Seismic Performance Assessment of Buildings

Volume 1 – Methodology

ATC-58-1 75% Draft

Prepared by

APPLIED TECHNOLOGY COUNCIL
201 Redwood Shores Parkway, Suite 240
Redwood City, California 94065
www.ATCouncil.org

Prepared for

U.S. DEPARTMENT OF HOMELAND SECURITY (DHS)
FEDERAL EMERGENCY MANAGEMENT AGENCY
Michael Mahoney, Project Officer
Robert D. Hanson, Technical Monitor
Washington, D.C.

PROJECT MANAGEMENT COMMITTEE
Christopher Rojahn (Project Executive Director)
Ronald O. Hamburger (Project Technical Director)
John Gillengerten
Peter J. May
Jack P. Moehle
Maryann T. Phipps*
Jon A. Heintz**
William T. Holmes **

STEERING COMMITTEE
William T. Holmes (Chair)
Roger D. Borcherdt
Anne Bostrom
Bruce Burr
Kelly Cobeen
Anthony B. Court
Terry Dooley
Dan Gramer
Michael Griffin
R. Jay Love
David Mar
Steven McCabe
Brian J. Meacham
William J. Petak

* ATC Board Contact
** ex-officio

STRUCTURAL PERFORMANCE PRODUCTS TEAM
Andrew S. Whittaker (Team Leader)
Gregory Deierlein
John D. Hooper
Yin-Nan Huang
Nicolas Luco
Andrew T. Merovich

NONSTRUCTURAL PERFORMANCE PRODUCTS TEAM
Robert E. Bachman (Team Leader)
Philip J. Caldwell
Andre Filiatrault
Robert P. Kennedy
Helmut Krawinkler
Manos Maragakis
Eduardo Miranda
Keith Porter

RISK MANAGEMENT PRODUCTS TEAM
John D. Hooper (Team Leader)
Craig Comartin (Team Leader)
Mary Comerio
Gregory Fenves
Mahmoud Hachem
Gee Hecksher
Judith Mitrani-Reiser
Farzad Naeim
Hope Seligson

May 2011

STRUCTURAL FRAGILITY DEVELOPMENT CONSULTANTS
Charles Ekiert
Andre Filiatrault
Aysegul Gogus
Kerem Gulec
Dawn Lehman
Jingjuan Li
Laura Lowes
Eric Lumpkin
Hussein Okail
Charles Roeder
Benson Shing
Christopher Smith
Victor Victorsson
John Wallace

FRAGILITY REVIEW PANEL
Bruce Ellingwood
Robert Kennedy
Stephen Mahin

NONSTRUCTURAL FRAGILITY DEVELOPMENT CONSULTANTS
Richard Behr
John Eidinger
Paul Kremer
Ali M. Memari
William O'Brien
John Osteraas
Xin Xu

RISK MANAGEMENT PRODUCTS CONSULTANTS
Peter Morris
Scott Shell

VALIDATION/VERIFICATION TEAM
Jack Baker
David Bonneville
Charles Scawthorn
Hope Seligson

Notice

This document has been prepared by the ATC-58 Project Team to assist interested parties in obtaining an understanding of the methodology as it is being developed, and to facilitate comment and feedback to the project team on its further development. The guidelines presented in this document are incomplete at this time. The data and procedures are not necessarily appropriate for use in actual projects at this time, and should not be used for that purpose. The information contained herein will be subject to further revision and enhancement as the methodology is completed.

Preface

In 2006 the Applied Technology Council (AT) was awarded the second in a series of five-year contracts with the Federal Emergency Management Agency (FEMA) to develop Next-Generation Performance-Based Seismic Design Guidelines for New and Existing Buildings (ATC-58-1 project). The principal work effort under this 5-year contract was the development of guidelines for *Seismic Performance Assessment of Buildings*, an activity that commenced under an earlier five-year contract with FEMA. Under that initial 5-year effort (ATC-58 project), ATC also prepared the FEMA 445 report, *Next-Generation Performance-Based Seismic Design Guidelines, Program Plan for New and Existing Buildings*, which sets forth the scope of work and program plan for implementing the overall work effort under this series of projects.

This document describes a recommended methodology for performing seismic assessments of individual buildings. The recommended methodology provides a framework for identifying the probable consequences, in terms of human losses (deaths and serious injuries), direct economic losses (building repair or replacement costs) and indirect losses (time of lost beneficial use of the building for its intended purpose), resulting from building response to ground shaking.

The companion Volume 2 provides guidance on implementing the methodology, including instructions on how to use an electronic Performance Assessment Calculation Tool (PACT) that has been developed to enable practical implementation of the methodology.

ATC gratefully acknowledges the numerous consultants involved in the development of this document, including Ronald Hamburger, who served as Project Technical Director, members of the Project Management Committee, members of the Project Steering Committee, the Nonstructural Performance Products Team, the Structural Performance Products Team, the Risk Management Products Team, and the consultants who assisted these teams. The names of individuals who served on these groups, along with their affiliations, are provided in the list of Project Participants at the end of this document.

ATC also gratefully acknowledges the guidance and support provided by the FEMA Project Officer, Michael Mahoney, and the FEMA Technical Monitor, Robert D. Hanson.

Christopher Rojahn, ATC Executive Director

Table of Contents

List of Figures

List of Tables

Glossary and Notation

Glossary

Annualized loss – over a period of many years, the average value of loss per year

Casualties – loss of life, or serious injury to persons, typically requiring hospitalization

Component – one of many parts, structural and nonstructural, that together comprise a building

Conditional Probability – The probability that an outcome will occur, given that a particular event occurs or condition exists.

Consequence function - a relationship that indicates the conditional probability of incurring loss as a function of a component or building damage state

Correlation - a mathematical relationship that defines the extent that the value of one parameter is dependent on the value of one or more other parameters

Damage function – for a specific damage state, a detailed description of the significant effects of the damage in terms of what is damaged, the repair actions that it necessitates, the effect on occupancy, and the effects that could result in casualties if persons are present

Damage State – for a particular building component, or the building as a whole, a range of damage conditions associated with unique consequences including required repair actions, occupancy interruption and potential injury or endangerment of persons

Decision-maker(s) – an individual or group of individuals who select the performance objectives for a performance-based design.

Demand – a parameter, such as peak floor (ground) acceleration, peak component deformation, peak or residual story displacement, peak floor (ground) velocity, or peak component force (stress) that is predictive of component or building damage states

Discount rate – a factor used to indicate the time-value of money in economic analysis

Distribution – a mathematical function that describes the statistical probability that subsets of elements in a set of elements, will have particular values

Dispersion – a measure of uncertainty associated with prediction of the true value of a random and/or otherwise uncertain behavior

Earthquake Scenario - a specific earthquake event, defined by a magnitude and geographic location relative to a building site

Fragility Function – a mathematical function that indicates the probability of incurring a damage state conditioned on the value of a single demand parameter

Fragility Group – a set of similar building components that have the same potential damage characteristics, fragility and consequence functions

Fragility Specification – a detailed description of potential component damage states, fragility and consequence functions

Geometric mean (geomean) –In characterization of ground motion intensity, the square root of the product of the value of a ground motion parameter in each of two orthogonal directions , i.e. $\sqrt{xy}$

Intensity – the severity of ground shaking as represented by a 5%-damped, elastic acceleration response spectrum or, the 5% damped spectral response acceleration at a particular natural period of vibration

Intensity-based Assessment – an assessment of a building's probable performance given that the building is subjected to ground motion with specific intensity

Lognormal distribution – a distribution of values, characterized by a median value and dispersion that has the property that the natural logarithm of the values is normally distributed.

Median – That value of an uncertain parameter (or of a population of values) that will be exceeded 50% of the time

Mean – the average value of a parameter (or population of values) having different possible values. If the population of values for the parameter is normally distributed the mean will be equal to the median. If the distribution of values is skewed, the mean may either be less than or greater than the median.

Mean Recurrence Interval – the average amount of time, typically expressed in years, between expected repeat occurrences of an event, such as a particular earthquake scenario or an earthquake loss.

Mutually Exclusive Damage States – A series of related damage states where the occurrence of any one type of damage will prevent the occurrence of the other types.

Net present value – for a particular discount rate, the present value of benefits that will be received in the future less the associated costs of these benefits

Normal Distribution – a symmetric distribution completely described by a mean value and standard deviation. When plotted as a probability density function, the normal distribution has the shape of a bell curve.

Non-structural Component – a building component that is not part of the structural system

Performance – the consequences of a building's response to earthquake shaking or other hazards expressed in terms of the probable consequences, potentially including number of casualties, occupancy interruption time, repair cost and environmental impacts

Performance group – a set of components described by a single fragility group that will all experience the same demand during a building's earthquake response

Performance Objective- an expectation as to the probable amount of damage and resulting consequences that a building may occur in future earthquakes

Period – the amount of time, in seconds, necessary for a structure to undergo one complete cycle of motion in free vibration

Realization - one possible performance outcome for a particular earthquake scenario or intensity comprising a unique set of demands, damage states and consequences

Repair cost – the cost, in present dollars, necessary to restore a building to pre-earthquake condition, or in the case of total loss, to replace the building with a new structure of similar type.

Replacement cost – the cost, in present dollars, necessary to completely replace a building that has been damage beyond a point of practicable repair, including costs associated with demolition and clearance of debris from the site.

Replacement time – the time, in weeks, necessary to completely replace a building that has been damage beyond a point of practicable repair, including time associated with demolition and clearance of debris from the site.

Return on investment – the annual income that can be derived from an investment divided by the present value of the investment

Return period – see mean recurrence interval

Scenario-based Assessment – an assessment of a building's probable performance given that the building is subjected to a specific earthquake scenario

Seismic Hazard Curve – a plot of the probabilities of exceedance of the possible values of a ground shaking intensity parameter

Sequential Damage States – A series of related component damage states that occur sequentially, that is only following the occurrence of an initial damage state, can an additional damage state or states occur.

Simulation – A vector set of demands representing the building's structural response in a particular realization.

Simultaneous Damage States – A series of unrelated component damage states that can, but need not necessarily, occur at the same time

Stakeholder – a person or group of persons who's well-being is affected by a building's performance including building owners, lenders, insurers, tenants, and the general public.

Structural Component – a building component that is part of the intended vertical or lateral force resisting system, or that provides measurable resistance to earthquake-induced building deformations

Structural System – the collection of building components that act together to resist either vertical or lateral loading, or both.

Time-based Assessment – an assessment of probable building performance over a specified period of time, considering all earthquake scenarios that could occur during that period of time, and the probability of occurrence of each.

Notation

a_i^*	in the simplified analysis method, estimated median peak floor acceleration at level "i"
b	the slope of a straight line fit to a series of data having x and y values
c	the y intercept of a straight line fit to a series of data having x and y values
d_i	the value of the demand at which a particular damage state was first observed to occur in specimen "i" in a series of M tests, or the maximum value of demand to which a specimen was subjected without occurrence of the damage state

$\overline{d}_j$ The maximum demand experienced by a series of test specimens in bin "j"

d_{max} The maximum demand, d, experienced by a specimen in a series of tests

d_{min} For a series of tests of specimens, the minimum value of demand, d, at which any specimen exhibited damage or distress

e_i In time-based assessment the mid-range intensity within an incremental range of intensities, Δe_i

h_j In the simplified procedure, the height of level "j" above the building base

i Interest rate, or expected rate of return on money

k in the simplified procedure, a coefficient used to account for nonlinear mode shape

m_j the number of specimens in bin "j" for which damage conforming to a particular damage state is observed

pga peak ground acceleration

t A period of years over which an investment decision is amortized

v_i^* in the simplified analysis method, estimated median peak floor velocity at level "i"

w_j In simplified analysis, weight lumped at a structure's level "j"

x_j the natural logarithm of $\overline{d}_j$

$\overline{x}$ the mean value of a series of values, x_j

y_j the inverse lognormal distribution value for the number of specimen tests that experienced a damage state in a bin "j" of specimen tests

$\overline{y}$ the mean of the values of y_j

A An amount of money that is earned or expended each year over a period of several years

C_1 In the simplified analysis procedure, a coefficient used to account for the difference in displacement response between elastic and inelastic structures, assuming non-degrading inelastic behavior

C_2 In the simplified analysis procedure, a coefficient used to account for the effects of stiffness degradation on displacement response

C_{sm} A coefficient used to derive an approximate estimate of the fraction of the structure's total mass effective in first mode response

C_q A coefficient that adjusts computed median strength capacity for construction quality

C_{vx} In the simplified analysis procedure, the fraction of the total pseudo lateral force, applied to level "*x*"

F_x In the simplified analysis procedure, the pseudo lateral force applied to level "*x*"

H In the simplified analysis procedure, total building height above the base

M the total number of test specimens for which test data is available and for which the damage state of interest occurred

M_A in a series of *M* tests, the number of specimens that did not experience any damage or distress but which experienced demands greater than or equal to a reference value, d_a

M_B in a series of *M* tests, the number of specimens that experienced some damage or distress but which did not experience the damage state of interest

M_j the number of test specimens in a bin "j" of a series of tests

NPV The net present value of a future stream of incomes or expenditures

PM_{10} That value of a performance measure, for example repair costs, that exceeds 10% of the possible range of values.

PM_{50} The median value of a performance measure, for example repair time, that exceeds 50% of the possible values.

PM_{90} That value of a performance measure, for example casualties, that exceeds 90% of the possible range of values.

$\overline{PM}$ The mean, value of a performance measure. Also termed the expected value and average value.

$P(C)$ The conditional probability of building collapse, given an intensity of shaking

$P(U_i)$ The probability, for a given intensity or scenario, that damage sustained by components in performance group "*i*" will result in an unsafe placard.

$P(U_T)$ The total conditional probability, given a specific intensity of motion or earthquake scenario, that a building will receive an unsafe placard

R_n nominal resistance in accordance with an appropriate LRFD design specification

S In the simplified analytical procedure, the ratio of elastic base shear force to the structure's yield shear strength

$S_a(T)$ Spectral response acceleration at period T.

S_a^{min} For time-based assessment, the minimum spectral response acceleration at which performance is assessed

S_a^{max} For time-based assessment, the maximum spectral response acceleration at which performance is assessed

T Period of structural response

T_1 Period of fundamental mode of vibration

T_1^X Period of fundamental mode of vibration in the "X" horizontal direction

T_1^Y Period of fundamental mode of vibration in the "Y" horizontal direction

$\overline{T_1}$ The average of the fundamental response periods about each of two orthogonal building axes

T_{min} The minimum period in a range of periods, used to scale ground motions for nonlinear response history analysis

T_{max} The maximum period in a range of periods, used to scale ground motions for nonlinear response history analysis

T_1^X The fundamental period of translational vibration in the first of two orthogonal directions of a structure's dynamic response

T_1^Y The fundamental period of translational vibration in the second of two orthogonal directions of a structure's dynamic response

$\overline{T}$ For structures with uncoupled first modes of translational vibration in each of two orthogonal directions, the average of the periods of the fundamental translation modes in each period

V In the simplified analysis procedure, a pseudo lateral force used to estimate story drifts

V_{yt} A structure's effective yield strength in first mode response.

W_1 In simplified analysis, the weight effective in the structure's first mode response

β A measure of uncertainty in the true value of a random parameter, also called dispersion.

β_a Uncertainty associated with record to record response variability

$\beta_{a\Delta}$ Record to record variability (dispersion) associated with story drift response

β_{aa} Record to record variability (dispersion) associated with floor acceleration response

β_c Modeling uncertainty associated with lack of definition of the way a building has actually been constructed

β_r In a series of data used to establish fragility functions, the random variability evident in the data

β_u A measure of uncertainty that represents the probability that conditions inherent in a data set used to establish fragility do not represent actual conditions a real component in a building will experience

β_{gm} Dispersion accounting for uncertainty in ground motion intensity as reflected in attenuation relationships

β_a Modeling uncertainty associated with inaccuracies in the structural model associated with imperfect hysteretic models, estimates of damping, and failure to include all elements in the model

β_m Modeling dispersion, representing the uncertainty in the predicted response obtained from structural modeling and analysis.

β_C Uncertainty associated with the quality of installation or construction of a component

β_D Uncertainty associated with the ability of a design equation to predict actual behavior when material strength is defined

β_M Uncertainty in material strength

β_{SD} In the simplified procedure, the total dispersion associated with story drift

δy Component deformation at yield

Δ_i In the simplified procedure, the uncorrected story drift at level "*i*"

Δ_i^* estimated median peak transient story drift at story "*i*"

Δ_r estimated median residual story drift

Δe_i In time-based assessments an incremental range of earthquake intensities

$\Delta\lambda_i$ In time-based assessments the probability of occurrence, in a period of time, of earthquake intensity with range Δe_i

Δ_y estimated transient story drift at development of yield strength

ϕ resistance factor as specified by an LRFD design specification

ϕ_{j1} In simplified analysis, the ordinate of the first mode deflection at floor level "*j*"

λ Mean annual frequency of exceedance of a ground motion parameter

μ the ratio of component deformation at the onset of damage to component deformation at yield

Chapter 1
Introduction

1.1 Purpose

This report describes a general methodology and recommended procedures to assess the probable earthquake performance of individual buildings based on their unique site, structural, nonstructural and occupancy characteristics. Performance measures include potential casualties, repair and replacement cost and schedule, and potential loss of use due to unsafe conditions. The methodology and procedures are applicable to performance-based design of new buildings, and performance assessment and seismic upgrade of existing buildings.

Performance measures are the probability of incurring casualties, repair costs, and occupancy loss. Performance can be assessed for particular earthquake scenarios or intensities, or considering all earthquakes that could occur, and the likelihood of each.

This volume is the fundamental product developed by the Applied Technology Council under a contract with the Federal Emergency Management Agency (FEMA) to develop next-generation "Performance-Based Seismic Design Guidelines" for buildings termed the ATC-58 Project. Companion products include an implementation guide; an electronic calculation tool and a companion technical manual; an electronic data base of component fragility specifications, and; a series of background technical reports.

The basic methodology and procedures presented herein can be applied to the seismic performance assessment of any building type, regardless of age, construction or occupancy. However, such application requires basic data on the susceptibility of structural and nonstructural components to damage as well as the casualty, occupancy, and repair consequences associated with this damage. An electronic data base contained in companion products permits application to buildings constructed with the structural systems indicated in Table 1-1 and having the architectural components, mechanical and electrical systems, contents and populations common to typical colleges and K-12 schools; offices, community hospitals, hotels and motels, single and multi-family residences, laboratories, shopping centers, and warehouses; and buildings containing combinations of these occupancies.

The necessary data for performance assessment of buildings constructed using other structural systems or having nonstructural components and/or occupancies different than those described above can be developed using basic procedures presented in companion volumes. These procedures involve the use of laboratory testing of individual building components and

assemblies, analytical evaluation, statistical information on the actual performance of buildings in past earthquakes, or expert judgment.

Table 1-1 Basic Structural Systems and Components

Material	System	Comments
Concrete	Beam-column frames	Conventionally reinforced, with or without modern seismic-resistant detailing
	Shear walls	Shear or flexurally controlled, with or without seismic-resistant detailing
	Slab-column systems	Post-tensioned or conventionally reinforced, with or without slab shear reinforcement
Masonry	Walls	Special or ordinary reinforced masonry walls, controlled by shear or flexure
Steel	Moment frames	Fully restrained, pre- or post-Northridge, Special, Intermediate and Ordinary detailing
	Concentric braced frames	"X"-braced, chevron-braced, single diagonals, special, ordinary or nonconforming detailing
	Eccentric braced frames	Flexure or shear links at mid-span of link beam
	Light-framed walls	With structural panel sheathing, steel panel sheathing or diagonal strap bracing
	Conventional floor framing	With concrete-filled metal deck, untopped steel deck or wood sheathing
Timber	Light-framed walls	With structural panel sheathing, gypsum board sheathing, cement plaster sheathing, let-in bracing, and with and without hold downs

Future products may include publications that suggest appropriate performance characteristics for buildings of differing occupancy and use; procedures to design new buildings or upgrade existing buildings to obtain desired performance; and data and tools that permit the assessment of environmental impacts and publications intended to assist design professionals, building regulators, developers, owners, tenants, lenders, insurers and other stakeholders to take advantage of the potential benefits of seismic performance assessment and performance-based design approaches.

1.2 The Performance-Based Design Process

Performance-based seismic design is a formal process for seismic design of new buildings or design of seismic upgrades for existing buildings with the specific intent that the buildings will be able to achieve specified performance objectives in future earthquakes. Performance objectives relate to the amount of damage the building may experience and the consequences of this damage including potential casualties; loss of use or occupancy; and repair and reconstruction cost. They can also include consideration of

potential environmental impacts including generation of waste, expenditure of energy and other resources, and creation of greenhouse gases.

The typical building design process is not performance-based. In the typical process designers select, proportion and detail building components to satisfy prescriptive criteria contained within the building code. Many of these code criteria were developed with the intent of providing some level of seismic performance; however, the intended performance is often not obvious to the designers and other stakeholders and the design's actual ability to provide this performance is seldom evaluated.

In the performance-based process, owners, designers and other stakeholders jointly identify the desired building performance characteristics at the project outset. Then as design decisions are made, the effect of these decisions on the building's performance capability is evaluated to assure that the final structure will be capable of achieving the target performance. Figure 1-1 presents a flow chart for the performance-based design process.

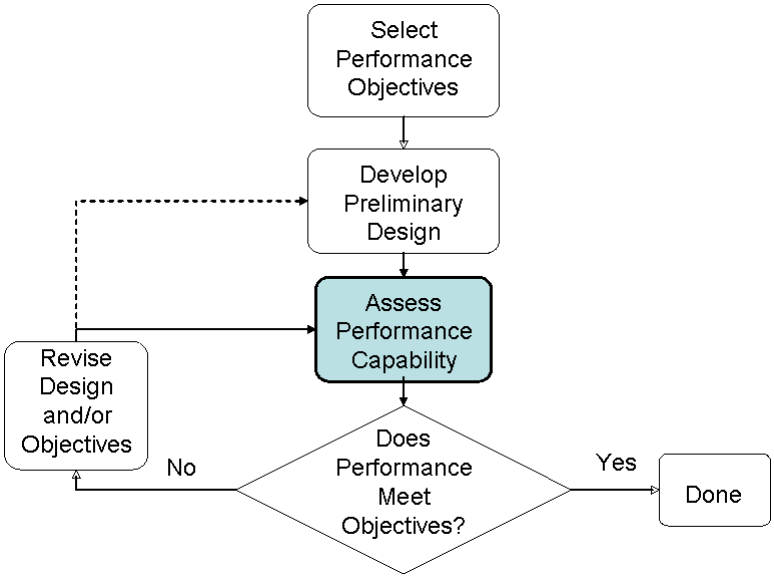

Figure 1-1 Performance-based design flow diagram

The process initiates with selection of one or more performance objectives. Each performance objective is a statement of the acceptable risk of incurring damage or loss for identified earthquake hazards. Building developers/owners, design professionals, and building officials will typically participate in the selection of performance objectives. When selecting performance objectives, these decision-makers may consider the needs and desires of a wider group of stakeholders including prospective tenants, lenders, insurers, the general public and others who have impact on a

building's value, but who generally do not have an opportunity to participate in the design process directly.

Once the decision-makers select the performance objectives, design professionals must develop their design to a sufficient level of detail to allow determination of the building's performance characteristics. For new buildings, this will include, as a minimum, identification of: (1) the location and characteristics of the site; (2) building size, configuration and occupancy; (3) type, location and character of finishes and nonstructural systems; (4) selection of structural system type and configuration; and, (5) developing estimates of the strength, stiffness and ductility of this system. In the case of existing buildings, these characteristics are already defined, and it is only necessary to determine what they are, and then define preliminary concepts for retrofit measures, if needed.

Performance assessment … is the primary subject of this methodology

Performance assessment (the shaded box in Figure 1-1) is the process used to determine the performance a design is capable of achieving. This step is the primary subject of this methodology. In this step, engineers conduct a series of structural analyses to predict the building's response when subjected to the earthquake hazards identified as part of the performance objectives and then use the information obtained from these analyses to assess the amount of damage that may occur and the probable consequences of this damage.

Following performance assessment, the engineer compares the predicted performance with the desired performance. If the assessed performance matches or exceeds the stated performance objectives, the design is adequate and the project can be completed, assuming that the cost of completion is acceptable. If the assessed performance does not meet the performance objectives, the design team must either revise the design or alter the performance objectives in an iterative process, until the assessed performance meets acceptable objectives.

1.3 Project Products

Project products include this volume, a companion Implementation Guide, the PACT electronic calculation tool, and background reports

This volume presents the overall ATC-58 seismic performance assessment methodology. Chapter 2 presents an overview of the methodology including discussion of the specific performance measures used and the types of assessments that can be conducted. Chapter 3 describes the development of building-specific performance models that include assembly of all that data necessary to assess a building's performance. Chapter 4 describes methods to characterize seismic hazards for use in the methodology. Chapter 5 provides guidelines for two alternative methods of structural analysis that can be used to predict building response. Chapter 6 presents alternative

procedures for characterizing a building's susceptibility to collapse as a function of ground shaking intensity. Chapter 7 describes the calculation procedures used to determine the probable damage the building will sustain and the consequences of this damage in terms of casualties, occupancy loss, and repair cost, as well as other potential impacts. Chapter 8 illustrates some methods to use data obtained from performance assessment in the project planning and design process.

Appendices to this report present background information that may be useful for some readers. Appendix A provides a basic tutorial on probability and statistics and the types of probabilistic distributions used to represent uncertainty in these performance assessment procedures; Appendix B provides detailed information on seismic hazard evaluation and attenuation relationships; Appendix C presents information on estimation of residual building drift and discussion of the inability of structural analysis to reliably predict residual drift. Appendix D lists the specific types of structural and nonstructural components and contents for which damage and consequence data are provided in the PACT databases; Appendix E presents recommended building population models for common building occupancies; Appendix F provides a tabulation of the typical quantities of nonstructural components and contents found in buildings of differing occupancy or use. Appendix G describes the algorithm used to generate multiple vectors of demands as part of the performance calculation process; and Appendix H provides guidelines for development of fragility functions for individual building components for use in building performance assessment.

There are a series of companion products to this volume that will assist engineers to implement the methodology. These include:

- *Performance Assessment Calculation Tool (PACT)* – PACT is an electronic calculation tool code and accompanying databases that performs the calculations described in Chapter 7 of this volume. It also includes a series of utilities that can be used to update or modify the performance databases referenced by the tool. It is provided on a CD-ROM with this volume. PACT is not maintained by the Federal Emergency Management Agency or the Applied Technology Council. However, it is written in C# and is public domain.
- *Implementation Guide* – The implementation guide provides specific instructions on how to assemble and prepare the data necessary for input to PACT. It includes a PACT user's manual, a PACT technical manual and a series of example applications of building performance assessment

- *Performance Parameter Database* – This database, also provided on the CD-ROM that accompanies this volume, contains printouts of the basic data on the damageability of structural and nonstructural components and contents, used by PACT as a default in performance calculations.
- *Background Reports* – These background reports document some of the studies conducted by the ATC-58 project team during development of the methodology. These studies underlie the basic methodology as well as data contained in the PACT databases.

Readers are cautioned to become thoroughly acquainted with the information contained in this volume before attempting to conduct building performance assessments using PACT.

1.4 Limitations

This report and its companion products provide a general methodology and recommended procedures to assess the probable performance of individual buildings when subjected to future earthquake shaking. Specifically, the methodology assesses the likelihood that building structural and nonstructural components and systems will be damaged by earthquake shaking, and estimates the potential casualties, repair costs, and interruption of beneficial building occupancy that could occur as a result of such damage. A companion project is expanding the methodology to address environmental impacts of earthquake damage. It is anticipated that a companion report and updated electronic calculation tools and data bases will be produced by that project.

Earthquake shaking can cause other significant effects including loss of offsite power, water and sewage, initiation of fires, inundation, and release of hazardous materials. Similarly, earthquake effects other than ground shaking including ground fault rupture, landslide, liquefaction, seiches and tsunamis, and lateral spreading can significantly affect building performance. While the general methodology presented in this volume could be used to assess these effects such assessment is beyond the scope of this volume and its companion products. Engineers conducting seismic performance assessments of buildings should, as a minimum perform qualitative evaluations of these other effects, and, if these effects appear significant, report this to decision-makers.

Assessment of a building's probable performance in future earthquakes inherently entails significant uncertainty. The methodology and procedures presented herein use state of art methodologies to express the effect of these uncertainties on projected building performance. Regardless, it is possible

that the performance of individual buildings in actual earthquakes may either be better or worse than indicated by assessments conducted in accordance with the procedures presented herein. Further the accuracy of performance assessments depends in large part on data and calculations generated by individual users. Neither the Federal Emergency Management Agency, nor the Applied Technology Council, their employees, directors nor consultants present any warranty expressed or implied as to the accuracy of performance assessments made using these procedures.

Chapter 2
Methodology Overview

2.1 Performance Measures

This methodology expresses performance in terms of probable earthquake impacts and their associated uncertainties rather than subjective judgments

A performance measure is a means of quantifying the consequences of a building's earthquake response in terms that are meaningful to decision makers. Historically, decision-makers have used a number of different performance measures.

Many financial institutions including lenders, investment funds and insurers use Probable Maximum Loss (PML), Scenario Expected Loss (SEL), and Scenario Upper Bound loss (SUL) as preferred performance measures. These performance measures are quantitative statements of probable building repair cost, typically expressed as a percentage of building replacement value. Some building owners, developers and tenants have also relied on these performance measures to quantify seismic performance.

Building officials and engineers commonly use a series of standard performance levels termed *Fully Functional*, *Immediate Occupancy*, *Life Safety* and *Collapse Prevention* to characterize expected building performance. These performance levels are defined by acceptable ranges of strength and deformation demand on structural and nonstructural components, with implicit qualitative relationship to probable levels of damage, casualties, post-earthquake occupancy and repair consequences.

In contrast to the above measures, this seismic performance assessment methodology uses probable future earthquake impacts as its measures of performance. The specific impacts considered are:

- casualties – the number of deaths and injuries of a severity requiring hospilization;
- repair cost – including the cost of repairing or replacing damaged buildings and their contents;
- repair time –the period of time necessary to conduct repairs or replace damaged contents, building components or entire buildings; and
- Unsafe Placards – the probability that a building will be deemed unsafe for post-earthquake occupancy.

For a number of reasons, described in more detail in Section 2.3, it is impossible to predict any of these impacts precisely. Therefore, this methodology expresses performance in the form of probable impacts, considering the inherent uncertainties. This method of measuring performance has several advantages. These performance measures (casualties, repair costs, construction time and occupancy loss) are more meaningful and useful to most decision makers than the standard performance levels described above. Also, the PML, SEL and SUL measures commonly used by many decision-makers can be directly and objectively derived using this approach. Finally, this approach explicitly acknowledges the uncertain nature of performance assessment and properly used, can assist design professionals to avoid liability associated with owners' and other stakeholder's possible perception of performance warranties associated with assessments and designs.

2.2 Factors Affecting Performance

The amount of earthquake damage a building experiences, and the consequences of this damage in terms of casualties, occupancy loss, repair cost and repair time depend on a number of factors. These include:

- the intensity of ground shaking and other seismic hazards the building experiences;
- the building's response to the ground shaking and other hazards, and the amount of force, deformation, acceleration and velocity experienced by the various structural and nonstructural components, contents and occupants
- the vulnerability of the building and its systems and contents to damage;
- the number of people present, their location in the building, and the type, location and amount of contents present when the earthquake occurs;
- the reactions of inspectors performing post-earthquake inspections to visible evidence of damage;
- the specific details and methods specified by design professionals performing repair design; and
- the availability of labor and materials, the efficiency of individual contractors and their desire for profit.

This methodology explicitly evaluates each of these factors in the development of building performance functions. However, there are other important factors associated with the actions people take in response to a future earthquake that the methodology does not consider because they are inherently unpredictable. Factors that are not considered, but which can affect the magnitude of earthquake impacts, include:

- the speed and quality of care given to injured individuals;
- the speed with which building owners engage design professionals and contractors to implement repair actions; and
- a decision to conduct repairs while a building remains occupied, requiring staged construction, or to vacate a building and turn it over to construction crews for efficient action.

2.3 Uncertainty in Performance Assessment

It is impossible to predict precisely the value of each of the individual factors that affect seismic performance. We do not know which fault will originate the next earthquake, where along the fault the rupture will initiate, what magnitude it will be, nor do we have a complete understanding of the subsurface conditions that seismic waves must pass through as they affect a building site. As a result, we are uncertain about the intensity, spectral shape, or specific wave form of shaking a building will experience.

> We are uncertain as to the intensity or wave form of future shaking…, our models are imprecise…, our assessment of damage is based on laboratory tests…but the tested components are not identical to those in our building; we don't know when the earthquake will occur or who will be inside the building…

While our ability to develop analytical models of structures is constantly improving, our models are still imprecise. We use default properties for structural elements based on assumptions of material strength and cross section construction. We estimate damping based on rules of thumb. We often neglect the effect of soil-foundation-structure interaction as well as the effect of many structural elements that resist only gravity loads, and nearly all nonstructural elements. Thus, our predictions of a building's response to ground shaking are somewhat inaccurate and we may not know whether we are over- or under-predicting a building's actual response.

With the results of our structural analyses, we can predict the levels of damage that structural and nonstructural components will sustain, based on the observed behavior of similar elements during laboratory tests and in past earthquakes. However, the tested components were likely not identical to the elements in our building, nor were the forces and deformations they experienced in the laboratory, identical to those predicted by our response analyses. Therefore, the types and amounts of damage we predict are also likely to be somewhat inaccurate.

lions express
incurring
ts… This
the
ted in this
e means of
rmance

We cannot predict the time of day, or day of the week when the earthquake occurs, which people will be present in the building, or what contents and furnishings the buildings may have. We don't know exactly which repair techniques will be specified to repair damaged components, or how efficiently contractors will conduct repairs. The result of these uncertainties and many others is that it is not possible to predict precisely any building's earthquake performance, whether measured by casualties, repair costs, downtime or other impacts.

However, it is possible to assess these performance measures in the form of performance functions. Performance functions are probability distributions that indicate the probability that losses of specified or larger magnitude will be incurred as a result of future earthquakes. Appendix A provides a brief introduction to probability distributions.

Figure 2-1 presents a typical performance function for a hypothetical building. In the figure, the horizontal axis represents the size of the impact (e.g., number of casualties or days of construction time) while the vertical axis indicates the probability that the actual impact will be equal to or less than this amount.

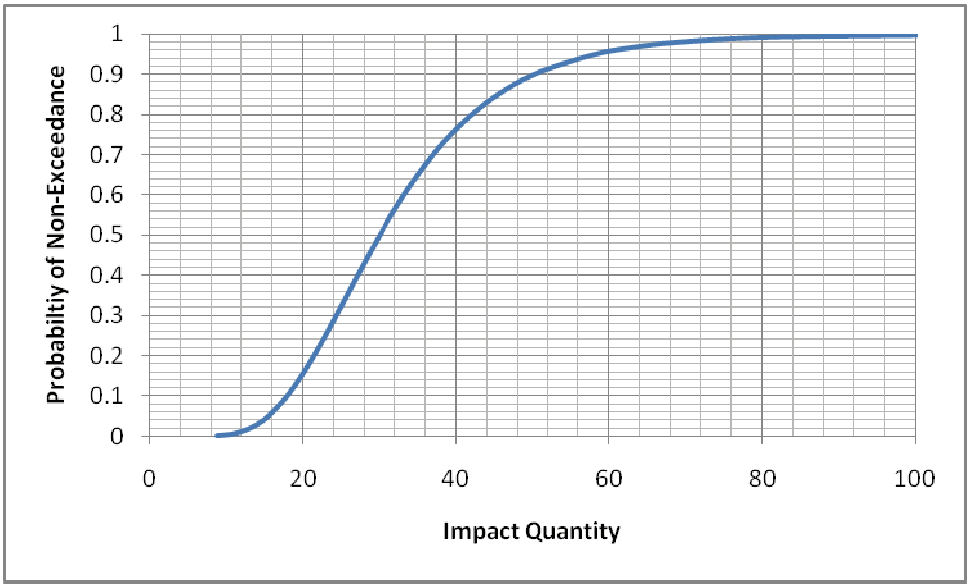

Figure 2-1 Hypothetical Peformance Function for Building

The methodology and procedures presented in this report describe the means of determining these performance functions.

2.4 Types of Performance Assessment

This methodology can be used to develop three types of performance assessment: intensity-based, scenario-based and time-based.

2.4.1 Intensity-Based Assessments

Intensity-based assessments evaluate a building's probable performance assuming that it is subjected to a specific intensity of shaking. Shaking intensity is defined by 5% damped, elastic acceleration response spectra. This assessment type can be used to assess a building's performance in the event it is subjected to the design earthquake shaking specified by the building code or to assess performance for shaking represented by any other response spectrum.

Intensity-based assessments evaluate performance for a user-selected acceleration response spectrum

2.4.2 Scenario-Based Assessments

Scenario-based assessments evaluate a building's probable performance assuming that it is subjected to the effects of a specific magnitude earthquake occurring at a specific location relative to the building site. Scenario assessments may be useful for decision makers with buildings located close to one or more known active faults. They can be used to inform decision-makers of the building's probable performance in the event that a historic earthquake on these faults is repeated, or a projected event occurs.

Scenario-based assessments evaluate performance for a user-defined earthquake magnitude and site distance

Scenario-based assessments are very similar to intensity-based assessments except that uncertainty in the earthquake intensity, given the scenario, is considered. The results of scenario-based assessments are performance functions like that of Figure 2-1 except that the probable performance is expressed conditioned on the occurrence of the scenario earthquake, rather than a specific intensity of shaking.

2.4.3 Time-Based Assessments

Time-based performance assessments evaluate a building's performance over a period of time, e.g. 1-year, 30-years, 50-years, considering all earthquakes that may occur in that period of time, and the probability that each will occur. Time-based assessments consider uncertainty in the magnitude and location of future earthquakes as well as the intensity of motion resulting from these earthquakes.

Time-based assessments evaluate performance over time, considering all possible earthquakes and their probability of occurrence

The period of time over which a time-based assessment is performed is dependent on the interests and needs of the individual decision makers. Assessments based on a single year are useful for cost-benefit evaluations used to decide between alternative performance criteria. Assessments using

longer time-periods may be more useful for other decision-making approaches. Chapter 8 provides additional information on these uses.

Time-based assessments provide performance functions that are similar in form to that shown in Figure 2-1, except that the vertical axis of the function expresses the probability that an impact magnitude (number of casualties, repair costs, etc.) will not be exceeded in a period of time, typically one year. Once the performance function for a particular period of time has been developed, it can easily be converted to apply to other time periods.

2.5 The Methodology

This Section provides a brief introduction to the several steps that comprise the performance assessment methodology. Figure 2-2 is a flow chart that illustrates the relationship of these steps in the methodology and also identifies the Chapters that present more detailed discussion of each step.

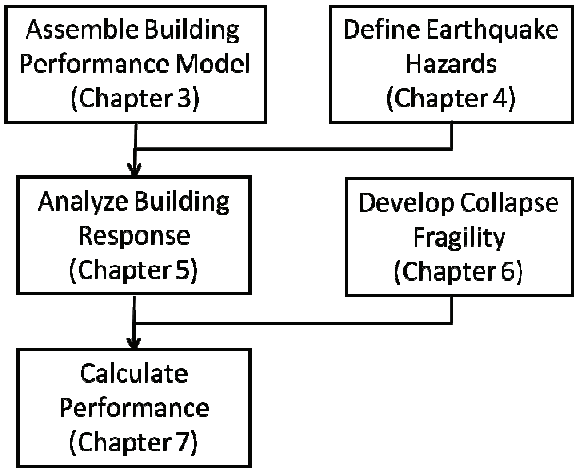

Figure 2-2 Performance Assessment Methodology

2.5.1 Assemble Building Performance Model

ormance
building
their
ic hazards

The building performance model is an organized collection of all data needed to define the building assets at risk and their exposure to seismic hazards. This data includes definition of the:

- Structural systems and components – consisting of all those structural components that provide measurable resistance to seismic loading, or, which can be damaged by the building's response to earthquake shaking. The data must be adequate to permit structural analysis and calculation of gravity and seismic demands. In addition, the data must include information on the types of damage these components can sustain; the structural demands that cause this damage; and the consequences of this

damage in terms of risk to human life, post-earthquake building occupancy, repair methods, costs and time.

- Nonstructural systems, components and contents – consisting of all those building components that do not provide significant resistance to gravity or earthquake loading but which can be damaged by the building's earthquake response, resulting in significant consequences. Data includes the location of these components, their vulnerability to damage of different types; the consequences of this damage, in terms of generation of life-threatening debris, influence on post-earthquake building occupancy and necessary repair actions.
- Occupancy – including the distribution of people within the building and the variability of this distribution with time of day and day of the year.

Chapter 3 describes the categorization of these components by fragility groups and performance groups. Fragility groups are sets of similar components that have the same damage vulnerability and consequences. Performance groups are fragility group subsets that will experience the same earthquake demands. Chapter 3 also describes the fragility specification used to categorize the fragility group damage and consequence data.

Fragility groups are sets of components with similar damage characteristics… Performance Groups are subsets of components that experience the same demands

2.5.2 Define Earthquake Hazards

Earthquake effects include ground shaking, ground fault rupture, liquefaction, lateral spreading, land sliding, and tsunami inundation. Each of these effects can occur with different levels of severity, or intensity, ranging from imperceptible to highly damaging. Earthquake hazard is a quantification of the intensity of these earthquake effects and the site-specific probability that effects of given intensity will be experienced.

This methodology addresses the earthquake consequences associated with building damage caused by earthquake ground shaking. However, the methodology can be extended to include consideration of the other hazards including permanent ground deformation, inundation, etc.

This methodology addresses earthquake performance associated with ground shaking, but it can be extended to other hazards

Ground shaking hazards are specified in different ways, depending on the type of assessment desired and the type of structural analysis used to quantify the building's earthquake response.

For intensity-based assessments the methodology considers the effect of building response to a single acceleration response spectrum. Depending on the type of structural analysis that will be used, ground shaking intensity is characterized in the form of discrete spectral response accelerations extracted

from this spectrum, or suites of ground motion records that have been selected and scaled for compatibility with this spectrum.

For scenario-based assessments the methodology considers the effect of building response to an earthquake having a defined magnitude and distance from the site. Shaking hazards are represented by a median acceleration response spectrum and period-dependant dispersions obtained from the attenuation relationship used to derive this spectrum. Analyses are conducted using discrete spectral response accelerations derived from the spectrum, or ground motion records that are scaled to be compatible with the spectrum.

For time-based assessments ground shaking hazards are characterized by a series of mean seismic hazard curves at different structural periods. Each hazard curve is a plot of the probability of exceedance of the spectral response acceleration at a particular structural period as a function of intensity. Using these hazard curves a series of acceleration response spectra are derived to represent ground shaking intensities across the meaningful range of exceedance probabilities and structural response. Analyses are conducted using discrete spectral response accelerations derived from these spectra, or ground motion records that are scaled to be compatible with the spectra.

Chapter 4 provides more complete discussion of the use of seismic hazards in this methodology.

2.5.3 Analyze Building Response

Chapter 5 describes the use of structural analysis to predict the damage-causing demands on a building's structural and nonstructural components resulting from the building's response to ground shaking. Demands typically include peak transient story drift and acceleration in each of two orthogonal directions as well as residual story drift at each level. However, it is possible to use additional demand parameters including peak floor velocity and component strength demand if a building has components for which damage is best predicted using these other parameters.

Two methods of analysis: nonlinear response history; or a simplified procedure based on equivalent lateral forces can be used to simulate building response

Chapter 5 describes the use of two methods of analysis, nonlinear response history analysis and a simplified analysis based on equivalent lateral force methods. Nonlinear response history analysis can be used for any structure and will provide values for any demand parameters desired. Simplified analysis is valid only for regular structures with limited nonlinear response and will provide values for peak transient floor acceleration, floor velocity

and story drift. An approximate procedure can be used to estimate residual drift from peak story drift and story yield displacement.

2.5.4 Develop Collapse Fragility

Most casualties (deaths and serious injuries) that occur in buildings during earthquakes occur as a result of partial or total building collapse. Therefore, in order to assess potential casualties it is necessary to define the probability of incurring structural collapse, as a function of ground motion intensity, and the modes of structural collapse (e.g. single story, multi-story) that can occur. These are represented in the form of collapse fragility functions. Chapter 6 describes means of establishing collapse fragilities using a combination of structural analysis and judgment.

2.5.5 Performance Calculations

Chapter 7 describes the performance calculation procedures used to assess the probable consequences of a building's response to earthquake shaking. In order to account for the many uncertainties inherent in the factors affecting performance, this methodology uses a Monte Carlo process to perform these calculations. This is a highly repetitive procedure in which the building's performance is calculated for a large number (hundreds to thousands) of realizations. Each realization represents one possible performance outcome for the building, considering a single combination of possible values of each of the uncertain factors. As a matter of practicality, these calculations must be performed using a digital computer and appropriate calculation tools, such as the PACT tool provided as a companion to this volume.

Each realization represents one possible performance outcome. The methodology uses Monte Carlo analysis to explore the possible range of outcomes

For intensity and scenario-based assessments, the performance calculations are nearly identical, as described in the Section below. For time-based assessments a more complex process is used as described in the following section.

Intensity- and Scenario-based Assessments

Figure 2-3 is a flow chart for the performance calculation process used in intensity and scenario-based assessments. For either assessment type, this process is repeated many times, in order to explore the effect of uncertainty on the predicted performance outcome. Each repetition is termed a realization and represents one possible performance outcome for the particular earthquake intensity or scenario being analyzed. Descriptions of the several steps in this flow chart are described below.

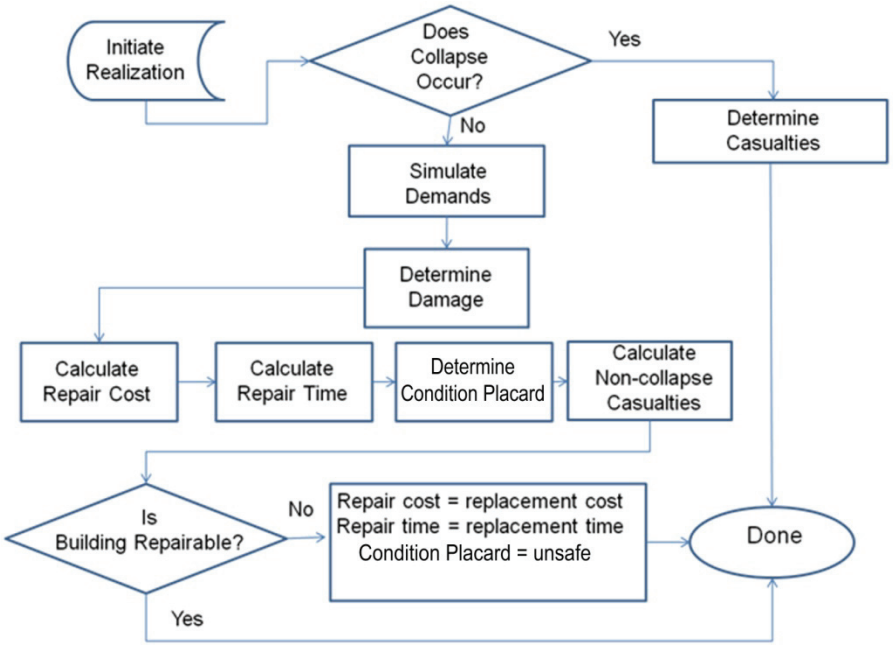

Figure 2-3 Loss calculation flow chart

Most casualties occur as a result of building collapse

Does Collapse Occur? - The first step in each realization is to determine if the building has collapsed using the collapse fragility function. The collapse fragility function, described in Chapter 6, indicates the probability of building collapse, given the ground motion intensity, and the mode of collapse if it occurs. By entering the collapse fragility function with the intensity of ground motion for the realization, the probability of collapse is determined. Then, a random number generator is used to select an integer between 1 and 100. If the selected number is less than or equal to the probability of collapse indicated by the collapse fragility, then the building is deemed to have collapsed. When collapse occurs, the building is assumed to be a total loss and the repair cost and time are taken as the building replacement values, including consideration of demolition and site clearance effort.

Calculate Building Collapse Casualties - In order to calculate casualties it is necessary to determine a time of day and day of the week at which the realization occurs using a random number generation process. Then, using this day and time, and a population function appropriate to the building's occupancy, the number of people present in the area o f collapse is determined. Depending on the type of construction, and casualty functions appropriate to the construction type, percentages of the population at risk in the collapsed area will be classified as serious injuries and fatalities.

Simulate Demands - If the random number generation and collapse fragility suggest the building does not collapse for a realization, it is necessary to

determine a set of earthquake demands including peak and transient story drift and floor accelerations. This demand set is termed a simulation. For intensity-based assessment, the results of the structural analysis are used to define a distribution of possible demands, given that the intensity of shaking is experienced, accounting for uncertainties in the modeling and analysis, as well as record to record variability in response. The analysis results are assumed to be representative of a distribution of possible analysis results that is jointly lognormal. With this assumption in place, the analysis results are used to determine the median response state, the dispersion and the covariance matrix associated with the assumed distribution. Then for each realization, random number generation is used to derive a simulated set of demands.

In reality, formation of the distribution and determination of median demands, dispersions and covariance is performed only one time, before any realizations are developed, and at this same time, a large number of demand sets, equal to the number of realizations to be evaluated, is also generated and stored for later use. At this stage in the realization flow diagram (figure 2-3) one of these simulated demand sets is obtained and associated with the realization.

Scenario-based assessments use the same process except that the dispersion for the assumed jointly lognormal demand distribution is modified to account for uncertainty in the intensity of motion associated with the ground motion scenario.

Determine Damage – If the building has not collapsed in a realization, the set of demands is used to determine a damage state for each vulnerable component in the building on a performance group by performance group basis. As described in Chapter 3, each performance group has an associated series of damage states and fragility functions that describe the probability that components within the performance group will be damaged to a given level. Random number generation is used to determine which, if any damage state each components is in for the particular realization.

Calculate Consequences - Using these damage states and consequence functions, also described in more detail in Chapter 3, a determination is made as to the magnitude of consequences (e.g., casualties, repair cost, repair time, unsafe placards) associated with the damage sustained by each of the building components. In performing these calculations, consideration is given to the volume of repair of each type that must be conducted as well as uncertainties associated with repair technique, contractor efficiency and pricing.

Is Building Repairable? The simulated set of demands for the realization includes the maximum residual story drift at any building level. Following computation of the damage to each performance group, and the resulting consequences, this maximum residual story drift is used, together with a building repair fragility to determine whether the building is practically repairable or not. The repair fragility is a lognormal distribution, typically having a median value of 1% residual drift ratio, and a dispersion of 0.3, as shown in Figure 2-4. At a residual drift ratio of 0.5% this fragility indicates a virtual certainty that the building can be repaired and at 2% drift a virtual certainty it will not be repaired. As with collapse determination, a random number generator is used to select an integer between 1 and 100. If this number is equal to or less than the probability of irreparability determined from the repair fragility at the maximum residual drift ratio for the realization, then the building is deemed irreparable.

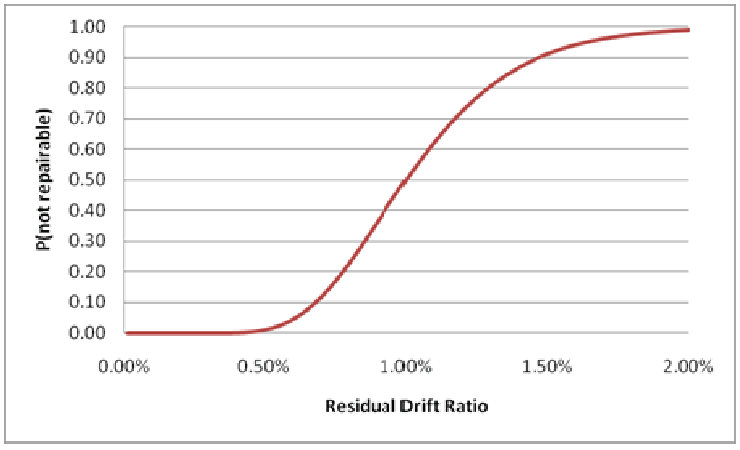

Figure 2-4 Typical building reparability fragility

If the building is determined to be irreparable the repair cost and repair time is taken as the building replacement cost and time, together with an allowance for demolition and site clearance of the damaged structure. The building is assumed to be assigned an unsafe placard.

The result of the process shown in Figure 2-3 and described above is one set of possible consequences of the building's earthquake response to a particular intensity or scenario. This process is repeated hundreds to thousands of times, resulting in a large set of possible outcomes. By ordering each of these outcomes (e.g. casualties) from smallest to largest and plotting the percentage of realizations with outcomes that exceed each value, it is possible to construct a performance curve, like that shown earlier in Figure 2-1.

Time-based Assessments

Time-based assessments compute the probable building performance outcomes considering all possible intensities of shaking the building may experience and weighting the outcome from each intensity by the probability that such shaking will be experienced.

In order to perform this calculation, it is necessary to obtain a hazard curve for the building site that shows the annual frequency of exceedance of ground motions having differing intensities. Chapter 4 and Appendix B provide detailed information on how to develop such hazard curves. Figure 2-5 is one such curve for a hypothetical site, showing the frequency of exceedance of a ground motion intensity parameter, *e*.

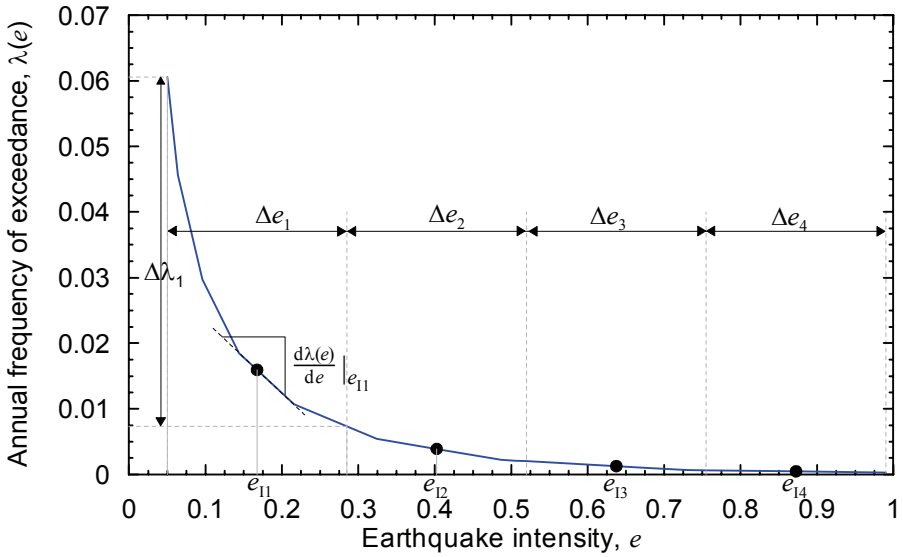

Figure 2-5 Seismic hazard curve and time-based loss calculations

In order to perform a time-based assessment, the hazard curve is divided into a series of segments, illustrated as the intervals Δe_i in the figure. The annual frequency of occurrence of ground motion having an intensity that falls within each interval is equal to the difference between the annual frequencies of exceedance of the ground shaking intensities at either end of the interval. For each intensity interval on the hazard curve, an intensity-based assessment is performed for the intensity at the interval mid-point. The resulting performance outcomes are then weighted by the annual frequency of occurrence of that interval. The results of these assessments are summed over all of the intervals to form a time-based assessment curve, like that shown in Figure 2-6.

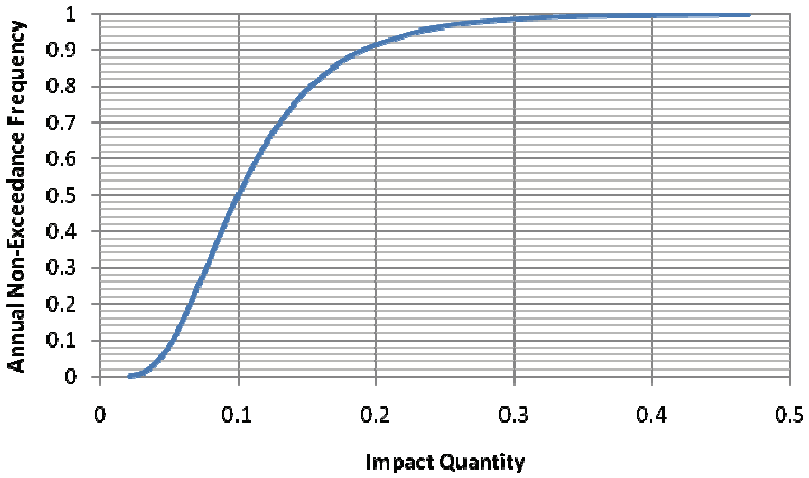

Figure 2-6 Example time-based performance curve

Chapter 3

Assemble Building Performance Model

3.1 Introduction

This chapter describes the building performance model assembly process. The building performance model is an organized collection of all the data necessary to define the building assets at risk. This data includes definition of the:

The building performance model is an organized collection of all the data necessary to define the building assets at risk

- structural systems and elements – in sufficient detail to quantify their location within the building and the demands they will experience during response to earthquake shaking; their vulnerability to damage caused by earthquake-induced deformations and forces; and the consequences of this damage, in terms of generation of life-threatening debris, influence on post-earthquake building occupancy and necessary repair actions.
- nonstructural systems, components and contents– in sufficient detail to quantify their location within the building and the demands they will experience during building earthquake response; their method of installation as it effects their vulnerability to damage; and the consequences of this damage, in terms of generation of life-threatening debris, influence on post-earthquake building occupancy and necessary repair actions.
- Occupancy – including the distribution of people within the building and the variability of this distribution with time of day and day of the year.

The building performance model is subcategorized into three separate groups: population models, fragility groups and performance groups. The subsections below describe each of these following a discussion of the basic building data and occupancy.

3.2 Basic Building Data

The basic building data required for performance assessment includes:

- number of stories, story height, floor areas; and
- total replacement cost, core and shell replacement cost, replacement time and total loss threshold.

l allows use
cost at
ikely to
e building.
suggested a
eplacement
threshold
s.

The total loss threshold is used to set a pre-determined level of repair effort, at which a building is likely to be replaced rather than repaired. Past studies have suggested that many owners elect to replace buildings rather than repair them, when the projected repair exceeds about 40% of replacement cost. Of course many factors, including the building's age, its occupancy, the economic health of its surrounding neighborhood and individual profitability affect these decisions. The Federal Emergency Management Agency uses a threshold of 50% when contemplating whether a damaged structure should be replaced or repaired.

Costs are presently expressed in monetary terms. Future enhancements could include consideration of environmental consequences associated with building replacement including volume of debris generated for placement in landfills; energy associated with building replacement and generation of greenhouse gases.

Figure 3-1 defines the system used to number floors and stories. Building roofs are designated Floor N+1, where "N' is the number of stories. In the figure, Floor 1 has been assigned to the ground floor. If significant damage and loss can occur in basement levels, floor numbering should initiate with the lowest level to be considered.

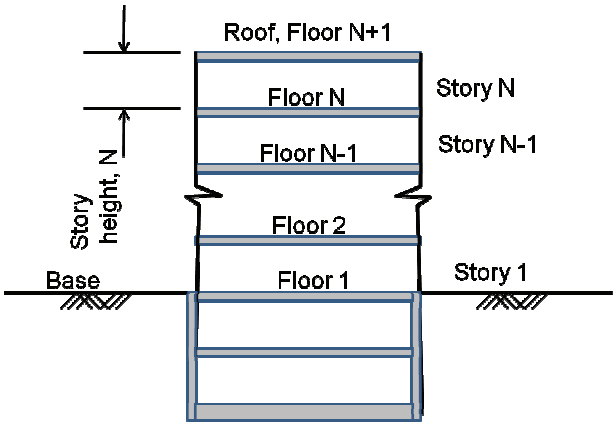

Figure 3-1 Definition of floor and story numbers and story height

orizes the
building or
ling

3.3 Occupancy

As used in this methodology, occupancy categorizes the primary use of a building or portion of a building. There are two primary functions for occupancy:

(1) Establish a population model, i.e., the number of people present, at different times of the day and different days of the year for use in assessing potential casualties and,

(2) Define on an approximate basis, without the need for performing a building-specific inventory, the quantities (termed normative quantities) of nonstructural building components and contents of different types, discussed further in Section 3.5.3.

Note that definition of occupancy is not an essential part of this methodology. If none of the default occupancies apply to a building, it is possible to create building-specific population models and inventories of nonstructural components and inventories. However, use of occupancies greatly facilitates the process of defining building performance models as indicated in the companion Implementation Guide.

Default population models and inventories are provided for the following occupancies:

Standard population and inventory model information is provided for eight occupancies. Users can modify this information or develop their own models.

- Commercial office;
- Education (K-12), with subcategories of Elementary, Middle and High School classroom buildings;
- Healthcare – general hospital;
- Hospitality;
- Multi-unit Residential;
- Research Laboratories;
- Retail (shopping malls); and
- Warehouse.

3.4 Population Models

Building population models define the number of people present per 1,000 square feet of building floor space. This is defined in terms of a peak population, that is, the maximum number of people likely to be present at times of peak occupancy, and the fraction of this peak population that is likely to be present at other times based on:

Population models define the number of people present in the building by occupancy, time of day, day of the week and month of the year

- Time of day;
- Day of the week (weekday or weekend); and
- Month of the year.

The population model also includes an Equivalent Continuous Occupancy (ECO). This is a time weighted average population. It represents the number of persons present, on average, throughout the year. Using the peak population, it is possible to generate a "worst-case" estimate of casualties,

assuming that the shaking occurs during peak occupancy. Using the ECO estimate it is possible to estimate the mean casualties, considering that earthquake occurrence is random in time. Using the point-in-time model of population, it is possible to develop an understanding of the variability in casualties with time of earthquake occurrence. However, it is necessary to perform a large number of realizations to do this in a meaningful way and this can be consume significant processing time.

Table 3-1 presents peak populations for each of the occupancies of Section 3.3. It also indicates the time of day during which these peak populations are expected to occur.

Table 3-1 Recommended Default Peak Population Models

Occupancy Description	Peak Population Model (Occupants per 1000 sq. ft.)	Peak Population Model - Time of Day
Commercial office	4.0	Daytime (3 pm)
Education (K-12): Elementary Schools	14.0	Daytime
Education (K-12): Middle Schools	14.0	Daytime
Education (K-12): High Schools	12.0	Daytime
Healthcare	5.0	Daytime (3 pm)
Hospitality	2.5	Nighttime (3 am)
Multi-unit residential	3.1	Nighttime (3 am)
Research Laboratories	3.0	Daytime (3 pm)
Retail	6.0	Daytime (5 pm)
Warehouse	1.0	Daytime (3 pm)

Population patterns vary with time of day (e.g., hours of operations, lunch time fluctuations), day of week (weekdays vs. weekends), and monthly population variations (e.g., due to building closures for holidays, extended breaks). Figure 3-2 plots the time-dependent variation of population, as a percentage of peak population, for commercial office occupancy. Appendix E contains similar data for the other occupancies shown above.

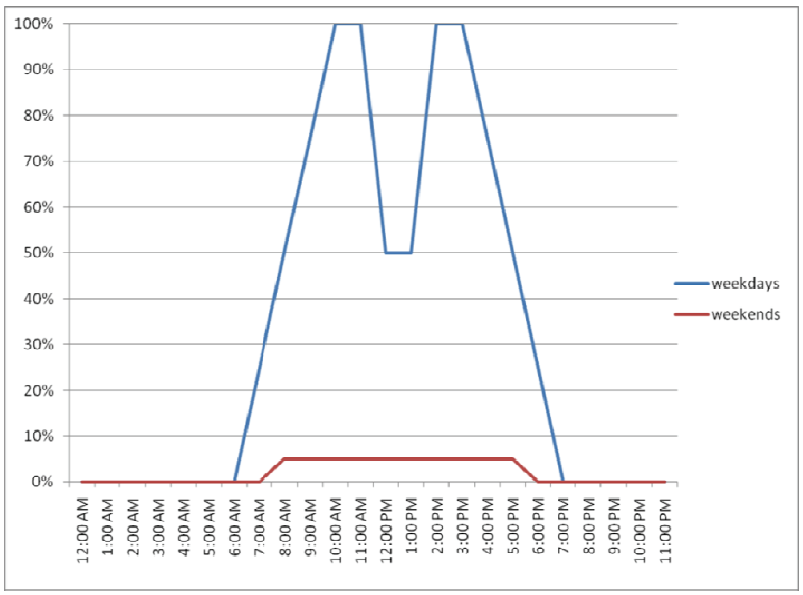

Figure 3-2 Graph illustrating the percent of peak occupancy, by hour and day present, for commercial office occupancy

3.5 Fragility and Performance Groups

All structural and nonstructural components and contents that can be damaged by building response to earthquake shaking are categorized by fragility group and performance group. A fragility group is a collection of similar components or systems, each of which has the same damageability and consequences of damage. Performance groups are a sub-categorization of fragility groups. A performance group is that set of members of a fragility group that are assumed to be subject to the same earthquake demands (e.g., story drift or peak floor acceleration at a particular level and in a particular direction). Section 3.5.1 and Section 3.5.2, respectively provide further discussion of fragility and performance groups.

a collection
nt or
nich has the
y and
mage. A
is that
group
demands

The quantity of nonstructural components and contents in a building and within each performance group can be determined by conducting a building-specific inventory, or default values can be used based on the building's occupancy, or occupancies and size. Section 3.5.3 describes typical quantities (termed normative quantities) for each of the occupancies described above, that can be used to generate the quantity of components in various performance groups.

3.5.1 Fragility Groups

A fragility group is a collection of components, or assemblies, all of which have similar:

- construction characteristics, including details of construction, details of manufacture and installation techniques;
- potential modes of damage;
- probability of incurring these damage modes, when subject to the effects of earthquake shaking; and
- potential consequences resulting from the damage, assuming that the components are installed in the same locations.

A fragility group can comprise individual components (e.g., pendant light fixtures), or assemblies of components (e.g., interior fixed partitions including the metal studs, gypsum board sheathing and wall coverings). Fragility groups are organized depending on whether they are part of the building's core and shell, or part of the building normally associated with individual tenant improvements and contents. Core and shell fragility groups include those associated with the structural systems, exterior cladding, elevators, major mechanical and electrical systems and similar items that are constructed independent of individual tenants' needs. Individual tenant improvements and contents fragility groups include ceilings, interior partitions, mechanical, electrical and plumbing distribution systems, office furnishings, computers and similar items.

Components and assemblies that are of similar, but not identical construction may have to be assigned to different fragility groups, in order to correctly characterize their susceptibility to damage and the consequences of such damage. For example, fixed interior partitions throughout a building could all be assigned to the same fragility group, if they are all of the same height, all installed in the same manner and all have the same wall coverings. However, if some of the interior partitions were installed with slip tracks at their top to permit the walls to move independently of the structure under seismic shaking and some are provided with fixed top connections, each type would have to be assigned to a different fragility group, as each would have different susceptibility to damage under the same earthquake shaking. Similarly, partitions with ceramic tile finish would cost more to repair than walls that are simply painted and should be assigned to different fragility groups.

Appendix D presents standard fragility groups that include many of the typical structural and nonstructural components found in buildings. Users can define additional fragility groups to cover unique situations. The following logic is recommended for establishing fragility groups, when the

default fragility groups provided in Appendix D are not adequate to define the building assets at risk:

1. **Identify the components that are likely to suffer damage and contribute to potential losses.** These are components that both can be damaged and will have significant impact on building performance if they are damaged. Components that are inherently rugged and not subject to significant damage for credible levels of demand need not be considered. For example, in a steel frame building the floor beams that are not part of the building's seismic force resisting system will not typically be damaged by earthquake shaking and generally need not be considered. Also, some nonstructural components (e.g., toilet fixtures) can often be neglected as they are inherently rugged and generally not damaged by earthquake shaking.

   Some components may not be damaged by earthquake shaking, but can be affected by damage or required repairs for other components. For example, a conduit embedded in an interior partition, by itself is inherently rugged. However, if the partition is sufficiently damaged to require complete replacement, it will be necessary to replace the conduit, even though the conduit was not damaged. In this case, the wall, and not the conduit, would be assigned to the fragility group. The fact that the wall contains the conduit, however, is acknowledged as discussed later in determining the consequences of wall damage. Similarly, if a fire sprinkler line breaks, the resulting water spray would damage carpets and furnishing below it that are otherwise rugged. As with the conduit embedded in the wall, it is not be necessary to define fragility groups for the carpet and other rugged items, but rather, to account for their potential damage as part of the consequences of sprinkler system failure.

2. **Group components into logical sets considering normal design and construction process and specification sections**. One logical fragility group for many buildings is interior partitions. These partitions are constructed out of a series of individual subcomponents including cold-formed steel framing, gypsum wallboard, fasteners, drywall tape, plaster, and paint. Since these items have both a design and construction relationship and tend to be damaged as an assembly, they should be included in a common fragility group. Despite the fact that these subcomponents are grouped together as an assembly, it is important to recognize that if the design or construction of one is changed, for example, the manner in which the studs attach to the floors above and below, this change will likely affect the damageability of all these

subcomponents. Similarly, repair of damage for one component is likely to involve others in the group.

3. **Group components into fragility groups such that all components in the group are damaged by a single demand parameter.** In this methodology, the probability that any building component (or collection) of components will be damaged must be tied to a single demand parameter such as peak story drift, peak floor acceleration, peak floor velocity, peak plastic rotation demand or similar quantity. All components within a fragility group must be assumed to be dependent on the same type of demand parameter, for example floor acceleration or story drift, as an indicator of the extent of damage they will experience. It is important to note, however, that not all components within a fragility group need to actually experience the same demands within the building. For example, if the partitions at the third story of a building are of the same type as those in the second story, they can be assigned to the same fragility group even though the demands (story drift) will likely be different in the third story than in the second story.

4. **Group components into fragility groups such that fragilities, damage states and consequence functions are logical for monitoring and repair.** All components placed in a single fragility group should have similar damage states and similar consequences of damage. Interior partitions and exterior cladding should be placed in different fragility groups because the damage states for each will likely be different—they will be damaged at different levels of drift—and the consequences of the damage to interior partitions are different than the consequences of damage to exterior cladding. In this methodology, these damage characteristics are categorized in the form of fragility functions, as discussed in Section 3.8.

Each fragility group is identified by a unique identification code per the National Institute of Standards and Technology Interagency Report (NISTIR) 6389 *Uniformat II Elemental Classification System for Building Specifications, Cost Estimating and Cost Analysis* (NIST, 1999).

This methodology uses the NISTIR Uniformat II classification system to uniquely identify fragility groups

The NISTR classifications take the form of A1234.567. The first letter in the NISTIR classification system indicates the overall category for the fragility and is one of the following:

- A–Substructure
- B–Shell
- C –Interiors

- D–Services
- E – Equipment and furnishings
- F – Special construction and demolition

The first two numbers provides the next categorization. For instance, B10 represents superstructure components while B20 represents exterior enclosures. The next two numbers identify a unique component. For example, the NISTIR classification for reinforced concrete shear walls is B1044. The identifiers after the decimal provide variations of the basic component and are used to identify different configurations, conditions of installation, material quantities, demand levels, and other attributes.

Appendix D contains a listing of standard fragility groups. Users can define new fragility groups or modify data associated with existing fragility groups in order to meet the needs of a specific building.

Table 3-2 lists a sample set of fragility groups that could be used to define the performance model for an example, 2-story, steel frame office building, including their NISTIR Classification per Appendix D, their type (core and shell or tenant improvements and contents), their description and the demand parameter that is predictive of the type of damage each incurs.

Table 3-2 Example Fragility Groups for 2-story Moment-resisting Steel Frame Office Structure

NISTIR Classification	Type	Description	Demand Parameter
B1035.011	Core and Shell	Structural Steel Special Moment Frame	Story drift parallel to frame
B2020.001	Core and Shell	Glazing	Story drift parallel to wall
D3031.000	Core and Shell	Mechanical Equipment	Floor acceleration
D1014.010	Core and Shell	Hydraulic Elevators	Peak ground acceleration
C1011.001	Tenant Improvement and Contents	Interior Partitions	Story drift parallel to wall
C3032.001	Tenant Improvement and Contents	Suspended Ceiling	Floor acceleration
E2022.010	Tenant Improvement and Contents	Bookcases & File Cabinets	Floor acceleration
E2022.020	Tenant Improvement and Contents	Desktop Equipment	Floor acceleration

The fragility groups listed in Table 3-2 are at an elementary level. Within each of these fragility groups there will typically be additional refinement with sub-groups assigned as necessary to identify slight differences in the damageability or consequences for the components in a fragility group. Thus the fragility group D3031.000 “Mechanical Equipment” will have a number of sub-groups including: D3031.011 “Chillers” and D3031.021

"Cooling Towers". Appendix D provides a complete listing of the standard fragility groups.

3.5.2 Performance Groups

ıps are a sub-
fragility
ıance group
ıme
nds

Performance groups are a further sub-categorization of fragility groups. A performance group is that set of fragility group members that are subject to the same earthquake demands (e.g., story drift or peak floor acceleration in a particular direction at a particular floor level). Figure 3-3 illustrates this concept. It depicts a three-story office structure, comprised of concrete frames and concrete shear walls.

As depicted in the figure, the majority of the performance groups are organized by-story (1st through 3rd) and by direction (N-S and E-W) since their predictive demand parameter is story drift parallel to their orientation. For instance, the 1st story N-S shear walls comprise one performance group, while the 2nd story N-S shear walls comprise a different performance group even though they are from the same fragility group: concrete shear walls (NISTR B1044.011). The same performance group approach holds true for the curtain walls and glazing.

The 3rd story contents, however, is a performance group independent of direction since the predictive demand parameter is floor acceleration. Although not shown in the figure, the 1st and 2nd story contents would be associated with their own unique performance groups since the floor accelerations vary by level. The 3rd story contents are also representative of other performance groups whose damage is associated with floor acceleration such as ceiling systems and mechanical equipment.

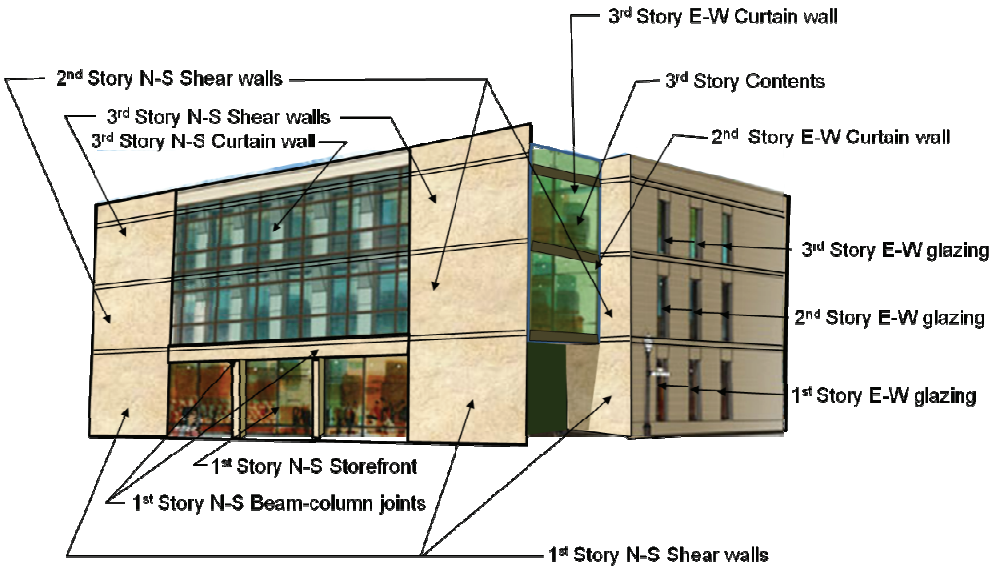

Figure 3-3 Three-story Office Building Performance Group Example

3.5.3 Unit and Normative Quantities

Standard units of measure and normative quantities are associated with typical fragility groups on an occupancy basis, to assist in the development of the building inventory

In order to conduct performance assessments it is necessary to identify the quantities of components in each performance group in meaningful units of measure. This methodology uses units of measure that are amenable to computation of damage in a logical manner that relates to damageability and the consequences of this damage. For example, large distinct components like elevators, air handlers, and beam-column moment connections are measured in individual units (or "each"). However, many other components have other units. For example, shear walls are measured in units of *H*x*H* panels because damage in these walls often can be segregated into panels of this size. Sprinkler piping is measured in units of thousands of linear feet because historically, when leaks have occurred in these systems, a leak rate of 1 per 1,000 feet is common. The units of measure for particular fragility groups are defined in the fragility specification form, described in Section 3.10. A complete listing of the units of measure for all fragility groups is contained in the electronic data base product that is a companion to this Volume.

The quantity of components that is present within a performance group is described by the number of units of measure present. Thus, for an office building, the performance group consisting of interior partitions at the fourth floor in the east-west direction might have 20 – 100-ft-long units, indicating the presence of a total of 2,000 linear feet. Quantities of performance group components in a particular building can be obtained either by performing a building-specific inventory, using drawings or on-site surveys, or by using typical (normative quantities) for given occupancies, factored by building size measures. Buildings can be assigned different occupancies on portions of each floor.

Databases of normative quantities are available that define the quantity of nonstructural components and contents in a building based on building's occupancy, or occupancies. While the quantity of nonstructural components and contents can be established from the building's design drawings (architectural, mechanical, electrical and plumbing), this level detail is not typically known until late in the design process and also is subject to change over the years. Normative quantities provide a reasonable estimate of the quantity of components and contents based solely on occupancy, by-passing the need to perform a detailed quantity take-off. Table 3-3 shows a portion of the normative quantity information for Healthcare Occupancies, which includes estimates for 10^{th}-, 50^{th}- and 90^{th}-percentile quantities. Typically, the 50-percentile values are sufficient for estimating the quantity of nonstructural components for a given occupancy. Where more information is

known about the building occupancy, values between the 10th- and 90th-percentile can be selected and is the primary purpose for their listing.

Appendix F provides a tabulation of similar normative quantities for all eight occupancies included in the methodology.

Table 3-3 Normative Quantities for Healthcare Occupancy

Normative Quantity Type	Unit of Measurement	10-Percentile Quantity	50-Percentile Quantity	90-Percentile Quantity
Cladding				
Windows or Glazing Area	100 SF per 1 gsf	4.0E-04	1.4E-03	3.1E-03
Interior Partition Length	100 LF per 1 gsf	7.5E-04	1.1E-03	1.4E-03
Ceilings				
Ceiling - Lay in tile percentage	%	N/A	80%	N/A
Ceiling - Gypsum board percentage	%	N/A	8%	N/A
Ceiling - Exposed percentage	%	N/A	8%	N/A
Ceiling - Other (high end) percentage	%	N/A	4%	N/A
Elevators	EA per 1 gsf	1.2E-05	2.8E-05	9.8E-05
Plumbing				
Cold Domestic Water Piping - 2 ½ inch diameter or smaller	1,000 LF per 1 gsf	8.0E-05	1.1E-04	1.3E-04
Gas supply piping	1,000 LF per 1 gsf	5.0E-06	1.0E-05	1.5E-05
HVAC				
Chiller capacity	TN per 1 gsf	2.9E-03	3.3E-03	3.7E-03
Boiler capacity	BTU per 1 gsf	40.000	50.000	65.000
Air Handling Units	CFM per 1 gsf	0.800	1.000	1.250
HVAC Ducts – less than 6 sq. feet	1,000 LF per 1 gsf	5.0E-05	7.5E-05	9.0E-05
HVAC in-line Drops & Diffusers	EA per 1 gsf	1.6E-02	2.0E-02	2.2E-02
Piping				
Steam & Chilled Water Piping - 2 ½ inch diameter or smaller	1,000 LF per 1 gsf	0.0E+00	2.0E-05	1.5E-05
Electrical				
Standby generators	KVA per 1 gsf	3.5E-03	5.0E-03	1.5E-02
Fire Protection				
Sprinkler Piping	20 LF per 1 gsf	1.0E-02	1.1E-02	1.3E-02
Sprinkler Drops	EA per 1 gsf	1.0E-02	1.2E-02	1.4E-02

3.6 Damage States

3.6.1 General

This methodology uses discrete damage states to characterize the different levels of damage

Building and component damage generally occurs as a continuum with the scope and extent of damage increasing as demand increases. In this methodology, rather than using a continuous range of possible damage states, each fragility group is assigned a series of discreet damage states to characterize the different levels of damage that can occur. Each damage state is defined by a unique set of consequences consisting of:

- probable repair action, and its likely consequences with regard to cost, repair time, and other consequences;
- potential for "unsafe" placard assignment;
- potential impact on occupancy or on casualties;

or a combination of these.

Not all damage states will have significant impact in all of these types of consequences. Damage states meaningful for one performance measure (e.g., repair action) may not be significant for another performance measure (e.g. casualties). Each damage state represents a unique set of consequences in these performance measures. For example, for a hypothetical exterior cladding component, meaningful damage states could include:

- No damage (and no consequences with regard to repair actions, occupancy or casualties).
- Cracking of sealant joints, permitting moisture and/or air intrusion. Such damage will have no consequences with regard to casualties, safety placard placement or long-lead times. However, over the long term, the damage will present building maintenance issues, and therefore will require repair consisting of replacing sealant joints. This will result in small repair and environmental costs with an associated short repair time.
- Damage consisting of visible cracking of the panels. To repair this unsightly damage, the cladding must be removed from the building and replaced. This damage will likely have more severe cost and environmental consequences and will result in a longer repair time. Casualties, safety placards and or long-lead times are not impacted in this damage state.
- Damage consisting of panel connection failure, and pieces of the cladding falling off the building. This damage will likely have similar repair consequences as that described previously (replacement of the

panels) but will also have potential casualty impacts (when the cladding falls from the building, although this methodology only tracks casualties within the building envelope) and may have severe occupancy impacts as the building might be deemed unsafe for occupancy and placarded as such, until the cladding is repaired.

3.6.2 Damage Logic

This methodology utilizes three types of damage states: sequential, mutually exclusive and simultaneous

Damage states for a fragility group will have a logical inter-relationship. The several possible logical relationships associated with damage states include:

- Damage states that must occur in sequential order, with one state occurring before another are termed *sequential*. Sequential damage states represent a progression of damage from none to higher and higher levels as demand increases. Generally, as the damage state increases, in sequence, more serious consequences accrue. For example, for a concrete component whose behavior is controlled by flexure, the damage states may include: 1) hairline cracking repaired with simple patching and painting; 2) large open cracks requiring injection with epoxy and 3) spalling with buckling of reinforcing steel, requiring replacement of bent or fractured reinforcing bars and crushed concrete.
- For some fragility groups the occurrence of one damage state will preclude the occurrence of other damages states. Such damage states are termed *mutually exclusive*. The implication for repair actions, occupancy and casualties will generally be different among the alternatives. Each mutually exclusive damage state must have a probability of occurrence, given that the component is damaged. For example, the concrete component previously discussed might reach a level of demand at which either (a) the flexural cracks lengthen and widen (80% chance) or (b) the behavior mode transitions to shear with the formation of a more serious crack pattern (20% chance). The probabilities for all mutually exclusive damage states must sum to 100 percent.
- *Simultaneous* damage states are those that can, but need not, coexist with one another. The repair actions, occupancy and casualty consequences for these damage states are generally independent of one another. As with mutually exclusive damage states, each of several simultaneous damage states is assigned a probability of occurrence given that the component is damaged. The sum of the probabilities for all simultaneous damage states will generally exceed 100% as some states will occur at the same time. Elevators are an example of a fragility group with simultaneous damage states. Damage can consist of one or more conditions each with its own independent probability of occurring, given

that the elevator has become damaged (e.g. damaged controls (30%), damaged vane and hoistway switches (20%), damaged entrance and car door (30%), oil leak in hydraulic line (10%). Other states are also possible, but not covered here for brevity.

3.6.3 Correlation

- In addition to definition of damage states as sequential, mutually exclusive or simultaneous, it is also possible to identify performance groups as having correlated or uncorrelated damage. If a performance group is designated as having correlated damage this means that all components within the group will always be in the same damage state. If a performance group is designated as having uncorrelated damage, then each performance group component can have different damage.

Performance groups can be identified as having correlated or uncorrelated damage

- Damage state correlation can be used to indicate the existence of a condition where failure of one element will necessarily require simultaneous failure of all elements within the performance group. An example of this condition would be a series of identical braced frames, all within a single line of resistance in a story. If lateral deformation of the brace line is sufficient to induce buckling in one of the braces in this frame, it is likely that all of the braces will buckle. Similarly, identical braces on separate lines of resistance will likely exhibit uncorrelated behavior as the building deformation along different framing lines will likely be different, resulting in different probabilities of damage on each line.
- From a practical perspective, designation of components within a performance group as having correlated damage results in reduced computation effort in the performance calculation process as for each realization, it is only necessary to identify a single damage state. For uncorrelated damage, it is necessary to determine a unique damage state for each component in the group, greatly increasing computation effort. However, in reality, most building components will not have perfectly correlated damage states. Designation of performance groups as having correlated damage states, when they are not, will not affect the mean performance outcomes, but can significantly affect the computed dispersion.

Specifying correlation significantly reduces computational effort and time but understates the potential dispersion in performance

3.7 Demand Parameters

All of the damage states for components within a fragility group are assumed to be related to a single demand parameter. The demand parameter selected for each fragility group is the one that best predicts the occurrence of the

The two most typical demand parameters used in this methodology are peak transient story drift and peak floor acceleration; other demand parameters can be defined

several damage states with the least amount of uncertainty. For most structural systems (e.g., shear walls, steel braces, steel and concrete moment frames) along with many nonstructural components, peak transient story drift is that demand parameter. The two most typical demand parameters used in this methodology are peak transient story drift and peak floor acceleration.

Other demand parameters can be developed as appropriate for the damage states being defined. For instance, plastic hinge rotation for beams and columns in moment frames could be used. For some nonstructural components, peak floor velocity may be a better indicator of damage than peak floor acceleration. Any single demand parameter can be selected; the one selected should best predict the onset of damage with the least amount of uncertainty. Each fragility group can use only one demand parameter for all of its damage states.

3.8 Component Fragility

3.8.1 Fragility Functions

Component fragility functions are distributions that indicate the conditional probability of incurring a damage state given a value of demand. This methodology assumes lognormal distributions.

The type and extent of damage a component will incur, given that it experiences a particular demand, is uncertain. Component fragility functions are statistical distributions that indicate the conditional probability of incurring a damage state given a value of demand. In this methodology, fragility functions are assumed to be lognormal distributions. A fragility function is required for each sequential damage state, and for each group of mutually exclusive or simultaneous damage states.

Figure 3-4 presents a representative family of fragility curves for a reduced beam section (RBS) special steel moment frame beam-column connection. For this fragility group, three damage states: DS_1, DS_2, and DS_3, are defined:

- DS_1: Beam flange and web local buckling in the beam requiring heat straightening of the buckled region.
- DS_2: Lateral-torsional distortion of the beam in the hinge region requiring partial replacement of the beam flange and web in the hinge region, and corresponding construction work to other structural and nonstructural components.
- DS_3: Low-cycle fatigue fracture of the beam flanges in the hinge region requiring replacement of a large length of beam in the distorted/fractured region, and corresponding construction work to other structural and nonstructural components.

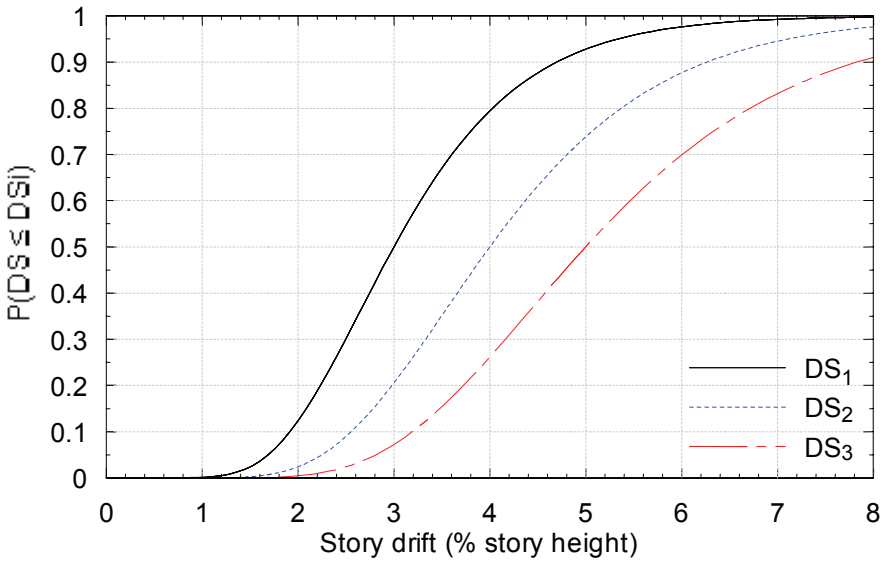

Figure 3-4 Example family of fragility curves for special steel moment frames

The fragility function for each damage state is defined by a median value of demand, θ_{DS}, at which there is a 50% chance that the damage state will initiate, and a dispersion β_{DS} that indicates the uncertainty that damage will initiate at this particular value of demand. If a large number of components are subjected to demand, θ_{DS}, and the performance of these components is uncorrelated, half of the components will have entered the damage state and half will not have. The dispersion, β_{DS}, is a measure of the scatter in demand values at which similar components will enter the damage state.

The dispersion is associated solely with the onset of the damage state as a function of building response (i.e., demand) and is independent of the uncertainty associated with the intensity of shaking or the prediction of demand. As the value of β_{DS} increases the shape of the curve becomes flatter, indicating a wider range of demand values over which there is significant probability for the damage state to initiate. The dispersion reflects variability in construction and material quality, the extent that the occurrence of damage is totally dependent on a single demand parameter, and the relative amount of knowledge or data on the components likely behavior.

For the family of fragility curves presented in Figure 3-3 above, for which medians and dispersion for the three damage states are (3% drift, 0.35) for DS_1, (4% drift, 0.35) forDS_2 and (5% drift ,0.35) for DS_3, the following interpretations are possible:

- At a story drift ratio of 4%, the probability of having some damage is the probability that DS_1 will have occurred, or 80%, since these damage

states are sequential, and DS_1 must occur before any of the other states can.

- At a story drift ratio of 4% the probability of no damage (neither Damage State DS_1, DS_2, nor DS_3have occurred) is 20% (=1.00-0.80), the probability of damage in state DS_1 (assumed to be representative of damage between curves DS_1 and DS_2) is 30% (=0.80-0.50), the probability of damage in state DS_2 is 24% (=0.50-0.26) and the probability of damage in state DS_3 is 26% (=0.26-0).
- For each realization in which building collapse is not predicted, the demands are used together with the component fragility functions for all performance groups in the building to determine the damage state for each component. Taken together, the damage states for all of the components that comprise the building define a building damage state.

3.8.2 Experimentally Derived Fragilities

The component fragilities may be developed by laboratory testing, from earthquake experience data, by analysis, by judgment or by a combination of these.

- Component fragility functions can be developed by laboratory testing, by collecting data on the behavior of similar components in real earthquakes, by analysis, by judgment, and by a combination of these methods. Appendix H presents quantitative procedures for developing fragility functions and a companion publication, FEMA 461 *Interim Testing Protocols for Determining the Seismic Performance Characteristics of Structural and Nonstructural Components* (FEMA, 2007), presents recommended procedures for performance of laboratory tests intended to develop fragility functions.

Appendix H provides detailed procedures for developing the median (θ) and dispersion (β) values for a fragility function for the following five conditions of data:

- Actual Demand Data: When test data is available from a sufficient number of specimens and each tested component actually experienced the damage state of interest at a known value of demand.
- Bounding Demand Data: When test data or earthquake experience data are available from a sufficient number of specimens, but the damage state of interest only occurred in some specimens. For the other specimens, testing was terminated before the damage state occurred or the earthquake did not damage the specimens. The value of the maximum demand to which each specimen was subjected is known for each specimen. This maximum demand need not necessarily be the demand at which the damage state initiated.

- Capable Demand Data: When test data or earthquake experience data are available from a sufficient number of specimens, but the damage state of interest did not occur in any of the specimens. The maximum value of demand that each specimen was subjected to is known.
- Derivation (analysis): When no test data are available, but it is possible to model the behavior and estimate the level of demand at which the damage state of interest will occur.
- Expert Opinion: When no data are available and analysis of the behavior is not feasible, but one or more knowledgeable individuals can offer an opinion as to the level of demand at which damage is likely to occur, based either on experience or judgment.

The fragility functions developed as part of this methodology utilized all five approaches or a combination thereof

3.8.3 Standard Fragilities

Using the procedures of Section 3.8.2 and available test data, numerous fragility functions for common structural and nonstructural components have been developed. Appendix D presents a complete listing of these fragilities. An electronic data base that is a companion to this Volume presents the actual fragility functions. Summaries of the data used to determine these fragility functions can be found in *Background Reports* published as another companion product to this Volume.

Over 600 standard fragilities have been developed as part of this methodology and are included in an electronic data base as a companion to this Volume.

The standard structural facilities cover common structural systems including:

- Moment-resisting steel frames;
- Moment-resisting concrete frames;
- Steel braced frames;
- Concrete shear walls;
- Masonry shear walls;
- Light-framed wood walls;
- Concrete slab-column frames; and
- Ordinary steel beam-column framing.

For many of the systems, fragilities are provided that capture the range from high ductility to ordinary ductility. For example, the overall steel braced frame category includes fragilities for those that:

- conform to AISC 341 requirements for special concentrically braced frames (high ductility)
- conform only to the requirements of AISC 360 (ordinary ductility)
- consist of different structural member sections, including HSS, WF, (high ductility to ordinary ductility)
- consist of gusset plate designs using varying limit state assumptions (high ductility to ordinary ductility)

In addition, variations based on configuration have also been developed. For steel braced frame systems, there are three configurations defined:

1. X-bracing;
2. Single diagonal; and
3. Chevron.

Similar variations are provided for the other structural system fragilities, including providing fragilities for both low- and high-aspect ratio concrete shear walls.

Nonstructural fragilities have been developed to account for the majority of the components that have been identified in the normative quantities for the occupancies described in Section 3.5.3. As with the structural fragilities, variations have been developed to account for configurations and situations that are likely to be encountered in buildings.

3.8.4 Calculated Fragilities

Some component types and damage modes require building-specific calculation of fragility. This methodology includes four separate procedures to calculate fragility parameters.

Some component types and damage modes, for example, anchorage failure of mechanical equipment, require building-specific calculation of the fragility parameters. The procedures below provide estimated fragility parameters for components with failure modes, the onset of which can be predicted using design formulations contained within industry standard design specifications, such as ACI 318 and AISC 360. These procedures can also be used to estimate fragility parameters for components and failure modes for which industry design standards do not provide a capacity, but which nonetheless, can be predicted using a rational calculation-based procedure based on considerations of engineering mechanics. Four separate procedures are presented, based on the type of limit state associated with the damage. These include procedures for:

i. Strength-limited damage states;

ii. Ductility-limited damage states;

iii. Displacement-limited damage states; and

iv. Code-based limit states.

These procedures should be used only when the standard fragilities of Section 3.8.3 are inapplicable and suitable test data for use with the procedures of Section 3.8.2 is unavailable.

Strength-limited Damage States

This procedure is applicable to the calculation of fragility parameters for damages states that occur as a limit to essentially elastic behavior. The procedure initiates by determining the component design strength ϕR_n in accordance with an appropriate industry standard. For ductile behavioral modes, such as flexure, determine the median strength as:

$$\theta_{ductile} = C_q e^{(2.054\beta)} \phi R_n \quad (3\text{-}1)$$

For brittle failure modes determine the median strength as:

$$\theta_{brittle} = C_q e^{(2.81\beta)} \phi R_n \quad (3\text{-}2)$$

where, the dispersion β and coefficient C_q are determined as described below.

Determine the total dispersion, β, as a function of the uncertainty in material strength (β_M), inherent variability in the design equation's ability to predict actual failure demand (β_D), and the uncertainties associated with construction quality (β_C).

Design equations for brittle failure modes have higher inherent uncertainty than do those for ductile failure modes. Material strength variability (β_M) is a function of the material itself. Wood tends to have higher variability than does concrete due to the uncertainty associated with grading procedures and the non-uniformity of individual pieces of wood. Some grades of steel, such as ASTM A992 have relatively low material strength variability, while others, such as A36, may have variability comparable to that of concrete.

The combined uncertainty β is computed from the equation:

$$\beta = \sqrt{\beta_D^2 + \beta_M^2 + \beta_C^2} \quad (3\text{-}3)$$

For ductile failure modes that are well predicted by classical methods of engineering mechanics, such as the yield strength of a prismatic member loaded in flexure, a value of the design uncertainty, β_D, equal to 0.05 is recommended. For ductile failure modes with more complex behavioral characteristics, such as elastic buckling of a bar, a larger value of the design uncertainty, on the order of 0.1, is recommended.

For brittle failure modes, such as tensile failure of a wood post, shear failure of lightly reinforced concrete, and crushing failure of masonry or concrete, a higher design uncertainty value is recommended. This can be attained either by reference to commentary underlying the design standard, or by reference to the fundamental research upon which the design standard is based. Alternatively, a default value for the design uncertainty, β_D, for brittle failure modes may be taken as 0.25.

Recommended values for the material strength uncertainty, β_M, may be obtained from industry data, or lacking this, the values shown in Table 3-4 may be used.

Table 3-4 Default Material Property Dispersions, β_M, for Structural Materials

Material	Condition	Dispersion, β_M
Steel	All grades except A36	0.10
	A36	0.15
Concrete	Ready-mix conforming to ASTM C-94	0.12
	Other – based on cylinder test results	a
Wood	Machine-stress graded	0.12
	Visually graded	0.20
	Ungraded	0.30
Masonry	Engineered concrete or brick masonry conforming to ACI 530.1	0.15
	Other masonry	0.25

For concrete with unknown construction control, compute β as the coefficient of variation obtained from tests on cores removed from the structure. If the coefficient of variation exceeds 0.15, not less than 6 tests should be performed to determine the coefficient of variation

Table 3-5 provides recommended values for the uncertainty associated with construction quality, β_C, based on consideration of the sensitivity of a particular behavioral mode to construction quality and the level of quality control that is provided in construction. For example, the yield strength of a steel bar will be essentially insensitive to the effects of construction quality, other than through the potential variability in cross section dimensions,

regardless of the extent of quality control provided. However, the strength of a post-installed expansion anchor is very sensitive to the quality of installation as reflected by hole size and tightening condition.

Table 3-5 Default Values of Uncertainty, β_C, Associated with Construction Quality

Sensitivity to Construction Quality	Degree of Construction Quality Control		
	Very Good	Average	Low
Low	0	0	0
Moderate	0	.1	.15
High	0	.15	.25

The coefficient, C_q, in equations 3-1 and 3-2 adjusts the value of the median based on the sensitivity of the behavioral mode to construction quality; the extent to which this is included in the resistance factors used to ascertain design strength; and the severity of the potential effects of poor construction quality. The C_q coefficient should be established based on judgment and an understanding of the probable value of the capacity, given poor quality control. The value of C_q will normally be taken as unity. However, in some conditions a lesser value is warranted. For example, a post-installed tension anchor, where it is uncertain whether the anchor has been properly set, a judgmental value taken as the average of that for a proper installation and that of an improper installation can be used.

Ductility-limited Damage States

Some damage states in ductile elements will initiate when inelastic deformation of the element reaches a particular ductility. Without appropriate test data to characterize the ductility at which some damage states occur, estimates of this ductility are, at best, highly uncertain. The following can be used to characterize ductility-limited damage states, when appropriate test data are not available:

1. Calculate the median value and dispersion for the onset of yield of the element, per the procedures for strength-limited damage states described above.

2. Calculate the median deformation of the element, δ_y, at the onset of yield, using elastic deformation analysis under the applied median yield load.

3. Classify the behavioral mode as one of "limited ductility",associated with a μ of 2, "moderate ductility" associated with a μ of 4, or high

ductility associated with a μ of 6, where μ is the ratio of deformation at onset of a damage state to deformation at yield.

4. Calculate the median displacement demand for the onset of the damage states as $\theta = \mu\delta_y$.

5. Calculate the dispersion β for the damage state as:

$$\beta = \sqrt{\beta_1^2 + 0.16} \leq 0.6 \tag{3-4}$$

where β_1 is the dispersion associated with the onset of yield, calculated per the procedures for strength-based damage states described above.

Displacement-limited Damage States

Some damage states are best characterized based on an imposed displacement. An example of this would be an expansion joint at which beams rest upon a bearing seat of limited length, or an attachment for a precast cladding panel, that relies on a slotted connection to accommodate movement. In such situations, the median displacement demand at initiation of failure should be taken as the calculated available length of travel based on the specified travel allowance dimension (for example, slotted hole length, length of bearing seat). The dispersion should be set based on an evaluation of the likelihood that the initial position of the structure is out of tolerance. The normal construction tolerance can be considered to represent one standard deviation on the displacement dimension. The dispersion can be taken as equal to the coefficient of variation calculated approximately as the standard deviation value divided by the median.

Code-based Limit States

In some cases, there may not be sufficient information available to calculate the capacity of a component, for example the anchorage of an equipment item, either because the anchorage itself has not yet been designed, or for an existing installation, the details of the anchorage are not known. In such cases, if the code-based design capacity that the installation should comply with is known, the procedures of this section can be used.

Repair costs include the cost of all construction activities necessary to return the damaged component to their pre-earthquake condition.

1. Compute the assumed design strength (or displacement capacity) of the installation in terms of a convenient demand parameter, such as spectral acceleration, force, or story drift. This presumed code-based capacity is taken as the value of ϕR_n.

2. Decide whether the damage state is a ductile or brittle mode. If it is unknown which of the two is likely, a separate calculation can be performed for each assumption, and the average results used. Regardless, use a value of the coefficient C_q of 0.5.

3. Assign a default dispersion, β, to the behavior, of 0.5.

4. If the mode is considered to be ductile, use equation 3-1 to determine the median value of the demand parameter, θ. If the mode is considered to be nonductile, use equation 3-2 to determine the median value.

3.9 Consequence Functions

Consequence functions are distributions of the likely consequences of a component damage state translated into repair costs, repair time, potential for unsafe placards, casualties and other impacts. For each damage state, fragility definitions include repair descriptions that provide the necessary information to develop the associated repair costs and times. To facilitate casualty estimation, each damage state description also includes a discussion as to whether life safety hazards are associated with the damage, and if they are, the affected area in which life safety hazards will likely occur. Damage state descriptions also include text describing the extent to which the occurrence of the damage is likely to result in an unsafe placard being posted on the building.

Consequence functions for each of these impacts are developed based on these descriptions, using the procedures described below.

Consequence functions are distributions of the likely consequences of component damaged translated into repair costs, repair time and other impacts.

3.9.1 Repair Costs

Repair costs include all the cost of all necessary construction activities to return the damaged components to their pre-earthquake condition. Repair costs do not include work associated with bringing a non-conforming installation or structure into compliance with newer criteria. They assume repair or replacement "in-kind". The repair costs are based on the repair measures outlined for the specific damage state and include all the steps a contractor would implement to conduct the repair including:

- Shore the surrounding structure (if necessary);
- Remove or protect contents adjacent to the damaged area;
- Protect the surrounding area from dust, noise, etc. with a temporary enclosure;

- Remove architectural and MEP systems, as necessary, to obtain access to the repair;
- Procure new materials and transport them to the site;
- Perform the repair;
- Replace architectural and MEP systems, as necessary; and
- Replace contents.

For many repairs, the cost of accessing the damaged area to perform the repair and to protect the surrounding area is greater than the cost of the repair itself.

The access available to conduct repairs will also affect repair costs. It is more difficult, and, hence, more costly, to repair damage on the 10th floor of a building than on the 1st floor. Likewise, the type of occupancy within the damaged area can affect repair costs. Occupancies such as healthcare and research laboratories will likely have access restrictions and will require enhanced protection measures, both of which will increase repair costs. This methodology includes factors, provided on a story-by-story basis, to take such effects into account.

This methodology includes efficiencies of scale in determining repair cost and repair time

Calculation of repair costs also includes consideration of efficiencies of scale in construction operations. When a large quantity of the same type of construction work is necessary, contractor mobilization, demobilization and overhead costs can be spread over a larger volume of work, resulting in reduced unit rates.

For each damage state, repair costs are described with the following parameters (see Figure 3-5):

- *Lower quantity:* the quantity of repair actions of a give type, below which there is no cost discount to reflect efficiency in construction operations
- *Maximum cost:* This is the cost to perform a unit damage state repair, without any efficiency of scale being obtained.
- *Upper quantity:* the quantity of repair work, above which no further efficiencies of scale are attainable
- *Minimum cost:* the minimum cost that can be attained for a unit repair operation, considering all possible efficiencies of scale
- *Dispersion:* the uncertainty associated with the unit cost.

Repair time is limited to the number of labor hours associated with the required repair.

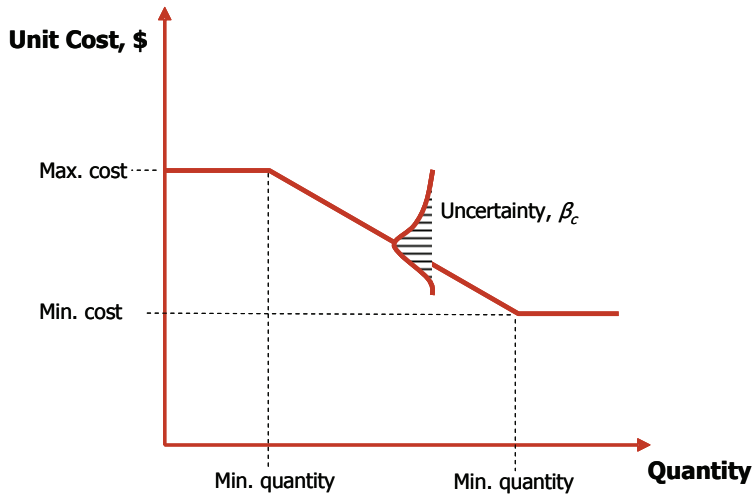

Figure 3-5 Sample consequence function for cost of repair

The distribution of the repair costs is derived from costs that represent the 10th-, 50th- and 90th-percentile estimates. Both lognormal and normal distributions are developed from the repair cost data and the curve with the best fit is used.

Repair cost is computed for a reference standard location in the United States at a reference period of time, neglecting uncertainty in contractor pricing strategies or construction cost escalation. Construction cost indices are used to adjust these standard costs for the building-specific location and to adjust for inflation. These procedures use the RSMeans Construction Cost Index; however, any convenient construction cost index can be used if normalized to the standard location and time.

3.9.2 Repair Time

The actual time that a building will be unusable for beneficial occupancy is very difficult to determine. Factors that can affect this include:

- The party responsible for performing repairs – i.e., the owner or tenants;
- Whether the party responsible for performing repairs has the necessary financial resources to pay for the needed repairs;
- The availability of design professionals to design repair operations and the availability of contractors to perform these operations;
- Whether or not the contractor has free access to the building to conduct the repairs or if the building remains in service and the contractor must limit their activity at any time to small portions of the building; and

- Whether the building has been placarded as "unsafe", and the length of time necessary to convince the building official that it is safe to conduct repair operations within the building.

These uncertainties make estimation of overall occupancy interruption time an intractable problem. Therefore, these procedures provide the following measures of occupancy interruption:

1. The length of time necessary to conduct repairs,
2. The need to procure items with long lead-times, and
3. The probability that the building will be placarded as unsafe for occupancy.

In order to estimate repair time, each damage state includes a time-related consequence function that indicates the number of labor hours associated with the required repair. An important parameter in developing repair time estimates is the number of workers that can occupy the building at the same time. The methodology includes a "maximum worker per square foot" parameter that accounts for this. This number can depend on whether the building is occupied during construction as well as the available labor in the region.

Repair time, like repair cost, can benefit from efficiency of scale when a large quantity of a specific repair action must be undertaken. These effects are described in the fragility specification through the following parameters:

- *Lower quantity:* the minimum quantity of a given repair action, below which there is no time efficiency.
- *Maximum time:* the maximum number of labor hours necessary to implement a repair action without efficiency of scale.
- *Upper quantity:* maximum quantity of a repair action above which there is no further efficiency.
- *Minimum time:* the minimum number of labor hours per unit repair action, considering possible economies of scale.
- *Dispersion:* the uncertainty associated with the labor effort associated with a given repair action.

Similar to repair costs, the distribution for repair time is derived from time allocations that represent the 10^{th}-, 50^{th}- and 90^{th}-percentile estimates. Both lognormal and normal distributions are developed from the repair time data and the curve with the best fit is used in the methodology

Both serial and parallel repair strategies are estimated as part of the methodology. The serial repair strategy assumes that repairs are performed on one floor at a time while parallel assumes that repairs can be done on all floors at the same time. Neither repair time estimate will likely represent the actual schedule used for a particular building; however, the two repair time estimates should bound the probable time required.

Finally, repair time can be greatly affected by long-lead times for procurement of critical equipment and components (e.g., HVAC equipment and elevators). If a damage state requires replacement of a component that is associated with a long-lead time, this is indicated in the fragility specification and is flagged as part of the methodology.

3.9.3 Unsafe Placards

Unsafe placards can be a primary source for damage-related downtime and could have an effect on the actual repair time given the presumed dangerous state of the building. An estimate of the downtime associated with such placards is not included as part of the methodology. However the likelihood of receiving an unsafe placard as a result of damage to a performance group is established. The actual time associated with this can then be estimated on a case-by-case basis and added to the repair time estimate.

Each damage state associated with a fragility group is identified as having a potential to result in an unsafe placard or not. The majority of nonstructural fragilities will not result in an unsafe placard. Although nonstructural damage could be an indicator of potential structural damage, it usually does not, by itself, pose a life safety risk. However, the most severe damage state in nearly all of the structural fragilities will trigger a potential for an unsafe placard since the structure's stability has been compromised sufficient to result in a life safety risk.

This methodology does not include specific downtime estimates associated with unsafe placards; rather the likelihood of such placards for each performance group is established.

For those damage states that are determined to have potential to produce unsafe placards, the median quantity of damage that would trigger such a placard is provided. For example, in damage state 3 for ACI-compliant special moment-resisting frames (NISTIR B1041.001), it is estimated that if 20% for the beam-column joints reach this damage state for a performance group an unsafe placard is likely.

The probability that the building will be receive an unsafe placard is computed by considering the probability that each of the individual performance groups, will result in such a placard, and then, assuming that the potential for receiving an unsafe placard for any performance group is not correlated with that for other performance groups, by computing the total

probability of receiving an unsafe placard, considering all performance groups. This is given by the formula:

$$P(U_T) = \begin{Bmatrix} 1-\left[1-P(U_1)\right]*\left[1-P(U_2)\right]*\cdots*\left[1-P(U_i)\right]* \\ \cdots*\left[1-P(U_n)\right]*\left[1-P(C)\right] \end{Bmatrix} \quad (3\text{-}5)$$

where, $P(U_T)$ is the total probability of receiving an unsafe placard; $P(U_i)$ is the probability of receiving an unsafe placard because of damage to performance group "i"; $P(C)$ is the probability of building collapse and "n" is the total number of performance groups. In the above, $P(U_i)$ is given by:

$$P(U_i) = \frac{k}{N} \quad (3\text{-}6)$$

where, k is the number of realizations in which performance group "i" resulted in an unsafe placard and N is the total number of realizations performed.

3.9.4 Casualties

Building collapse is the principle cause of earthquake casualties; this methodology does, however, estimate casualties associated with falling debris and other component damage.

Although building collapse is the principle cause of earthquake casualties (defined as death and serious injuries), some damage states associated with individual components or assemblies can have potential casualty consequences. These are generally associated with falling debris, for example glazing falling out of its frame and injuring nearby occupants, but can also be associated with the release of hot water, steam or toxic materials.

Casualties caused by building collapse are determined based on the building's collapse modes (See Section 6.5) and the number of estimated occupants.

For individual components, the fragilities include a "flag" indicating whether a life-safety hazard exists for the damage state. If the answer is "yes", then a casualty-affected planar area is estimated along with the probability that individuals within that affected area are likely to incur serious injury or death.

As the name implies, the casualty-affected planar area represents the planar area proximate to a component, where the component's damage could result in casualties. The affected area is typically larger than that occupied by the component to account for the uncertainty in the area where debris, spray or other release may occur. Not all of the occupants within the planar area will become casualties, resulting in the need to identify the percentage of individuals within the area that are likely to be injured. For example, for electronic equipment on wall mount brackets (NISTIR E2022.021), the

casualty-affected area is 16 SF, while the unit itself may only be 5-10 SF, and the percentage for serious injury and death is 10% and 5%, respectively. These statistics are judgmentally determined.

3.10 Fragility Specifications

All of the damage, fragility, and consequence data associated with a fragility group are recorded on a standard fragility specification form. Over 600 fragility specifications have been developed as part of the methodology and are available in an electronic database. Each fragility group is identified by a unique NISTIR classification.

Figure 3-6 illustrates the typical format for fragility specifications. Appendix D contains a compact tabulation of fragilities by NISTIR classification with brief descriptions.

NISTIR Classification	B1049.002a					Line 224
Name	Reinforced concrete flat slabs- columns without shear reinforcing .2<Vg/Vo<.4, no continuity reinf					
Description	Costing is on a per joint basis					
Construction Quality: [1]	ACI 318-56, ACI 318-63, ACI 318-89, ACI 318-95, ACI 318-99, ACI 318-05					
Seismic Installation Conditions:	Not applicable					
Normative Quantity (unit):	Each	Each				
Demand Parameter (unit):	Story Drift	Unit less				
Number of Damage States:	2					
Damage State:	DS1	DS2				
Type of Damage State:	Sequential	Sequential				
DS Hierarchy	Seq(DS1,DS2)					
Descriptions	Yield strain of the slab flexural reinforcement has been exceeded, spalling of concrete may/may not occur, slab exhibits large enough crack widths to allow epoxy injection	Punching occurs, causing significant spalling of concrete. Epoxy injection is no longer expected to be sufficient to restore the required strength and stiffness to the slab and the slab-column connection.				
Illustrations	B1049.001a-DS1-1.JPG	B1049.001a-DS2-1.JPG				
Damage State Probability:	1.00	1.00				
Fragility Parameters						
Median Demand, θ:	0.02	0.035				
Data dispersion, β_d:	0.4	0.4				
Uncertainty, β_u:	0.1	0.1				
Total Dispersion, β:	0.4	0.4				
Correlation (Yes / No)	NO					
Directionality (Yes / No)	NO					
Quality Ratings						
Data Quality	Average					
Data Relevance	Average					
Documentation Quality	Average					
Rationality	Superior					
Consequence Functions						
Repair Description	Prepare work area for epoxy injection, inject epoxy into 40 feet of crack (30 feet top, 10 feet bottom of slab) per 100 square feet of floor panel, replace and repair finishes; replace furnishings, ceilings, mechanical, electrical and plumbing systems.	Shore damaged area in the two stories below. Remove 100 square feet of concrete slab per column, preserving the slab reinforcement; lap splice 30 new 10 foot long rebar with existing rebar; place formwork; recast concrete slab; remove forms, replace and repair finishes; replace furnishings, ceilings, mechanical, electrical, and plumbing systems Cracks wide enough to be grouted are included in the portion of slab to be demolished and recast.				
Long Lead Time (Yes / No)	NO	NO				

Repair Costs:	P_{10}	P_{50}	P_{90}	P_{10}	P_{50}	P_{90}	P_{10}	P_{50}	P_{90}	P_{10}	P_{50}	P_{90}	P_{10}	P_{50}	P_{90}
Repair Cost by Damage State:	1.93E+04	3.62E+04	5.09E+04	3.43E+04	4.95E+04	7.67E+04									
Best fit mean:		3.55E+04			5.06E+04										
Best Fit Distribution:		Normal			LogNormal										
Quantity Plateau (Min Qty, Max Qty)	3.00		10.00	3.00		10.00									
Average Repair Cost (Min Qty, Max Qty)	3.99E+04		3.26E+04	5.45E+04		4.46E+04									
CV or beta (Min Qty, Max Qty)	0.35		0.35	0.32		0.32									
Quantity Unit:		EA			EA										
Repair Time:	P_{10}	P_{50}	P_{90}	P_{10}	P_{50}	P_{90}	P_{10}	P_{50}	P_{90}	P_{10}	P_{50}	P_{90}	P_{10}	P_{50}	P_{90}
Repair Time by Damage State:	4.77E+01	8.95E+01	1.26E+02	8.47E+01	1.22E+02	1.89E+02									
Best fit mean:		8.76E+01			1.25E+02										
Best Fit Distribution:		Normal			LogNormal										
Quantity Plateau (Min Qty, Max Qty)	3.00		10.00	3.00		10.00									
Average Repair Time (Min Qty, Max Qty)	9.85E+01		8.06E+01	1.35E+02		1.10E+02									
CV or beta (Min Qty, Max Qty)	0.35		0.35	0.32		0.32									
Quantity Unit:		EA			EA										
LifeSafety Hazard:															
Potential non-collapse casualties? (Yes / No)		NO			NO										
Casualty-affected Planar Area (sf) per Normative Unit:		Not Applicable			Not Applicable										
Serious Injury (Median, Dispersion)	0%	0.00		0%	0.00										
Death (Median, Dispersion)	0%	0.00		0%	0.00										
Post-event Tagging Flag:		NO			YES										
Red Tag Trigger (Median,	Not	Not													

Figure 3-6 Fragility specification format

Chapter 4
Define Earthquake Hazards

4.1 Introduction

This Chapter presents procedures for characterizing earthquake ground shaking for use in the performance assessment methodology. Procedures presented address development of data for intensity-based, scenario-based and time-based assessments using either the nonlinear response history or simplified analysis methods of Chapter 5.

Building sites can be subject to other seismic hazards that can cause damage and significantly impact performance. These hazards include ground fault rupture, liquefaction, lateral spreading, landslides, and inundation from offsite effects such as dam failure or tsunami. While this methodology could be expanded to address these other hazards it does not do so at this time. As a minimum, engineers using this methodology should conduct a qualitative assessment of the potential impact of these hazards and, if this impact is found significant acknowledge that performance outcomes predicted by this methodology do not include these effects.

This methodology addresses ground shaking. Engineers should perform qualitative assessment of other hazards that could cause damage including ground fault rupture, landslide, liquefaction, lateral spreading and tsunamis.

Earthquake shaking is completely defined by two orthogonal horizontal components and one vertical component. However, there is little evidence to suggest that vertical shaking is a key contributor to damage and loss in most buildings. Therefore these procedures address only horizontal earthquake shaking. Procedures to characterize vertical shaking effects, when deemed significant, are presented in Appendix B, along with background information on characterization of ground shaking hazard that may be useful for some readers.

For intensity-based assessments, ground shaking can be represented by any user-defined acceleration response spectrum. For scenario-based assessments, ground shaking intensity is represented by acceleration response spectra derived for a specific magnitude-distance pair, using attenuation relationships. For time-based assessments, ground shaking intensity is represented by a series of seismic hazard curves and acceleration response spectra derived from these curves associated with selected hazard exceedance probabilities.

For nonlinear response history analysis, the effects of shaking are considered by evaluating earthquake shaking effects simultaneously along each of two

principal orthogonal horizontal building axes. For simplified analysis, shaking is characterized by spectral response accelerations at the first mode period along each axis. For response-history analysis, shaking is characterized as pairs of ground motion histories scaled for compatibility with the response spectrum that represents the desired ground shaking intensity level.

Section 4.2 addresses site conditions and location. Section 4.3 introduces attenuation relationships. Section 4.4 presents procedures for selecting and scaling ground motions for use with nonlinear response-history analysis. Section 4.5 describes the characterization of ground motion demands for use with simplified analysis.

4.2 Building Location and Site Conditions

4.2.1 Seismic Environment and Hazard

Earthquake hazard is defined by the earthquake sources, the propagation of seismic waves to the building location and modifications applicable to the local site conditions.

Earthquake shaking hazards are dependent on site location with respect to causative faults and sources and, regional and site-specific geologic characteristics. Local topographic conditions (e.g., hills, valleys, canyons) can also modify the amplitude, frequency content and duration of earthquake shaking relative to that expected at a flat, level site. Where topographic effects are significant, e.g. on steep escarpments and hills, site response analyses using finite-element and finite-difference methods can be used to characterize these effects. However, this is not necessary for most sites and detailed discussion of this topic is not provided.

4.2.2 Location

Time-based assessments require seismic hazard curves that depict the annual frequency of exceedance of key spectral response parameters. In order to develop hazard curves, the site's exact location (longitude and latitude) must be identified. Latitude and longitude should be defined to a minimum of three decimal places.

For scenario-based assessments, the distance from the building site to the causative fault must be known. For intensity-based assessments, the site location need not be defined.

4.2.3 Local Soil Effects

The properties of site soils must be defined to:

- Select an appropriate shaped spectrum for intensity-based assessments;

- Select an appropriate attenuation relationship for scenario-based assessments; and/or
- Develop the seismic hazard curves and response spectra for time-based assessments,

It is generally sufficient to define the soil conditions within the upper 30 m (100 ft). As a minimum, it will be necessary to have sufficient data to characterize the Site Class in accordance with ASCE-7 so that site coefficients can be assigned. For sites categorized as Site Class E or F, more detailed information will be necessary to permit the necessary site response analysis. This information will generally include the depth, classification and shear wave velocity of materials in the soil column above bedrock.

4.3 Attenuation Relationships

Attenuation relationships are used to derive acceleration response spectra for use in scenario-based assessments, and also form the basis for probabilistic seismic hazard analyses used to develop the hazard curves needed for time-based assessments. Attenuation relationships provide estimated values of ground shaking intensity parameters, such as peak ground acceleration, peak ground velocity and spectral response acceleration at particular structural periods, for user-specified combinations of earthquake magnitude and site-to-source distance (e.g., $M_W 7$ from a source 13 km from the building site).

Attenuation relationships provide estimates of spectral response accelerations for specified earthquake magnitude and site to source distance based on statistical analysis of past strong ground motion recordings.

Attenuation relationships are derived by performing regression analyses of the values of intensity parameters obtained from strong motion recordings of past earthquakes against distance, magnitude and other parameters. Horizontal ground shaking is a vector quantity that varies in orientation and amplitude throughout an earthquake's duration. Strong motion recordings used to develop attenuation relationships are typically obtained from pairs of instruments arranged to capture orthogonal components of motion. At any instant of time, each component of recorded motion will have different amplitude and neither may be the maximum. Most attenuation relationships now provide geometric mean (geomean) spectral response accelerations, $S_{gm}(T)$ which represents the quantity:

$$S_{gm}(T) = \sqrt{S_x(T) \bullet S_y(T)} \qquad (4\text{-}1)$$

where $S_x(T)$ and $S_y(T)$ are orthogonal components of spectral response acceleration at period T. The X and Y directions may represent the actual recorded orientations, or may represent a rotated axis orientation. Some attenuation relationships rotate the motion to capture fault-normal and fault-parallel orientations, while others use an arbitrary rotation intended to

capture a maximum orientation. The geomean approximately represents a statistical mean response, with actual shaking response in any direction as likely to be higher as it is lower than the geomean. Maximum response acceleration can be as much as 130% or more of the geomean while the minimum response acceleration can be as little as 80% or less than the geomean. The direction of actual peak response is random and varies with period.

Scenario assessments can be used to assess the effects of a repeat of a historic earthquake or to explore the effects of a maximum-magnitude event on a nearby fault. The US Geological Survey posts information on best-estimate maximum magnitudes for active faults in the Western United States and the Inner Mountain seismic region at http://earthquake.usgs.gov/hazards/qfaults/.

If the building site is within 15 km of the presumed zone of fault rupture and the selected earthquake magnitude is M_W 6.5 or greater, fault directivity effects should be considered. Fault directivity characterizes whether the progression of rupture along the fault is towards the site or away from the site and can have substantial effect on the amplitude and period content of shaking. Directivity should be specified as: forward directivity (rupture progresses towards the site); reverse directivity (rupture progresses away from the site); null directivity; or unspecified directivity (random direction of rupture progression). Appendix B provides guidance on fault-rupture directivity and how to include it in hazard calculations.

At sites located within the forward directivity zone, and within a few kilometers of the rupture zone of large magnitude (M_w 6.5 or greater) strike-slip faulting, shaking in the fault normal direction often exhibits significant velocity pulses as well as significantly larger amplitude than does shaking in the fault parallel direction. This effect is known as directionality. Assessments on sites within a few (less than 5 kilometers) of strike slip faults should account for these effects.

Although some attenuation relationships are quite complex, the base form of many attenuation relationships is:

$$\ln Y = c_1 + c_2 M - c_3 \ln R - c_4 R + \gamma \qquad (4\text{-}2)$$

where Y is the median value of the strong-motion parameter of interest (e.g., spectral acceleration at a particular period), M is the earthquake magnitude, R is the source-to-site distance, and γ is a standard error term. Typical attenuation relationships are more complicated than the basic equation given above. Additional terms can be used to account for other effects including

near-source directivity, faulting mechanism (strike slip, reverse and normal), site conditions (different relationships), and hanging wall/footwall location of the site.

Although many attenuation relationships have been developed, most apply to only a specific geographic region, based on the data set of ground motion records used to develop the relationships. It is important to ensure that the selected attenuation relationship is appropriate to the particular building site and earthquake source.

Appendix B presents selected North American attenuation relationships. The Open Seismic Hazard Analysis website, http://www.opensha.org/, provides an attenuation relationship plotter (under the dialog box Applications). The plotter can be downloaded from the website and used to generate median spectra and dispersions for the listed relationships including the three Next Generation Attenuation relationships (Boore and Atkinson, B_A; Campbell and Bozorgnia, C_B; Chiou and Youngs, C_Y) used by the USGS to produce the national seismic hazard maps referenced by ASCE 7-10.

For a particular earthquake scenario and site, different attenuation relationships can provide significantly different estimates of the probable values of spectral response acceleration. These differences result from differences in the data set of records used to develop each relationship and differences in the functional form of the relationships. Figure 4-1 illustrates these differences by presenting the value of 0.2-second spectral response acceleration derived using three different relationships for an M_w 7.25 event and an M_w 5.0 event over site to source distances ranging from 1 km to 100 km. This variation between attenuation relationships is one source of uncertainty associated with ascertaining ground motion intensity for a scenario.

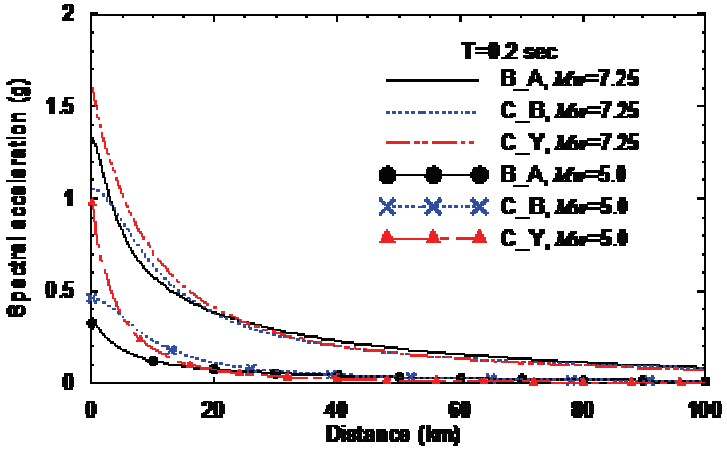

Figure 4-1 Illustration of the relative differences between several attenuation relationships.

Some attenuation relationships use shear-wave velocity in the upper 30 *m* of soil as an input variable while others are applicable only for particular reference shear wave velocities (e.g., 760 *m/sec*). If the selected attenuation relationship has an input variable for shear wave velocity in the upper 30 *m*, the site-specific value should be used for seismic hazard calculations.

If the selected attenuation relationship uses a generic description of the reference soil type (e.g., soft rock) and reports the reference shear wave velocity, spectra so calculated should be adjusted for the site-specific shear wave velocity in the upper 30 *m* of the soil column using either site-response analysis tools or site class factors such as those used in ASCE-7 and other references.

Attenuation relationships can be used to develop an acceleration response spectrum for a site by repeating the attenuation calculations for many values of period across the period range of interest (typically 0.01 to 5 second). In addition to uncertainties associated with the differences in response accelerations derived from different attenuation relationships, each attenuation relationship itself includes a measure of uncertainty associated with the lack of perfect fit between the values predicted by the attenuation relationship and the measured values of acceleration upon which they were based. Many attenuation relationships permit derivation of response acceleration values associated with different probabilities of exceedance. Figure 4-2 illustrates this by indicating response spectra associated with different probabilities of exceedance, all derived from a single attenuation relationships for an M 7.25 earthquake

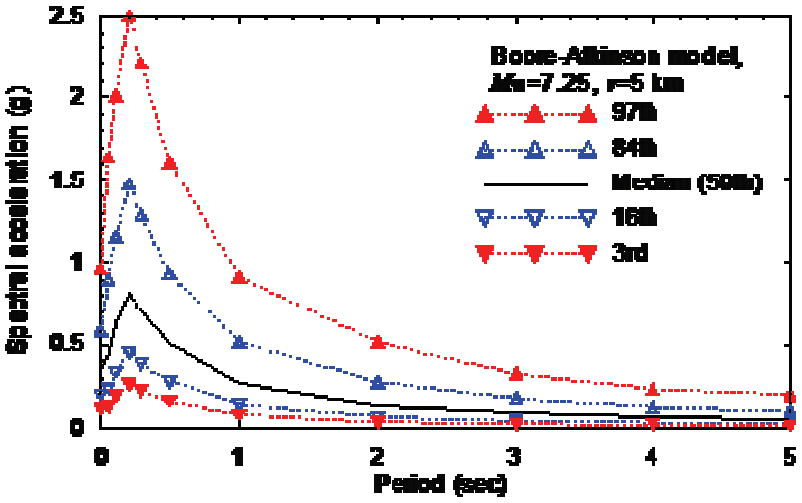

Figure 4-2 Response spectra with different probabilities of exceedance derived from a single attenuation relationship for a earthquake scenario.

4.4 Nonlinear Response-History Analysis

4.4.1 Introduction

This section describes recommended procedures for selecting and scaling acceleration histories for use with nonlinear response history analysis. The basic procedure consists of:

1. development of an appropriate target acceleration response spectrum;
2. selection of an appropriate suite of earthquake ground motions; and
3. scaling of the motions for compatibility with the target spectrum.

The basic procedures includes: 1) development of appropriate target response spectra; 2) selection of a suite of ground motions; and 3) scaling that suite for compatibility with the spectrum.

The procedures presented in this Section are applicable to intensity-based, scenario-based and time-based assessments. Appendix B, Section B.7 presents an alternate procedure to develop ground motion pairs for use with scenario-based assessments, wherein the dispersion in ground motion is considered explicitly.

4.4.2 Target Acceleration Response Spectra

The procedure for developing an appropriate spectrum depends on the type of assessment:

- For intensity-based assessments any spectrum of the user's choice can be used. The spectral shape should be consistent with the site's geologic characteristics.
- For scenario-based assessments, the target spectrum should be derived directly from appropriate attenuation relationships as described in Section 4.3.
- For time-based assessments, one spectrum is required for each of the several seismic hazard intervals, selected from the seismic hazard curve for the site (see Section 2.5.5). Either Uniform Hazard Spectra or Conditional Mean Spectra can be used. For frequent events (high annual frequency of exceedance), the Uniform Hazard and Conditional Mean spectra are similar. For low-probability events, the use of conditional mean spectra improves the estimate of median drift response and results in lower dispersion. Appendix B provides information on the development of Uniform Hazard and Conditional Mean Spectra.

4.4.3 Scaling Parameters

The building's primary orthogonal horizontal axes are respectively denoted X and Y. If the building has identifiable modes associated primarily with translational response aligned approximately with these axes, the

corresponding fundamental translational periods associated with each axis are denoted T_1^X and T_1^Y. $\overline{T}_1$ is taken as the average of T_1^X and T_1^Y.

For buildings with individual translational response modes in each of the *X* and *Y* axes, T_{max} is taken as twice the larger of the building's fundamental translational periods T_1^X and T_1^Y. T_{min} should typically be taken as the smaller of $(0.2T_1^X, 0.2T_1^Y)$.

For buildings without identifiable response modes in each of the X and Y axes, $\overline{T}_1$ is taken as the period of the fundamental mode T_1, T_{max} should be taken as twice the fundamental period T_1 for the building and T_{min} as $0.2T_1$. If substantial response and damage can occur due to response in modes having periods smaller than T_{min} (e.g., in high-rise buildings where multiple higher modes may contribute significantly to the acceleration and drift response) T_{min} should be selected sufficiently small to capture these important response modes.

4.4.4 Ground Motion Selection and Scaling

Select records with spectral shape similar to that of the target spectrum. Where good fit is obtained, as few as 3 pairs of motions may be adequate. When poorer fit is obtained, as many as 11 pairs may be needed.

The intent of ground motion selection is to derive a set of motions that when used with nonlinear response history analysis will produce unbiased estimates of median structural response. Limited study suggests that when good fit between the shape of the selected motions and target spectrum is obtained, as few as three records can provide reasonable prediction of median response. When there is significant scatter in spectral shape of the selected records or poor fit to the target spectrum, as many as eleven pairs of motions may be needed to produce reasonable estimates of median response. To the extent possible, select pairs of earthquake ground motions that have spectral shape similar to that of the target spectrum over the range of periods T_{min}, T_{max}. Additional factors to consider include selecting records having faulting mechanism, earthquake magnitude, site-to-source distance and local geology that are similar to those that dominate the seismic hazard at the particular intensity level; however, these are not as significant as the overall spectral shape. Ground motions are available from a number of sources, including www.peer.berkeley.edu and www.cosmos-eq.org.

Intensity-Based Assessment

Earthquake intensity is defined by a user-specified 5%-damped, elastic acceleration response spectrum, representing the geomean spectrum of the two horizontal components. The following process should be used:

1. Select or construct a target response spectrum.

2. Select a candidate suite of ground motion pairs from available data sets of recorded motions.
3. For each ground motion pair, construct the geomean spectrum for the pair, using equation 4-1 over a range of periods T_{min}, T_{max}. Compare the geomean shape with that of the target. Select ground motion pairs with geomean spectra that are similar in shape to the target response spectrum of Step 1 within the period range of $T_{\min}$ to $T_{\max}$. Discard motion pairs that do not fit the shape of the target spectrum adequately. Where good fit is obtained over the period range T_{min}, T_{max} as few as three records may be used for analysis. Where fit is poor, a significantly larger suite may be required. Typically, not more than 11 pairs of motions will be needed to predict the median response with sufficient accuracy.
4. Amplitude-scale both components of each ground motion pair by the ratio of $S_a(\overline{T})$ obtained from the target spectrum of Step 1 over the geometric mean $S_a(\overline{T})$ of the two records components for the pair.

Scenario-Based Assessments

Earthquake intensity is defined by probabilistic distributions in spectral demand for the specified magnitude-distance combination. Ground motion intensity is assumed to be lognormally distributed with median value, θ, and dispersion, β. In this procedure, dispersion is not directly considered because it is addressed indirectly in the procedures for response calculation (Chapter 5). Instead, the intent is to select motions that will produce median estimates of response. Appendix B, Section B.7 presents an alternate procedure for selection of motions that explicitly considers ground motion dispersion.

Ground motions are selected and scaled using the following steps:

1. Select the magnitude and site-to-source distance for the scenario event.
2. Select an appropriate attenuation relationship(s) for the region, site soil type and source characteristics.
3. Establish the period range ($T_{\max}$, $T_{\min}$).
4. Construct a median spectrum in the period range ($T_{\max}$, $T_{\min}$) using the attenuation relationship(s) of Step 2.
5. Select and scale suites of *n* ground motion pairs per Steps 2 through 4 of Section 4.4.4.1 (intensity-based assessment).

Time-Based Assessments

Time-based performance assessments utilize seismic hazard curves for spectral acceleration $S_a(\overline{T})$ and suites of ground motion pairs selected and scaled to match spectra derived from the seismic hazard curves over a range of exceedance probabilities. The hazard curve includes an explicit consideration of ground motion uncertainty. Appendix B provides summary information on the inclusion of uncertainty in seismic hazard analysis.

Step 1 – Select Intensity Range

The procedure initiates with selection of a range of ground motion exceedance probabilities and corresponding spectral response accelerations $S_a(\overline{T})$. The range should include intensities that produce building response that causes negligible damage to complete loss. For new buildings, designed to conform to a recent edition of ASCE 7 an acceptable range is:

- Minimum $S_a(\overline{T}) = S_a^{\min} = 0.05\ g$ for $\overline{T} \le 1$ second and $0.05 / \overline{T}\ g$ otherwise
- Maximum $S_a(\overline{T}) = S_a^{\max}$ = two times the spectral acceleration for an annual frequency of exceedance = 0.0004 (4×10^{-4}). $S_a^{\max}$ need not exceed the median collapse capacity $\hat{S}_a(\overline{T})$ per Chapter 6

where $\overline{T}$ is the effective fundamental period of the building, as defined in Section 4.4.3.

Older, non-ductile buildings are much more likely to experience damage at low levels of shaking and to collapse at moderate levels of shaking than modern code-compliant buildings. For such buildings, the range of spectral accelerations suggested above should be modified. Specifically the upper limit should be adjusted so that no more than 2 of the intensities of shaking described below trigger collapse. The lower bound limit on spectral acceleration should be selected such that it does not result in damage to either structural or nonstructural components.

Step 2 – Select Analysis Intensities

Structural analysis will be performed at a series of intensities spanning the range of intensities selected in Step 1. To identify the analysis intensities, perform the following steps:

1. Develop a seismic hazard curve for $S_a(\overline{T})$.
2. Compute the spectral accelerations $S_a^{\min}$ and $S_a^{\max}$ per Step 1 above.
3. Split the range of spectral acceleration, $S_a^{\min}$ to $S_a^{\max}$ *g*, into *m* (suggested m = 8) intervals; identify the midpoint spectral acceleration in each

interval and the corresponding mean annual frequency of exceedance (Refer to Figure 4-3).

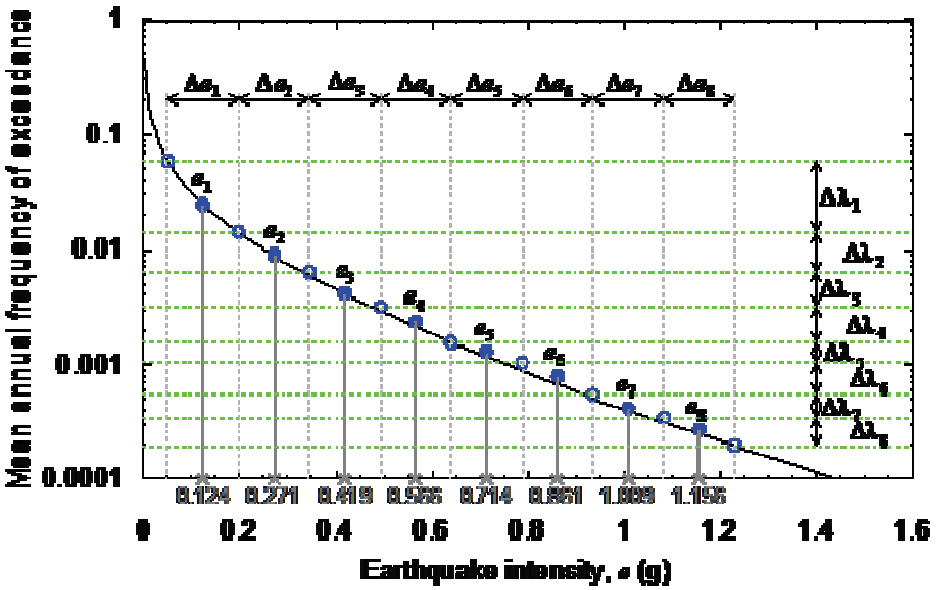

Figure 4-3 Example hazard curve showing selection, intensity intervals, midpoints and corresponding mean annual frequencies of exceedance.

4. Calculate the mean annual frequency of spectral demand in each interval $\Delta\lambda_i$ from the hazard curve and record these frequencies

5. Develop a target spectrum (either uniform hazard or conditional mean spectrum) for the mean annual frequency of exceedance of each midpoint spectral acceleration. Appendix B provides information on these spectral types.

6. For *each* target spectrum, select and scale suites of *n* ground motion pairs per Steps 2 through 4 of Section 4.4.4.1 (intensity-based assessment).

4.5 Hazard Characterization for Use with Simplified Analysis

4.5.1 Introduction

Use the procedures below to characterize earthquake hazards for use with simplified analysis.

4.5.2 Intensity-Based Assessment

Earthquake intensity is defined by any, user-defined 5%-damped, elastic horizontal acceleration response spectrum. Simplified analysis uses the spectral response accelerations at the fundamental period of translational

response in each of two orthogonal directions, T_1^X and T_1^Y, derived from that spectrum.

4.5.3 Scenario-Based Assessment

Characterize earthquake hazard with the following steps:

1. Select the magnitude and site to source distance for the scenario event.
2. Select an appropriate attenuation relationship for the region, site and source characteristics.
3. Determine the median values of the spectral response acceleration at the periods of the first translational mode along each axis of the building, T_1^X and T_1^Y.

4.5.4 Time-Based Assessment

Time-based assessment makes use of site-specific seismic hazard curves. Divide the hazard curve into *m* intervals (8 is recommended – See Section 4.4.4.3) of spectral acceleration, $S_a(\overline{T})$, where $\overline{T}$ is the average of the period of fundamental translation response in each of the building's two orthogonal response directions. The *m* intervals of spectral acceleration should span the range of interest from shaking that causes no damage to complete loss. Refer to Section 4.4.4.3 for guidance no selection of an acceptable range.

Characterization of the earthquake hazard involves the following steps (see Section 4.4.4.3 for additional explanation):

1. Develop a seismic hazard curve at $\overline{T}$.
2. Compute the spectral accelerations $S_a^{\min}$ and $S_a^{\max}$.
3. Split the range of spectral acceleration, $S_a^{\min}$ to $S_a^{\max}$ g, into *m* intervals; identify the midpoint spectral acceleration in each interval and the corresponding mean annual frequency of exceedance, λ, at each end.
4. Calculate the mean annual frequency of spectral demand in each interval $\Delta\lambda_i$ (see Figure 4-3) from the hazard curve and record these frequencies
5. Develop a uniform hazard spectrum for each mean annual frequency of exceedance of Step 3.
6. For *each* of the *m* uniform hazard spectra, determine the values of the spectral response acceleration at the periods of the first translational mode along each axis of the building, T_1^X and T_1^Y.

Chapter 5
Analyze Building Response

5.1 Scope

Structural analysis is used to evaluate building response to earthquake shaking and produce median estimates of key structural response parameters that are predictive of structural and nonstructural damage including peak floor accelerations and velocities, peak story drifts and transient drift. This chapter presents two alternative structural analysis procedures that can be used for this purpose and to estimate dispersion in structural response. These procedures are not suitable for evaluation of building collapse. The procedures of Chapter 6 should be used for that purpose.

Structural analysis provides estimates of median values of key structural response parameters that are predictive of damage including peak floor acceleration, peak story drift and transient drift.

Section 5.2 presents guidelines for using nonlinear response-history analysis to predict median response and dispersion. Section 5.3 describes a simplified procedure to predict median response and dispersion based on elastic static analysis and knowledge of the structure's yield strength. Section 5.4 presents equations for calculating residual drift, based on the results of either nonlinear response-history analysis or simplified analysis.

5.2 Nonlinear Response-History Analysis

5.2.1 Introduction

The procedures of this section are appropriate for calculating median estimates of story drift, floor acceleration, and deformations and forces in structural components.

Buildings should be modeled, analyzed and assessed as a three-dimensional assembly of components, including foundation and soil-structure interaction effects as appropriate. All structural framing and nonstructural components that contribute significant stiffness and/or strength should be explicitly included in the analytical model. Although a complete treatment of the subject is beyond the scope of this report, Subsection 5.2.2 provides limited guidance on mathematical modeling of structural and nonstructural components. Further guidance on nonlinear modeling considerations can be found in NEHRP Seismic Design Technical Brief #4, *Nonlinear Structural Analysis For Seismic Design* (Deierlein et al., 2010), and PEER/ATC 72-1, *Interim Guidelines on Modeling and Acceptance Criteria for Seismic Design and Analysis of Tall Buildings* (ATC, 2010). Subsection 5.2.3 describes

recommended procedures to characterize uncertainties in the calculated demand parameters.

5.2.2 Modeling

General

Models should include all elements that provide measurable resistance to lateral displacement. Models should use nonlinear representation of components, unless it can be demonstrated they will remain elastic.

Nonlinear representation of force-deformation behavior should typically be used for all modeled components. Elastic component representations can be substituted for nonlinear component models only if elastic response is confirmed for the shaking intensities analyzed. Components can be modeled using a variety of techniques, ranging from frame elements with concentrated springs or hinges through to detailed finite element type models. Whatever type model is used, it should be verified against test data and/or appropriate idealized backbone response curves, such as those in ASCE 41 (2006) and PEER/ATC 72-1 (ATC 2010). Strength and stiffness degradation in all components and elements should be considered to the extent they are expected to significantly influence the structural response for the ground motion intensities considered.

The goal of analysis is to predict the central tendency of the building's response and that of its components to earthquake shaking. If the probability distributions of the model parameters (e.g., initial stiffness, Q_y, or Δ_p in the force-deformation relationship of Figure 5-1) are known, each parameter should be defined using its median value. However, mean (expected) values are more commonly available than median values and are considered reasonable to estimate the central tendency where insufficient information is available to accurately characterize the distribution.

Component force--deformation relationships

Element and component models will often be enveloped by force-displacement relationships like those shown in Figure 5-1, with a single force parameter (axial, shear or moment), Q, compared to a characteristic displacement (or rotation) parameter, Δ. For convenience, the curves shown in the figure are idealized as piecewise linear plots, but actual behavior is typically curvilinear. Regardless, the discrete characteristic strength and deformation quantities shown in the figure are useful indices to either calibrate or validate component models.

Hysteretic models should be benchmarked against cyclic laboratory test data or be referenced to standard industry approaches

Such component backbone relationships are generally distinguished between envelopes of response under monotonic or cyclic loading. Cyclic envelopes are not unique and depend on the cyclic loading protocol used in testing of the component. The force-deformation behavior is typically characterized by an initial stiffness, yield strength, peak strength, plastic deformations to the

peak and ultimate points, and a residual strength. As shown, the deformation capacities, peak and residual strengths typically degrade with cyclic loading.

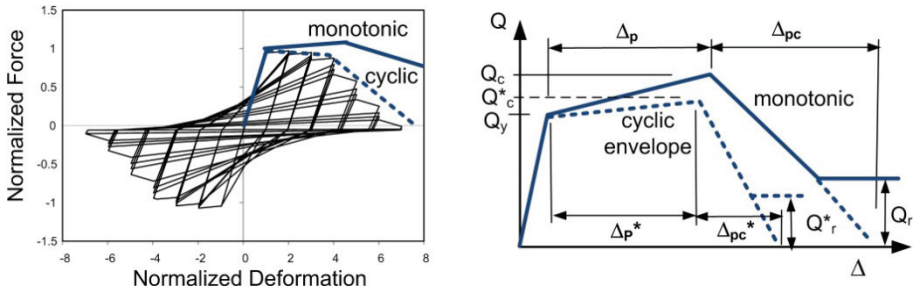

Figure 5-1 Generalized component force-deformation behaviors

Many force-deformation relationships used for seismic assessments, such as those presented in ASCE 41 (ASCE, 2006), and reproduced in Figure 5-2, are defined based on a cyclic envelope curve so as to approximately capture cyclic effects that are not modeled directly in the analysis. Ideally, the cyclic envelope should be based on tests conducted using a standard loading protocol, such as given by ATC-24 (ATC, 1992), which represents the loading demands of a characteristic earthquake. Referring to Figure 5-2, the "a", "b" and "c" parameters of the nonlinear force-deformation relationships of ASCE 41 are comparable to the Δ_p^*, Δ_{pc}^* and Q_r^* parameters of Figure 5-1.

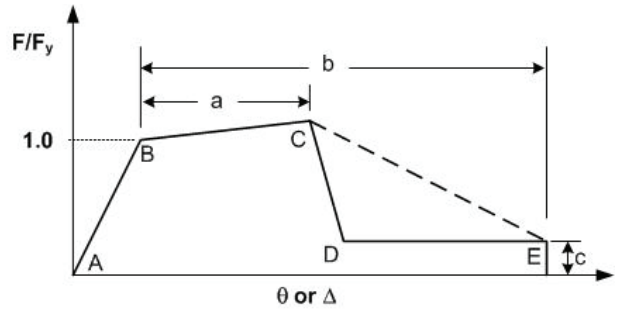

Figure 5-2 Generalized force-deformation relationship of ASCE 41

For nonlinear dynamic analysis, the choice of backbone curve (monotonic or cyclic) will depend on whether the analysis model is capable of directly simulating the degradation of the backbone curve. Direct modeling of cyclic degradation begins with a monotonic backbone curve and degrades this relationship as the analysis proceeds, specifically in accordance with the load path that is imposed on the component. Indirect modeling of cyclic degradation does not adjust the component backbone curve based on the load path, but instead, uses the cyclic envelope to define the component backbone in analysis. While it is desirable to employ direct modeling, relatively few commercial analysis software codes employ elements capable of this and therefore, indirect modeling must often be used.

Component models should account for cyclic and in-cycle strength degradation, either explicitly or implicitly

In general, the envelope of component response described by the backbone curve has a more significant effect on response than the characteristics of the cyclic loading (such as pinching behavior) between the peak excursions. As shown in Figure 5-3, cyclic degradation is often differentiated between "cyclic" and "in-cycle" degradation. Cyclic degradation is associated with the decrease in stiffness and yield strength that occurs between subsequent cycles, whereas "in-cycle" degradation occurs during a loading excursion within a cycle. Studies have shown that in-cycle degradation has a more significant effect on response, especially at large deformations beyond the peak strength (ATC, 1996; FEMA 2005) than does "cyclic" degradation. The differences between the two are less significant for ductile components where the imposed deformations do not exceed the peak strength (less than Δ_p or Δ_p* in Figure 5-1). Further details on modeling degradation and its effects on behavior are provided in PEER/ATC 72-1 (ATC, 2010), NEHRP Technical Brief #4 (Deierlein et al., 2010), FEMA 440 (FEMA, 2005), and Ibarra et al. (2005).

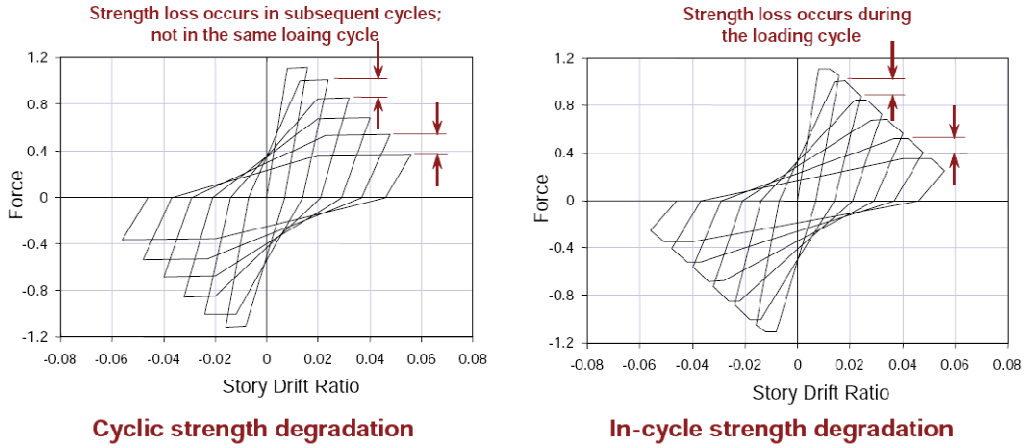

Figure 5-3 Cyclic versus in-cycle degradation of component response

Geometric Nonlinear Effects

The destabilizing effects of gravity loads acting on the deformed geometry of the structure, so-called P-Δ effects, should be accounted for in nonlinear analysis, even where elastic design provisions would otherwise allow them to be neglected, since P-Δ effects can significantly increase displacements and internal member forces in the post-yield region of response.

Gravity Loads

The gravity loads incorporated in the analysis should be based on the seismic mass that is stabilized by the lateral force resisting system and based on the expected dead and live loads. For seismic analysis of overall building

response, it is usually appropriate to include about 25% of the specified design live load.

Damping

In nonlinear dynamic analyses, most of the energy dissipation is modeled directly through hysteretic response of the structural components. Therefore, equivalent viscous damping assigned to the dynamic analysis model should be limited to that which represents the energy dissipation that is not otherwise captured in the analysis model. Generally, this includes energy dissipation in (1) components that are modeled as elastic but where limited cracking or yielding occurs; (2) architectural cladding, partitions and finishes, that are not modeled; and (3) foundations and the soil (if the soil-structure interaction effects are not modeled). The equivalent viscous damping should typically be assigned in the range of 1% to 5% of critical damping in the predominant vibration modes of the building. Values of 3% or less are recommended for tall buildings and other structures where the damping effect of foundations and nonstructural cladding is small relative to the structural characteristics. PEER/ATC 72-1 (ATC, 2010) provides further guidance on modeling of damping.

Most energy dissipation should be explicitly modeled. Equivalent viscous damping to account for components that are not modeled should typically be limited to 5% or less. In tall buildings, equivalent viscous damping should be limited to 3% or less.

Where energy dissipation components (dampers) are installed in a structural system, these components should be modeled explicitly using appropriate component models, including velocity terms to capture viscous effects and/or nonlinear springs to capture hysteretic effects.

Floor diaphragms

Floor diaphragms should be modeled using appropriate stiffness assumptions. A diaphragm can be classified as rigid if the maximum lateral deformation of the diaphragm is less than one half of the average story drift above and below the subject diaphragm. Diaphragms that do not meet this criterion and diaphragms where significant shear transfer between vertical lines of resistance will occur, such as at out-of-plane offset discontinuities, should not be considered rigid and should be modeled explicitly using finite elements. Mass should be distributed across the footprint of diaphragms to capture torsional and in-plane response. If diaphragms are incapable or remaining elastic at the response levels investigated, nonlinear representation should be used.

Foundation rocking and sliding should be modeled, where this will occur. Soil-foundation-structure interaction should be modeled for structures on soft sites, that are deeply embedded, have large footprints and short fundamental periods.

Soil-foundation-structure interaction

Foundations likely to uplift or slide at the ground shaking intensities of interest should be modeled to capture these effects. Where foundation compliance will either significantly alter the structure's dynamic properties

or change the structure's deformation pattern, this should also be modeled. Where this is the case, nonlinear models should be used. Simplifying assumptions, such as composite elements composed of vertical grouped foundation components (e.g., piles associated with a single pile cap) can be used for this purpose. The hysteretic properties of each element under generalized loadings should be developed based on test data and soil mechanics principles

Nonlinear models of soil in the immediate vicinity of the building should be included in the numerical model if (a) the soil-structure-foundation interaction substantially modifies the free-field demand, or (b) the soil is prone to liquefaction or ground failure. Soil-structure-foundation interaction is most significant for structures that are deeply embedded, are located on soft sites, have large footprints and which have relatively short fundamental modes of vibration (less than 0.5 second).

Appendix B presents guidance on modeling soil-foundation-structure system together with a discussion of the likely impact of soil-foundation-structure interaction as a function of building and foundation type and geometry, soil type and depth to bedrock, and related issues.

Foundation embedment

Seismic hazard assessments are routinely conducted for sites that are assumed to be in the free field, namely, sites far removed from buildings or other structures. Depending on the site and the building dynamic characteristics, free-field motions may differ substantially from those experienced by a building's embedded foundation, with the greatest differences for deep foundations and/or soft soil sites. For structures with basements exceeding one story in depth, consideration should be given to developing estimates of ground motion at the structure's base, rather than free-field motion. Site response analysis can be used for this purpose. Preliminary guidance is provided in Appendix B.

Non-simulated deterioration and failure modes

Ideally, all significant modes of component deterioration and failure should be incorporated directly in the nonlinear analysis model. In new buildings that employ ductile detailing and capacity design concepts, the analysis can usually simulate the complete response, since the inelastic deformations are concentrated in ductile elements and force demands in non-ductile (strength-controlled) elements are shielded by the yielding elements. However, in many existing buildings and new buildings that do not have well-defined yield zones protected by ductile detailing, there may be non-ductile rapid

degradation in response that is not captured in the nonlinear analysis. For example, sudden degradation in response may occur through premature shear failures in concrete columns or walls, torsional-flexural buckling of laterally unbraced steel members, or connection and splice failures. In such cases, these failure modes should be considered when processing the analysis data by adjusting the calculated demand parameters and associated building performance. Particular attention should be given to failure modes that may affect the building collapse safety and warrant more rigorous analysis.

5.2.3 Number of analyses

The number of analyses required for each scenario or intensity level depends on the extent that spectra for the ground motions match the target spectrum.

The number of pairs of ground motions necessary to obtain valid estimates of median response depends on the extent that the geomean spectral shape of the scaled motions matches that of the target spectrum in the period range T_{min} to T_{max}, as defined in Chapter 4. Recent studies indicate that for structures dominated by first mode response as few as three ground motion pairs can provide good estimates of median response if the spectral match of the scaled motions and target motion is superior. When the spectral shape of the individual ground motions varies considerably from that of the target, many more analyses are needed to obtain reasonable estimates of median response. When ground motions are selected without consideration of spectral shape, analyses using eleven pairs of motions, scaled in accordance with the recommendations of Chapter 4, can provide a reasonable estimate (+/-20%) of median response with 75% confidence.

For time-based assessments, nonlinear analyses are conducted for m sets of n ground motion pairs each, scaled to appropriate intensity values using the procedures of Section 4.4.4.3. It is recommended that m be taken as having a value of 8 unless it is demonstrated that suitable stable results can be obtained by a lesser number of intensities.

5.2.4 Quality Assurance

Nonlinear analysis is a complex process. To assure meaningful results, models should be carefully checked to establish their reliability.

Owing to the complexity of nonlinear analysis, models should be carefully checked to establish their reliability. The following are suggested steps:

- Results of linear dynamic analyses (response spectrum) should be compared to results of the nonlinear response history analyses to assess the degree of nonlinearity in the structure under various ground motion intensities and to confirm that under low intensity motion, the nonlinear model is behaving in a manner consistent with the linear model.

- Nonlinear static lateral and gravity load analyses should be used to interrogate inelastic mechanisms, plastic deformations, and inelastic force redistributions and to confirm these with expected behavior.
- Nonlinear analyses should be run with and without P-Δ effects to establish the sensitivity of the results to gravity loads and large deformations.
- Hysteretic response plots of selected components (from nonlinear response history analysis) should be reviewed for conformance with the modeled response.

5.2.5 *Uncertainty*

It is usually impractical to perform sufficient numbers of analyses to obtain reliable data on record to record variability and other uncertainties. Therefore, dispersion in the demand parameters are judgmentally estimated.

In this methodology, nonlinear analysis is used to estimate *median* values of demand parameters (component deformations and forces, story drift, floor acceleration, and floor velocity) and the relationships between the values of these parameters. It is usually not practical to perform sufficient analyses to obtain valid information on the dispersion in these response parameters. Therefore, d*ispersions* in the demand parameters are estimated through judgments about the uncertainty inherent in response calculation.

Modeling Uncertainty

Statistics (median and dispersion) to characterize the displacement and acceleration response for a given intensity of earthquake shaking can be established by use of *best estimate* (deterministic) structural and nonstructural component models to calculate the median response and a user-specified dispersion for modeling uncertainty. Alternatively medians and dispersions can be obtained through development and *probabilistic analysis* of a large family of building models whose component mechanical properties are random variables with user-specified distributions. Although probabilistic analysis is more rigorous than the best-estimate deterministic analysis, the computational effort is increased by orders of magnitude. Therefore, the use of the deterministic best-estimate analysis is assumed here.

Modeling uncertainty, β_m, accounts for our imprecise knowledge of a building's actual construction and also in accuracies in our ability to precisely model their inelastic behavior.

Modeling uncertainty, β_m, results from inaccuracies in component modeling, damping and mass assumptions. For convenience this is categorized as uncertainties associated with building definition and quality assurance, β_c, and the quality and completeness of the nonlinear analysis model, β_q. The first of these, β_c, accounts for the possibility that the actual properties of structural elements, e.g. material strength, section dimensions, and rebar locations, may be different than those believed to exist. The latter,

β_q, recognizes that our hysteretic models may not accurately capture the behavior of these elements, even if their construction is precisely known. The total modeling dispersion can be estimated using equation (5-1) and the information presented in the tables below.

$$\beta_m = \sqrt{\beta_c^2 + \beta_q^2} \quad (5\text{-}1)$$

Building definition and construction quality assurance. The value of the dispersion, β_c, is assigned on the basis of the level of definition of the building and how well the design intent is (or will be) implemented through close adherence to the construction documents. Table 5-1 provides recommended values for β_c under representative conditions. Analysts should use individual judgment and guidance provided by the table to assess β_c for individual projects.

Table 5-1 Default descriptions and values for β_c

Definition and Construction Quality Assurance	β_c
Building definition: The building is completely designed and well represented by drawings and specifications (i.e., construction documents are available). *Construction quality*: The building was or will be constructed using rigorous construction quality assurance measures, including special inspection, materials testing and structural observation	.10
Building definition: The building is completely designed or nearly completely designed but available drawings do not completely define all details of construction (i.e., design development documents or equivalent are available). *Construction quality*: For existing buildings, the structure is sited in a region and is of an age in which rigorous construction quality assurance measures were likely implemented. For new construction, the building will be constructed using reasonable construction quality assurance measures.	0.25
Building definition: The design is incomplete (i.e., schematic documents are available), or, for an existing building is known only on the basis of limited field observation and testing. *Construction quality*: For new or existing buildings, little information on the construction quality assurance program is available.	0.40

Model quality and completeness: The value of the dispersion, β_q, should be assigned on the basis of the completeness of the mathematical model and how well the structural component deterioration and failure mechanisms are understood and implemented. The dispersion should be selected on the basis of the user's understanding of how sensitive the response is to certain structural parameters (e.g., strength/stiffness, deformation capacity, in-cycle and between cycle degradation of structural components) and the likely degree of inelastic response and deterioration. Table 5-2 provides guidance on the selection of β_a values.

The selection of a value for β_q from Table 5-2 should be guided by the expected degree of inelastic response and likelihood of component failure and building collapse. For example, the component models in a building that is shaken in the elastic range only (i.e., no structural damage) need not address component deterioration and failure modes need not be simulated; a value of $\beta_q = 0.1$ is likely appropriate in this instance. Conversely, if collapse simulations are being performed, robust numerical models are required for all components expected to suffer significant damage. If such models have not been validated by large-scale testing, model confidence should not be high, and a value of β_q in the range of 0.3 to 0.5 is likely appropriate. Regardless of the relative values of β_a and β_c, derived using the above tables, total uncertainty computed using equation 5-1 should never be taken greater than about 0.5.

Table 5-2 Default descriptions and values for β_q

Model Quality and Completeness	β_q
Model quality: The numerical model for each component is robust over the anticipated range of displacement or deformation response. Strength and stiffness deterioration and all likely failure modes are modeled explicitly. Model accuracy is established with data from large-scale component tests through failure. *Completeness*: The mathematical model includes all structural components and nonstructural components in the building that contribute strength and/or stiffness.	.10
Model quality: The numerical model for each component is robust over the anticipated range of displacement or deformation response. Strength and stiffness deterioration is fairly well represented, though some failure modes are simulated indirectly. Accuracy is established through a combination of judgment and large-scale component tests. *Completeness*: The mathematical model includes most structural components and nonstructural components in the building that contribute significant strength and/or stiffness.	0.25
Model quality: The numerical model for each component is based on cyclic envelope curve models of ASCE 41 or comparable guidelines, where strength and stiffness deterioration and failure modes are incorporated indirectly. *Completeness*: The mathematical model includes all structural components in the lateral-force-resisting system.	0.40

Table 5-3 presents default values of modeling dispersion, β_m, based on the data presented in Tables 5-1 and 5-2 (in addition to record-to-record dispersion, $\beta_{a\Delta}$ and β_{aa}, and ground motion dispersion, β_{gm}). Values are presented as a function of effective fundamental period, $\overline{T}$, and a strength ratio, S, which is given by

$$S = \frac{S_a(\overline{T})W}{V_{y1}} \tag{5-2}$$

Table 5-3 Default Dispersions for Record-to-Record Variability, Modeling Uncertainty and Ground Motion Variability

$\bar{T}, T_1$ (sec)	$S = \frac{S_a(T_1)W}{V_{y1}}$	$\beta_{a\Delta}$	β_{aa}	β_m	β_{gm} [1]		
					WNA	CEUS	PNW
0.20	≤ 1.00	0.05	0.10	0.25	0.60	0.53	0.80
	2	0.35	0.10	0.25			
	4	0.40	0.10	0.35			
	6	0.45	0.10	0.50			
	≥ 8	0.45	0.05	0.50			
0.35	≤ 1.00	0.10	0.15	0.25	0.60	0.55	0.80
	2	0.35	0.15	0.25			
	4	0.40	0.15	0.35			
	6	0.45	0.15	0.50			
	≥ 8	0.45	0.15	0.50			
0.5	≤ 1.00	0.10	0.20	0.25	0.61	0.55	0.80
	2	0.35	0.20	0.25			
	4	0.40	0.20	0.35			
	6	0.45	0.20	0.50			
	≥ 8	0.45	0.20	0.50			
0.75	≤ 1.00	0.10	0.25	0.25	0.64	0.58	0.80
	2	0.35	0.25	0.25			
	4	0.40	0.25	0.35			
	6	0.45	0.25	0.50			
	≥ 8	0.45	0.25	0.50			
1.0	≤ 1.00	0.15	0.30	0.25	0.65	0.60	0.80
	2	0.35	0.30	0.25			
	4	0.40	0.30	0.35			
	6	0.45	0.30	0.50			
	≥ 8	0.45	0.25	0.50			
1.50	≤ 1.00	0.15	0.35	0.25	0.67	0.60	0.85
	2	0.35	0.35	0.25			
	4	0.40	0.30	0.35			
	6	0.45	0.30	0.50			
	≥ 8	0.45	0.25	0.50			
2.0+	≤ 1.00	0.25	0.50	0.25	0.70	0.60	0.90
	2	0.35	0.45	0.25			
	4	0.40	0.45	0.35			
	6	0.45	0.40	0.50			
	≥ 8	0.45	0.35	0.50			

1. WNA = Western North America; CEUS = Central and Eastern United States; PNW = Pacific North West. Values established using the attenuation relationships of Boore and Atkinson (2008) and Campbell and Bozorgnia (2008) for WNA, Campbell (2003) for CEUS, and Atkinson and Boore (2003) for the PNW; moment magnitudes between 6.5 and 7; and rock sites.

where V_{y1} is the (estimated) yield strength of the building in first mode response, and W is the total reactive weight. Linear interpolation can be used to estimate β for intermediate values of T_1 and S. V_{yt} should be determined by a suitable nonlinear static analysis procedure, such as that contained in ASCE 41-06.

The default values provided for β_m in Table 5-3 were computed using equation 5-1 and rounding to the nearest 0.05. The dispersion, β_c, was set equal to 0.25, assuming the level of information typically available at the design development project phase. If only schematic level information is available, this should be adjusted to a value of 0.4. If complete construction details are available, a value of 0.1 should be used.

Dispersions in response due to ground motion record-to-record variability

In these procedures, pairs of earthquake ground motion records are scaled to be compatible with a target spectrum. For structures that have nonlinear response, or response in multiple modes, each record will produce somewhat different response, resulting in record to record variability or dispersion. Unless a very large number of ground motion pairs, on the order of 20 or more, are used, dispersion values obtained from the analyses will generally not accurately represent the true record-to-record dispersion. Therefore, these *Guidelines* recommend use of the default values of record-to-record variability, denoted β_a presented in columns 2 and 3 of Table 5-3. These values were established using data presented in Huang et al. (2009) and Ruiz-Garcia and Miranda (2003). Separate values are presented for story drift ($\beta_{a\Delta}$) and floor acceleration (β_{aa}). Values vary as a function of effective fundamental period and strength ratio.

Dispersions in ground motion conditioned on magnitude and distance

For scenario-based assessments, it is necessary to account for uncertainty in the shape and amplitude of the target spectrum computed for the particular scenario. Attenuation relationships, introduced in Chapter 4, describe the uncertain distribution of spectral demand as a function of moment magnitude, site-to-source distance and other parameters. Table 5-3 lists default values for ground motion spectral demand dispersion, β_{gm}, computed using widely accepted attenuation relationships for Western North America (WNA); the Central and Eastern United States (CEUS); and the Pacific North West (PNW), assuming subduction-zone earthquakes. Alternate values of β_{gm} appropriate to the particular attenuation relationship used to derive the target spectrum can be used.

5.3 Simplified Analysis

5.3.1 Introduction

The simplified procedure uses linear mathematical structural models, and an estimate of the structure's lateral yield strength to estimate median values of response parameters. Structures are assumed to have independent translational response in each of two horizontal axes (denoted *X* and *Y* in Chapter 4). Separate analysis is performed along each axis. The affects of vertical earthquake shaking, torsion and soil-foundation-structure interaction are neglected.

Simplified procedures use linear structural models and estimate of the structure's lateral yield strength to estimate median values of response parameters.

Assumptions that underlie the simplified procedure include:

(a) building framing is independent along each horizontal axis, permitting the framing systems along each axis to be uncoupled and torsional response to be ignored;

(b) the building is regular in plan and elevation (i.e., there are no substantial discontinuities in lateral strength and stiffness);

(c) story drifts do not exceed 4 times the corresponding yield drift, so that the assumptions of elastic-plastic (bilinear) response at the component level is not compromised by excessive degradation in strength and stiffness;

(d) P- Δ effects are not included, therefore, the story drifts are limited to 4%, beyond which may P-Δ may become important; and

(e) the building is less than 15 stories in height.

To the extent that buildings do not conform to these assumptions, the results of simplified analysis may not be reliable. Even for buildings that to conform to the above assumptions, the use of these simplified procedures entails much greater uncertainty both as to the true value of the medians and also as to the dispersion associated with the demands. Therefore, this procedure will result in projections of performance that entail greater uncertainty than when the nonlinear methods are used and may not agree in the mean.

5.3.2 Modeling

The mathematical model should appropriately represent the building's distribution of mass and stiffness. All elements that contribute significantly to either the building's lateral strength or stiffness should be considered in developing the model, whether or not these elements are considered to be

The mathematical model should appropriately represent the building's distribution of stiffness and mass and should include all elements that significantly contribute to the building's lateral strength or stiffness, whether or not they are considered structural or part of the lateral force resisting system.

structural or nonstructural, or part of the seismic force-resisting system. ASCE 41-06 provides guidance for modeling the strength and stiffness of typical building elements.

The mathematical model is used to establish the building's first mode period and shape in each of two orthogonal axes. These periods and mode shapes are used to compute pseudo lateral forces which are statically applied to the mathematical model to determine story drifts. Together with an estimate of the structure's yield strength, these story drifts are converted into median estimates of peak floor acceleration, velocity and story drift in each direction.

The structure's lateral yield strength can be estimated by either nonlinear static analysis, per ASCE 4-061, plastic analysis or, for building's designed in accordance with recent editions of ASCE-7, using the response modification factor, R, and the strength factor, Ω_0. This latter approach is appropriate only when minimal information is available as to the structure's actual design, as may occur during schematic or preliminary design phases. In these phases, the structure's yield strength can be taken in the range given by formula 5-3 below. Individual judgment as to the structure's actual strength must be applied in evaluating formula 5-3.

$$\frac{1.5S_a(T)W}{R/I} \le V_y \le \frac{\Omega_o S_a(T)W}{R/I} \tag{5-3}$$

In the above formula, $S_a(T)$ is the structure's design spectral response acceleration, evaluated at its fundamental period in the direction under consideration, and R, I and Ω_o are the elastic design coefficients appropriate to the structure's occupancy and structural system.

Modeling of seismically isolated structures should follow the equivalent linear procedures of ASCE 41-06.

5.3.3 Analysis Procedure

An independent analysis for each of two principal orthogonal building axes is required.

Figure 5-4 presents the definitions of floor and story numbers and story height adopted for use with the analysis procedures of this section.

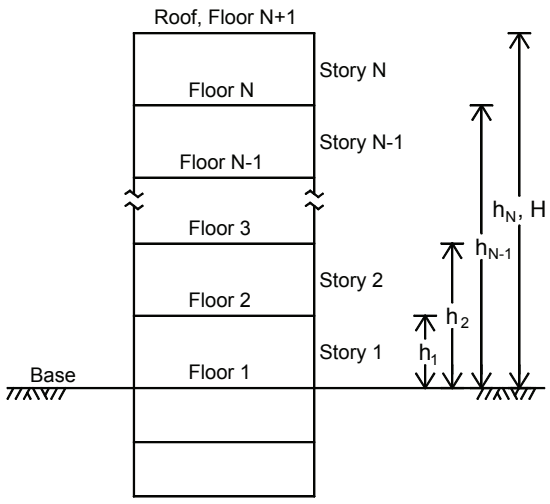

Figure 5-4 Definition of floor, story numbers and floor heights above grade

Pseudo Lateral Force

A pseudo lateral load, *V*, is used to compute story drifts. The load, *V,* is computed in each of two orthogonal directions using equation 5-4:

$$V = C_1 C_2 S_a(T_1) W_1 \tag{5-4}$$

where C_1 is an adjustment factor for inelastic displacements; C_2 is an adjustment factor for cyclic degradation; $S_a(T_1)$ is the 5% damped spectral acceleration at the fundamental period of the building in the direction under consideration, for the selected level of ground shaking; and W_1 is the building's first modal weight in the direction under consideration, but cannot be taken as less than 80% of the total reactive weight, *W*.

The first modal weight, W_1, can be calculated as

$$W_1 = \frac{(\sum_{j=2}^{N+1} w_j \phi_{j1})^2}{\sum_{j=2}^{N+1} w_j \phi_{j1}^2} \tag{5-5}$$

where w_j is the lumped weight at floor level *j* (see Figure 5-2), ϕ_{j1} is the *j*th floor ordinate of the first mode deflected shape and *N* is the number of floors in the building *above* the base. In the absence of calculation per equation 5-5, W_1 can be set equal to $C_{sm}W$, where C_{sm} is defined in ASCE 41. W_1 should not be taken less than 80% of the building's total mass above grade.

The adjustment factor, C_1, is computed as:

$$C_1 = 1 + \frac{S-1}{0.04a} \quad \text{for } T_1 \le 0.2\,\text{sec}$$
$$= 1 + \frac{S-1}{aT_1^2} \quad \text{for } 0.2 < T_1 \le 1.0\,\text{sec} \qquad (5\text{-}6)$$
$$= 1 \quad \text{for } T_1 > 1.0\,\text{sec}$$

where T_1 is the fundamental period of the building in the direction under consideration, *a* is a function of the soil site class (= 130, 130, 90, 60 and 60 for ASCE-7-10 site classes A, B, C, D and E, respectively) and S is a strength ratio given by equation (5-2) with the effective fundamental period replaced by T_1.

The adjustment factor C_2 is computed as:

$$C_2 = 1 + \frac{(S-1)^2}{32} \quad \text{for } T_1 \le 0.2\,\text{sec}$$
$$= 1 + \frac{1}{800}\frac{(S-1)^2}{T_1^2} \quad \text{for } 0.2 < T_1 \le 0.7\,\text{sec} \qquad (5\text{-}7)$$
$$= 1 \quad \text{for } T_1 > 0.7\,\text{sec}$$

If the building incorporates viscous or viscoelastic damping devices, the 5% damped spectral acceleration ordinate should be replaced by the value that corresponds to the first mode damping in the building. The procedures of ASCE 4-06 can be used to estimate the damping in a building equipped with viscous or viscoelastic energy dissipation devices and to adjust the response spectrum for the effects of damping other than 5%.

Median Estimates of demand

Estimates of median story drift, Δ_i^*; floor acceleration, a_i^*, and floor velocity V_i^* are computed in the following steps:

1. Determine the distribution of the pseudo lateral force *V* over the building height.
2. Apply the lateral forces to the elastic model described in Section 5.3.2. and compute the floor displacements and uncorrected story drifts.
3. Correct the story drifts to account for inelastic action and higher mode effects.
4. Convert peak ground acceleration to peak floor acceleration.
5. Convert peak ground velocity to peak floor velocity.

Details of the steps are provided below.

Step 1 – Determine Vertical Distribution of Force.

The pseudo lateral force, F_x, at floor level *x*, is given by:

$$F_x = C_{vx} V \tag{5-8}$$

where C_{vx} is a vertical distribution factor given by:

$$C_{vx} = \frac{w_x h_{x-1}^k}{\sum_{j=2}^{N+1} w_j h_{j-1}^k} \tag{5-9}$$

where w_j is the lumped weight at floor level *j*; h_{j-1} (h_{x-1}) is the height above the effective base of the building to floor level *j*; and *k* is equal to 2.0 for a first mode period greater than 2.5 seconds and equal to 1.0 for a first mode period less than or equal to 0.5 second (linear interpolation can be used for intermediate periods).

Step 2 – Compute floor displacements and story drifts

Simultaneously apply the lateral forces, F_x, to the linear mathematical building model. Compute the displacement of each floor relative to the base under these applied forces. Compute the uncorrected story drift at each level, Δ_i, as the difference between the lateral displacements of the floors immediately above and below the story..

Step 3 – Correct story drifts for inelastic behavior

Median estimates of story drift, Δ_i^*, at level "*i*" are obtained from the formula:

$$\Delta_i^* = H_{\Delta i}(S, T_1, h_i, H)\Delta_i \tag{5-10}$$

where $H_{\Delta i}(S, T_1, h_i, H)$ is the drift correction factor for story *i* computed using equation (5-11):

$$\ln H_{\Delta i} = a_0 + a_1 T_1 + a_2 S + a_3 \frac{h_i}{H} + a_4 (\frac{h_i}{H})^2 \qquad S \geq 1, i = 1 \text{ to N} \tag{5-11}$$

where the values of the coefficients a_0 through a_4 are presented in Table 5-4 for braced frame, moment-frame and shear-wall buildings, respectively; S is the strength ratio previously defined; T_1 is the first mode period; and H is the total building height above the base..

Step 4 – Convert Peak Ground Acceleration to Floor Acceleration

At the base of the building, the peak floor acceleration is taken as the peak ground acceleration. At other floor levels, *i*, the estimated median peak floor acceleration, a_i^*, is derived from peak ground acceleration using the formula:

Table 5-4 Correction Factors for Story Drift, Floor Acceleration and Floor Velocity

	Frame type	a_0	a_1	a_2	a_3	a_4
Story Drift	Braced	0.72	0.048	0.012	-2.64	2.09
	Moment	0.65	0.027	-0.010	-2.58	2.30
	Wall	1.12	-0.22	-0.059	-2.70	1.29
Floor acceler.	Braced	0.57	-0.16	-0.089	0	0
	Moment	0.67	-0.28	-0.080	0	0
	Wall	0.33	0.22	-0.081	0.53	0
Floor velocity						
		See reader note below				

$$a_i^* = H_{ai}(S, T, h_i, H) * pga_i \qquad i = 2 \text{ to N+1} \tag{5-12}$$

where $H_{ai}(S, T_1, h_i, H)$ is the acceleration correction factor for floor *i* (see Figure 5-4) calculated using equation 5-13; and *pga* is the peak ground acceleration.

$$\ln H_{ai} = a_0 + a_1 T_1 + a_2 S + a_3 \frac{h_{i-1}}{H} \qquad S \geq 1, i = 2 \text{ to N+1} \tag{5-13}$$

Table 5-4 presents the values for the coefficients a_0 through a_3 in the above formula for braced frame, moment-frame and shear-wall buildings.

Step 5 – Convert peak ground velocity to floor velocity

Reader Note: The equations and correction factors for computing floor velocity are scheduled for inclusion in the final Guidelines.

Median Residual Story Drift

Calculate residual story drifts using the peak transient story drifts computed above and the procedures of Section 5.4. Note that the simplified elastic procedure should not be used for computing story drifts in excess of four times the yield story drift. The yield story drift should be computed as discussed previously.

Dispersions in response calculations

To conduct performance assessments, it is necessary to develop distributions of story drift, floor acceleration and floor velocity, where the distributions capture the uncertainty in ground motion, β_{gm}, analysis, $\beta_{a\Delta}$ and β_{aa}, and

modeling, β_m. Table 5-3 lists default values of the dispersion to be used with the simplified analysis procedure. Linear interpolation can be used to estimate β for intermediate values of T_1 and S.

For intensity-based assessments and time-based assessments, separate values of dispersion for acceleration and drift demands are required. Drift ratio dispersion is given by:

$$\beta_{SD} = \sqrt{\beta_{a\Delta}{}^2 + \beta_m{}^2} \tag{5-14}$$

Dispersion in acceleration demands is given by:

$$\beta_{FA} = \sqrt{\beta_{aa}{}^2 + \beta_m{}^2} \tag{5-15}$$

For scenario-based assessments, the values of story drift dispersion and floor acceleration dispersion must also include uncertainty in attenuation, β_{gm}, and is respectively given by:

$$\beta_{SD} = \sqrt{\beta_{a\Delta}{}^2 + \beta_m{}^2 + \beta_{gm}{}^2} \tag{5-16}$$

$$\beta_{FA} = \sqrt{\beta_{aa}{}^2 + \beta_m{}^2 + \beta_{gm}{}^2} \tag{5-17}$$

5.4 Residual Drift

Residual drifts predicted by nonlinear analysis are highly sensitive to the assumed component models including the post-yield hardening/softening slope and unloading response. Accurate statistical simulation of residual drifts requires the use of advanced component models with careful attention paid to cyclic hysteretic response and a large number of ground motion pairs.

Nonlinear analysis using standard models does not provide accurate assessments of residual drift.

Since such analysis is not presently practical for wide scale implementation, median residual story drift, denoted Δ_r, should be calculated as:

$$\begin{aligned} \Delta_r &= 0 && \Delta \le \Delta_y \\ \Delta_r &= 0.3(\Delta - \Delta_y) && \Delta_y < \Delta < 4\Delta_y \\ \Delta_r &= (\Delta - 3\Delta_y) && \Delta \ge 4\Delta_y \end{aligned} \tag{5-18}$$

where Δ is the median peak transient story drift calculated by analysis and Δ_y is the median story drift at yield calculated by analysis. Appendix C provides background information on the basis for these relationships.

The yield drift ratio, Δ_y, is the story drift at which significant yielding in the structure occurs. For concentrically steel braced frame systems (or for squat wall systems), the yield drift can be calculated as the story drift associated with imposed story shear forces equal to the expected yield strength of the

braces (or the expected shear strength of the walls). For moment frame systems, the yield drift can be calculated as the story drift associated with story shear forces that cause (a) the beams and/or columns to reach their expected plastic moment capacity, taking into account the effect of axial forces in the members, or (b) the beam-column joint panel to reach its expected yield strength. The distribution of forces in the story under consideration can be calculated either based on the forces induced using equivalent lateral forces, or alternatively, by applying a shear force at the floor above the story being evaluated with a lateral support imposed at the floor below the story being evaluated. In shear wall systems whose behavior is dominated by flexural yielding, the yield drift is equal to the story drift associated with the wall reaching its expected flexural strength under a lateral load distribution that reflects the dynamic response of the building.

When nonlinear response history analysis is used, calculate the residual drift, Δ_i, using equation 5-18 and the median of the peak transient drifts calculated from the suite of analyses at each level. When simplified analysis is used, calculate the residual drift, Δ_r, at each level using value of median transient drift, Δ_i^*, calculated using the procedures of Section 5.3.

The dispersion in the residual drift is generally larger than that of the peak story drift. Unless substantiating data are available, the total dispersion in the residual drift due to both record-to-record variability, β_a, and modeling, β_m, should be set equal to 0.8 (Ruiz-Garcia and Miranda, 2005).

Chapter 6
Develop Collapse Fragility

6.1 Introduction

Collapse fragility functions express the probability of building collapse, in one or modes, as a function of spectral acceleration at the first mode period. Collapse fragilities are assumed to follow a lognormal distribution and are defined by a median value, $\hat{S}_a(T)$, and a dispersion, β. Collapse fragilities are necessary to perform meaningful assessments of potential casualties.

Collapse fragilities are necessary for meaningful assessment of casualties. Collapse is considered to occur if excessive sidesway leads to P-Δ instability or the portions of the gravity load carrying system lose an ability to continue to support gravity loads.

This chapter presents several alternative procedures to establish building-specific collapse fragility functions. Collapse fragilities can be developed for any building using the Incremental Dynamic Analysis procedure. Collapse fragilities for low-rise buildings can also be approximated using a simplified procedure. Collapse fragilities for buildings conforming to the requirements of recent building codes can also be inferred based on target collapse resistance inherent in the building code.

Building collapse is generally associated with failure of the gravity-load framing system, either locally or globally. There are few examples of buildings overturning, aside from those that experienced soil or foundation (pile) failures. Excessive story displacements, which can lead to a near-complete loss of lateral stiffness, can trigger a failure of both vertical and horizontal components. In this methodology, collapse is defined as either:

1. Sidesway failure as characterized by loss of lateral stiffness and development of P-Δ instability, or
2. Loss of vertical load carrying capacity of gravity framing members due to earthquake-induced building drifts.

Vertical collapse is not simulated directly because currently available numerical tools are unable to do so. Instead, vertical collapse is inferred when numerical instability occurs in dynamic structural analysis or predicted lateral displacements exceed the modeling validity range. Loss of vertical capacity in gravity framing components is included in the collapse assessment and development of collapse fragility functions.

6.2 Incremental Dynamic Analysis

6.2.1 Introduction

Incremental Dynamic Analysis, though numerically complex and calculation-intensive, can be used to derive collapse fragilities for any structure.

Incremental Dynamic Analysis is a rigorous method to determine collapse fragilities. In this method, a suite of suitable ground motion pairs is selected and each is scaled to a geomean spectral response acceleration for the building at period $\overline{T}$, at which the building will remain linear. A response-history analysis is performed to determine the peak drift in each story. The geomean spectral acceleration for each ground motion pair is then incremented a number of times and response-history analysis repeated, until collapse is indicated. For each ground motion pair, the maximum drift in any story along either axis should be plotted as a function of geometric mean spectral acceleration. Collapse can be inferred to occur where small increment in spectral acceleration produces large increment in spectral displacement, when the analysis encounters numerical instability or when demands predicted by the analysis indicate that non-simulated collapse modes will occur.

6.2.2 Mathematical Models

Ideally, models should simulate all possible modes of deterioration or failure. Nonsimulated modes, which are not included in the model must be indirectly evaluated for potential initiation at response levels below those at incipient simulated collapse

Three-dimensional mathematical models should generally be used for collapse assessment. Two-dimensional (planar) models may be acceptable for buildings with regular geometries where the response in each orthogonal direction is independent and torsional response is not significant. When two-dimensional models are used, the median collapse capacity, $\hat{S}_a(T)$, should be taken as the smaller of the value obtained for either direction.

Best-estimate models should be used for each component. Best-estimate models use median, or if median values are unavailable, mean properties of all force-deformation parameters (e.g., yield strength, yield deformation, post-yield stiffness, maximum strength, deformation corresponding to maximum strength). Chapter 5 presents additional guidance for modeling structural components across the entire range of response, from elastic behavior through complete loss of resistance.

Ideally, nonlinear models should simulate all, or nearly all, possible modes of component deterioration and failure (e.g., axial, flexure, flexure-axial interaction, shear, and flexure-shear interaction). If a mode of deterioration or failure is not included in the model, its effect on collapse must be accounted for indirectly as a *non-simulated* mode (see Section 6.2.4). Some building components (e.g., gravity-load resisting columns) may not be included in the building model but must be checked to either ensure they do not fail at story drifts smaller than those predicted by analysis at incipient building collapse, or the results of the analysis must be adjusted to account for the non-

simulated failures. Non-simulated deterioration in components included in the mathematical model and components not included in the mathematical model should be assessed using appropriate collapse (loss of load-carrying capacity) limit state checks against demand parameters.

Energy dissipation will occur prior to the onset of inelastic structural response and damage. Such dissipation in structural and nonstructural components may be modeled through equivalent viscous damping and implemented in a variety of ways, including Rayleigh damping and modal damping. For typical buildings, damping under earthquake motions is generally assumed to range between 2% and 5% of critical, depending on the building height, construction materials, and nonstructural components, with smaller values expected for high-rise, steel-framed buildings and larger values for low-rise, concrete framed buildings. Care must be exercised so as not to overestimate the effects of equivalent viscous damping following yielding of the structural frame because hysteretic energy dissipation is included explicitly in the nonlinear analysis.

6.2.3 Ground Motion Characterization

For each ground motion analyzed, Incremental Dynamic Analysis (IDA) produces a plot of maximum story drift at any level, versus spectral acceleration at the building's effective first mode period. When an IDA curve becomes horizontal, or nearly so, this implies that the lateral deformations are uncontrolled, and the value of $S_a(T)$ at which this occurs is the collapse capacity for that record.

Figure 6-1 presents a sample plot for a hypothetical building using 22 different ground motions. The horizontal axis is maximum drift in any building story and the vertical axis, spectral acceleration at the effective first mode period. The lognormal distribution at the right of the plot represents the probability of collapse as a function of first mode spectral acceleration demand and is derived from the suite of analyses by determining the median and an appropriate dispersion.

Two different methods for selecting and scaling ground motions for use in this procedure are presented below. One uses uniform hazard spectra and the other, conditional mean spectra, both of which are described in Appendix B. In both procedures, a sufficient number of ground motions should be used to provide stable estimates of the median collapse capacity. In limited studies, the use of 11 pairs of motions, that are rotated 90 degrees to produce a total of 22 motion sets have been found to be sufficient for this purpose. For some structures, stable prediction of median collapse capacity may be possible with smaller suites of motions.

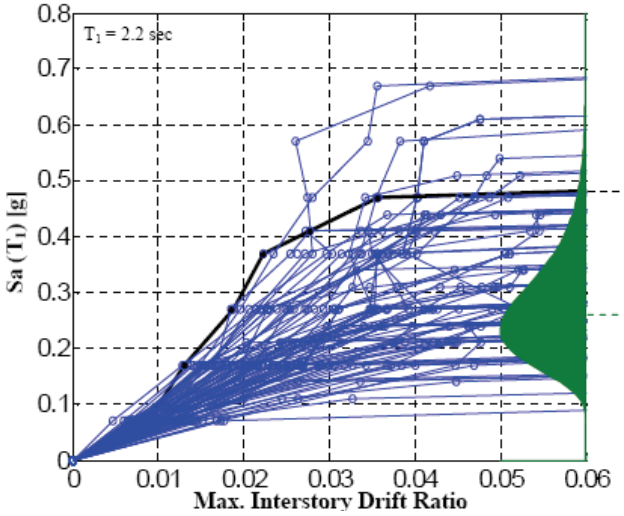

Figure 6-1 Sample Results of Incremental Dynamic Analysis for a Hypothetical Building

Method A – Uniform Hazard Spectra:

1. Estimate the median collapse capacity, $\hat{S}_a(\overline{T})$, and the mean annual frequency of exceedance of $\hat{S}_a(\overline{T})$ For typical structures conforming to the detailing criteria contained in recent editions of ASCE-7, $\hat{S}_a(\overline{T})$ can be estimated as being approximately 3 times the value of the design shaking spectral ordinate at period, $\overline{T}$.
2. Develop a Uniform Hazard Spectrum consistent with the mean annual frequency of exceedance for $\hat{S}_a(\overline{T})$ estimated in Step 1
3. Select an appropriate suite of ground motion pairs with geometric mean spectra that have a similar shape to the Uniform Hazard Spectrum of Step 2

If the estimate of median collapse capacity in Step 1 is significantly larger or smaller than the value computed using the suite of records and incremental dynamic analysis, a new Uniform Hazard Spectrum should be determined for the mean annual frequency of exceedance corresponding with the value of $\hat{S}_a(\overline{T})$ determined by the analysis. If the shape is significantly different from that developed in Step 2, a new suite of motions should be selected per Step 3 to match the new spectrum and the analysis repeated.

Method B – Conditional Mean Spectrum:

1. Estimate the median collapse capacity, $\hat{S}_a(\overline{T})$, and the mean annual frequency of exceedance of $\hat{S}_a(\overline{T})$ as described above for Method A.
2. Deaggregate the seismic hazard at this annual frequency of exceedance (refer to Appendix B) to determine the magnitude and distance of characteristic events that dominate the hazard at this probability.

3. Generate a Conditional Mean Spectrum at period $\overline{T}$ per Appendix B for the $[M, r, \varepsilon]$ of the events selected in Step 2 using an appropriate attenuation function. Normalize the Conditional Mean Spectrum so that the peak ordinate is equal to 1.0
4. Select an appropriate suite of ground motions with geometric mean spectra that have a similar shape and period at peak spectral response to the Conditional Mean Spectrum.

As with the Uniform Hazard Spectrum procedure, if the estimate of median collapse capacity in Step 1 is significantly higher or lower than that determined by incremental dynamic analysis, using this suite of motions, a new annual exceedance frequency should be determined for the value of $\hat{S}_a(\overline{T})$ determined from analysis, and a new Conditional Mean Spectrum generated. If the shape of the spectrum has changed significantly, a new suite of ground motions should be selected and the Incremental Dynamic Analysis process repeated.

6.2.4 Development of Collapse Fragility

Regardless of the method used to select ground motion pairs, the amplitude of each ground motion pair should be incremented, and nonlinear response history analysis performed until either numerical instability occurs in the analysis, indicating collapse, story drift or forces producing non-simulated collapse modes are predicted, or predicted drifts become larger than the valid range of modeling. The value of $S_a(\overline{T})$ at which either occurs should be noted. If numerical instability or a non-simulated collapse mode is not predicted, the analysis should be repeated, with incremental amplitude adjustment for the ground motion pair until a small increment in the value of $S_a(\overline{T})$ produces a large increment in the maximum predicted story drift, numerical instability occurs, or demands associated with non-simulated modes are predicted. In this case, the value of $S_a(\overline{T})$ at which this occurs should be taken as the collapse capacity for this ground motion pair.

The median collapse capacity is taken as that value of $S_a(\overline{T})$ at which 50% of the ground motion pairs produce either:

1. Numerical instability or simulated collapse,
2. Predicted response that would result in non-simulated collapse,
3. Large increment in story drift for small increase in $S_a(\overline{T})$, or
4. Story drifts at which the analytical model is no longer believed to be reliable.

Figure 6-2 presents a collapse fragility plot constructed using the median and dispersion values obtained from Figure 6-1 and the assumption of a lognormal distribution. Note that the dispersion in Figure 6-2, which is based on analysis of a mathematical model constructed using *best estimate* mechanical properties, does not include all sources of uncertainty. These additional sources of uncertainty, identified below, must also be considered in developing the collapse fragility dispersion.

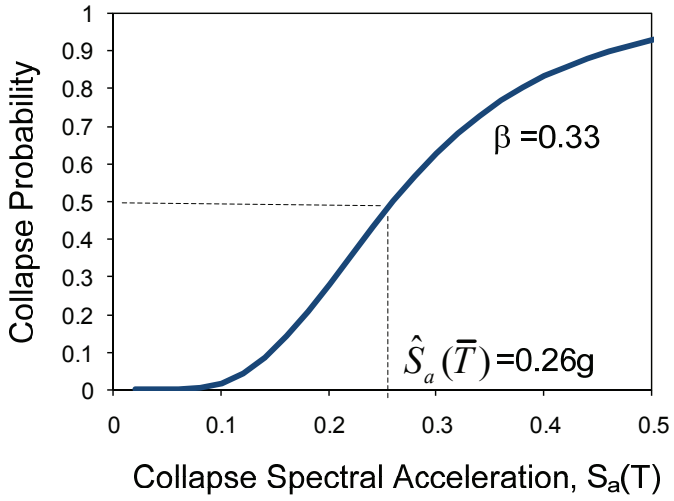

Figure 6-2 Transforming results of IDA to a collapse fragility curve

Collapse fragility dispersion should account for three sources of uncertainty:

1. Variation in collapse capacity among different ground motion records, $\beta_{a\Delta}$, (also termed record-to-record uncertainty);
2. Variations due to building definition and construction quality assurance, β_c; and,
3. Uncertainty associated with the quality and completeness of the nonlinear analysis model, β_q.

Chapter 5 provides recommendations for the second and third sources of uncertainty and groups these together as modeling uncertainty, β_m. Total dispersion can be estimated using equation (6-1) and the information presented below. Alternately, a default dispersion value of 0.6 can be used.

$$\beta = \sqrt{\beta_{a\Delta}^2 + (\beta_c^2 + \beta_q^2)} = \sqrt{\beta_{a\Delta}^2 + \beta_m^2} \qquad (6\text{-}1)$$

a. *Record-to-record uncertainty.* The record to record dispersion in collapse capacity, $\beta_{a\Delta}$, can either be selected from the values presented as a function of structural period and geographic region in column 3 of Table 5-3, or taken as 0.45.

b. *Building definition and construction quality assurance.* Table 5-1 provides default values for β_c.

c. *Model quality and completeness:* Table 5-2 provides default values for β_q. Given that few models account for strength and stiffness deterioration through component failure have been validated by large-size experimentation, β_q should typically have a value between 0.3 and 0.5.

6.3 Simplified Nonlinear Analysis to Derive Collapse Fragility Curves

Nonlinear static analysis can be used wih the SPO2IDA tool to provide representative collapse fragilities for regularly configured structures with uncoupled fundamental modes in each direction of response and limited higher mode behavior.

Vamvatsikos and Cornell (2005) developed an analysis tool, known as SPO2IDA, to facilitate the development of approximate incremental dynamic analysis curves based on the results of nonlinear static analysis. The spreadsheet tool, which is available for download at http://www.ucy.ac.cy/~divamva/software.html, uses a user-defined global force-displacement relationship and a database of results from large-scale analyses of nonlinear single-degree-of-freedom models of varying profiles to generate surrogate incremental dynamic analysis curves, which include some record-to-record variability. Use of this tool should be limited to low-rise structures that are regular in both plan and elevation, and whose seismic response is dominated by independent first translational modes along each principal axis.

To use the SPO2IDA tool, a pushover analysis, similar to that described in ASCE-41 as the nonlinear static procedures is performed. The global base-shear, V, versus roof displacement, Δ, relationship is transformed to a relationship between a normalized spectral acceleration and global displacement ductility. Figure 6-3 presents sample information. The spectral acceleration, SA, is computed as $SA = V / (C_m W / g)$, where all terms have been defined previously. The spectral acceleration is normalized by a variable, S_y, which is equal in value to SA at the first control point as seen in the figure. The global displacement ductility, μ, is the ratio of the roof displacement, Δ, to the roof yield displacement. The coordinate of the yield point (first control point) in the SPO2IDA space is $\left(\mu, SA / S_y = 1,1\right)$.

Building-specific nonlinear static analysis can be performed to generate the normalized force-displacement relationship of Figure 6-3. Procedures for performing nonlinear static analysis are provided in ASCE 41 (ASCE, 2006).

Figure 6-3 Global force-displacement relationship in SPO2IDA

Figure 6-4 presents sample output from the SPO2IDA tool, which includes the results of the nonlinear static analysis per Figure 6-3 and the IDA predictions, including the 16th, 50th (median) and 84th percentile predictions. The median collapse capacity, $\hat{S}_a$, for this example is approximately $5.1S_y$. Since a best estimate model is used to derive the relationship of Figure 6-4, dispersions due to record-to-record variability and modeling should be computed and used to derive the collapse fragility curve. The default dispersion of 0.6 is recommended for use with the SPO2IDA tool.

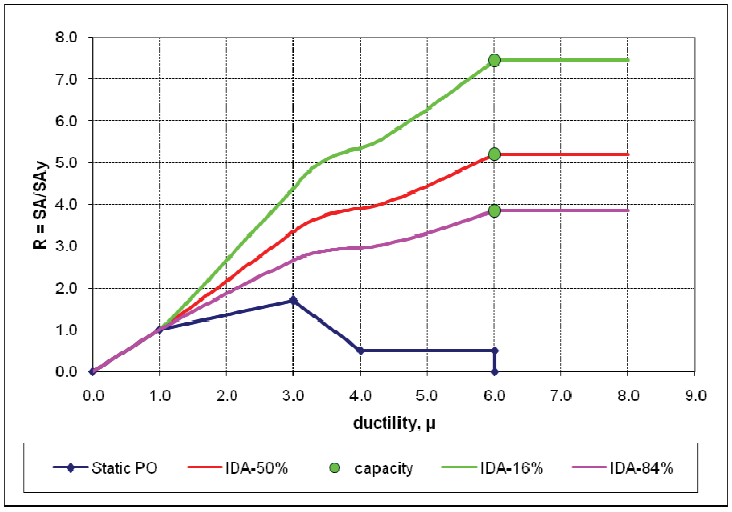

Figure 6-4 Sample SPO2IDA results for the example of Figure 6-3

6.4 Judgment-based Collapse Fragility

Collapse fragility curves can also be developed based on engineering judgment. As with any exercise of engineering judgment, the resulting assessments of performance will be only as good as the judgment used to develop the fragility.

The seismic design procedures contained in ASCE-7 are intended to provide less than a 10% chance that structures conforming to the requirements will collapse if they experience Maximum Considered Earthquake shaking as defined in that standard. Recent studies funded under the National Earthquake Hazards Reduction program have used the FEMA P-695 methodology to confirm that some structural systems for which ASCE-7 specifies seismic design criteria are capable, on average, of meeting this criteria. These studies have generally used well-configured, regular structures. Further, some typical structures used in these studies have easily met this collapse resistance goal, while others have not. It can be expected that irregular structures with unfavorable configuration will not provide the same collapse reliability as that intended by ASCE-7.

Judgment can be used to form approximations of collapse fragility but should not be regarded as reliable measures of a structure's collapse resistance

Regardless, these criteria can be used to rapidly establish approximate collapse fragilities for structures that generally conform to the ASCE-7 criteria. These procedures assume significantly larger uncertainty than the other two methods described above, and consequently, even if an appropriate median collapse capacity is used, will result in greater assessed likelihood of collapse and resulting casualties than would be obtained using the more rigorous methods. The following procedure can be used:

1. Determine the highest value of the spectral acceleration, $S_a(T)$, for which the structure would fully conform to the design requirements of ASCE-7 and its referenced standards, assuming an occupancy importance factor of 1.0 and a redundancy coefficient of 1.0.
2. Compute the inferred median collapse capacity, $\hat{S}_a(\overline{T})$, as having a value of 3 times the value of $S_a(T)$ determined in Step 1.
3. Take the dispersion as having a value of 0.7 for regular, well-configured structures, and 0.8 or higher for irregular structures or structures having configurations that otherwise are unfavorable to good seismic performance.

For archaic construction, the median value can be estimated on the basis of past experience; a dispersion of no less than 0.6 should be assumed.

6.5 Collapse Modes for Casualty Assessments

To permit assessment of casualties it is necessary to provide a brief qualitative narrative that describes the likely mode(s) and extent of collapse. Each narrative should include information on the dominant deterioration modes and triggers of collapse, whether the collapse is dominated by sidesway or by loss in vertical load carrying capacity, and whether the collapse is likely to involve the entire building area or to affect just portions

of the structure (e.g., select stories or regions of the plan area). Information on the likely stories involved in the collapse should be provided, if available.

In addition to determining the distribution of collapse probability it is necessary to estimate the probable extent of structure involved in collapse.

Collapse area ratios are used to supplement the collapse fragility curves with information on the portion of the building area that is likely to be involved in the collapse. These ratios take the form of a probability equation to predict the total amount of collapsed floor area as the sum of the fractional collapse on each floor of the building. These fractions are presented independently of the ground motion intensity using the format of Table 6-1 below. The sum of the probabilities in the table total 1.00. The fractional area of collapse area is the sum of (probability) × (% of stories) × (% plan area). Using the sample probabilities in Table 6-1 below, the expected fractional area of the building involved in collapse would be 0.31.

Table 6-1 Sample probabilities that the specified portion of a building will be involved in the collapse

		Amount of Plan Area		
		25% of plan area	50% of plan area	100% of plan area
Number of stories involved in the collapse	25% of stories	0.05	0.15	0.05
	50% of stories	0.1	0.3	0.1
	100% of stories	0.05	0.15	0.05

Chapter 7
Calculate Performance

7.1 Introduction

This chapter describes the algorithms used to determine performance in these procedures. This section introduces the overall approach and subsequent sections outline the specific processes associated with collapse, casualties, repair costs, repair time, demand generation, damage calculation and loss calculations. The material presented outlines the process for intensity-based assessments. Scenario-based assessments are performed in a similar manner. The final section outlines the modifications to the process necessary to perform time-based assessments as a series of occurrence probability-weighted, intensity-based assessments.

The methodology uses a Monte Carlo process to assess performance measures

The methodology uses a Monte Carlo process to explore variability in building performance outcomes for a particular intensity (or scenario) motion. Ideally, this process would include performing structural analyses using a large suite of input ground motions, each representing the particular motion intensity of interest, with the properties of the analytical model randomly varied to account for modeling uncertainty. The analytical model would include structural and nonstructural systems and would be able to predict damage to each component as it occurs. Each single analysis would represent one possible building damage state, and the results of the large suite of analyses (thousands) would produce a smoothed distribution of possible damage states that could be used to evaluate repair costs, casualties, and other earthquake consequences. At present, however, such an approach is impractical because the necessary modeling capability does not exist, there are an insufficient number of ground motions available for use in the analyses and the solution time would be excessive.

Instead, this methodology uses analysis to predict demands that are indicative of damage. These demands are used together with the fragility and consequence functions described in Chapter 3 to predict earthquake consequences over a distribution of possible earthquake response states. In this process, a limited number of structural analyses are performed to predict an estimate of the median value of key building response parameters such as story drifts and floor accelerations.

The median estimates of demand developed from the structural analyses are converted into distributions of demand based on the assessed variability of each of the random parameters, for example damping or yield strength of a structural element, and the likely effect of this variability on structural response. This approach, albeit indirect and lacking the precision of analysis using appropriate distributions of strength and hysteretic properties, is computationally efficient and better suited to the analysis tools available at this time.

Realizations are used to determine the statistical distribution of performance outcomes. Each realization is one possible outcome.

In the Monte Carlo process used to assess performance, each possible earthquake outcome, including a set of demands (floor accelerations and velocities, story drifts,), damage, and performance consequences, is termed a *realization*. As part of the process of constructing realizations, the statistical distribution of demands derived from the structural analyses is used to construct a series of possible response states for the particular intensity of motion, termed *simulations*. The simulated demand set, or simulation, for each realization represents one possible set of peak response quantities that is consistent with the particular intensity of motion. Section 7.4 describes the demand generation process. Hundreds, and perhaps thousands, of realizations and the associated simulations are needed to predict the distribution of building damage for a particular intensity of motion.

Subsequent sections describe the method of determining a building damage state from a single set of demands or realization. These procedures are repeated many times to determine the distribution of building damage and consequences over many realizations. Figure 7-1 shows the performance calculation process used to assess damage, and then consequences in each realization, as described in the following sections.

7.2 Realization Initiation

Each realization initiates with determination of the time of day, and day of the year at which the earthquake has occurred. This information is used, together with the building's population model, to determine the number of people present. If desired, the number of people present can be assumed to be the peak population, or alternatively, the mean population. Chapter 3 provides additional information on population models.

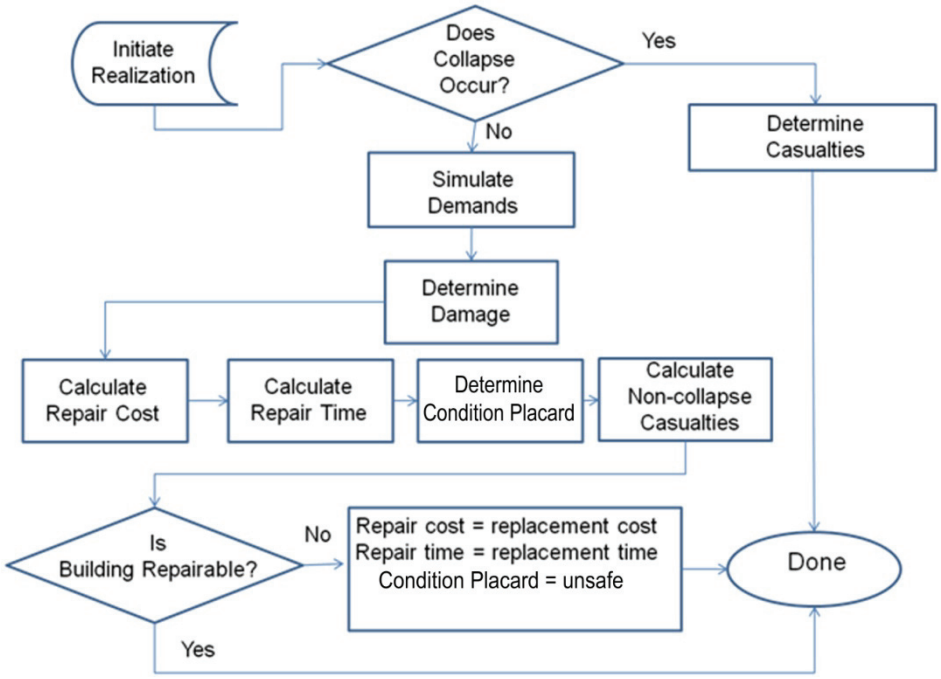

Figure 7-1 Performance calculation flow chart

7.3 Collapse Determination

For each realization, a determination is made as to whether the building has collapsed, using the collapse fragility described in Chapter 6. Figure 7-2 presents a collapse fragility function for a hypothetical building.

For each realization, a determination as to whether collapse has occurred is initially checked.

For example, at an intensity of motion having a spectral acceleration at the building's fundamental period of 0.5g, Figure 7-2 indicates a 15% probability of building collapse. To determine if collapse has occurred, a random integer in the range of 1 to 100 is generated. For the example case of 0.5g ground shaking, if the random number is less than or equal to the conditional probability of collapse, factored by 100 (15 in this case), the realization would judge that collapse had occurred, defining the building's damage state. If the random number is greater than 15, this would indicate that collapse had not occurred, and the performance calculation would go to the next step in the process, Demand Simulation (see Section 7.4), as depicted in Figure 7-1.

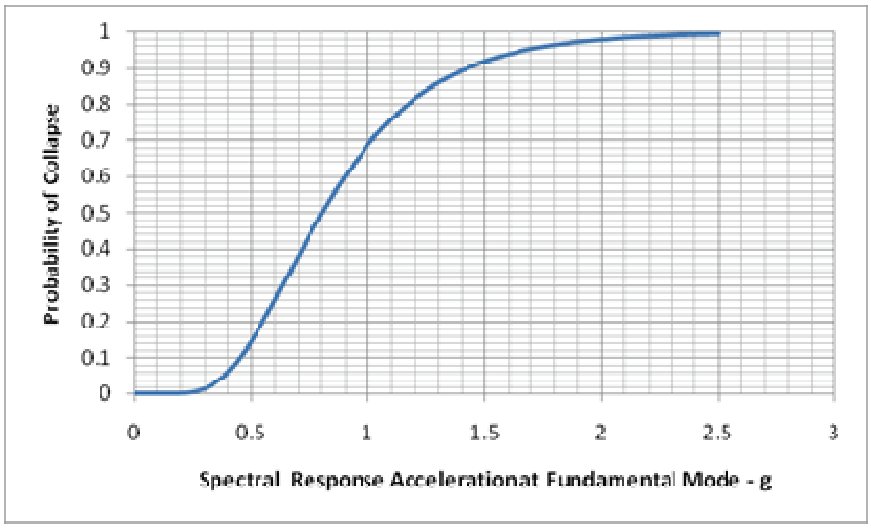

Figure 7-2 Representative collapse fragility for a hypothetical building structure

7.3.1 Collapse Mode

allows for
tiple

In general, structures may experience any of several collapse modes, including collapse that involves a portion of a single story or stories; an entire story or stories; or the entire structure. Given a prediction that collapse has occurred, the collapse mode must be determined to permit estimation of the casualties. As described in Chapter 6, the collapse fragility must include identification of the possible collapse modes and the conditional probability of occurrence of each of these modes, given that collapse occurs. For each mode the fraction of the floor subject to collapse debris must also be provided. For complete collapse, the mode would identify that 100% of the floor area on each level is subject to collapse debris. For a single story collapse, with minor collapse on other floors, the mode would identify nearly 100% for the floor area on the level associated with story collapse and lesser collapse debris percentages on other floors.

To determine which collapse mode has occurred in a realization, the collapse modes probabilities are assembled into an array ranging from 1 to 100, with n_i sequential numbers assigned to each mode, where n_i is the conditional probability of occurrence for each mode, factored by 100. Then, a random number between 1 and 100 is generated and the range in the array in which this number falls indicates the collapse mode that has occurred. For example, if a two story building has three potential collapse modes, consisting of first story collapse (50% probability), second story collapse (25% probability) and complete collapse (25%) these probabilities would be used to construct an array with numbers 1 through 50 assigned to collapse

mode 1; numbers 51 to 75 to collapse mode 2 and 76 to 100 assigned to collapse mode 3. A random number selection of 64 would indicate collapse mode 2 had occurred for this realization.

7.3.2 Casualties

Given determination that a collapse mode has occurred, the number of casualties is estimated based on the associated fraction of floor area at each level subject to collapse together with additional casualty-specific information. For each collapse mode there are mean fatality and injury rate ratios. These ratios describe, based on limited data from past earthquakes, for the population present, the percent of occupants that will suffer death or injury. These probabilities are factored by the percent of building area subject to debris and the population present in the building to predicted deaths and injuries for the realization.

The demands used in the performance calculation are based on the analysis procedure used.

7.3.3 Repair Cost and Time

Given that the realization predicts collapse, repair cost and repair time are set equal to the building replacement values.

7.4 Demand Simulation

If collapse has not occurred, it is necessary to generate a vector of demands that are used to predict the damage sustained by individual structural and nonstructural components and systems. Two different approaches are used for this purpose, depending on whether simplified analysis or nonlinear response history analysis has been performed.

7.4.1 Simplified Analysis

The simplified analysis procedure of Chapter 5 results in a single set of peak floor acceleration, velocity, peak story drift and transient drift demands and associated dispersions. The set of peak accelerations, velocities and story drifts are assumed to represent a median response state and the distribution in these demands is assumed to be lognormally distributed with the dispersions obtained from the analysis.

For simplified analysis, a single set of peak demands are required.

For each realization, a random number between 1 and 100 is generated. This random number represents the percentile, within the lognormal distribution for determination of demands for this realization, respectively, using the dispersions for acceleration and story drift, as appropriate. In essence, this approach assumes that the building maintains the same response profile, regardless of the ground motion, an assumption that is obviously incorrect for multi-degree of freedom structures. Figure 7-3 illustrates this process by

showing assumed deformed shapes for a hypothetical structure at different percentiles for four simulations. As described in Section 7.1, hundreds, and perhaps thousands, of simulations are needed to predict the distribution of building damage for a particular intensity of motion.

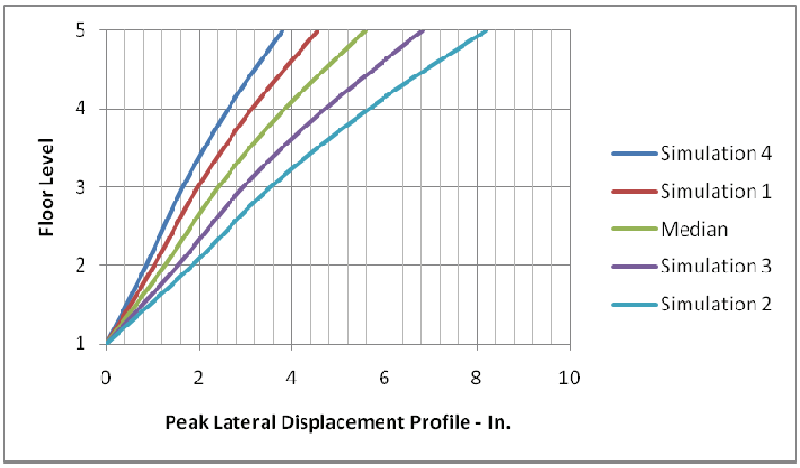

Figure 7-3 Illustration of assumed variability in demands associated with Simplified Analysis

7.4.2 Nonlinear Response History Analysis

When nonlinear response history analysis is performed, the analysis produces a limited suite of demands, each of which represents one possible response state. The demands from each analysis are assembled into a vector containing the value of each of the demands (peak floor acceleration and velocity, peak and residual story drift at each level in each direction) for that analysis. These vectors are assembled into a matrix, each column of the matrix being one analysis and each row, one demand parameter. This matrix is assumed to be representative of a joint lognormal distribution that includes a median vector of demands (assumed to be the median vector derived from the suite of analyses), dispersion, and a correlation matrix that indicates how each demand parameter varies with respect to other demand parameters. This resulting joint probability distribution recognizes that when some demand parameters are disproportionately high (e.g., from formation of an inelastic soft story), other demands (e.g., drift in stories other than the soft story) may be significantly reduced. Figure 7-4 illustrates this behavior for the same hypothetical structure of Figure 7-3. As can be seen, the structure's response profile varies in amplitude and shape from simulation to simulation. This is a much more realistic treatment of potential variability than is possible using the simplified approach. As with the simplified procedures discussed previously, random number generation is used together with the medians, dispersion and joint correlation matrix to determine individual simulated

demand vectors for use in each realization. Appendix G presents the mathematics used to generate simulations using this approach.

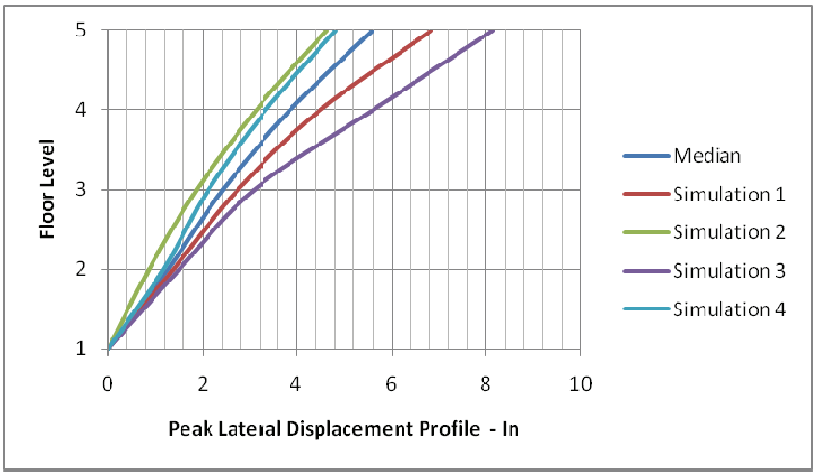

Figure 7-4 Illustration of variability in demands associated with Nonlinear Analysis and assumed joint lognormal distribution

7.5 Damage Calculation

For each realization in which collapse is not predicted, a damage state is determined for each component utilizing the simulated set of demand vectors and the performance groups. Once the damage state is determined, the losses (e.g., repair costs, repair time, casualties) are calculated as described in Section 7.6. The overall building damage is computed as the aggregate of the damage from all of the performance groups.

The process for determining the damage state for a performance group varies by the damage state type (sequential, simultaneous or mutually exclusive) and whether the damage is correlated or uncorrelated. One consistent aspect of the process is the use of random number generation to serve as the basis for determining the damage state. For correlated damage states, every element of the performance group is assumed to have the same damage and the damage determination process is performed only one time for the performance group. For uncorrelated damage, each element of the performance group can have different damage and the random number generation process must be applied *n* times, where *n* is the number of elements in the performance group.

rmining the

varies by
and
e is
related.

7.5.1 Sequential Damage States

Sequential damage states are states of increasing damage, with the logical relationship that one damage state cannot occur until the prior, less severe damage state has occurred. Each sequential damage state is assigned a range of numbers; damage state 1 ranging from (P_1 x 100) to (P_2 x 100), damage

state 2 ranging from ($P_2 x\ 100$+1) to (P_3 x 100), and so on, where P_i is the inverse probability of incurring damage state "*i*" at the demand level for the realization, as indicated by the performance group fragility. A random number below ($P_1 x\ 100$) indicates that no damage has occurred; a random number between (P_i x 100) and (P_{i+1} x 100) indicates damage state P_i has occurred. Figure 7-5 illustrates this process for a representative performance group. The figure shows the hypothetical fragility functions for these three damage states and a hypothetical realization demand of 0.25g.

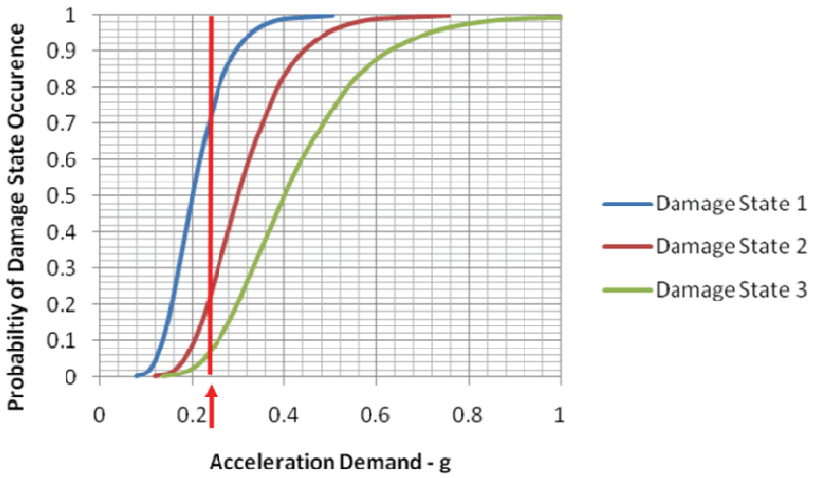

Figure 7-5 Illustration of determining sequential damage state for a performance group for a given realization

For this hypothetical case, the probability of not incurring damage state 1 or higher is P1 = 1 - 0.8 = 0.2; the probability of not incurring damage state 2 or higher is 1 - P2 = 1 -.27 = 0.73; and the inverse probability of not incurring damage state 3 is P3 = 1 - .09 = 0.91. Therefore, the range of numbers assigned to no damage is from 1 to 20; the range to damage state 1 is from 21 to 73; for damage state 2 from 74 to 91; and for damage state 3 from 92 to 100. A random number of 93 for a realization falls within the highest range and would indicate that damage state 3 had occurred.

7.5.2 Simultaneous Damage States

For simultaneous damage states, a first random number is selected to determine whether damage has occurred or not. If the random number is less than the probability of incurring damage, than damage of some type has occurred. Each simultaneous damage state has an associated conditional probability of occurrence, given that the component is damaged. These conditional probabilities of occurrence are combined to determine the probability of all possible outcomes. For a component with *N* possible simultaneous damage states, there will be *N!+1* possible combinations of damage states. Thus, if there are two possible damage states, there would be

3 possible combinations of simultaneous damage states. If there are 3 possible damage states there would be 7 possible combinations. Table 7-1 illustrates the possible combinations of simultaneous damage states for a component that has three possible states, D_1, D_2, and D_3, and also shows the probability of each combined state occurring, assuming that the probability of occurrence of these states is respectively 50%, 50% and 20%. Appendix A describes the procedures used to calculate these combined probabilities.

Table 7-1 Illustration of possible simultaneous damage states

Combination	D_1 P=0.5	D_2 P=0.5	D_3 P=0.2	Probability	Index
1	Yes	No	No	0.2	1-20
2	Yes	Yes	No	0.2	21-40
3	Yes	No	Yes	.05	41-45
4	Yes	Yes	Yes	.05	46-50
5	No	Yes	No	0.2	50-70
6	No	Yes	Yes	.05	70-75
7	No	No	Yes	.05	75-80
Total				0.8	

Once the possible combinations of damage are determined, each possible combination is assigned a number and these are arbitrarily ordered with indices assigned based on the individual probabilities of occurrence for each of the combinations starting with 1, and ranging to P_T, where P_T is the 100 times the sum of all combination probabilities. Then a random number is selected, just as for sequential states, and the unique combination of damage states that has occurred for the realization is selected, based as previously described for sequential states. In the example of Table 7-1, if a random number of 55 were selected, this would indicate combination 5 (only Damage State 2 having occurred) is selected.

7.5.3 Mutually Exclusive Damage States

For mutually exclusive damage states each damage state has a conditional probability of occurrence, given that damage occurs, and the sum of the conditional probabilities of occurrence must add up to 100%. The mutually exclusive damage states, DS_1, DS_2, and so on, are each assigned an array of numbers with the array for damage state 1 ranging from 1 to $P(DS_1) \times 100$, that for array 2 ranging from $(P(DS_1) \times 100+1)$ to $P(DS_1 + PDS_2) \times 100$, and so on. A random number is then generated between 1 and 100, and whichever range it falls within is the type of damage that occurs for the particular realization.

As an example, consider a hypothetical component that has three mutually exclusive damage states, DS_1, DS_2 and DS_3, with respective conditional probabilities of occurrence of 20%, 30% and 50%. The range of numbers assigned to damage state 1 is 1 to 20; for damage state 2 from 21 to 50; for damage state 3 from 51 to 100. A random number of 42 for a realization would indicate that damage state 2 has occurred.

7.6 Loss Calculation

Given that collapse does not occur, the losses are computed for each realization using the damage states for each component, calculated as described in the previous section. As described in Section 3.9, consequence functions are developed for each damage state that specify the likely consequences in terms of repair cost, repair time, casualties and environmental impacts and are used to calculate the associated losses for the given realization.

Each realization enables the development of a performance group damage state and the calculation of a single value of the loss. This loss value includes the efficiency of scale for the performance group as described in Section 3.9 and also takes into account the uncertainty in the calculation by taking into account the dispersion, β_c. Since the overall building loss is computed as the aggregate of the losses from all of the individual performance groups, global efficiencies of scale are not taken into account.

As described in Section 2.5, following computation of the damage states and consequences for all performance groups, the maximum residual drift is evaluated to determine if it is sufficient to render the building impractical to repair. If the building is deemed irreparable, then the computed repair cost and time for the realization are discarded and the total replacement cost and times are used for the realization, instead.

The loss distributions are developed by repeating realization-specfic damage and loss calculations many times.

The loss distribution is developed by repeating the realization-specific damage and loss calculation many times and sorting the losses in ascending or descending order to enable the calculation of the probability that the total loss will be less than a specific value for the given intensity of shaking. For example, if loss calculations are performed for 1,000 realizations, and the realizations are assembled in ascending order, the repair cost with a 90% chance of exceedance will be the repair cost calculated for the realization with the 100^{th} largest cost, as 90% of the realizations will have a higher computed cost.

Figure 7-6 shows sample results of a scenario or intensity-based cumulative loss distribution function for repair costs. In the figure, each dot represents a realization result.

Any value of total loss can also be de-aggregated into performance group losses as shown in Figures 7-7, by summing up, on a realization basis, the sources of the loss, in this case, repair costs. Results for other consequences are similar. Casualties can be de-aggregated into those due to collapse in different modes and those caused by various non-collapse hazards associated with performance groups.

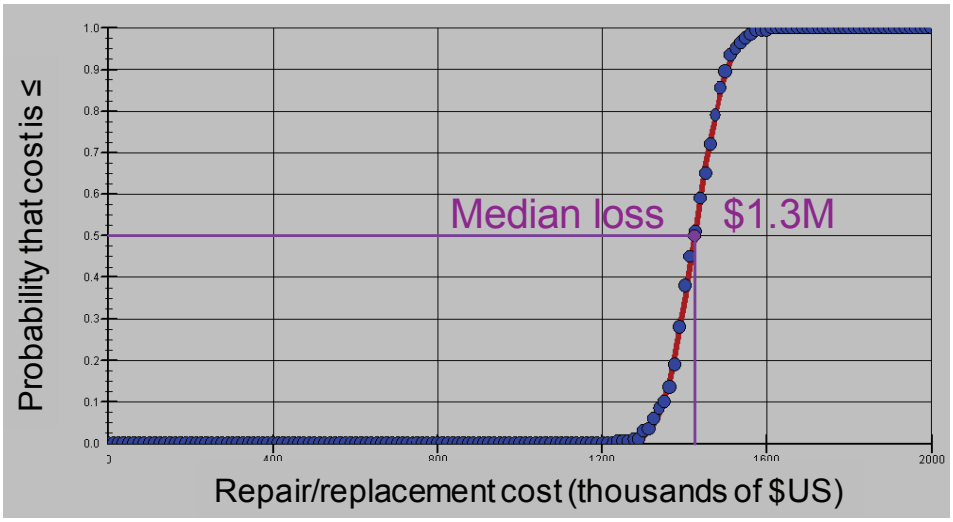

Figure 7-6 Sample repair/replacement losses for a scenario or intensity-based assessment.

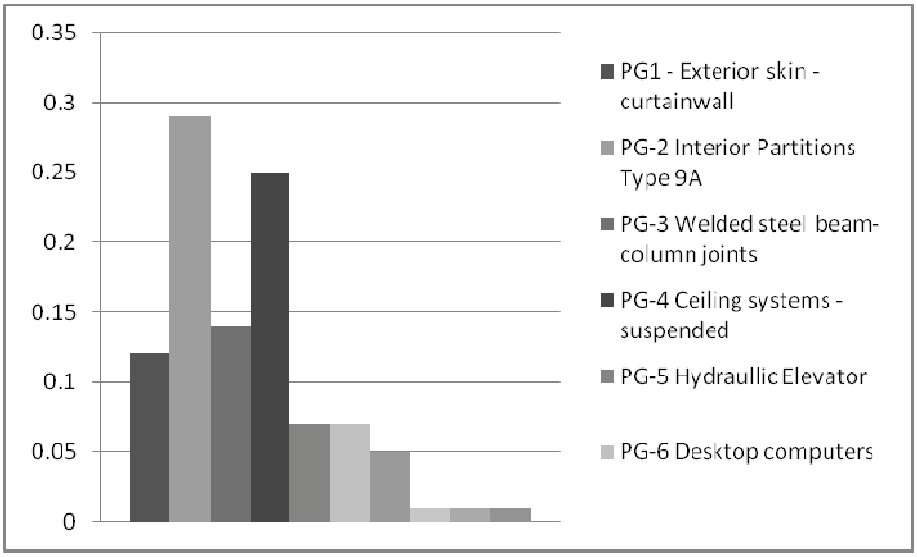

Figure 7-7 Sample Repair/replacement losses de-aggregated by performance group (PG) for a scenario or intensity-based assessment.

7.7 Time-based Assessments

The product of time-based assessment is a curve of the type shown in Figure 7-8, which plots the total repair cost (or other consequence measure), as a function of the annual rate of exceeding these losses. The curve shown in Figure 7-8 is constructed using the results of a series of intensity-based assessments and an appropriate seismic hazard curve for the site.

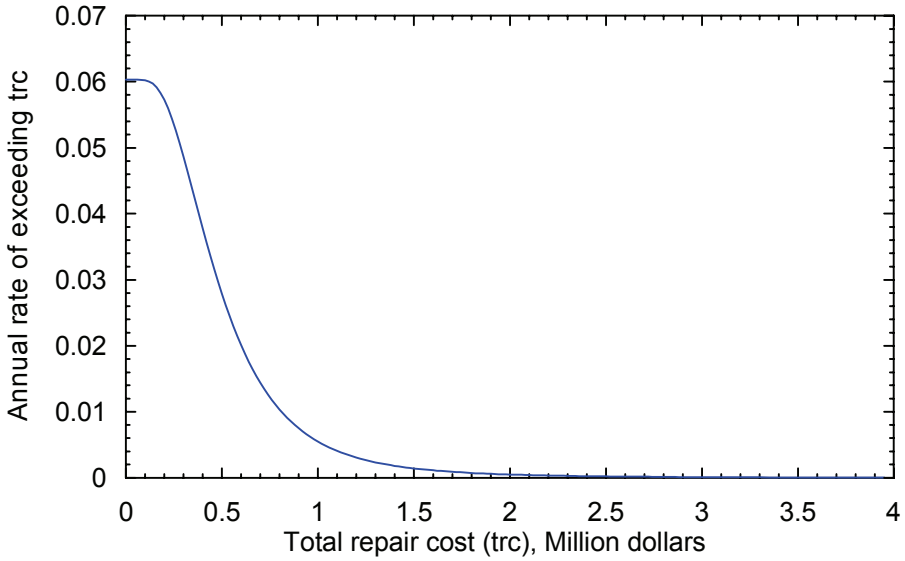

Figure 7-8 Distribution of mean annual total repair cost

Figure 7-9 shows a representative seismic hazard curve, where the annual frequency of exceeding an earthquake intensity, $\lambda(e)$, is plotted against the earthquake intensity, e, where the typical earthquake intensity is spectral acceleration at the first mode period of the building.

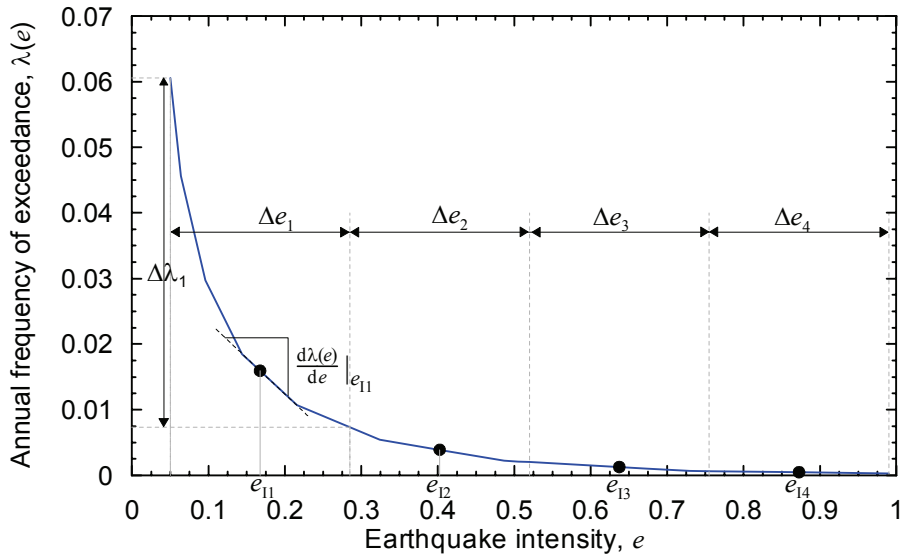

Figure 7-9 Seismic hazard curve and time-based loss calculations

Hazard curves like that shown in Figure 7-9 are used together with Equation (7-1) to calculate the annual probability that the loss *L* will exceed a value *l*:

$$P(L > l) = \int_{\lambda} P(L > l \,|\, E = e)\, d\lambda(e) \qquad (7\text{-}1)$$

where the term $P\left(L > l \,|\, E = e\right)$ is the product of an intensity based assessment for intensity e. Equation (7-1) is solved by numerical integration.

In order to perform this numerical integration, the spectral range of interest is divided into *n* intervals, Δe_i. The spectral range of interest will typically range from a very low intensity that results in no damage to a very large intensity that produces a high probability of collapse. The midpoint intensity in each interval is e_{Ii}, and the annual frequency of earthquake intensity in the range Δe_i is $\Delta\lambda_j$ where the parameters Δe_i, e_{Ii} and $\Delta\lambda_j$ are defined in Figure 7-9 for a sample hazard curve using *n* = 4. This small value for *n* is chosen for clarity. In real time-based assessments, a larger number, *n*, of intensities will typically be necessary.

An intensity-based assessment is performed at each of the *n* midpoint intensities, e_{I1} through e_{In}. The number, n, of intensities required to implement this process will vary from structure to structure, and will depend on the steepness of the hazard curve and the ability of the structure to survive a wide range of ground shaking intensities. Earthquake intensity at intensity e_{I1} is assumed to represent all shaking in the interval Δe_1. The product of the *n* intensity-based assessments is *n* loss curves of the type shown in Figure 7-10. The annual probability of shaking of intensity e_{Ij}, $\Delta\lambda_j$, is calculated directly from the seismic hazard curve. A sample calculation is shown in Figure 7-9 for interval, Δe_1, for which $\Delta\lambda_1 = 0.054$. Figure 7-8 is constructed by: (1) multiplying each loss curve by the annual frequency of shaking in the interval of earthquake intensity used to construct the loss curve; and (2) summing the annual frequencies for a given value of the loss.

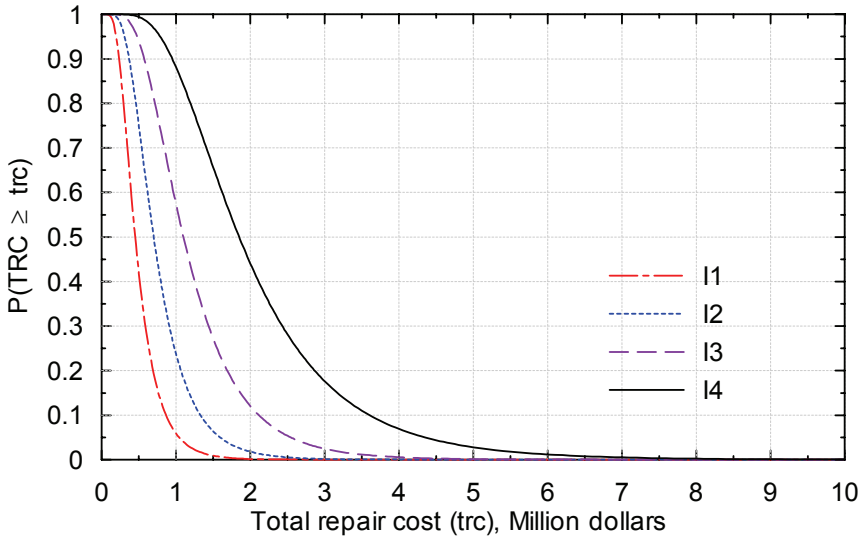

Figure 7-10 Example cumulative probability loss distributions for a hypothetical building at four ground motion intensities

Chapter 8
Decision Making

8.1 Introduction

In addition to being part of the performance-based design process, as described in Chapter 1, performance assessment can provide useful information for many decisions associated with real property. These include:

Performance assessment can provide useful information for many decisions associated with real property.

- Demonstrating equivalence of alternative design approaches;
- Selection of appropriate design criteria for new buildings;
- Determining if existing buildings constitute an acceptable risk for a particular planned use;
- Determining if an existing building should be upgraded, and if so, to what level; and
- Determining whether insurance is a cost-effective risk management technique.

This Chapter illustrates how data obtained from performance assessments can be used as an aid to making such decisions.

8.2 Code Equivalence

For many years the building code has permitted building officials to accept alternative designs and construction techniques that do not conform to the code's prescriptive criteria. This permission is subject to the building official's satisfaction that the proposed design or construction is capable of providing performance equivalent to that expected of code-conforming buildings. The performance assessment process can be used to directly indicate whether an alternative design is capable of providing equivalent performance.

Under ASCE 7-10, Occupancy Category I and II buildings should have less than 10% chance of collapse given MCE shaking, Occupancy Category III buildings a 6% chance of collapse, and Occupancy Category IV buildings a 3% chance of collapse.

Commentary to ASCE 7-10 Section 1.3 establishes the intended minimum safety-related seismic performance of building structures conforming to any of four Risk (or Occupancy) Categories. This performance is measured in terms of probability of collapse, given that the structure is subjected to MCE shaking. The procedures of Chapter 6 can be used to develop a collapse fragility and to determine directly, the probability of collapse for MCE shaking, individual scenarios, or on a time-basis.

Future building codes will likely include quantitative criteria that address performance issues in both a broader and more direct manner. Rather than considering the probability of collapse, future codes will likely set safety-related performance goals in terms of the risk of life loss, rather than collapse. Additional performance measures likely to be considered and quantified by future codes and standards include the potential for loss of beneficial use and for damage of critical function-related equipment. The intensity-based assessment procedures can be used to indicate probable building performance for Design Earthquake shaking or Maximum Considered Earthquake shaking, as defined in the building code, or for any other response spectrum.

8.3 Scenario-based Assessments

Scenario-based assessments can be useful for decision makers with buildings located close to major active faults.

Scenario-based assessments can be useful for decision makers with buildings that are located close to a major active fault, and who have come to believe that a particular magnitude earthquake is likely to occur on this fault within a time-horizon that is meaningful to them, often ranging from 10 to 30 years.

Scenario-based assessments will provide direct information as to the probable repair costs for such an occurrence, the potential for life loss, and the potential for long term loss of use. Scenario-based assessments quantify these impacts in the form of performance curves that indicate the probability that loss will exceed a certain value, over the full range of possible values. Many decision-makers are unable to use this probabilistic information and want a specific answer to the question: how bad will the loss be? It is probably best to provide this answer in the form of an expected performance together with upper and lower bounds.

Expected performance can be mathematically derived from the performance curve through numerical integration. Figure 8-1 illustrates this process. The figure shows a scenario performance curve for an unidentified performance-measure. In Figure 8-1, the performance curve has been divided into 5 equal stripes, each stripe having a probability of occurrence of 20%, conditioned on the occurrence of the earthquake scenario. Also identified in the figure is a central value for each stripe. The value of the mean performance measure is given by the formula:

$$\overline{PM} = \sum_{i=1}^{k} P(i) PM_i \qquad (8\text{-}1)$$

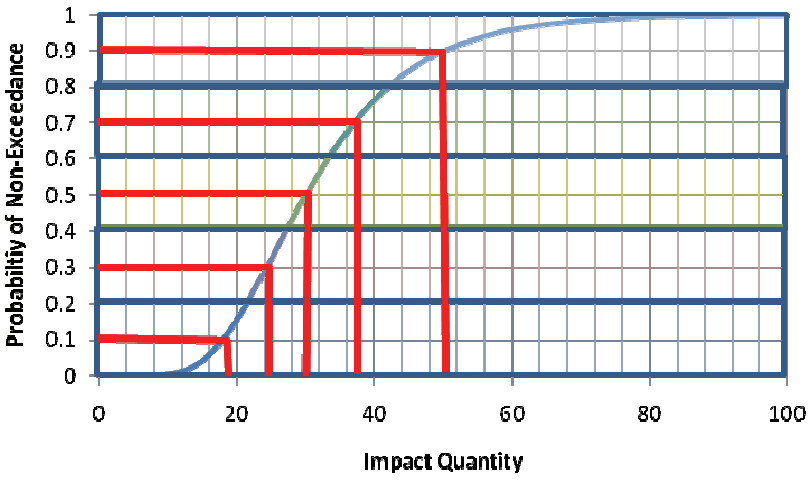

Figure 8-1 Hypothetical Peformance Function for Building Illustrating Calculation of Mean value of Performance Measure

Where, $\overline{PM}$ is the mean value of the performance measure; *P(i)* is the probability of occurrence of a value of the performance measure within strip "*i*"; PM_i is the central value of the performance measure for stripe "*i*"; and *k* is the number of stripes. For the case illustrated in the figure, in which each stripe represents a probability of occurrence of 0.2, the mean value is given by 0.2 (19 + 24 +30 + 38 + 50) = 32. It should be noted that this is modestly larger than the median value, which in this case has a value of 30. As the distribution's skew increases, so too does the difference between the median and mean values, with the mean typically being larger than the median. Any number of stripes can be used in this integration process and the stripes do not need to be of uniform size. As the number of stripes used in the integration is increased, the accuracy of the integration will also increase.

An alternative means of finding the mean value is to assume that the performance curve is approximated by a lognormal distribution, with median value, PM_{50}, and dispersion, β. The median value is the value exceeded 50% of the time, which in the case of the figure, is a value of 30, as previously stated. The dispersion can be approximated as:

$$\beta = 0.43\left(\frac{PM_{50}}{PM_{10}} - .782\right) \qquad (8\text{-}2)$$

where, PM_{50} and PM_{10} are the 50th and 10th percentile values read off the loss curve. The mean value can be determined as:

$$\overline{PM} = PM_{50}e^{\beta^2/2} \qquad (8\text{-}3)$$

where all terms have been previously defined. For the example loss curve of Figure 8-1, these equations provide a value of β of 0.34 and a value of the

mean of 31.8, which compares well with the value of 32 computed by numerical integration, and which is also approximate.

It is also important to specify bounds on this performance for decision-makers wanting to use mean performance measures, so that they have some understanding of the chance that performance will either be superior or inferior to the mean. Often the PM_{10} and PM_{90} values are appropriate bounds for this purpose.

8.4 Time-based Assessments

ments
ge annual
iance
useful in
ies.

Time-based assessments can be used to provide the average annual value of a performance measure. The average annual value of a performance measure is useful in cost-benefit analyses and also for determining a reasonable insurance premium for a property.

The average annual value is the mean value obtained from a time-based performance curve, such as that shown in Figure 2-4. It can be obtained in the same way mean values are obtained from scenario-based performance curves as described in the previous section. Figure 8-2 illustrates this process for a hypothetical annual performance curve. For this example, the computed mean annual value is 0.2 (0.05 + 0.07 + 0.1 + .0.14 + 0.19) = 0.11 per year. If the performance measure were in casualties, this would indicate an average annual casualty rate of 0.11. If the performance measure were repair costs, in millions of dollars, this would indicate an annual average repair cost of $110,000.

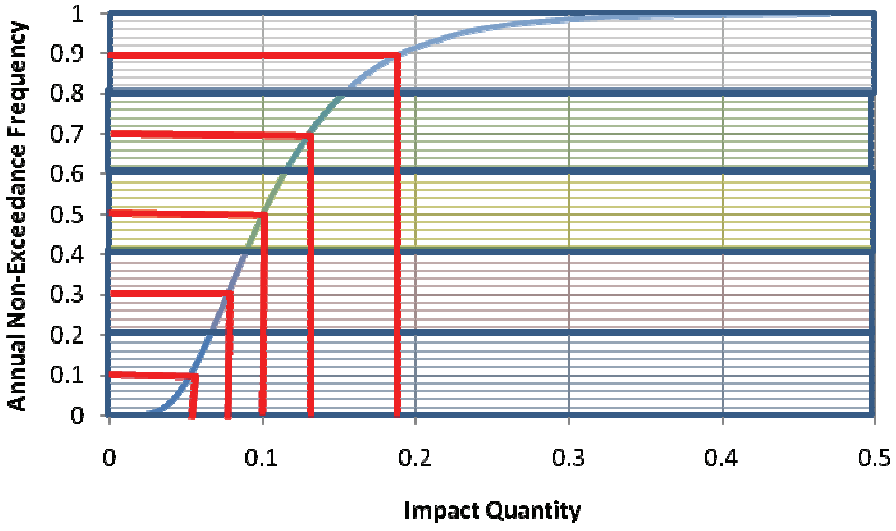

Figure 8-2 Hypothetical Annual Performance Function for Building Illustrating Calculation of Mean Annual value of Performance Measure

Of course, earthquake losses do not really occur in annual increments. However, over a period of many years, the average annual loss should approximate the total loss well in that period of time, divided by the number of years in that period. As such, when the performance measure is repair cost, the average annual value of repair cost is a reasonable measure of the insurance premium that one should be willing to pay to insure against possible future repair costs. If the performance measure is expanded to include the probable costs associated with loss of use, this can also indicate the reasonable value of insurance premiums to cover occupancy interruption costs.

Average annual repair costs are a good measure of the insurance premium a person should be willing to pay.

The average annual performance measure can also be used as an input to cost-benefit studies that are useful in deciding how much should be invested in providing seismic resistance in a building, over and above any legal requirements. Essentially this process is performed by evaluating the present value of the average annual costs associated with future earthquake damage that is avoided by enhanced resistance, against the present value of the costs associated with enhanced seismic resistance. The Net Present value of a stream of future expenditures is given by the formula:

$$NPV = A\left[\frac{1-\frac{1}{(1+i)^t}}{i}\right] \tag{8-4}$$

where *NPV* is the net present value of a stream of equal annual expenditures (or avoided expenditures), *A*, conducted over a period of years *t*. The variable, "*i*", in this equation is variously called the internal rate of return, or the interest rate. It represents either the amount of interest one would expect to incur if one borrowed money from others, or the amount of return on one's investment one expects to make.

For decisions associated with property with an anticipated life of more than 40 years, the annual average cost or saving can be considered an annuity of infinite term. In this case, Equation 8-4 reduces to the simpler form:

$$NPV = \frac{A}{i} \tag{8-5}$$

As an example of the use of this analysis, consider a hypothetical company (Acme) with operations in a single building in an earthquake-prone region. A performance assessment of the building indicates negligible risk of life endangerment; however, it does indicate an annual average repair cost of

$150,000 and average annual repair times of 5 days. ACME estimates that each day of downtime costs the company $100,000 in profit. ACME's engineer has determined that a seismic upgrade of the building will reduce the average annual repair cost to $50,000 and the average annual repair time to 3 days. The estimated cost of the upgrade, including design fees and ACME's internal costs is $3,000,000. ACME uses an internal rate of return for their investments of 7%. If ACME expects to remain in the building for 10 years should they invest in the upgrade? If ACME expects to remain in the building indefinitely, should they invest in the upgrade?

The average annual benefit of performing the upgrade is the avoided average annual repair cost ($150,000 - 50,000 = $100,000) and the avoided lost profit per year ((5 days - 3 days) ($100,000) = $200,000) for a total reduction in average annual loss of $300,000.

The Net Present Value of the avoided average annual loss for 10-year and an indefinite period is given by:

$$NPV_{10\,years} = \$300{,}000\left[\frac{1-\frac{1}{1.07^{10}}}{.07}\right] = \$2{,}108{,}000$$

$$NPV_{indefinite} = \frac{\$300{,}000}{.07} = \$4{,}290{,}000 \qquad (8\text{-}6)$$

Since the Net Present Value of the avoided annual average loss over a 10-year period is less than the cost of the upgrade, it would not make economic sense for the company to invest in this upgrade. However, if the company anticipates remaining in this building indefinitely, there would be a net benefit to investing in the upgrade.

Time-based assessments provide a convenient means to determine the maximum loss likely in a specified return period, a useful tool for some risk-adverse decision makers.

While cost benefit analyses of this type are useful tools for some decision-makers, not all decision makers prefer this approach. In the above example, it is possible, though unlikely, that within 10 years of the date that the company elects not to upgrade their building, an earthquake actually occurs resulting in real cost to the company that is substantially in excess of the $3,000,000 upgrade cost. In this unlikely, but possible scenario, the company would have been economically better off if they had invested in the seismic upgrade than not.

Some decision-makers, who are risk-adverse, would want to avoid the realistic possibility of such a scenario. These risk-adverse decision-makers would prefer basing decisions on a loss with a specific anticipated probability

of occurrence, or return period, such as a 10-year, 50-year or 100-year losses Time-based assessments can also be used to provide this type of information.

Return period is equal to the inverse of the annual frequency of exceedance. Thus, if one were interested in a 50- year loss, one could enter the time-based performance curve for the loss at an annual probability of exceedance of 2% (1/50) and determine the loss directly at this level. A risk-adverse decision maker, with a risk tolerance of 50-years, might be willing to spend as much as the amount of this projected loss, but not more, to avoid incurring the loss.

8.5 Probable Maximum Loss

Many commercial lenders and real estate investors use a measure of seismic risk known as Probable Maximum Loss (PML). Many such investors will either not make an investment in a property, or require the purchase of earthquake insurance, when the projected PML exceeds a threshold value, often 20%.

Intensity-based assessments directly provide Scenario Expected losses, Scenario Upper bound losses and Probable losses as described in ASTM E-2026 and ASTM E-2557.

Two ASTM Standards, E-2026 and E-2557 set standard procedures for seismic evaluations and the development of PMLs for use by the financial industry. These standards define several types of PML including:

- *Scenario Expected Loss* – this represents the mean repair cost, expressed as a percentage of building replacement value, for a particular intensity of ground motion, typically defined as that ground motion having a 475-year return period.
- *Scenario Upper Loss* – this represents the 90th percentile repair cost, expressed as a percentage of building replacement value, for a particular intensity of ground motion, typically defined as that ground motion having a 475-year return period.
- *Probable Loss* – that amount of loss, having a specific probability of exceedance, over a specified number of years.

Both the Scenario Expected Loss and Scenario Upper Losses can be determined by performing intensity-based assessments for response spectra having the specified return period. The Scenario Expected Loss is obtained by computing the mean repair cost for the assessment. The Scenario Upper Loss is determined directly from the performance curve for repair cost at the 90th percentile.

Probable loss can be derived directly from a time-based assessment using an appropriate return period for the assessment.

Appendix A
Probability, Statistics & Distributions

A.1 Introduction

This appendix provides a brief tutorial on probability and statistics including methods of expressing probabilities in the form of statistical distributions. It is intended to provide readers unfamiliar with these topics the basic information essential to understanding the process used to account for the inherent uncertainties in performance assessment. Interested readers can obtain additional information on this subject by referring to textbooks on probability and statistics, and on structural reliability theory. In particular, Benjamin and Cornell (Benjamin and Cornell, 1970) contains a wealth of information on this topic.

A.2 Statistical Distributions

Statistical distributions are mathematical representations of the probability of encountering a specific outcome given a set of possible outcomes. The set representing all possible outcomes is termed a population. There are generally two broad types of populations considered in statistical studies. The first of these is a finite population of outcomes, where each possible outcome has a discrete value representing one of the finite number of possible outcomes. The second of these is an infinite population of possible outcomes. Each is discussed separately, below.

A.2.1 Finite Populations and Discrete Outcomes

Consider the classic case of a coin thrown in the air to determine an outcome. One of two possible outcomes will occur each time the coin is tossed. One potential outcome is that the coin will land "heads-up" and the other that it will land "heads-down." Which way the coin will land on a given toss is a function of a number of factors including which way the coin is held before the toss; the technique we use to toss the coin; how hard or high the coin is tossed, how much rotation it is given, and how, it lands. We could never hope to precisely simulate each of these factors, and therefore, the occurrence of a "heads-up" or "heads-down" outcome in a given coin toss appears to be a random phenomena, that is not predictable. There is an equal chance that

the coin will land "heads up" or "heads down," and we can not know before tossing the coin, which way it will land.

If we toss a coin in the air one time there are two possible outcomes. These two outcomes – coin lands "heads-up" and coin lands "heads-down" completely define all possibilities for one coin toss and therefore, the probability that the coin will land either heads up or heads down is 100%. In essence, this illustrates the total probability theorem, that is, that the sum of the probabilities of all possible outcomes will be 100%, which can also be expressed as 1.0.

The probability that the coin will land "heads-up" is 50%, or 0.5. The probability that it will land "heads-down" is the inverse of this, calculated as one minus the probability of "heads-up," or (1-0.5) = 0.5, also 50%.

If we toss the coin in the air many times, we would expect that we would get a "heads-up" outcome in half of these tosses and "heads-down" outcome in the other half. This does not mean that every second toss of the coin will have a "heads-up" outcome. We might obtain several successive "heads-up" outcomes or several successive "heads-down" outcomes; however, over a great many tosses, we should have approximately the same number of each possible outcome.

A.2.2 Combined Probabilities

A combined probability is the probability of experiencing a specific combination of two or more independent outcomes. We can calculate the combined probability of two independent events as the product of the probability of outcome 1 and the probability of outcome 2. That is:

$$P(A+B) = P(A) * P(B) \qquad \text{(A-1)}$$

To illustrate this, if we toss the coin into the air two times, there is a 50% chance, each time, that the coin will land "heads-up." The chance that the coin will land "heads-up" both times is calculated, using equation A-1, as the probability of landing "heads-up" the first time (0.5) multiplied by the probability that it will land "heads-up" the second time (0.5), or (0.5 x 0.5) = 0.25, or 25%.

This probability means that if we toss a coin into the air twice in succession, a large number of times, and record the number of "heads-up" outcomes, in each pair of tosses, approximately 25% of the total number of pairs of tosses will have two successive heads-up outcomes. The 25% probability does not mean that every fourth time we make a pair of coin tosses we will get two successive heads-up outcomes. There is some possibility that we will get

two successive heads-up outcomes several times in a row and there is also a possibility that we will have to make more than four pairs of coin tosses to obtain an outcome of two heads-up in any of the pairs of tosses. However, over a very large number of pairs of tosses, one fourth of the pairs should be successive heads-up outcomes.

If we toss the coin into the air three times, there is again a 50% chance on each toss that the coin will land "heads-up." The probability that the coin will land "heads-up" all three times is given by the probability that it will land "heads-up" the first two times (25%) multiplied by the probability that it will land "heads-up" the third time (50%), or (0.25 x 0.5) = 0.125, or 12.5%. If we repeat this exercise with 4 coin tosses, the probability that all four will land "heads-up" will be the probability that the first three tosses will land "heads-up" (12.5%) times the probability that the fourth toss will land "heads-up" or (0.125 x 0.5 = 0.0625) or 6.25%. That is, there is approximately a 6% chance that we will have two successive pairs of coin tosses both having two heads-up outcomes.

A.2.3 Mass Distributions

A probability mass distribution is a plot of the probability of occurrence of each of the possible outcomes in a finite population of discrete outcomes, such as a coin landing either "heads-up" or "heads-down" a specified number of times in N-throws.

Consider the case of four coin tosses. As shown in the previous section, there is a 6.25% chance that all four coin tosses will land "heads-up." There is also a 6.25% chance that all four coin tosses will land "heads-down" or that none of the coin tosses will land "heads-up." The chance that three of the four coin tosses will land "heads-up" is equal to the combined chance of any of the following outcomes: "T, H, H, H"; "H, T, H, H"; "H, H, T, H" or "H, H, H, T," where "H" indicates "heads-up" and "T" "heads-down ." The chance of each of these outcomes is the same as having all four tosses landing "heads-up" or 6.25%. Therefore, the chance of exactly three out of four tosses landing "heads-up" is equal to 6.25% for the "T, H, H, H" combination, plus 6.25% for the "H, T, H, H" combination, plus 6.25% for the "H, H, T, H" combination, plus 6.25% for the "H, H, H, T" combination, or a total of 25% (6.25% + 6.25% + 6.25% +6.25%). Similarly, the probability that exactly three of the four tosses will be "heads-down," or that only one of the tosses will land "heads-up" is 25%. We can use similar approaches, to show that the probability that exactly half the tosses will land "heads-up" is 37.5%.

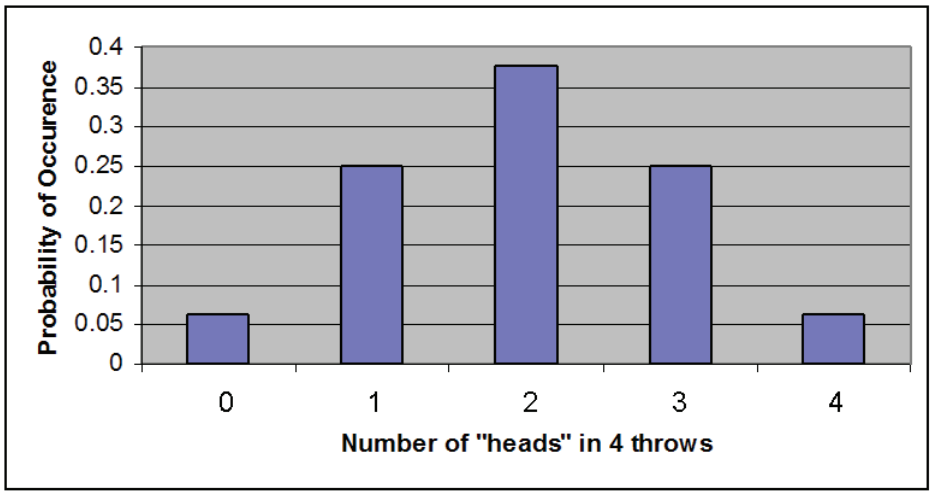

Figure A-1 Probability mass function indicating the probability of "n" numbers of "heads-up" outcomes in four successive coin tosses

Figure A-1 is a plot that shows the probability of obtaining zero, one, two, three, or four "heads-up" outcomes from four coin tosses. Plots of this type are termed probability mass distributions. By entering the plot along the horizontal axis, at a particular outcome, for example – "1 heads-up" out of four throws, we can read vertically to see the probability of this outcome, which is 25%. The probability of having not more than one "heads-up" toss in four tosses, is calculated as the sum of the probability of no "heads-ups", which is 6.25% plus the probability of 1 "heads-up" which is 25%, for a cumulative probability of 31.25%. Another way to say this is that the probability of non-exceedance for "1 heads-up in 4 coin tosses" is 31.25%. The inverse of this is that the cumulative probability of more than "1 heads-up" is 1–0.3125 or 68.75%. This could also be called the probability of exceedance of "1 heads-up toss in 4 tosses."

A.2.4 Continuous Distributions

The distribution of possible "heads-up" throws in a finite number of coin tosses is an example of a discrete distribution. That is, there are only a finite number of possible outcomes, and these have discrete values, in the example above, 0, 1, 2, 3 or 4 "heads-up" outcomes in 4 coin tosses.

For many situations, the possible outcomes are not a finite number of discrete possibilities but rather a continuous range of possibilities. An example of such a continuous distribution is that of possible compressive strengths obtained from concrete cylinder compression tests, where all cylinders are from concrete mixed using the same mix design. Such a distribution will have the form shown in Figure A-2, where the dispersion in strength is due to minor variability in the amounts of cement, amount of water, strength of

aggregates, cylinder-casting technique, curing technique, and other factors. There are an infinite number of possible outcomes for the strength of any particular cylinder test. The form of the distribution shown in Figure A-2 is termed a probability density function.

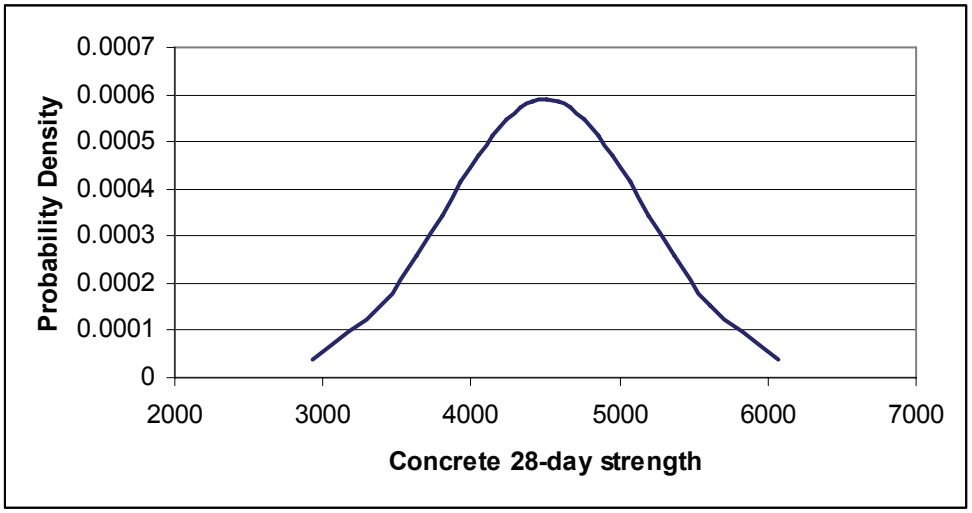

Figure A-2 Distribution of possible concrete cylinder strengths for a hypothetical mix design

The area under the curve of a probability density function, between any two points along the horizontal axis gives the probability that the value of any member of the population will be within the range defined by the two values. Figure A-3 illustrates this. In the figure, the probability that a single cylinder test, conforming to the population represented by Figure A-2 will have strength that is greater than 4,000 psi but less than or equal to 5,000 psi is given by the area under the curve between the two strength values, which in this case has a calculated probability of 54%. That is, there is a 54% chance that any cylinder test in this population will have strength between 4,000 psi and 5,000 psi.

A.3 Common Forms of Distributions

A.3.1 Normal Distributions

The probability density function illustrated in Figure A-2 has a special set of properties known as a normal distribution. In a normal distribution the "median" outcome, that is, the outcome that is exceeded 50% of the time is also equal to the average or "mean" outcome, which is the total value of all possible outcomes, divided by the number of possible outcomes. In the example above, the median outcome is that the concrete has a compressive strength of 4,500 psi. The average strength of all cylinders tested is also 4,500 psi. Normal distributions are also symmetric. That is, there is an equal

probability of having a value at a defined measure above the average, say 1,000 psi above the mean (5,500 psi in Figure A2), as there is of having a value the same defined distance below the average, in this example, 1,000 psi below the mean or 3,500 psi.

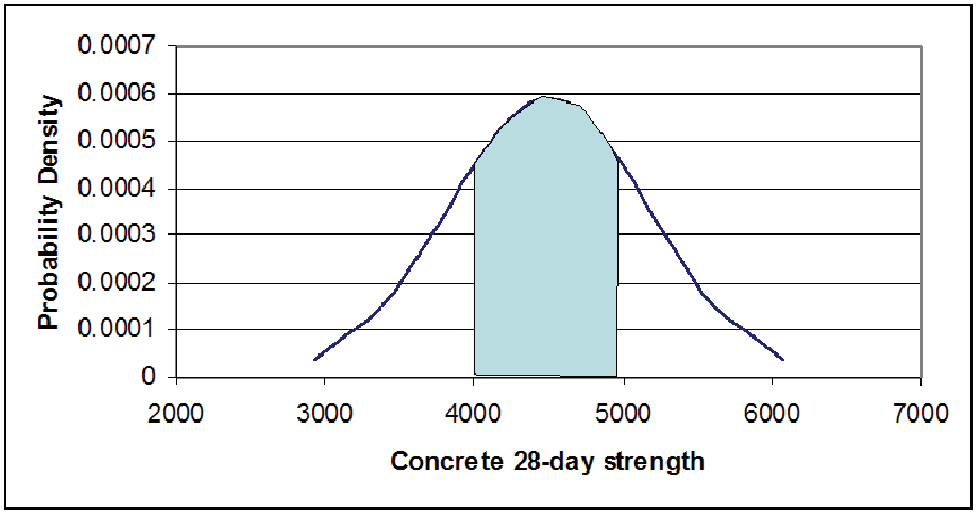

Figure A-3 Calculation of probability that a member of the population will have a value within a defined range.

Two parameters are used to uniquely specify the characteristics of a normal distribution, namely, the mean value $\bar{x}$ and standard deviation, σ. Equations A-2 and A-3, define these values for a random variable x (e.g. compressive strength of concrete as measured by cylinder testing) and a sample of size N:

$$\bar{x} = \frac{\sum_{i=1}^{N} x_i}{N} \tag{A-2}$$

$$\sigma = \sqrt{\frac{1}{N-1}\sum_{i=1}^{N}\left(x_i - \bar{x}\right)^2} \tag{A-3}$$

where N is the size of the population. If a parameter is normally distributed, that is, its population of possible outcomes is represented by a normal distribution, having mean value $\bar{x}$ and standard deviation σ, it is possible to determine the value x of an outcome that has a specific probability of exceedance, based on the number of standard deviations that the value x lies away from the mean, $\bar{x}$. For example, there is a 97.7% chance that the value of any single outcome x will be greater than $\bar{x}$ -2σ, an 84.1% chance that the value of any single outcome x will be greater than $\bar{x}$ - σ, a 50% chance it will be greater than $\bar{x}$, a 15.8% chance it will exceed $\bar{x} + \sigma$ and a 2.3% chance that it will be greater than $\bar{x}$ +2σ. Standard tables that are available

in most texts on probability theory indicate the probability that the value of any outcome in a normally distributed population of potential outcomes will exceed a value that is a defined number of standard deviations from the mean. The number of standard deviations above or below the mean that will have a specified probability of exceedance is sometimes termed the Gaussian variate and the probability tables that give these values, Gaussian tables. Table A-1 indicates some representative values of the Gaussian variate for several commonly referenced probabilities.

Table A-1 Gaussian Variate for Normal Distribution for Common Probabilities

Probability of Non Exceedance	Number of Standard Deviations below Mean		Probability of Non Exceedance	Number of Standard Deviations Above Mean
.02	-2.0		.60	.25
.05	-1.64		.70	.52
.10	-1.28		.80	.84
.158	-1.0		.84	1.0
.20	-.84		.90	1.28
.30	-.52		.95	1.64
.40	-.25		.98	2.0
.50	0			

Structural engineers use normal distribution to represent the distribution of values for many random quantities (e.g., concrete compressive strength). In addition to the mean, median and standard deviation, another often-used parameter to characterize the properties of a normal distribution is the coefficient of variation (COV). The coefficient of variation is calculated as the standard deviation, σ, divided by the mean value $\bar{x}$. It is useful because it represents a normalized measure of the scatter inherent in a normally distributed population. Figure A-4 plots probability density functions for several normal distributions, all having mean values of 1.0 and coefficients of variation of 0.1, 0.25, and 0.5, respectively.

A.3.2 Cumulative Probability Functions

An alternative means of plotting probability distributions is in the form known as a cumulative probability function. A cumulative probability function plot shows the probability that an outcome in the population of possible outcomes will have a value that is less than or equal to the specified value *x*. This probability is sometimes termed the probability of non-exceedance. Cumulative density plots are obtained by integrating over the probability density function to determine the area under the curve between the lowest possible value of *x* and any other value of *x*. Figure A-5 presents

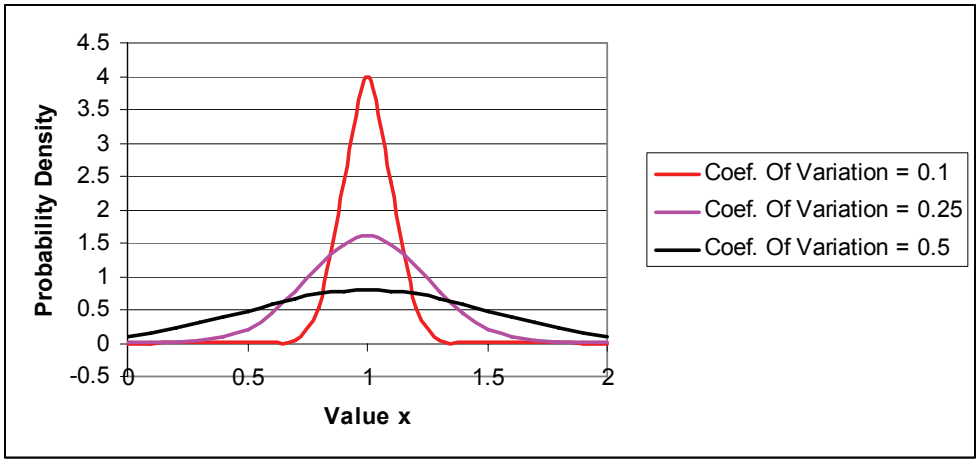

Figure A-4 Probability density function plots of normal distributions with mean values of 1.0 and coefficients of variation of 0.1, 0.25 and 0.5.

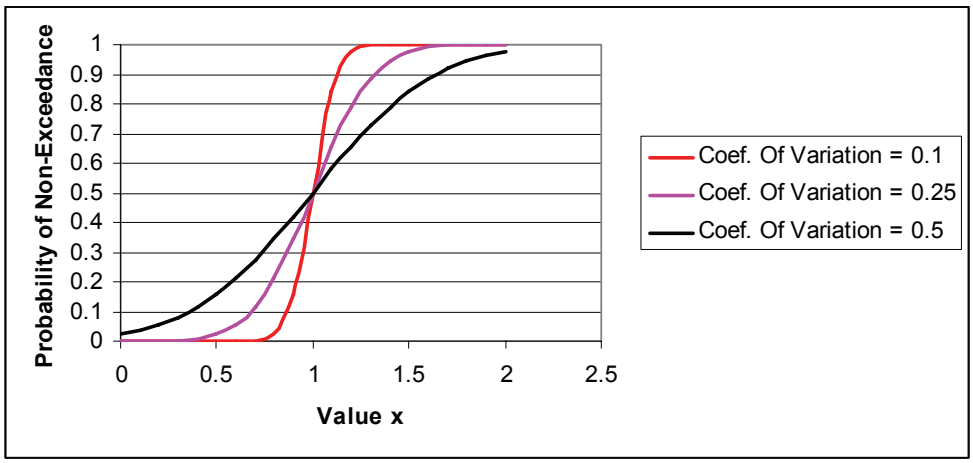

Figure A-5 Cumulative probability plots of normal distributions with coefficients of variation of 0.1, 0.25, and 0.5.

cumulative probability plots for the same normally distributed populations previously shown in Figure A-4. From either series of plots, it is possible to observe that the larger the coefficient of variation becomes, the greater the amount of scatter in possible outcome values.

A.3.3 Lognormal Distributions

Although normal distributions represent some random variables well, they do not represent all variables well. Some variables have skewed distributions. In skewed distributions, the mean value, $\bar{x}$, will be either greater than or less than the median value. In structural reliability applications, such as performance assessment, it is common to use a specific type of skewed distribution known as a lognormal distribution. This is because the skew inherent in lognormal distributions can reasonably represent the distributions

observed in many structural engineering phenomena, such as the distribution of strength in laboratory specimens.

The lognormal distribution has the property that the natural logarithm of the values of the population, $\ln(x)$, are normally distributed. The mean and the median of the natural logarithms of the population have the same value, which is equal to $\ln(\theta)$, where θ is the median value. In these guidelines, the standard deviation of the natural logarithms of the values, $\sigma_{\ln(x)}$, is called the dispersion and is denoted by the symbol, β. For relatively small values of dispersion, the value of β is approximately equal to the coefficient of variation for x. Together, the values of θ and β completely define the lognormal distribution for a population.

Figure A-6 plots probability density functions for three lognormally-distributed populations having median values of 1.0 and dispersions of 0.1, 0.25 and 0.5 respectively. Figure A-7 plots this same data in the form of cumulative probability functions.

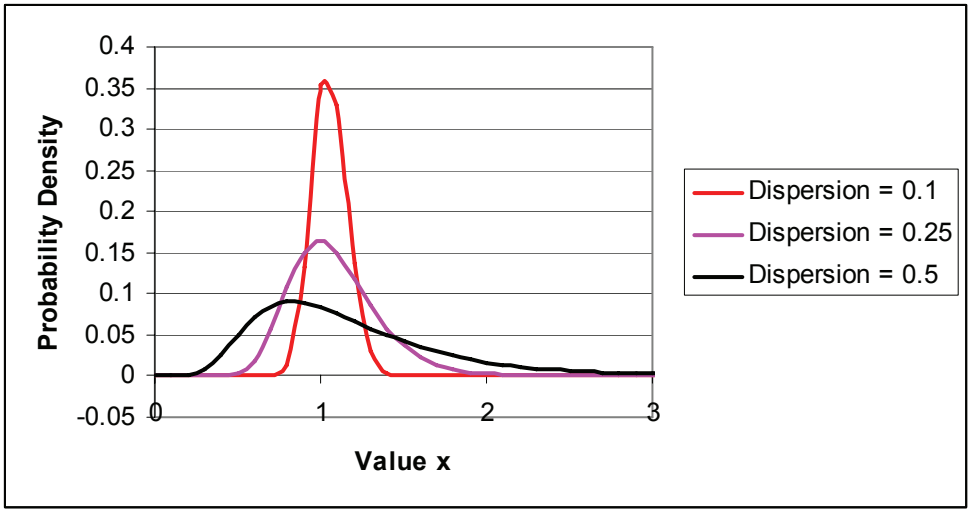

Figure A-6 Probability density function plots of lognormal distributions with median values of 1.0 and dispersions of 0.1, 0.25 and 0.5.

As can be seen from the plots, for small values of the dispersion, the distribution approaches the shape of the normal distribution, but as the dispersion increases in value, the distribution becomes more and more skewed. This skew is such that there is nil probability of incurring a negative value in the distribution (because the logarithm of a negative number is positive) and extreme values above the median are substantially more probable than extreme values below the median. Consider the distribution of possible actual yield strengths of various steel parts, all conforming to a specific ASTM specification and grade. Since this variable (yield strength) cannot take on values of less than zero, the lognormal distribution could be

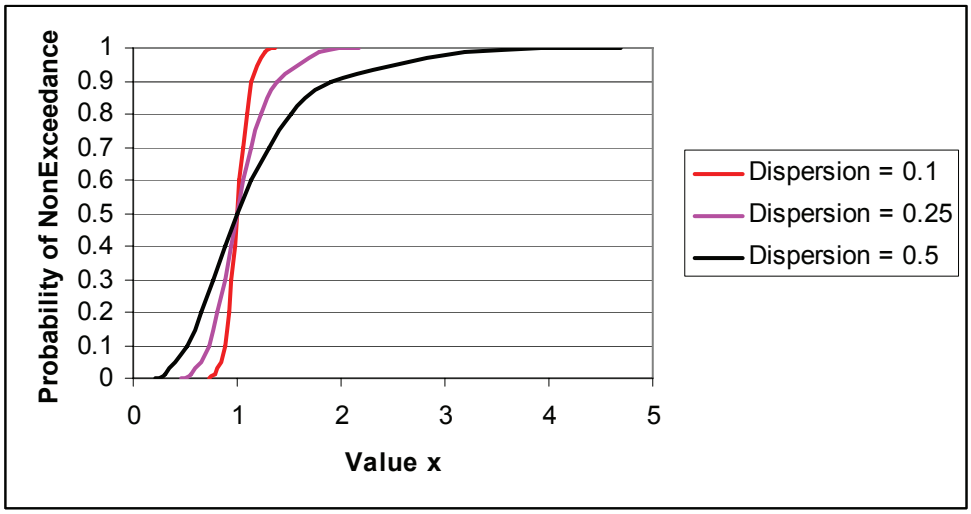

Figure A-7 Cumulative probability plots of lognormal distributions with median values of 1.0 and dispersions of 0.1, 0.25, and 0.5.

used to describe the variation in possible steel strength using a median value and dispersion. In this example, the median value will be substantially higher than the minimum specified value, which, is intended to have a very low probability of non-exceedance by any steel conforming to the specification.

The procedures presented in these guidelines use lognormal distributions to represent many uncertain factors that affect performance including: the distributions of intensity for a scenario earthquake; the values of response parameters given an intensity; the probability of incurring a damage state as a function of response parameter, herein termed a fragility; and the probability of incurring a specific level of direct economic loss, downtime and casualties, given a damage state. These lognormal distributions are derived in a variety of ways. Specifically,

- Intensity distributions are obtained based on statistical analysis of actual ground motion data recorded from past earthquakes, and represented in the form of equations known as attenuation relationships
- Response parameter distributions are obtained by performing suites of structural analyses using multiple ground motion recordings and varying the strength, stiffness, damping, and ductility capacity of the structural elements
- Fragility distributions are obtained primarily through laboratory testing or observation of actual damage in past earthquakes
- Loss distributions are obtained through performing multiple calculations of loss, varying the factors that affect the loss, such as contractor

efficiency, and number of persons likely to be occupying a building at the time of the earthquake

Regardless of how these distributions are derived, they are represented by two variables, the median value, θ, and dispersion, β.

The mean m_Y and standard deviation, σ_Y, of a lognormal distribution, *Y*, can be calculated from θ_Y and β_Y as follows:

$$m_Y = \theta_Y \exp\left(\frac{\beta_Y^2}{2}\right) \tag{A-4}$$

$$\sigma_Y^2 = m_Y^2\left[\exp\left(\beta_Y^2\right) - 1\right] \tag{A-5}$$

The coefficient of variation, ν_Y, is given by

$$\nu_Y = \frac{\sigma_Y}{m_Y} = \sqrt{\exp(\beta_Y^2) - 1} \tag{A-6}$$

Many common spreadsheet applications also have embedded within them, functions that will automatically solve lognormal distribution problems. For example, in Microsoft Excel, the LOGNORMDIST function will determine the cumulative probability of non-exceedance of any value in a population *Y*, based on input of the value, *y*, the natural logarithm of the median, $\ln\theta_Y$, and the dispersion, β_Y. The Excel input is of the form =LOGNORMDIST (*y,* $\ln\theta_Y$, β_Y). Similarly, the LOGINV function can be used to determine the value of *y*, at a given cumulative probability of non-exceedance, based on the desired probability, *p*, which must be less than 1.0, the natural logarithm of the median $\ln\theta_Y$ and the dispersion, β_Y. The Excel input is of the form =LOGINV(*p,* $\ln\theta_Y$, β_Y).

Appendix B
Ground Shaking Hazards

B.1 Scope

This appendix presents supplemental information on characterization of ground shaking hazards and an alternate procedure for scaling ground motions for scenario-based assessments.

B.2 Attenuation Relationships

Attenuation relationships relate ground motion parameters to the magnitude of an earthquake and the distance away from the fault rupture. Relationships have been established for many ground motion parameters including

- Peak horizontal ground acceleration, velocity, displacement and corresponding spectral terms
- Peak vertical ground acceleration, velocity, displacement and corresponding spectral terms

Attenuation relationships are developed by statistical evaluation of large sets of ground motion data. Relationships have been developed for different regions of the United States (and other countries) and different fault types (i.e., strike-slip, dip-slip and subduction). These relationships are only as good as the dataset from which they were derived; the greater the size of the data set, the more robust the relationship.

Chapter 4 presents the basic construction of ground motion attenuation relationships. Attenuation relationships generally return a geometric mean[1] of two horizontal spectral ordinates.

Table B-1 presents selected North American ground motion attenuation relationships. These attenuation relationships all use moment magnitude,

[1] For a given pair of horizontal earthquake histories, the geometric mean ($\overline{S}_g$ of the spectral ordinates of the two components (S_x and S_y) is generally used to characterize the pair of histories: $\overline{S}_g = \sqrt{S_x S_y}$. Since the functional form of the attenuation relationship involves the natural log of the ground motion parameter, the geometric mean of the ordinates (which is equivalent to the arithmetic mean of the logs of the ordinates) is used instead of the arithmetic mean.

M_W, to define earthquake magnitude but use different definitions of site-to-source distance. Figure B-1 defines some of these distance parameters.

Table B-1 Ground Motion Attenuation Relationships

Model	Calculated[1]	Site Conditions[2]	Variables[3]	Ranges		
				T_n (secs)	r (km)	M_W [4]
Western North America (WNA)						
Abrahamson and Silva, 2008	PHA, PHV, Sah	$180 \le V_{S30} \le 2000$ [5]	M, r_{rup}, r_{jb}, V_{S30}, F, H, B	0-10	0-200	5-8.5
Boore and Atkinson, 2008	PHA, PHV, Sah	$180 \le V_{S30} \le 1300$	M, r_{jb}, V_{S30}, F			5-8
Campbell and Bozorgnia, 2008	PHA, PHV, Sah	$150 \le V_{S30} \le 1500$	M, r_{rup}, r_{jb}, V_{S30}, F, H, B			4-8.5 (s) 4-8 (r) 4-7.5 (n)
Chiou and Youngs, 2008	PHA, PHV, Sah	$150 \le V_{S30} \le 1500$	M, r_{rup}, r_{jb}, V_{S30}, F, H, B			4-8.5 (s) 4-8 (r&n)
Idriss, 2008	PHA, Sah	$V_{S30} > 900$, $450 \le V_{S30} \le 900$	M, r_{rup}, F			4.5-8[5]
Central and Eastern North America (CENA)						
Atkinson & Boore, 1997	PHA, Sah	Rock	M, r_{hypo}	0-2	10-300	4-9.5
Campbell, 2003	PHA, Sah	Hard rock	M, r_{rup}	0-4	1-1000	5-8.2
Toro et al., 1997	PHA, Sah	Rock	M, r_{jb}	0-2	1-100	5-8
Subduction Zones						
Atkinson & Boore, 2003	PHA, Sah	Rock to poor soil	M, r_{hypo}, +	0-3	10-300	5.5-8.3
Youngs et al., 1997	PHA, Sah	Rock, Soil	M, r_{rup}, F, H	0-4	0-100	4-9.5

1. PHA = peak horizontal ground acceleration, PHV = peak horizontal ground velocity, Sah = horizontal spectral acceleration
2. V_{S30} = Average shear wave velocity in the upper 30 meters of sediments, unit: m/s
3. r_{rup} = closest distance to the rupture surface, r_{jb} = closest horizontal distance to the vertical projection of the rupture, r_{hypo} = hypocentral distance, M = magnitude, F = fault type, H = hanging wall, B = 3-D basin response.
4. s = strike-slip faulting, r = reverse faulting, n = normal faulting.
5. Ranges are not specified (Abrahamson and Silva 2008; Idriss 2008) but are estimated based on the datasets.

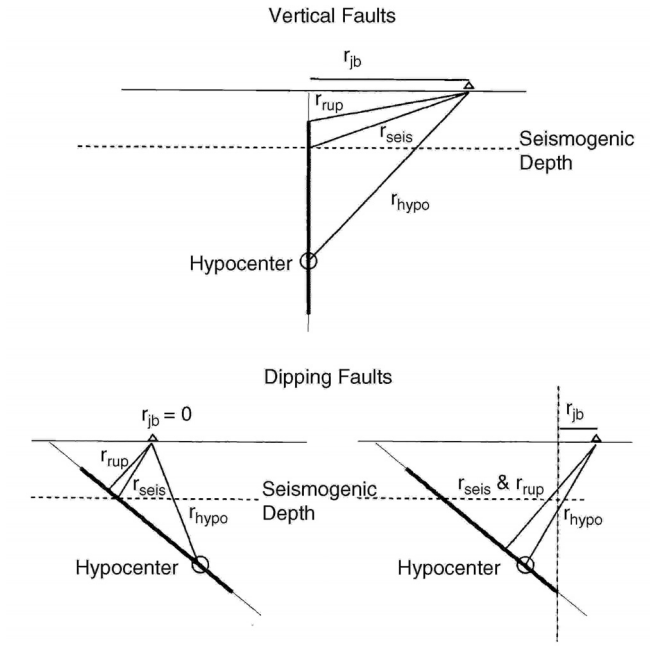

Figure B-1 Site-to-source distance definitions (Abrahamson and Shedlock, 1997)

B.3 Fault Rupture Directivity and Maximum Direction Shaking

Rupture directivity causes spatial variation in the amplitude and duration of ground motions in the regions surrounding faults. Propagation of rupture towards a site produces larger amplitudes of shaking at periods longer than 0.6 second and shorter strong-motion durations than for average directivity conditions.

Somerville et al. (1997) developed modifications to the empirical attenuation relations of Abrahamson and Silva (1997) to account for these variations. This and other attenuation functions of that time were constructed from strong motion databases that included few near-fault records and so could not adequately represent the spectral demands associated with near-fault shaking.

Somerville (1997) identified fault rupture directivity parameters θ and X for strike-slip faults and ϕ and Y for dip slip faults as shown in Figure B-2; and developed three ground motion parameters to characterize directivity: (1) *Amplitude factor*: bias in average horizontal response spectrum acceleration with respect to Abrahamson and Silva (1997); (2) *Duration factor*: bias in duration of acceleration with respect to Abrahamson and Silva (1997); and (3) *Fault-normal/Average amplitude*: ratio of fault normal to average (directivity) horizontal response spectrum acceleration. Bounds were set on the range of applicability of the directivity model.

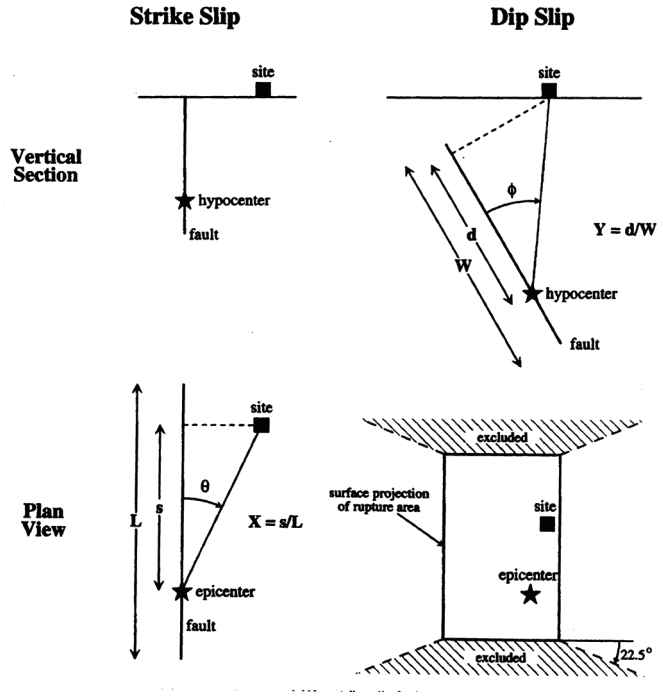

Figure B-2 Fault rupture directivity parameters (Somerville et al., 1997)

The recently developed Next Generation Attenuation (NGA) relationships for the Western United States were developed using a database that included many near-fault ground motion recordings. These relationships predict geomean spectral demand of recorded near-fault motions (i.e., average directivity) well with little bias (Huang et al. 2008a, 2008b). Huang et al. also report the median and 84th percentile ratios of maximum and minimum direction spectral demand to NGA-calculated geomean spectral demand for average directivity (i.e., all near-fault records) and the forward directivity region.

B.4 Probabilistic Seismic Hazard Assessment

B.4.1 Introduction

Performance-assessment will often utilize site-specific characterization of the ground shaking associated with different probabilities of exceedance or return periods. Such characterizations are routinely performed using Probabilistic Seismic Hazard Assessment. The following subsections provide introductory information on this technique, drawing substantially from Kramer (1996), McGuire (2004) and Bozorgnia and Bertero (2004).

B.4.2 Probabilistic Seismic Hazard Assessment Calculations

General

In this technique, probability distributions are determined for the magnitude of each earthquake on each source, $f_M(m)$, the location of the earthquake in or along each source, $f_R(r)$, and the prediction of the response parameter of interest $P(\text{pga} > \text{pga}' | m, r)$. Kramer describes this as a four-step process enumerated below and depicted in Figure B-3.

1. Identify and characterize (geometry and potential M_W) of all earthquake sources capable of generating significant shaking (say $M_W \geq 4.5$) at the site. Develop the probability distribution of rupture locations within each source. Combine this distribution with the source geometry to obtain the probability distribution of source-to-site distance for each source.
2. Develop a distribution of earthquake occurrence for each source using a recurrence relationship. This distribution can be random or time-dependent.
3. Using predictive (attenuation) relationships, determine the ground motion produced at the building site (including the uncertainty) by earthquakes of any possible size or magnitude occurring at any possible point in each source zone.
4. Combine the uncertainties in earthquake location, size, and ground motion prediction to obtain the probability that the chosen ground motion parameter (e.g., peak horizontal ground acceleration, spectral acceleration at a specified frequency) will be exceeded in a particular time period (say 10% in 50 years).

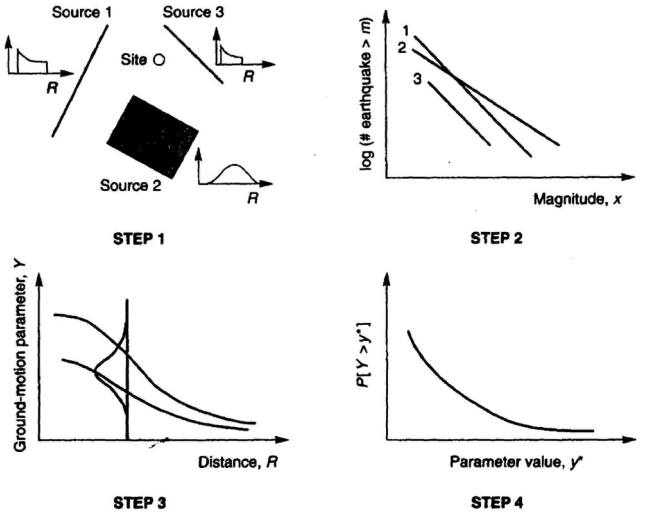

Figure B-3 Steps in probabilistic seismic hazard assessment (Kramer, 1996)

The sections below present summary information on parts of each step in this process. Kramer (1996) and McGuire (2004) provide much additional information.

Earthquake Source Characterization

Characterization of an earthquake source (there can be a number of sources for some sites) requires consideration of the spatial characteristics of the source, the distribution of earthquakes within that source, the distribution of earthquake size within that source, and the distribution of earthquakes with time. Each of these characteristics involves some degree of uncertainty, which is explicitly addressed by the process.

Spatial Uncertainty

Earthquake source geometries are typically characterized, as shown in Figure B-4 from Kramer (1996) a) as *point sources* (e.g., volcanoes); b) two-dimensional *areal sources* (e.g., a well-defined fault plane); and, c) three-dimensional *volumetric sources* (e.g., areas where earthquake mechanisms are poorly defined such as the Central and Eastern USA). These representations can have varying level of accuracy.

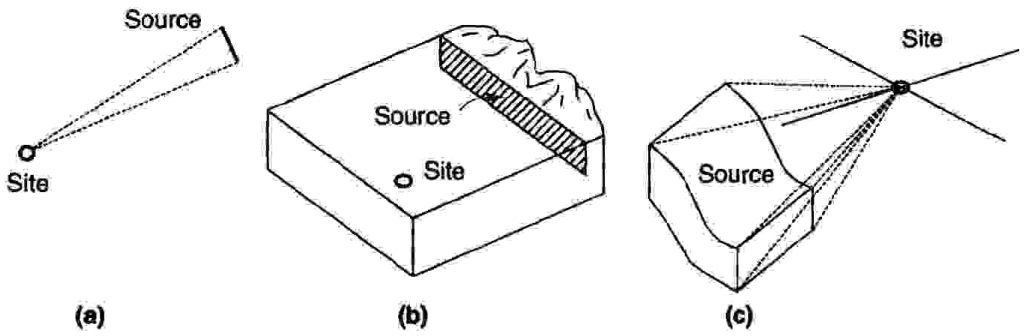

Figure B-4 Source zone geometries (Kramer, 1996)

Since attenuation relationships express ground motion parameters in terms of a measure of the source-to-site distance, the spatial uncertainty must be described with respect to the appropriate distance parameter. The uncertainty in source-to-site distance can be described by a probability density function as shown in Figure B-5.

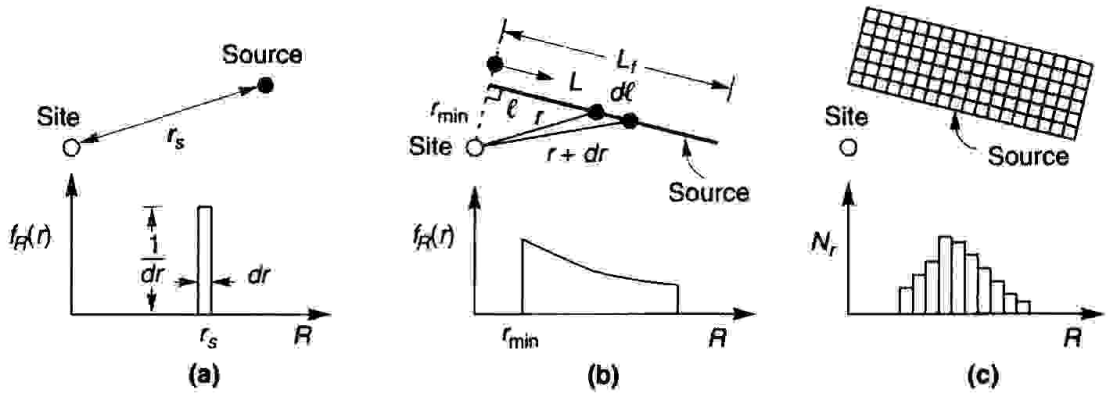

Figure B-5 Variations in site-to-source distance for three source zone geometries (Kramer, 1996)

As shown in Figure B-5, for the point source, the distance *R* is r_S; the probability that $R = r_s$ is 1.0 and that $R \neq r_s$ is 0. For more complex source zones, it is easier to evaluate $f_R(r)$ by numerical integration. For example, the source zone of part c. of the figure above is broken up into a large number of discrete elements of the same area. A histogram that approximates $f_R(r)$ can be constructed by tabulating the values of *R* that correspond to the center of each element.

Size Uncertainty

Recurrence laws describe the distribution of probable earthquake sizes over a period of time. One basic assumption is that past recurrence rates for a source are appropriate for the prediction of future seismicity. The best known recurrence law is that of Gutenberg and Richter (1944), who collected data from Southern Californian earthquakes over a period of years and plotted the data according to the number of earthquakes that exceeded different magnitudes during that period. The number of exceedances of each magnitude was divided by the length of the time period used to assemble the data to define a *mean annual rate of exceedance* λ_m of an earthquake of magnitude *m*. The reciprocal of the mean annual rate of exceedance of a particular magnitude is termed the return period of earthquakes exceeding that magnitude. Guttenberg-Richter plotted the logarithm of the annual rate of exceedance (of earthquakes in Southern California) against earthquake magnitude and obtained the linear regression relationship:

$$\log \lambda_m = a - bm \qquad \text{(B-1)}$$

where λ_m is defined above, 10^a is the mean yearly number of earthquakes of magnitude greater than or equal to magnitude *m*, and *b* describes the relative likelihood of large and small earthquakes. As the value of *b* increases, the number of larger magnitude earthquakes relative to smaller magnitude earthquakes decreases. The mean rate of small earthquakes is often under-

predicted because historical records are often used to supplement the instrumental records and only the larger magnitude events from part of the historical record.

The Guttenberg-Richter recurrence law can also be expressed as

$$\lambda_m = 10^{a-bm} = \exp(2.303a - 2.303b) \quad \text{(B-2)}$$

In this form, the implies that earthquake magnitudes are exponentially distributed and that the range of magnitude is from $-\infty$ to ∞. Small magnitude earthquakes are of little significance to the built environment and can be ignored in terms of hazard assessment. The law also predicts non-zero mean rates of exceedance from magnitudes up to ∞, which is not physically possible. Bounded (lower and upper) recurrence laws have been proposed to deal with these practical bounds on magnitude.

The Guttenberg-Richter law was originally developed from regional data and not for specific source zones. Paleoseismic studies over the past 30 years have indicated that individual points on faults (or fault segments) tend to move by approximately the same distance in successive earthquakes, suggesting that individual faults repeatedly generate earthquakes of a similar (with 0.5 magnitude unit) size, known as *characteristic earthquakes* at or near their maximum capable magnitude. Geological evidence indicates that characteristic earthquakes occur more frequently than would be implied by extrapolation of the law from high exceedance rates (of low magnitude events) to low exceedance rates (of high magnitude), resulting in a more complex recurrence law than that given by equation B-2.

Attenuation Relationships

Predictive (or attenuation) relationships are generally empirically obtained using least-squares regression on a strong-motion dataset. Scatter or randomness in the results is inevitable because of differences in site conditions, travel path and fault rupture mechanics. The scatter can be characterized by confidence limits or by the standard deviation of the predicted parameter.

The probability that a ground motion parameter, Y, exceeds a certain value, y, for an earthquake of magnitude, m, occurring at a distance, r, is given by

$$P[Y > y | m, r] = 1 - F_y(y) \quad \text{(B-3)}$$

where $F_Y(y)$ is the value of the cumulative distribution function of Y at m and r. The value of $F_Y(y)$ depends on the probability distribution used to describe Y. As noted previously, ground motion parameters are generally

assumed to be lognormally distributed. Figure B-6 illustrates the conditional probability of exceeding a particular value of the ground motion parameter for a given combination of *m* and *r*.

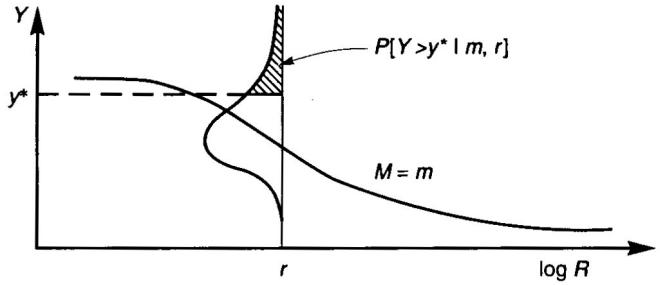

Figure B-6 Conditional probability calculation (Kramer, 1996)

Temporal Uncertainty

The distribution of earthquake occurrence with time must be computed or assumed to calculate the probabilities of different earthquake magnitudes occurring in a given time period. Earthquakes are assumed to occur randomly with time and the assumption of random occurrence permits the use of simple probability models.

The temporal occurrence of earthquakes is commonly described as a *Poisson* process: one that yields values of a random variable describing the number of occurrences of a particular event during a given time interval (or spatial region). In a Poisson process: (a) the number of occurrences in one time interval are independent of the number that occur in any other time interval; (b) the probability of occurrence during a very short time interval is proportional to the length of the time interval; and (c) the probability of more than one occurrence in a very short time interval is negligible. Events in a Poisson process occur randomly, with no memory of the time, size or location of any preceding events. Cornell showed that the Poisson model is useful for probabilistic hazard analysis unless the hazard is dominated by a single source zone that produces characteristic earthquakes and the time period since the previous significant event exceeds the average inter-event time.

For a Poisson process, the probability of a random variable *N*, representing the number of occurrences of a particular event in a given time period is given by

$$P[N = n] = \frac{\mu^n e^{-\mu}}{n!} \qquad \text{(B-4)}$$

where μ is the average number of occurrences of the event in the time period. To characterize the temporal distribution of earthquake recurrence for PSHA, the Poisson probability is normally expressed as

$$P[N = n] = \frac{(\lambda t)^n e^{-\lambda t}}{n!} \quad \text{(B-5)}$$

where λ is the average rate of recurrence of the event and *t* is the time period. When the event is the exceedance of a particular earthquake magnitude, the Poisson model can be combined with a suitable recurrence law to predict the probability of at least one exceedance in a period of *t* years by

$$P[N \geq 1] = 1 - e^{-\lambda_m t} \quad \text{(B-6)}$$

Probability Computations and Seismic Hazard Curves

S*eismic hazard curves* identify the annual probability of exceedance of different values of a selected ground motion parameter. Development of these curves involves probabilistic calculations that combine the uncertainties in earthquake size, location and frequency for each potential earthquake source that could impact shaking at the site under study.

The seismic hazard curve calculations are straightforward once the uncertainties in earthquake size, location and frequency are established but much bookkeeping is involved. The probability of exceeding a particular value, *y*, of a ground motion parameter, *Y*, is calculated for one possible source location and then multiplied by the probability of that magnitude earthquake occurring at that particular location. The calculation is then repeated for all possible magnitudes and locations and the probabilities of each are summed to compute the $P[Y > y]$ at the site. A summary of this process is presented below. Kramer (1996) and McGuire (2004) provide much additional information.

For a given earthquake occurrence, the probability that a ground motion parameter, *Y*, will exceed a particular value, *y*, can be computed using the total probability theorem (Cornell and Benjamin, 1968) as:

$$P[Y > y] = P[Y > y|\mathbf{X}]P[\mathbf{X}] = \int P[Y > y|\mathbf{X}] f_x(\mathbf{X})\, dx \quad \text{(B-7)}$$

where $\mathbf{X}$ is a vector of random variables that influence *Y*. In most cases, the quantities in $\mathbf{X}$ are limited to the magnitude *M* and distance *R*. Assuming that *M* and *R* are independent, the probability of exceedance can be written as

$$P[Y > y] = \iint P[Y > y|m,r] f_M(m) f_R(r)\, dm\, dr \quad \text{(B-8)}$$

where $P[Y > y|m,r]$ is obtained from the predictive relationship and $f_M(m)$ and $f_R(r)$ are the probability density functions for magnitude and distance, respectively.

If the building site is in a region of N_s potential earthquake sources, each of which has an average rate of threshold exceedance $\nu_i = \exp(\alpha_i - \beta_i m)$, the total average exceedance rate for the region is given by the equation:

$$\lambda_y = \sum_{i=1}^{N_s} P[Y > y|m,r] f_{Mi}(m) f_{Ri}(r)\, dm\, dr \tag{B-9}$$

This equation is typically solved by numerical integration. One simple approach described by Kramer is to divide the possible ranges of magnitude and distance into N_M and N_R segments, respectively. The average exceedance rate can then be calculated using the multi-level summation:

$$\begin{aligned}\lambda_y &= \sum_{i=1}^{N_s}\sum_{j=1}^{N_m}\sum_{k=1}^{N_R} \nu_i P[Y > y|m_j,r_k] f_{Mi}(m_j) f_{Ri}(r_k)\, \Delta m\, \Delta r \\ &= \sum_{i=1}^{N_s}\sum_{j=1}^{N_m}\sum_{k=1}^{N_R} \nu_i P[Y > y|m_j,r_k] P[M = m_j] P[R = r_k]\end{aligned} \tag{B-10}$$

where the terms are $m_j = m_0 + (j - 0.5)(m_{\max} - m_0)/N_M$, $\Delta r = (r_{\max} - r_{\min})/N_r$, $r_k = r_{\min} + (k - 0.5)(r_{\max} - r_{\min})/N_R$ and $\Delta m = (m_{\max} - m_0)/N_M$. The above statement is equivalent to assuming that each source is capable of generating only N_M different earthquakes of magnitude, m_j at only N_R different source-to-site distances of r_k. The accuracy of this method increases with smaller segments and thus larger values of N_M and N_R.

Figure B-7 presents a sample seismic hazard curve for peak ground acceleration at a site in Berkeley, California (McGuire, 2004). The figure shows the contributions to the annual frequency of exceedance from 9 different seismic sources.

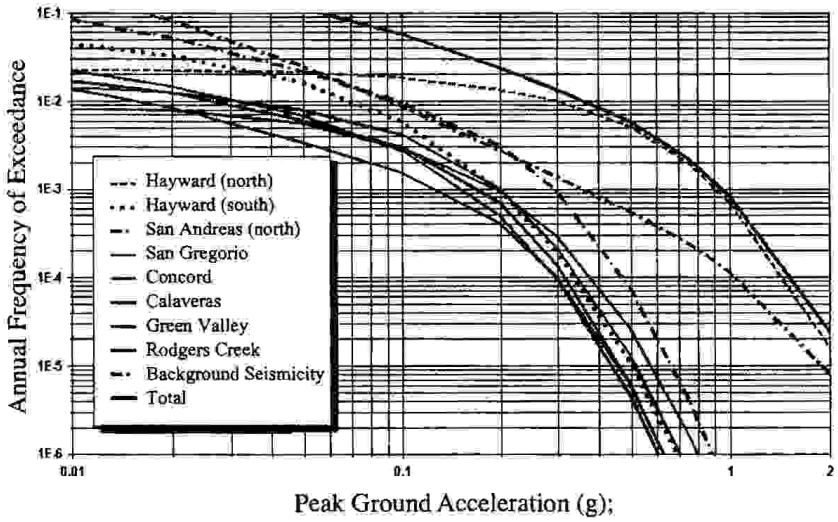

Figure B-7 Seismic hazard curve for Berkeley, California (McGuire, 2004)

Probabilities of exceedance in a selected time period can be computed using seismic hazard curves combined with the Poisson model. The probability of exceedance of y in a time period T is

$$P[Y_T > y] = 1 - e^{-\lambda_y T} \tag{B-11}$$

As an example, the probability that a peak horizontal ground acceleration of 0.10 g will be exceeded in a 50-year time period for the site characterized by the hazard curve above is:

$$P[\text{PHA} > 0.1g \text{ in 50 years}] = 1 - e^{-\lambda_y T} = 1 - e^{-(0.060)(50)} = 0.950 = 95\% \tag{B-12}$$

An alternate, often made, computation is the value of the ground motion parameter corresponding to a particular probability of exceedance in a given time period. For example, the acceleration that has a 10% probability of exceedance in a 50-year period would be that with an annual rate of exceedance, calculated by re-arranging the second-to-last equation, namely

$$\lambda_y = -\frac{\ln(1 - P[Y_T > y])}{T} = -\frac{\ln(1 - 0.10)}{50} = 0.00211 \tag{B-13}$$

Using the hazard curve from Figure B-13 for all nine sources, the corresponding zero-period spectral acceleration is approximately 0.75 g.

Hazard curves can be developed for specific oscillator periods (0.2 second and 1.0 second are widely used) and the above calculations of probability of exceedance can be extended to the spectral domain. This permits development of probabilistic estimates of spectral demands for different probabilities of exceedance or return periods. Hazard curves have been

developed for many different response quantities and characterizations of earthquake ground motion.

B.4.3 Inclusion of Rupture Directivity Effects

If the building site is located within 20 *km* of an active fault capable of generating an M_w 6.5 earthquake or greater, rupture directivity effects should be considered.

Average rupture directivity effects can be included directly in probabilistic seismic hazard analysis if the attenuation relationships are either a) constructed using a database of recorded ground motions that include directivity effects (i.e., the NGA relationships described previously), or b) corrected to account for rupture directivity in a manner similar to that described by Somerville et al. (1997) and Abrahamson (2000). Note that the ratio of median maximum demand to geomean demand in the near-fault region is period-dependant and can be as great as 2 (Huang et al. 2008a, 2008b).

B.4.4 Deaggregation of Seismic Hazard Curves and Epsilon

The probabilistic seismic hazard analysis procedures described previously enable the calculation of annual rates of exceedance of ground motion parameters (e.g., spectral acceleration at a selected period) at a particular site based on aggregating the risks from all possible source zones. Therefore, the computed rate of exceedance for a given parametric intensity value is not associated with any particular earthquake magnitude, *m*, or distance, *r*.

For a given building site and hazard curve, it is possible to establish the combinations of magnitude, distance and source that contribute most to particular values of an intensity. This process is termed de-aggregation (or disaggregation). Hazard deaggregation requires expression of the mean annual rate of exceedance as a function of magnitude and distance of the form:

$$\lambda_y(m_j, r_k) = P[M = m_j]\,P[R = r_k]\sum_{i=1}^{N_s} \nu_i P[Y > y \,|\, m_j, r_k] \qquad \text{(B-14)}$$

McGuire (2004) provides detailed information on hazard deaggregation.

Figure B-8 shows sample deaggregation results for horizontal spectral acceleration at periods of 0.2 second and 1.0 second for a site in the Western United States, for a 2% probability of exceedance in 50 years. Consider the 1-second deaggregation data of part b of Figure B-8. The plot shows the contribution to the 1-second uniform hazard spectral ordinate as a function of

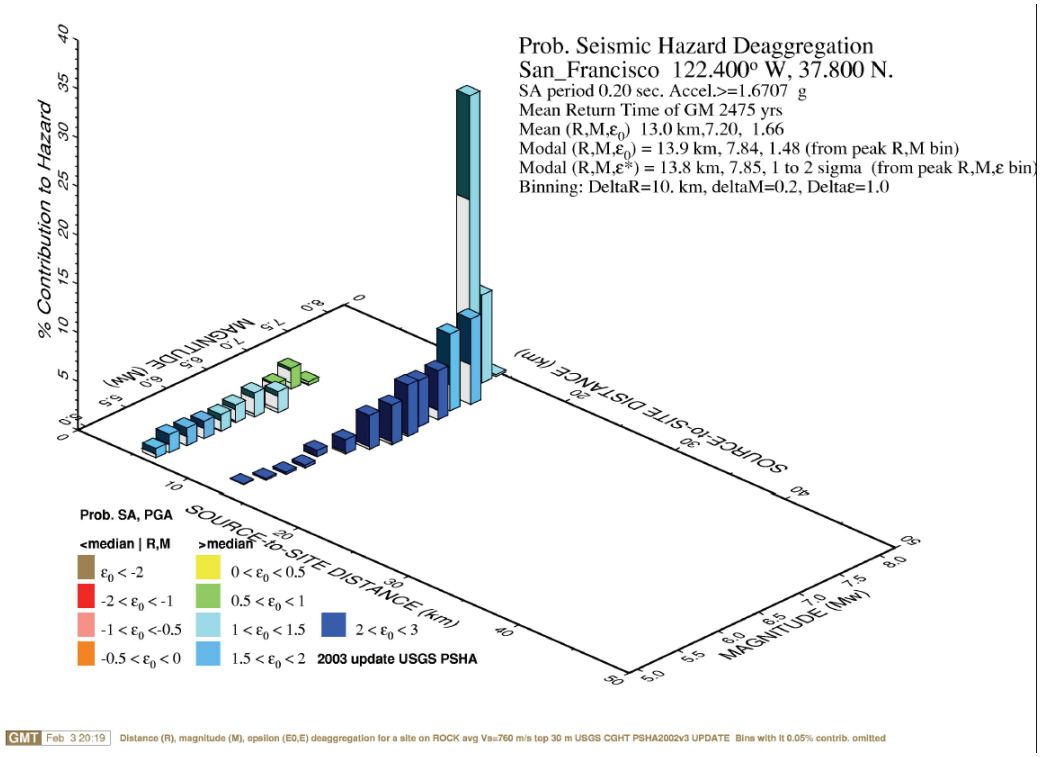

a. 0.2 second deaggregation

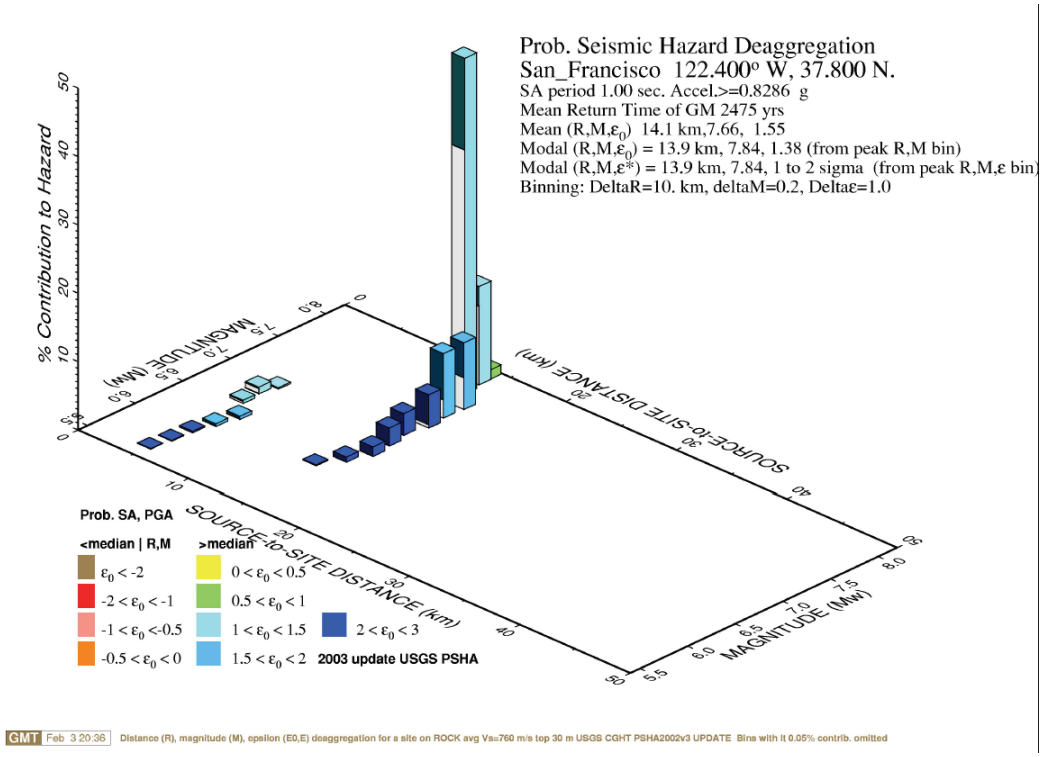

b. 1.0 second deaggregation

Figure B-8 Sample de-aggregation of a hazard curve (from www.usgs.gov)

moment magnitude and distance. The figure shows that approximately 50% of the total 1-second seismic demand can be ascribed to a moment magnitude 7.8 earthquake at a distance of 14 *km* – the [*M*, *r*] pair that dominates the 1-second spectral demand at this site is [7.8, 14].

This figure also introduces another important ground motion variable, epsilon, ε. One straightforward definition of ε is:

$$\varepsilon = \frac{S_a - \theta}{\beta} \tag{B-15}$$

where all variables vary as a function of period and: S_a is the computed spectral acceleration for a given probability (e.g., 2%) of exceedance in a specified time period (e.g., 50 years) and equal to 0.829*g* in this instance at a period of 1 second; θ is the median value of spectral acceleration computed by an appropriate attenuation relationship(s) for the dominant [*M*, *r*] pair (equal to [7.8, 14] in this instance), and β is the dispersion in the attenuation relationship. In this example, and using the modal [*M*, *r*, ε] triple, we see that ε ranges between 1 and 2, meaning that less than 15% of moment magnitude 7.8 earthquakes at a distance of 14 *km* would produce *geomean* spectral demands in excess of 0.829 *g*.

Baker and Cornell (2005, 2006) observed that ε is an indicator of spectral shape, with a positive (negative) value of ε at a given period tending to indicate a relative peak (valley) in the acceleration response spectrum at that period. Figure B-9 illustrates these trends using six bins of 20 ground motions defined by $\varepsilon \geq 2.25$, $-0.06 \leq \varepsilon \leq 0.06$ and $\varepsilon \leq -2.25$, respectively, at periods of 0.8 (Figure B-9a) and 0.3 second (Figure B-9b). The relative peak (valley) in the spectra for the $+\varepsilon$ ($-\varepsilon$) bin of motions at the two periods is clearly evident. No relative peak or valley at the reference periods is associated with the ε-neutral bin.

B.4.5 Conditional Mean Spectrum and Spectral Shape

Chapter 4 introduced Probabilistic Seismic Hazard Assessment and the development of Uniform Hazard Spectra and noted that the ordinates of Uniform Hazard Spectra are each associated with the same annual frequency of exceedance.

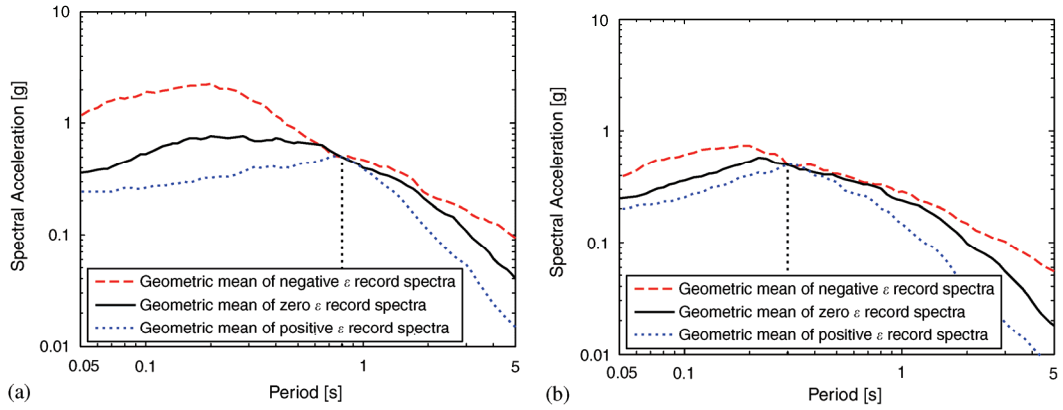

Figure B-9 Sample geometric-mean response spectra for negative-, zero- and positive-ε record sets with each record in the sets scaled to a) $S_a(0.8s) = 0.5\ g$ and b) $S_a(0.3s) = 0.5\ g$ (Baker and Cornell, 2006)

Building code and seismic design standard provisions for nonlinear response history analysis recommend scaling ground motions to match a target uniform hazard spectrum over a wide period range. Although convenient for design and likely conservative, such scaling procedures ignore the fact that:

1. If the spectral ordinates of a uniform hazard spectrum are governed by multiple scenario events, the spectral shape will not represent that for any of the governing events, regardless of the return period (Cornell 2006, Baker and Cornell, 2006).

2. For long-return-period earthquake shaking, the spectral ordinates of Uniform Hazard spectra are typically associated with a high value (greater than 1) of ε across a wide range of period (Harmsen, 2001). For the case where the geomean spectral ordinate of a ground motion pair attains the uniform hazard spectrum ordinate at a given period, the geomean spectrum of the pair is unlikely to have ordinates as large as those of the uniform hazard spectrum at other periods. The geomean spectra for the $+\varepsilon$ record sets in Figure B-9 support this observation.

Baker and Cornell (2005, 2006) introduced the Conditional Mean Spectrum which considers the correlation of spectral demands (represented by values of ε) at different periods, to address these two issues. Conditional Mean Spectra estimate the median geomean spectral acceleration response of a pair of ground motions given an [M, r] pair and a target spectral ordinate, $\overline{S}_a(T_1)$ (from which ε_{T_1} is back-calculated using an appropriate attenuation relationship). Baker and Cornell (2005) used the following equation to generate conditional mean spectra:

$$CMS_{\overline{S}_a(T_1)}(T_2) = \theta(M, r, T_2) \cdot \exp\left[\beta(M, r, T_2) \cdot \rho_{\varepsilon(T_1),\varepsilon(T_2)} \cdot \varepsilon_{T_1}\right] \qquad \text{(B-15)}$$

where $CMS_{\bar{S}_a(T_1)}(T_2)$ is the ordinate of the spectrum at period T_2 given that the spectral demand at T_1 is $\bar{S}_a(T_1)$; $\theta(M,r,T_2)$ and $\beta(M,r,T_2)$ are the median and logarithmic standard deviation of spectral acceleration at T_2 computed using a ground motion attenuation relationship for the [*M*, *r*] pair of interest; ε_{T_1} is the value of ε associated with $\bar{S}_a(T_1)$; and $\rho_{\varepsilon(T_1),\varepsilon(T_2)}$ is the correlation coefficient for ε between T_1 and T_2.

Baker and Jayaram (2008) developed a model for $\rho_{\varepsilon(T_1),\varepsilon(T_2)}$ using the Next Generation Attenuation ground motion database (www.peer.berkeley.edu) :

$$\begin{aligned} &\text{if } T_{\max} < 0.109 && \rho_{\varepsilon(T_1),\varepsilon(T_2)} = C_2 \\ &\text{else if } T_{\min} > 0.109 && \rho_{\varepsilon(T_1),\varepsilon(T_2)} = C_1 \\ &\text{else if } T_{\max} < 0.109 && \rho_{\varepsilon(T_1),\varepsilon(T_2)} = \min(C_2, C_4) \\ &\text{else} && \rho_{\varepsilon(T_1),\varepsilon(T_2)} = C_4 \end{aligned} \tag{B-16}$$

where $T_{\min} = \min(T_1, T_2)$, $T_{\max} = \max(T_1, T_2)$ and

$$C_1 = 1 - \cos\left(\frac{\pi}{2} - 0.366 \ln\left(\frac{T_{\max}}{\max(T_{\min}, 0.11)}\right)\right) \tag{B-17}$$

$$C_2 = \begin{cases} 1 - 0.105\left(1 - \dfrac{1}{1+e^{100T_{\max}-5}}\right)\left(\dfrac{T_{\max}-T_{\min}}{T_{\max}-0.01}\right) & \text{if } T_{\max} < 0.2 \sec \\ 0 & \text{otherwise} \end{cases} \tag{B-18}$$

$$C_3 = \begin{cases} C_2 \text{ if } T_{\max} < 0.11 \sec \\ C_1 \text{ if } T_{\max} \geq 0.11 \sec \end{cases} \tag{B-19}$$

$$C_4 = C_1 + 0.5(\sqrt{C_3} - C_3)\left(1 + \cos\left(\frac{\pi T_{\min}}{0.11}\right)\right) \tag{B-20}$$

Conditional mean spectra can be constructed using the following procedure:

1. Determine the value of $\bar{S}_a(T_1)$ from the probabilistic seismic hazard analysis at the desired mean annual frequency of exceedance.
2. De-aggregate the hazard at $\bar{S}_a(T_1)$ and identify the modal [*M*, *r*, ε] triple.
3. Select an appropriate ground motion attenuation relationship.
4. Generate the spectrum using (E-15) through (E-20) and the selected attenuation relationship for the [*M*, *r*, ε] triple of Step 2.
5. Amplitude scale the spectrum to recover $\bar{S}_a(T_1)$.

To illustrate this procedure, consider the deaggregation results of Figure B-8b for a site in San Francisco. As presented in Figure B-8b, the value of $\overline{S}_a(T_1)$ is 0.83 g for a return period of 2475 years and the modal [M, r, ε] triple for the hazard is [7.8, 14 km, 1 to 2]. A value of $\varepsilon = 1.5$ (midpoint of 1 and 2) was used for this example. In this example, the Chiou-Youngs NGA relationship was selected. Figure B-10 presents the results of Steps 4 and 5 using dotted and solid lines, respectively. (If $\varepsilon = 2$ is used in Step 4, the scale factor for Step 5 is 1.) The figure also presents the uniform hazard spectrum for this site at a return period of 2475 years. Except at period, T_1, the ordinates of the uniform hazard spectrum are greater than those of the scaled conditional mean spectrum.

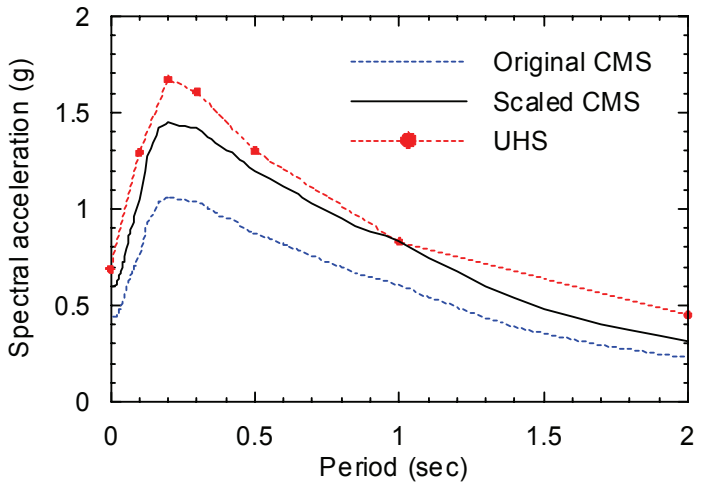

Figure B-10 Uniform Hazard Spectra (UHS) for a 2% probability of exceedance in 50 years and original and scaled Conditional Mean Spectrum (CSM) for a rock site in San Francisco.

B.5 Vertical Earthquake Shaking

B.5.1 Introduction

This section presents procedures that can be used to generate vertical response spectra for most buildings, where important vertical periods of response are less than or equal to 1.0 second. For buildings with important natural periods of vertical response in excess of 1.0 second, site-specific analysis should be conducted.

B.5.2 Procedure for Site Classes A, B and C

For structural periods less than or equal to 1.0 second, the vertical response spectrum can be constructed by scaling the corresponding ordinates of the horizontal response spectrum, S_a, as follows.

For periods less than or equal to 0.1 second, the vertical spectral acceleration, S_v, can be taken as

$$S_v = S_a \quad \text{(B-21)}$$

For periods between 0.1 and 0.3 second, the vertical spectral acceleration, S_v, can be taken as

$$S_v = (1 - 1.048[\log(T) + 1])S_a \quad \text{(B-22)}$$

For periods between 0.3 and 1.0 second, the vertical spectral acceleration, S_v, can be taken as

$$S_v = 0.5S_a \quad \text{(B-23)}$$

B.5.3 Procedure for Site Classes D and E

For structural periods less than or equal to 1.0 second, the vertical response spectrum can be constructed by scaling the corresponding ordinates of the horizontal response spectrum, S_a, as follows.

For periods less than or equal to 0.1 second, the vertical spectral acceleration, S_v, can be taken as

$$S_v = \eta S_a \quad \text{(B-24)}$$

For periods between 0.1 and 0.3 second, the vertical spectral acceleration, S_v, can be taken as

$$S_v = (\eta - 2.1(\eta - 0.5)[\log(T) + 1])S_a \quad \text{(B-25)}$$

For periods between 0.3 and 1.0 second, the vertical spectral acceleration, S_v, can be taken as

$$S_v = 0.5S_a \quad \text{(B-26)}$$

In equations (B-24) through (B-26), η can be taken as 1.0 for $S_s \le 0.5g$; 1.5 for $S_s \le 1.5g$; and $(1 + 0.5(S_s - 0.5))$ for $0.5g \le S_s \le 1.5g$.

B.6 Soil-Foundation-Structure Interaction

B.6.1 General

Structural response to earthquake shaking is affected by the dynamic properties of the three components of the soil-foundation-structure system and the interactions between these components. Soil-foundation-structure interaction analysis involves either direct or indirect analysis of the three-component system to prescribed free-field inputs, which are typically imposed as bedrock motions.

Traditional structural analysis neglects soil-foundation-structure interaction. As illustrated in Figure B-11a, such analysis assumes the base of the structure is rigid (components fixed at their base) and the input motions at the base of the foundation are derived assuming one of the standard soil categories described in the building code and its referenced standards. The use of such fixed base models is inappropriate for structural framing systems that incorporate stiff vertical components for lateral resistance (e.g., reinforced concrete shear walls, steel braced frames) because the response of such systems can be sensitive to small base rotations and translations that are neglected by the fixed base assumption. Relatively flexible lateral framing systems such as moment-resisting frames are often not significantly affected by soil-foundation-structure interaction effects.

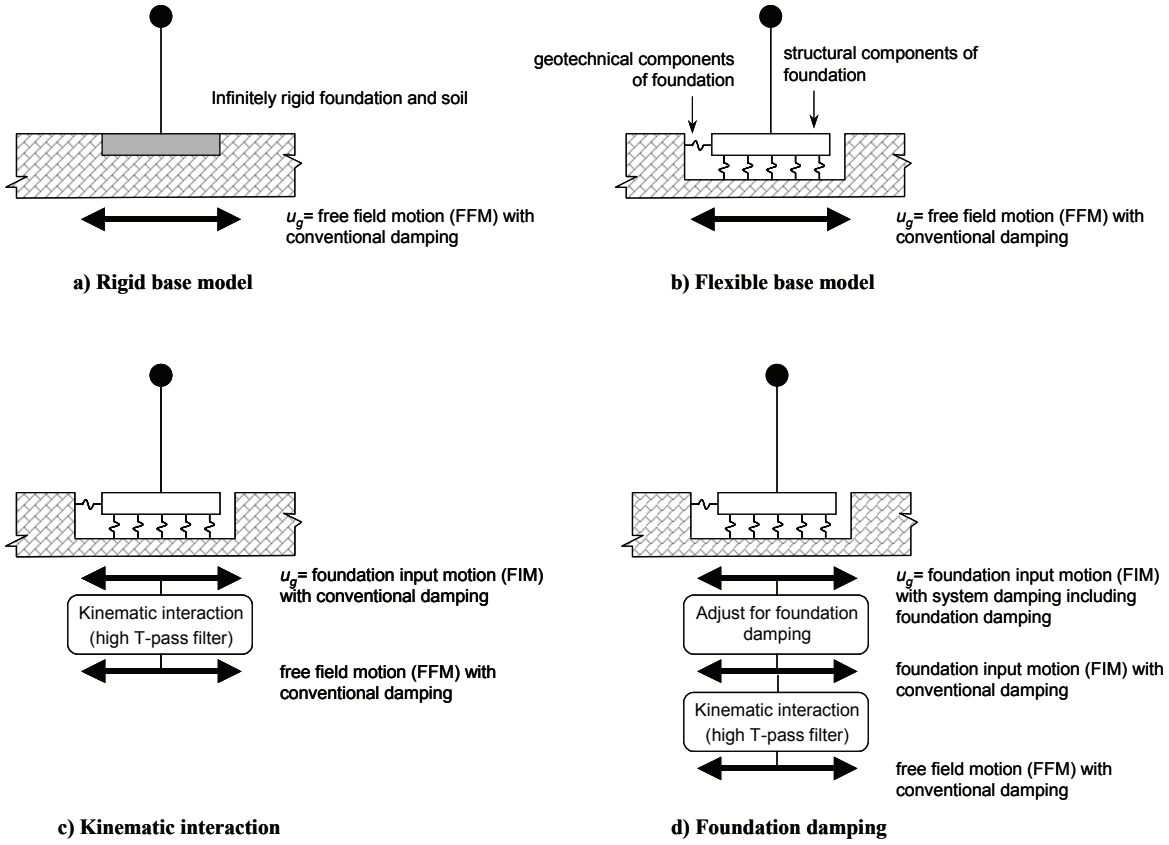

Figure B-11 Analysis for soil foundation structure interaction (FEMA, 2005)

B.6.2 Direct Soil-Foundation-Structure-Interaction Analysis

Soil-foundation-structure interaction can be directly analyzed using finite-element models that represent the soil as discretized solid finite elements. Soil elements can either use equivalent linear properties, or full nonlinear representation. Such direct analysis can address the three key effects of soil-foundation-structure interaction: foundation flexibility, kinematic effects, and

foundation damping. Solution of the kinematic interaction problem is often difficult without customized finite element codes because typical finite element codes cannot account for wave inclination and wave incoherence effects, both of which can be important.

Response-history analysis requires the development of a three-dimensional numerical model of the soil-foundation-structure system. Stress-strain or constitutive models (linear, nonlinear or equivalent linear) for the soils in the model should be developed based on test data. Appropriate and consistent frequency-dependant stiffness and damping matrices should be developed for the edges or boundaries of the soil in the numerical model.

B.6.3 Simplified Soil-Foundation-Structure-Interaction Analysis

Simplified Procedures

This section presents simplified procedures for including the effects of soil-foundation-structure interaction in response analysis. The procedures are based on those presented in FEMA 440, *Improvement of Nonlinear Static Seismic Analysis Procedures* (FEMA, 2005). More rigorous procedures are available in Appendix A of FEMA 440.

For the discussion below, soil-foundation-structure interaction is parsed into three key effects:

- foundation flexibility
- kinematic effects (filtering of the ground shaking to the building)
- foundation damping (dissipation of energy from the soil structure system through radiation and hysteretic soil damping).

Figure B-11b illustrates the incorporation of foundation flexibility into the numerical model of a building frame. Current analysis procedures in guidelines such as ASCE 41, *Seismic Rehabilitation of Existing Buildings* (ASCE, 2006) and ATC 40, *Seismic Evaluation and Retrofit of Concrete Buildings* (ATC, 1996) partially address the flexible foundation effect by providing guidance on the stiffness and strength of the geotechnical (soil) components of the foundation in the structural analysis model. However, these analysis procedures do not characterize the reduction of the shaking demand on the structural framing system relative to the free-field motion due to kinematic interaction or the foundation damping effect, both of which are described below. Guidance on including these effects in a simplified manner for nonlinear dynamic response analysis is provided below. Numerical simulation using models like that illustrated in Figure B-11b predicts global

response that includes elastic and inelastic deformations in the structural and geotechnical parts of the foundation system. These deformations are sometimes referred to as an *inertial soil-structure-interaction effect*. The inclusion of foundation flexibility in the numerical model can provide significantly different and more accurate response predictions than those computed assuming a fixed base (Figure B-11a). Further, foundation response and failures (e.g., rocking, soil bearing failure, pier/pile slip) can be explicitly evaluated using this appraoch.

Kinematic soil-structure interaction (Figure B-11c) results from the presence of relatively stiff foundation elements atop or within soil that causes the foundation motions to deviate from free-field motions. Base slab averaging and embedment are two kinematic effects. Ground motion shaking is spatially variable (i.e., in the absence of a foundation, each point beneath a building footprint, would experience somewhat different shaking at the same instant in time). Placement of a structure and foundation across these spatially variable motions produces an averaging effect and the weighted or overall motion experienced by the building is less than the localized maxima that would have occurred in the free-field, particularly at short period. The embedment effect is associated with the reduction of ground motion with depth into a soil deposit. Both base slab averaging[2] and embedment[3] affect the characteristics of the foundation-level motion (sometimes called the foundation input motion) in a manner that is independent of the superstructure (i.e., the portion of the structure above the foundation) with one exception. The effects are strongly period dependent, being maximized at short periods. The effects can be visualized as a filter applied to the high-frequency components of the free-field ground motion. The impact of those effects on superstructure response will tend to be greatest for short-period buildings. A simplified procedure to reduce the free field motion to a foundation input motion is presented below. The foundation input motion can be applied to a fixed base model or combined with a flexible base model. Kinematic effects tend to be important for buildings with relatively short

[2] Base slab averaging occurs to some extent in virtually all buildings. The slab averaging effect occurs at the foundation level for mats or spread footings interconnected by either grade beams or reinforced concrete slabs. Even if a laterally stiff foundation system is not present, the averaging can occur at the first elevated level of buildings with rigid diaphragms. The only case where base slab averaging effects should be neglected is for buildings without a laterally connected foundation system and with flexible floor and roof diaphragms.

[3] Embedment effects should not be considered for buildings without basements, even if the footings are embedded. Embedment effects tend to be significant when the depth of basements is greater than about 10 feet.

fundamental periods (e.g., less than 0.5 second), large plan dimensions and basements embedded 10 feet or more in soil materials.

Figure B-11d illustrates foundation damping effects that are another result of *inertial soil-structure interaction*. Foundation damping results from the relative movements of the foundation and free-field soil. It is associated with radiation of energy away from the foundation and hysteretic damping within the soil. The result is an effective decrease in the spectral ordinates of ground motion experienced by the structure. Foundation damping effects tend to be greatest for stiff structural framing systems (e.g., reinforced concrete shear walls, steel braced frames) and relatively soft foundation soils (e.g., Site Classes D and E per ASCE-7-10). Simplified procedures for incorporating foundation damping in a numerical model analysis are described below.

Simplified Procedure for Kinematic Interaction

A ratio-of-response-spectra factor can be used to represent kinematic interaction effects. This is the ratio of the response spectral ordinates imposed on the foundation (i.e., the foundation input motion, FIM) to the free-field spectral ordinates. Two phenomena should be considered in evaluating the ratio: base-slab averaging and foundation embedment. Foundation embedment effects should be considered for buildings with basements. The simplified procedure of Chapter 8 of FEMA 440 (FEMA, 2005) can be used for assessment of kinematic interaction. The following information is needed for such assessment: dominant building period (as measured by % mass participating in the elastic base shear computation), building foundation plan dimension, foundation embedment, peak horizontal ground acceleration, and shear wave velocity. Section 8 of FEMA 440 specifies limitations on the applicability of the simplified procedure Figures B-12a and B-12b (from FEMA 440) provide summary information on the reductions in spectral demand due to base-slab averaging and embedment. The 5% damped free-field spectrum is multiplied by the product of the period-dependant reduction factors for base-slab averaging and embedment to derive the foundation input motion spectrum. Since the embedment computation is dependant on the peak horizontal ground acceleration, the computation must be repeated for every level of hazard considered for the performance and loss assessment.

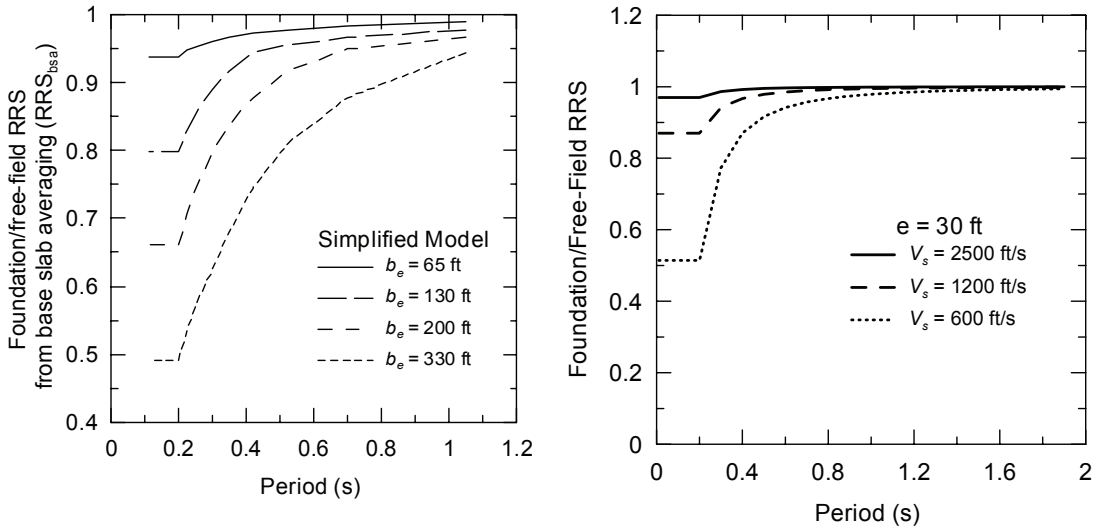

a. base slab averaging b. embedment

Figure B-12 Reductions in spectral demand due to kinematic interaction

Simplified Procedure for Foundation Damping

Soil-foundation interaction can significantly increase the effective damping in associated with a structure's dynamic response to earthquake shaking.

The simplified procedure of FEMA 440 can be used for assessment of foundation damping. In this procedure foundation radiation damping effects reduce the ordinates of the 5% damped acceleration response spectrum, typically used as the basis for selecting and scaling ground motions used in analysis. Hysteretic damping in the soil should be captured directly through the use of nonlinear soil springs. The following information is needed for such an assessment: dominant (first mode) building period (as measured by % mass participating in the elastic base shear computation), T_1; first modal mass; building foundation plan dimension; building height; foundation embedment; strain-degraded soil shear modulus and soil Poisson's ratio. Section 8 of FEMA 440 presents limitations on the use of the simplified procedure. The 5% damped free-field spectrum is modified in the period range $T \geq 0.75T_1$.

B.7 Alternate Procedure for Hazard Characterization for Scenario-Based Assessment Using Nonlinear Response-History Analysis

Scenario-based assessments consider uncertainty in spectral demand. Ground motion intensity is assumed to be lognormally distributed with median value θ, and dispersion, β.

Eleven values of spectral acceleration at each user-selected period are used to characterize the distribution of seismic demand for scenario-assessments as follows:

$$S_{ai} = \theta e^{\beta \eta_i} \qquad i = 1, 11 \tag{B-27}$$

where S_{ai} is the i^{th} target spectral acceleration at a given period and values of η_i are listed in Table B-2.

Table B-2 Values of η_i for Generating a Distribution of $S_{ai}(T)$

i	η_i	*I*	η_i	*i*	η_i
1	-1.69	5	-0.23	9	0.75
2	-1.10	6	0	10	1.10
3	-0.75	7	0.23	11	1.69
4	-0.47	8	0.47		

Figure B-13 illustrates this process for a scenario earthquake having median spectral acceleration of 0.3 *g* and dispersion equal to 0.4. The figure shows the cumulative probability distribution represented by this median and dispersion. Horizontal lines across the plot divide the distribution into eleven striped-regions, each having a probability of occurrence of 9.09%. For each stripe, the central or midpoint value of the probability of exceedance is shown by × with values of 4.55%, 13.64%, 22.73%, 31.82%, 40.91%, 50%, 59.09%, 68.18%, 77.27%, 86.36% and 95.45%. A dashed horizontal line is drawn across the plot from the vertical axis to intersect the cumulative distribution function and dropped vertically to the horizontal axis, where spectral acceleration values of .153 *g*, .193 *g*, .222 *g*, 0.248 *g*, 0.274 *g*, 0.300 *g*, 0.329 *g*, 0.362 *g*, 0.405 *g*, 0.465 *g* and 0.590 *g*, respectively, are read off.

The values of spectral acceleration, S_{a1} to S_{a11}, characterize the distribution of spectral acceleration shown in the figure and can be obtained from the following equation:

$$S_{ai} = \theta \cdot e^{\beta \cdot \Phi^{-1}(P_i)} \tag{B-28}$$

where Φ^{-1} is the inverse standardized normal distribution and P_i is the midpoint cumulative probability for region *i*. The values for η_i in Table B-2 are calculated from $\Phi^{-1}(P_i)$ for 11 target spectral accelerations. Alternatively, these values can be generated using an Excel spreadsheet and the function LOGINV (p, $\ln\theta$, β), where values of p = (0.04545 ….. 0.9545), $\ln\theta$ (ln(0.3)=-1.204) is the mean, and β (=0.4) is the dispersion.

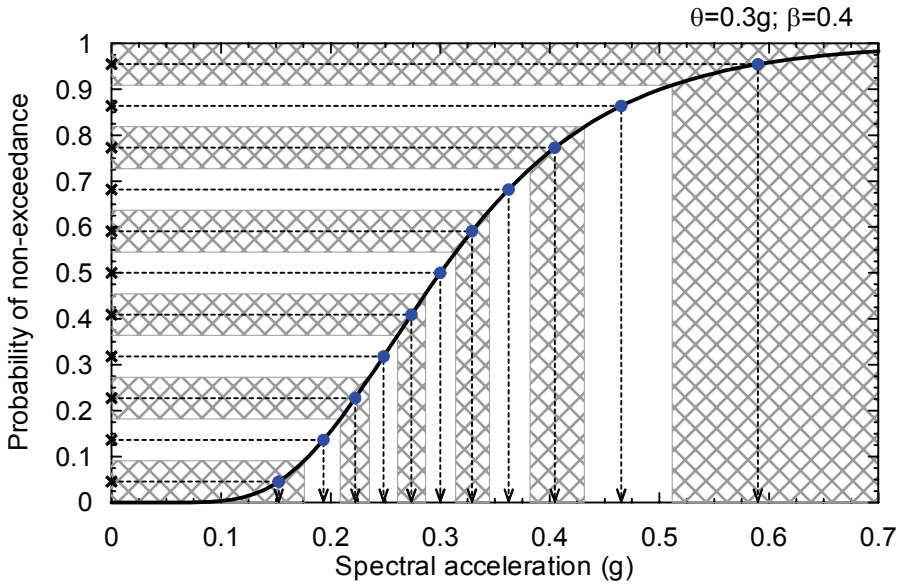

Figure B-13 Calculation of spectral accelerations given a lognormal distribution

Identical to the procedures of Section 4. involving the Uniform Hazard Spectrum, the user must specify a period range (T_{max}, T_{min}) for scaling pairs of ground motions. The characterization of the earthquake hazard can involve the following steps:

1. Select the magnitude and site-to-source distance for the scenario event
2. Select an appropriate attenuation relationship(s) for the region, site soil type and source characteristics
3. Establish the period range (T_{max}, T_{min}) for scaling pairs of ground motions
4. Determine the median spectral acceleration demands, θ, and the corresponding dispersions, β, in the period range (T_{max}, T_{min}) using the attenuation relationship(s) of Step 2
5. Establish 11 target spectra, $S_{ai}(T), i = 1, 11$, using the medians and dispersions from Step 4 and equation (4-*) in the period range (T_{max}, T_{min})
6. Select 11 pairs of ground motions
7. Construct a geomean spectrum for each pair of ground motions
8. For each target spectrum of Step 5, scale a pair of motions such that for each period in the range (T_{max}, T_{min}), the geomean spectrum matches the response spectrum $S_{ai}(T)$
9. Repeat Step 8 for the remaining 10 spectra.

This procedure will result in 11 pairs of earthquake histories to represent the potential range of intensities associated with the scenario.

Step 8 in this procedure requires the selection of pairs of motions in Step 6 with geomean spectra in the period range ($T_{\max}$, $T_{\min}$) that are similar in shape to the target spectra of Step 5. If appropriate pairs of motions are unavailable, an alternative to Steps 7, 8 and 9 is to spectrally match pairs of motions to the target spectra of Step 5, with each component in a pair matched to the same target spectrum.

A refinement to the above 9-step procedure involves the use of Conditional Mean Spectra and the effective fundamental period $\overline{T}$ as defined in Section 5.6.1. Steps 4 through 9 above are altered as follows:

1. Determine the median spectral acceleration demand, θ , and the corresponding dispersion, β , at effective fundamental period $\overline{T}$, using the attenuation relationship(s) of Step 2
2. Compute 11 target values of spectral acceleration, $S_{ai}(\overline{T}), i = 1,11$, using the medians and dispersions from Step 3 and (4-7)
3. Generate Conditional Mean Spectra (CMS_i) for the 11 target values of $S_{ai}(\overline{T})$ given magnitude and distance from Step 1 and η from Section 4.*.*
4. Select 11 pairs of ground motions, $p_i, i = 1,11$ such that the shape of the geomean spectrum for p_i is similar to that of the CMS_i of Step 5 over a user-specified range of period, which must include T_1^X and T_1^Y
5. Amplitude scale the geomean spectral acceleration of the two components of p_i to $S_{ai}(\overline{T})$
6. Repeat Step 8 for the remaining 10 spectra.

Similar to the first procedure presented in this section, spectral matching of pairs of motions can be used in lieu of selecting pairs of ground motions with geomean spectral shapes that are similar to CMS_i .

Appendix C
Residual Drift

C.1 Introduction

Residual (permanent) drift is an important consideration in judging a structure's post-earthquake safety and the economic feasibility of repair. Modest amounts of residual drift may require costly and difficult adjustments to nonstructural components (e.g., re-plumbing of elevator rails, adjustments to building facades) and can also lead to judgments that a building is unsafe during post-earthquake inspections. Larger residual drifts may require straightening of the structural frame or alternative measures to strengthen the frame for stability. At some stage, residual drifts may be large enough to seriously jeopardize structural stability to earthquake aftershocks and uneconomical to repair, in which case the cost of repair is on par with complete building replacement.

Research has shown that residual drifts predicted by nonlinear analysis are highly variable and sensitive to the assumed modeling features, including the post-yield hardening/softening slope and unloading response, and that residual drift may be larger under near-fault records with forward directivity pulses or under long-duration records that cause many cycles of significant response. Accurate statistical simulation of residual drifts requires advanced nonlinear response-history analyses, with a large number of ground motions and with careful attention paid to cyclic hysteretic response of the models and numerical accuracy of the solution. Since the requirements for direct simulation of residual drifts are computationally complex for general implemenation, equations are provided to *estimate* residual drifts as a function of the peak transient response.

Past studies on the residual story drifts are presented in Section C.2. Section C.3 presents a simplified procedure for computing residual story drifts. Section C.4 proposes global building damage states associated with residual story drift.

C.2 Prediction of Residual Story Drifts

Analytical studies by Riddell and Newmark (1979) and Mahin and Bertero (1981) first identified some of the key behavioral aspects associated with calculating residual drifts. More recent studies (including MacRae and

Kawashima, 1997; MacRae, 1994; Christopoulos et al., 2003; Christopoulos and Pampanin, 2004; Pampanin et al., 2003; and Ruiz-Garcia and Miranda 2005, 2006a-c) have confirmed that residual drifts are largely dependent on the following parameters: (1) magnitude of peak transient inelastic drifts, (2) lateral strength of the structure relative to the earthquake demand, (3) inelastic post-yield stiffness, (4) cyclic unloading response,(5) pulses in the ground motions, and (6) duration of ground shaking. In many respects these parameters are all inter-related and affect transient and residual drifts. Some of these factors are implicitly accounted for in the peak transient drift assessment. It is desirable that analytical models account for variations in post-yield stiffness and the cyclic unloading response, since these parameters are structural parameters that can be influenced by design. For example, the residual drift assessment should differentiate between conventional structures and ones that employ self-centering features that are designed to minimize residual drifts.

Figure C-1 presents a schematic plot relating predicted peak transient and residual story drift under increasing earthquake intensity. Point "a" corresponds to the onset of inelastic response, prior to which residual drifts cannot occur. Point "c" corresponds to the collapse point, where residual and transient response converges and point "b" corresponds to regions between these two limits, where the residual drifts represent some fraction of the peak transient drift. As this figure clearly indicates, the ratio of residual to transient drifts is not constant but it may be reasonable to treat the ratio as a constant. Much of the existing literature has evaluated residual drifts at intermediate levels of response, sometimes distinguishing between the degree of inelasticity by varying the strength of the structure, either adjusting the strength using a response modification factor or by adjusting the transient story ductility demand.

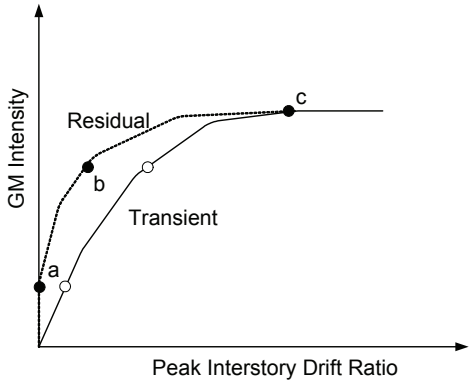

Figure C-1 Idealized incremental dynamic analysis presenting transient and residual story drift ratios as a function of ground-motion (GM) intensity

A structure's unloading characteristics are significant behavioral effects that impact residual displacements. Figure C-2 presents load versus deflection plots representing the basic aspects of unloading response that have been identified as important in prior research. These studies have consistently shown that residual displacements are largest in elastic-plastic (EP) systems, due to their tendency to preserve the inelastic displacements upon unloading. This is in contrast to general inelastic (GI) response, where pinching or other effects lead to smaller unloading stiffness. Most recently, researchers have been examining the benefits of so-called self-centering (SC) systems that are specifically designed with unloading characteristics that are intended to minimize (or potentially eliminate) residual displacements. There are also behavioral effects, such as foundation rocking, which have natural self-centering tendencies.

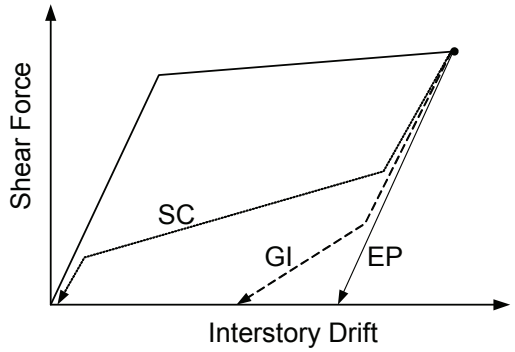

Figure C-2 Idealized response characteristics for elastic-plastic (EP), general inelastic (GI) and self-centering (SC) systems

Due to the variety of approaches and parameters addressed by various researchers, it is difficult to generalize the results of previous research. However, in the interest of developing a simplified model, the following discussion summarizes some overall results and observations from published analytical studies.

MacRae and Kawashima (1997) investigated residual displacements in single degree-of-freedom bilinear oscillators with a focus on bridge design, where the presence of residual displacements was cited as a major factor in bridge closures and replacement. They proposed a model to estimate residual displacements as a function of the peak inelastic displacement, unloading properties of the inelastic oscillator, and a statistical coefficient based on inelastic response history analyses. In an illustrative example, they predicted residual displacements equal to about 0.16 times the maximum transient displacement. According to their proposed model, the residual displacement ratio could be disaggregated into the following product, 0.16 = 0.67 x 0.9 x 0.27, where 0.67 is the ratio of plastic to total drift (equal to the sum of the

elastic and plastic drift), 0.9 reflects the effect of the reduced unloading stiffness, and 0.27 is a statistical parameter accounting for inelastic dynamic response. The specific value of 0.27 represents the mean plus standard deviation from a range of analyses for systems with modest strain hardening and a ductility demand ratio of 4.

Christopoulos et al. (2003) conducted analyses of single-degree of freedom models with the primary emphasis on characterizing the effect of post-yield hardening stiffness and hysteretic unloading behavior on response. The models were generally representative of modern ductile moment frame buildings, ranging in height from 4 to 20 stories designed with base shear yield ratios (V_y / W) ranging from 0.26 to 0.11, respectively. They applied ground motions to represent both design and maximum earthquakes. Maximum drift ratios observed in their analyses were in the range of 2% to 3%. Analyses of elastic-plastic (EP) models with zero hardening had residual displacements ranging from 0.1 to 0.4 times the peak inelastic transient displacements. These ratios reduced to 0.1 to 0.2 for systems with 5% strain hardening and increased up to 0.7 for systems with 5% strain softening (-5% hardening). The largest residual displacements and peak transient ductility (up to 5 times yield) were observed in the 4-story (period approximately equal to 1 second) building with strain softening. Comparable analyses run with a general inelastic model (the Takeda model) had significantly smaller residual drifts, ranging between 7 to 12% of the peak transient drifts for systems with zero or positive strain hardening and 10 to 15% for systems with strain softening. In related studies of multi-degree-of-freedom models (Pampanin et al., 2003) the researchers reported residual drifts equal to 0.05 to 0.25 times the total transient drift, depending on the hardening and hysteretic model.

Ruiz-Garcia and Miranda (2005, 2006a-c) conducted an extensive parametric study of single and multi degree-of-freedom systems with the goal to characterize probabilistic residual drift hazard curves. They generally expressed their results in terms of a parameter, C_r, which related residual drifts to *elastic spectral displacement*. Thus, for consistency with the previous studies, this parameter would need to be modified to account for the difference between peak inelastic transient displacement and the elastic spectral displacement. Presumably, this adjustment is close to unity where the equal displacement rule applies (long period single mode dominated systems under small to moderate displacements). For elastic-plastic models with periods greater than 1 second and elastic demand to yield strength ratios of R = 1.5 to 6, they reported median values of C_r = 0.25 to 0.5. This ratio increased to C_r = 0.8 for oscillators with period between 0.5 and 1 second,

and became even larger for smaller periods. Since the ratio is conditioned on elastic spectral displacement, the large amplification at small periods probably reflects the amplification between elastic and inelastic transient displacements. For stiffness degrading systems, the median value coefficient reduced to C_r = 0.1 to 0.3. They also reported dispersion in C_r of about 0.8, which was fairly constant across various periods and building strengths.

C.3 Model to Calculate Residual Story Drifts

Prior studies have indicated that for ductility demands of about 4, residual drifts were on the order of 0.15 to 0.30 times the peak transient drifts. Using this as a guide, a set of equations are proposed to relate residual story drift, Δ_r, to peak transient story drift, Δ:

$$\begin{aligned} \Delta_r &= 0 && \Delta \le \Delta_y \\ \Delta_r &= 0.3(\Delta - \Delta_y) && \Delta_y < \Delta \le 4\Delta_y \\ \Delta_r &= (\Delta - 3\Delta_y) && 4\Delta y < \Delta \end{aligned} \qquad \text{(C-1)}$$

where Δ_y is the story drift at yield. Figure C-3 illustrates these equations.

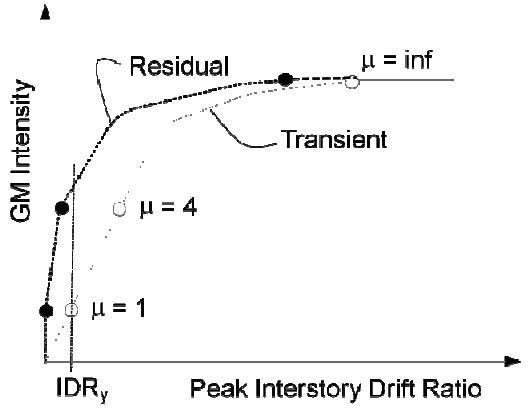

Figure C-3 Idealized model to estimate residual story drift from peak transient drift as a function of ground-motion (GM) intensity

These equations are calibrated such that at a story ductility ratio of 4, the ratio of residual to peak transient drift is 0.23. At ductility ratios of 2 and 6, the ratios of residual to peak transient drift are 0.15 and 0.5, respectively. Ultimately, as the collapse point is reached the residual drift will approach the peak transient drift. As an example, consider a steel moment frame with a yield drift ratio of 1%. At 3% total drift, the predicted residual drift ratio would be 0.6%, or about 0.20 times the peak transient. At 5% total drift, the predicted residual would be about 1.9%, or about 0.38 times the peak transient. At 7% total drift (approaching the collapse point), the residual drift would be about 3.9%, or 0.56 times the peak transient.

The proposed equations apply to typical building systems and do not distinguish between many of the behavioral effects that are known to affect residual drifts. For example, whereas previous studies of idealized models has shown a correlation between post-yield stiffness and residual drifts, this is not reflected in the equations except insofar as the post-yield stiffness affects the peak transient drift ratio. The equations are presented in this simple format owing to the lack of physical data to validate modeling of residual displacements and due to the complexity of obtaining significant improvements in the residual drift estimates.

Per Ruiz-Garcia and Miranda, the dispersion for residual drift estimates is about 0.8. Two alternative ways to consider this in the assessment would be to either (1) calculate the median residual drift demand fragility using equation C-1 based on the median transient and yield drift ratios, and then apply a dispersion of 0.8, or (2) calculate the residual drift probability based on the integration of the conditional probability of residual drift and the transient drift. In this case, the dispersion on the conditional probability of residual drift should be reduced by the record-to-record variability in the transient drift.

C.4 Proposed Damage States for Residual Story Drifts

Table C-1 proposes four damage states associated with residual building drift, ranging from the onset of damage to nonstructural components to near-collapse. The proposed median story drift ratios (residual drift as a percentage of story height) are approximate and based on a combination of judgment and limits that have been previously suggested in FEMA 356, *Prestandard and Commentary for the Seismic Rehabilitation of Buildings* (Table C1-3). For damage state DS4, the limits on the residual drifts that are expressed in terms of the design shear force are intended to cover cases in regions of low seismicity where the destabilizing effects of $P-\Delta$ may dominate at smaller drift ratios than the values noted.

Further work remains to establish appropriate parameters to describe the uncertainty in these limits and loss functions to define the direct economic loss and downtime losses associated with these damage states. For example, damage state DS1 may require repairs to nonstructural components that may not otherwise be damaged, except for the need to realign components. Similarly, depending on the type of system, damage state DS2 requires extensive structural repairs beyond those evident from the assessment of structural component damage.

The relationship between transient and residual drift demands, per C-1, can be combined with the information in Table C-1 to relate these damage states to the associated peak transient drifts. Through the yield drift ratio, the relationship between the residual drift damage states and peak transient drift will depend on the stiffness of the system. A few example relationships are summarized in Table C-2, which are based on the assumed yield drift ratios noted in the table.

Table C-1 Damage states for residual story drifts

Damage state	Description	Residual story drift ratio, [1]
DS1	No structural realignment is necessary for structural stability; however, the building may require adjustment and repairs to nonstructural and mechanical components that are sensitive to building plumb (e.g., elevator rails, curtain walls, doors).	0.2% (equal to the maximum out of plumb typically permitted in new construction)
DS2	Realignment of structural frame and related structural repairs required to both maintain permissible drift limits for nonstructural and mechanical components and to limit degradation in structural stability (collapse safety)	0.5%
DS3	Major structural realignment is required to restore safety margin for lateral stability; however, the required realignment and repair of the structure may not be economically and practically feasible (i.e., the structure might be at total economic loss).	1%
DS4	Residual drift is sufficiently large that the structure is in danger of collapse from earthquake aftershocks. For this reason the performance point might be considered as equal to collapse, albeit with greater uncertainty.	High Ductility Systems $4\% < 0.5V_{design}/W$
		Moderate Ductility Systems $2\% < 0.5V_{design}/W$
		Limited Ductility Systems $1\% < 0.5V_{design}/W$

1. *h* is the story height

Table C-2 Sample transient story drift ratios, Δ / h, associated with the residual story drift damage states of Table C-1

		Δ / h			
Sample framing system	Δ_y / h	**DS1**[1]	**DS2**[1]	**DS3**[1]	**DS4**[2]
Steel ductile moment resisting frame	1%	1.5%	2.7%	4.1%	7.1%
Reinforced concrete wall	0.5%	1%	2.2%	2.6%	3.6%
Timber shear wall	1%	1.5%	2.7%	4.1%	5.1%

1. Δ_r / h = 0.2%, 0.5% and 1.0% for DS1, DS2 and DS3, respectively.

2. Δ_r / h = 4%, 2% and 2% for steel moment resisting frames, reinforced concrete walls, and timber shear walls, respectively.

Appendix D
List of Default Fragilities

D.1 Default Fragilities

Table D-1 provides a summary listing of all the structural and nonstructural fragilities that were developed as part of the methodology. The table also indicates the number of "sub" fragilities that were developed for each category. In total, over 600 fragility specifications are provided in the electronic database.

Table D-1 Default Fragilities

System Designation	NISTIR Number	Description	Number of Sub Fragilities
Miscellaneous Structural Steel Components/Connections	B1031.001	Bolted shear tab gravity connections	1
	B1031.011	Steel column base plates	3
	B1031.021	Welded column splices	3
Structural Steel Special Concentric Braced Frame	B1033.001	Special Concentric Braced Frame with WF braces, balanced design criteria, Chevron Brace	3
	B1033.002	Special Concentric Braced Frame with Wide Flange (WF) braces, balanced design criteria, Single Diagonal Brace	3
	B1033.003	Special Concentric Braced Frame with WF braces, balanced design criteria, X Brace	3
	B1033.011	Special Concentric Braced Frame with Hollow Structural Section (HSS) braces, balanced design criteria, Chevron Brace	3
	B1033.012	Special Concentric Braced Frame with HSS braces, balanced design criteria, Single Diagonal Brace	3
	B1033.013	Special Concentric Braced Frame with HSS braces, balanced design criteria, X Brace	3
	B1033.021	Special Concentric Braced Frame with HSS braces, tapered gusset plates & design to AISC minimum standard, Chevron Brace	3

Table D-1 Default Fragilities (continued)

System Designation	NISTIR Number	Description	Number of Sub Fragilities
Structural Steel Special Concentric Braced Frame	B1033.022	Special Concentric Braced Frame with HSS braces, tapered gusset plates & design to AISC minimum standard, Single Diagonal Brace	3
	B1033.023	Special Concentric Braced Frame with HSS braces, tapered gusset plates & design to AISC minimum standard, X Brace	3
	B1033.031	Special Concentric Braced Frame, design to AISC minimum standards, Chevron Brace	3
	B1033.032	Special Concentric Braced Frame, design to AISC minimum standards, Single Diagonal Brace	3
	B1033.033	Special Concentric Braced Frame, design to AISC minimum standards, X Brace	3
	B1033.041	Special Concentric Braced Frame with double angle braces, Chevron Brace	3
	B1033.042	Special Concentric Braced Frame with double angle braces, Single Diagonal Brace	3
	B1033.043	Special Concentric Braced Frame with double angle braces, X Brace	3
Structural Steel Ordinary Concentric Braced Frame	B1033.051	Ordinary Concentric Braced Frame with compact braces, Chevron Brace	3
	B1033.052	Ordinary Concentric Braced Frame with compact braces, Single Diagonal Brace	3
	B1033.053	Ordinary Concentric Braced Frame with compact braces, X Brace	3
	B1033.061	Ordinary Concentric Braced Frame, braces design to ductile slenderness limits, Chevron Brace	3
	B1033.062	Ordinary Concentric Braced Frame, braces design to ductile slenderness limits, Single Diagonal Brace	3
	B1033.063	Ordinary Concentric Braced Frame, braces design to ductile slenderness limits, X Brace	3
	B1033.071	Braced frame, design for factored loads, no additional seismic detailing, Chevron Brace	3
	B1033.072	Braced frame, design for factored loads, no additional seismic detailing, Single Diagonal Brace	3

Table D-1 Default Fragilities (continued)

System Designation	NISTIR Number	Description	Number of Sub Fragilities
Structural Steel Ordinary Concentric Braced Frame	B1033.073	Braced frame, design for factored loads, no additional seismic detailing, X Brace	3
Structural Steel Moment Frame	B1035.001	Post-Northridge Reduced Beam Section (RBS) connection with welded web, beam one side	2
	B1035.011	Post-Northridge RBS connection with welded web, beams both sides	2
	B1035.021	Post-Northridge welded steel moment connection other than RBS, beam one side	2
	B1035.031	Post-Northridge welded steel moment connection other than RBS, beams both sides	2
	B1035.041	Pre-Northridge Welded Unreinforced Flange-Bolted (WUF-B) beam-column joint, beam one side	2
	B1035.051	Pre-Northridge WUF-B beam-column joint, beam both sides	2
Reinforced Concrete Special Moment Frame	B1041.001a	ACI 318 Special Moment Frame (SMF), beam one side	3
	B1041.001b	ACI 318 SMF, beam both sides	3
	B1041.011a	MF with SMF-conforming beam and column flexural and confinement reinforcement but weak joints, beam one side	3
	B1041.011b	Moment Frame (MF) with SMF-conforming beam and column flexural and confinement reinforcement but weak joints, beam both sides	3
Reinforced Concrete Intermediate Moment Frame	B1041.021a	ACI 318 Intermediate Moment Frame (IMF), beam one side	3
	B1041.021b	ACI 318 IMF, beam both sides	3
Reinforced Concrete Ordinary Moment Frame	B1041.031a	ACI 318 Ordinary Moment Frame (OMF) with weak joints and beam flexural response, beam one side	3
	B1041.031b	ACI 318 OMF with weak joints and beam flexural response, beam both sides	3
	B1041.041a	ACI 318 OMF with weak joints and column flexural response, beam one side	3

Table D-1 Default Fragilities (continued)

System Designation	NISTIR Number	Description	Number of Sub Fragilities
Reinforced Concrete Ordinary Moment Frame	B1041.041b	ACI 318 OMF with weak joints and column flexural response, beam both sides	3
	B1041.051a	ACI 318 OMF with weak beams and weak joints, beam flexural or shear response, beam one side	3
	B1041.051b	ACI 318 OMF with weak beams and weak joints, beam flexural or shear response, beam both sides	3
	B1041.061a	ACI 318 OMF with weak columns, beam one side	3
	B1041.061b	ACI 318 OMF with weak columns, beam both sides	3
	B1041.071a	ACI 318 OMF with weak columns and high axial load, beam one side	3
	B1041.071b	ACI 318 OMF with weak columns and high axial load, beam both sides	3
Reinforced Concrete Non-conforming Moment Frame	B1041.081a	Non-conforming MF with weak joints and beam flexural response, beam one side	3
	B1041.081b	Non-conforming MF with weak joints and beam flexural response, beam both sides	3
	B1041.091a	Non-conforming MF with weak joints and column flexural response, beam one side	3
	B1041.091b	Non-conforming MF with weak joints and column flexural response, beam both sides	3
	B1041.101a	Non-conforming MF with weak beams and strong joints, beam one side	3
	B1041.101b	Non-conforming MF with weak beams and strong joints, beam both sides	3
	B1041.111a	Non-conforming MF with weak columns, beam one side	3
	B1041.111b	Non-conforming MF with weak columns, beam both sides	3
	B1041.121a	Non-conforming MF with weak columns and strong joints, beam both sides	3
	B1041.121b	Non-conforming MF with weak columns and strong joints, beam one side	3

Table D-1 Default Fragilities (continued)

System Designation	NISTIR Number	Description	Number of Sub Fragilities
Reinforced Concrete Non-conforming Moment Frame	B1041.131a	Non-conforming MF with inadequate development of reinforcing, beam one side	3
	B1041.131b	Non-conforming MF with inadequate development of reinforcing, beam both sides	3
Reinforced Concrete Low Aspect Ratio Planar Wall	B1044.001	Rectangular low aspect ratio concrete walls, 8" or less thick	3
	B1044.011	Rectangular low aspect ratio concrete walls, 8" to 16"	3
	B1044.021	Rectangular low aspect ratio concrete walls, 18" to 24" thick	3
Reinforced Concrete Low-rise Wall	B1044.031	Low-rise reinforced concrete walls with return flanges, less than 8" thick	3
	B1044.041	Low-rise reinforced concrete walls with return flanges, 8" to 16" thick	3
	B1044.051	Low-rise reinforced concrete walls with return flanges, 17" to 24" thick	3
	B1044.061	Low rise reinforced concrete walls with boundary columns, less than 8" thick	3
	B1044.071	Low rise reinforced concrete walls with boundary columns, 8" to 16" thick	3
	B1044.081	Low rise reinforced concrete walls with boundary columns, 17" to 24" thick	3
Reinforced Concrete Flat Slab	B1049.001	Reinforced concrete flat slabs - joints without shear reinforcing	6
	B1049.011	Reinforced concrete flat slabs - joints with shear reinforcing	2
	B1049.021	Post-tensioned concrete flat slabs - joints without shear reinforcing	4
	B1049.031	Post-tensioned concrete flat slabs - joints with shear reinforcing	2
	B1049.041	Reinforced concrete flat slabs drop panel or drop capital - joints without shear reinforcing	4

Table D-1 Default Fragilities (continued)

System Designation	NISTIR Number	Description	Number of Sub Fragilities
Reinforced Masonry Ordinary Wall	B1051.001	Ordinary reinforced masonry walls with partially grouted cells, 4" to 6" thick, shear dominated	2
	B1051.003	Ordinary reinforced masonry walls with partially grouted cells, 4" to 6" thick, flexure dominated	2
	B1051.011	Ordinary reinforced masonry walls with partially grouted cells, 8" to 12"' thick, shear dominated	2
	B1051.013	Ordinary reinforced masonry walls with partially grouted cells, 8" to 12" thick, flexure dominated	2
	B1051.021	Ordinary reinforced masonry walls with partially grouted cells, 16" thick, shear dominated	2
	B1051.023	Ordinary reinforced masonry walls with partially grouted cells, 16" thick, flexure dominated	2
Reinforced Masonry Special Wall	B1052.001	Special reinforced masonry walls with fully grouted cells, 8" or 12" thick, shear dominated	2
	B1052.003	Special reinforced masonry walls with fully grouted cells, 8" to 12" thick, flexure dominated	2
	B1052.011	Special reinforced masonry walls with fully grouted cells, 16" thick, shear dominated	2
	B1052.013	Special reinforced masonry walls with fully grouted cells, 16" thick, flexure dominated	2
Light-framed Wood Wall	B1071.001	Light framed wood walls with structural panel sheathing, gypsum wallboard	2
	B1071.002	Light framed wood walls with structural panel sheathing, stucco	2
	B1071.031	Wood walls with diagonal let-in bracing	1
Glazing	B2022.001	Glazing	15
Tile Roof	B3011.011	Concrete tile roof, tiles secured and compliant with UBC94	1
	B3011.012	Clay tile roof, tiles secured and compliant with UBC94	1
	B3011.013	Concrete tile roof, unsecured tiles	1

Table D-1 Default Fragilities (continued)

System Designation	NISTIR Number	Description	Number of Sub Fragilities
Tile Roof	B3011.014	Clay tile roof, unsecured tiles	1
Wall Partition	C1011.001	Wall Partition, Type: Gypsum	3
	C3011.001	Wall Partition, Type: Gypsum + Wallpaper	3
	C3011.002	Wall Partition, Type: Gypsum + Ceramic Tile	3
	C3011.003	Wall Partition, Type: High End Marble or Wood Panel	3
Ceiling	C3032.001	Suspended Ceiling	16
Elevator	D1014.010	Traction elevator	1
	D1014.021	Hydraulic elevator	2
Piping	D2021.001	Domestic Cold Water Piping	4
	D2031.001	Sanitary Waste Piping - flexible coupling	4
	D2031.002	Sanitary Waste Piping - bell & spigot coupling	4
Chiller	D3031.011a	Chiller - Anchorage fragility only	8
	D3031.011e	Chiller - Equipment fragility only	8
	D3031.011i	Chiller - Combined anchorage & equipment fragility	8
Cooling Tower	D3031.021a	Cooling Tower - Anchorage fragility only	8
	D3031.021e	Cooling Tower - Equipment fragility only	8
	D3031.021i	Cooling Tower - Combined anchorage & equipment fragility	8
Compressor	D3032.011a	Compressor - Anchorage fragility only	8
	D3032.011e	Compressor - Equipment fragility only	8
	D3032.011i	Compressor - Combined anchorage & equipment fragility	8
HVAC Distribution	D3041.001	HVAC Fan In Line Fan, Fan independently supported and vibration isolators	4

Table D-1 Default Fragilities (continued)

System Designation	NISTIR Number	Description	Number of Sub Fragilities
HVAC Distribution	D3041.002	HVAC Fan In Line Fan, Fan independently supported but not on vibration isolators	4
	D3041.011	HVAC Galvanized Sheet Metal Ducting	8
	D3041.021	HVAC Stainless Steel Ducting	8
	D3041.031	HVAC Drops / Diffusers in suspended ceilings	2
	D3041.032	HVAC Drops / Diffusers without ceilings	4
	D3041.041	Variable Air Volume (VAV) box with in-line coil	2
	D3041.101a	HVAC Fan - Anchorage fragility only	2
	D3041.101b	HVAC Fan - Equipment fragility only	2
	D3041.101c	HVAC Fan - Combined anchorage & equipment fragility	2
Domestic Steam Piping	D3043.001	Domestic Steam Piping - Small Diameter Threaded Steel	4
	D3043.002	Domestic Steam Piping - Large Diameter Welded Steel	4
Domestic Water Piping	D3044.001	Domestic Hot Water Piping - Small Diameter Threaded Steel	4
	D3044.002	Domestic Hot Water Piping - Large Diameter Welded Steel	4
	D3045.001	Domestic Chilled Water Piping - Small Diameter Threaded Steel	4
	D3045.002	Domestic Chilled Water Piping - Large Diameter Welded Steel	4
Packaged Air Handling Unit	D3063.011a	Packaged Air Handling Unit - Anchorage fragility	8
	D3063.011e	Packaged Air Handling Unit - Equipment fragility only	8
	D3063.011i	Packaged Air Handling Unit - Combined anchorage & equipment fragility	8
Control Panel	D3067.011a	Control panel - Anchorage fragility only	2

Table D-1 Default Fragilities (continued)

System Designation	NISTIR Number	Description	Number of Sub Fragilities
Control Panel	D3067.011b	Control panel - Equipment fragility only	2
	D3067.011c	Control panel - Combined anchorage & equipment fragility	2
Fire Sprinkler Water Piping	D4011.001	Fire Sprinkler Water Piping - Horizontal Mains and Branches - New Style Vitaulic / Threaded Steel	4
	D4011.002	Fire Sprinkler Water Piping - Horizontal Mains and Branches - Old Style Vitaulic	4
Fire Sprinkler Drop	D4011.011	Fire Sprinkler Drop Standard Threaded Steel - Dropping into unbraced lay-in tile SOFT ceiling	4
	D4011.012	Fire Sprinkler Drop Standard Threaded Steel - Dropping into unbraced lay-in tile HARD ceiling	2
	D4011.013	Fire Sprinkler Drop Standard Threaded Steel - Dropping into braced lay-in tile SOFT ceiling	2
	D4011.014	Fire Sprinkler Drop Standard Threaded Steel - Dropping into braced lay-in tile HARD ceiling	2
	D4011.015	Fire Sprinkler Drop Standard Threaded Steel - No Ceiling	4
Motor Control Center	D5010.011a	Motor control center - Anchorage fragility only	2
	D5010.011b	Motor control center - Equipment fragility only	2
	D5010.011c	Motor control center - Combined anchorage & equipment fragility	2
Transformer/Primary Service	D5011.011a	Transformer/Primary Service - Anchorage fragility only	8
	D5011.011e	Transformer/Primary Service - Equipment fragility only	8
	D5011.011i	Transformer/Primary Service - Combined anchorage & equipment fragility	8
Low Voltage Switchgear	D5012.021a	Low voltage switchgear - Anchorage fragility only	8
	D5012.021e	Low voltage switchgear - Equipment fragility only	8
	D5012.021i	Low voltage switchgear - Combined anchorage & equipment fragility	8

Table D-1 Default Fragilities (continued)

System Designation	NISTIR Number	Description	Number of Sub Fragilities
Distribution Panel	D5012.031a	Distribution panel - Anchorage fragility only	8
	D5012.031e	Distribution panel - Equipment fragility only	8
	D5012.031i	Distribution panel - Combined anchorage & equipment fragility	8
Battery Rack	D5092.011a	Battery Rack - Anchorage fragility only	2
	D5092.011b	Battery Rack - Equipment fragility only	2
	D5092.011c	Battery Rack - Combined anchorage & equipment fragility	2
Battery Charger	D5092.021a	Battery Charger - Anchorage fragility only	2
	D5092.021b	Battery Charger - Equipment fragility only	2
	D5092.021c	Battery Charger - Combined anchorage & equipment fragility	2
Diesel Generator	D5092.031a	Diesel generator - Anchorage fragility only	8
	D5092.031e	Diesel generator - Equipment fragility only	8
	D5092.031i	Diesel generator - Combined anchorage & equipment fragility	8
Miscellaneous Contents	E2022.010	Fragile objects on shelves	4
	E2022.020	Electronic equipment	4

Appendix E

Population Models

E.1 Population Models

Table E-1 presents the default population models, Figure E-1 plots the variation graphically and Table E-2 presents the default monthly variation of occupancy, relative to peak, for the occupancies that are supported by the methodology:

- Commercial office
- Education (K-12), with subcategories of Elementary, Middle and High School classroom buildings
- Healthcare – general hospital
- Hospitality
- Multi-unit Residential
- Research Laboratories
- Retail (shopping malls)
- Warehouse

The peak population values are defined in Table 3-1 of the Main Volume.

Table E-1 Default Time of Day and Day of Week Population Variations

	Commercial Office		Education - Elementary Schools		Education - Middle Schools		Education - High Schools		Healthcare	
Time of Day	Week-days	Week-ends	Week-days	Week-ends	Week-days	Week-ends	Week-days	Week-ends	Week-days	Week-ends
12:00 AM	0%	0%	0%	0%	0%	0%	0%	0%	40%	40%
1:00 AM	0%	0%	0%	0%	0%	0%	0%	0%	40%	40%
2:00 AM	0%	0%	0%	0%	0%	0%	0%	0%	40%	40%
3:00 AM	0%	0%	0%	0%	0%	0%	0%	0%	40%	40%
4:00 AM	0%	0%	0%	0%	0%	0%	0%	0%	40%	40%
5:00 AM	0%	0%	0%	0%	0%	0%	0%	0%	40%	40%
6:00 AM	0%	0%	0%	0%	5%	0%	5%	0%	40%	40%
7:00 AM	25%	0%	5%	0%	50%	0%	50%	0%	40%	40%
8:00 AM	50%	5%	100%	2%	100%	2%	100%	2%	40%	40%
9:00 AM	75%	5%	100%	2%	100%	2%	100%	2%	60%	50%
10:00 AM	100%	5%	100%	2%	100%	2%	100%	2%	80%	65%
11:00 AM	100%	5%	100%	2%	100%	2%	100%	2%	100%	80%

Table E-1 Default Time of Day and Day of Week Population Variations (continued)

	Commercial Office		Education - Elementary Schools		Education - Middle Schools		Education - High Schools		Healthcare	
Time of Day	Week-days	Week-ends	Week-days	Week-ends	Week-days	Week-ends	Week-days	Week-ends	Week-days	Week-ends
12:00 PM	50%	5%	100%	2%	100%	2%	100%	2%	100%	80%
1:00 PM	50%	5%	100%	2%	100%	2%	100%	2%	100%	80%
2:00 PM	100%	5%	100%	2%	100%	2%	100%	2%	100%	80%
3:00 PM	100%	5%	50%	2%	100%	2%	100%	2%	100%	80%
4:00 PM	75%	5%	5%	2%	50%	2%	50%	2%	100%	80%
5:00 PM	50%	5%	5%	2%	25%	2%	25%	2%	100%	80%
6:00 PM	25%	0%	5%	0%	5%	0%	5%	0%	100%	80%
7:00 PM	0%	0%	0%	0%	0%	0%	0%	0%	100%	80%
8:00 PM	0%	0%	0%	0%	0%	0%	0%	0%	80%	65%
9:00 PM	0%	0%	0%	0%	0%	0%	0%	0%	60%	50%
10:00 PM	0%	0%	0%	0%	0%	0%	0%	0%	40%	40%
11:00 PM	0%	0%	0%	0%	0%	0%	0%	0%	40%	40%
	Hospitality		Multi-Unit Residential		Research Laboratories		Retail		Warehouse	
Time of Day	Week-days	Week-ends	Week-days	Week-ends	Week-days	Week-ends	Week-days	Week-ends	Week-days	Week-ends
12:00 AM	100%	100%	100%	100%	10%	10%	0%	0%	0%	0%
1:00 AM	100%	100%	100%	100%	10%	10%	0%	0%	0%	0%
2:00 AM	100%	100%	100%	100%	10%	10%	0%	0%	0%	0%
3:00 AM	100%	100%	100%	100%	10%	10%	0%	0%	0%	0%
4:00 AM	100%	100%	100%	100%	10%	10%	0%	0%	0%	0%
5:00 AM	100%	100%	100%	100%	10%	10%	0%	0%	0%	0%
6:00 AM	100%	100%	80%	100%	25%	25%	0%	0%	0%	0%
7:00 AM	80%	100%	60%	100%	25%	25%	0%	0%	25%	0%
8:00 AM	70%	100%	40%	100%	50%	25%	5%	5%	50%	2%
9:00 AM	50%	75%	20%	75%	75%	25%	10%	10%	100%	2%
10:00 AM	50%	50%	20%	50%	100%	25%	20%	25%	100%	2%
11:00 AM	50%	25%	20%	50%	100%	25%	40%	50%	100%	2%
12:00 PM	50%	25%	20%	50%	50%	25%	60%	75%	100%	2%
1:00 PM	50%	25%	20%	50%	50%	25%	60%	100%	100%	2%
2:00 PM	50%	25%	25%	50%	100%	25%	60%	100%	100%	2%
3:00 PM	50%	25%	30%	50%	100%	25%	60%	100%	100%	2%
4:00 PM	50%	25%	35%	50%	75%	25%	60%	100%	100%	2%
5:00 PM	50%	25%	50%	50%	50%	25%	60%	100%	100%	2%
6:00 PM	50%	25%	67%	50%	25%	25%	60%	75%	50%	0%
7:00 PM	50%	25%	84%	50%	25%	25%	60%	50%	25%	0%
8:00 PM	50%	50%	100%	50%	10%	10%	40%	25%	0%	0%
9:00 PM	50%	50%	100%	75%	10%	10%	20%	10%	0%	0%
10:00 PM	100%	100%	100%	100%	10%	10%	5%	5%	0%	0%
11:00 PM	100%	100%	100%	100%	10%	10%	0%	0%	0%	0%

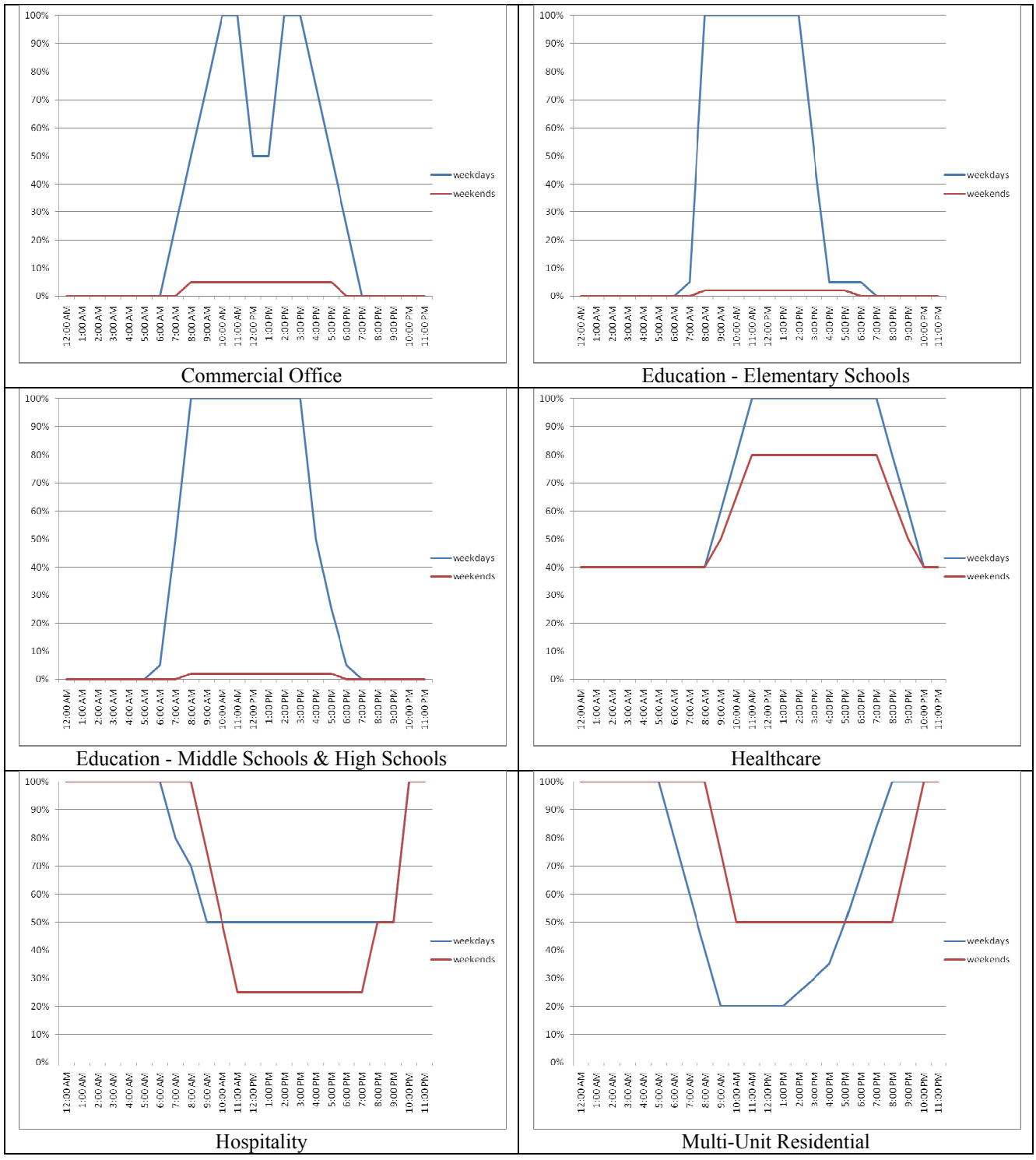

Figure E-1 Charts of Recommended Default Time of Day Population Variations (relative to Expected Peak Population) by Occupancy Class.

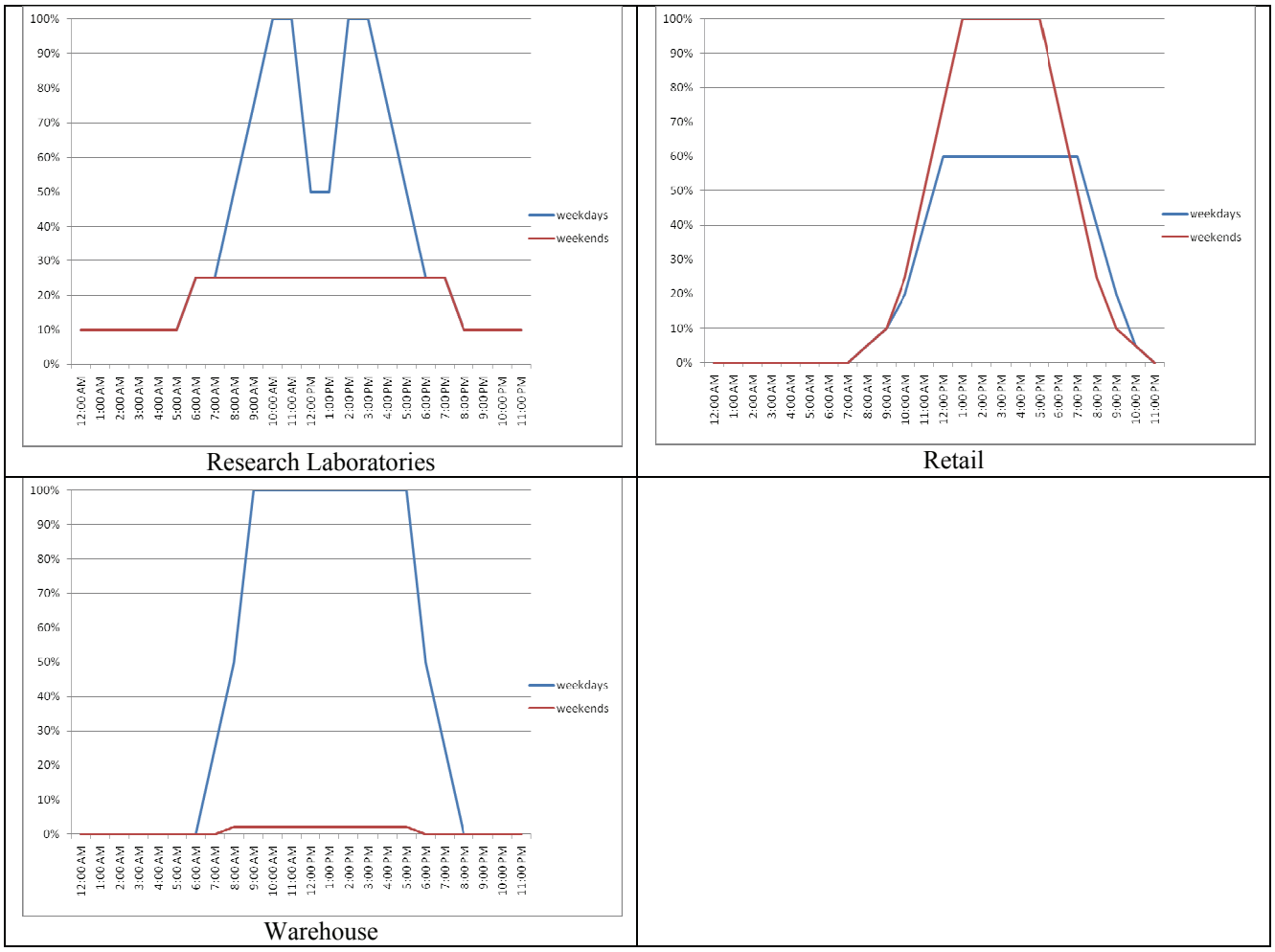

Figure E-1 Charts of Recommended Default Time of Day Population Variations (relative to Expected Peak Population) by Occupancy Class (Continued)

Table E-2 Monthly Population Variations (Relative to Expected Peak Population)

	Commercial Office		Education - Elementary Schools		Education - Middle Schools		Education - High Schools		Healthcare	
Month	Week-day	Week-end	Week-day	Week-end	Week-day	Week-end	Week-day	Week-end	Week-day	Week-end
Jan.	91%	100%	73%	100%	73%	100%	73%	100%	100%	100%
Feb.	95%	100%	90%	100%	90%	100%	90%	100%	100%	100%
March	100%	100%	100%	100%	100%	100%	100%	100%	100%	100%
April	100%	100%	77%	100%	77%	100%	77%	100%	100%	100%
May	95%	100%	95%	100%	95%	100%	95%	100%	100%	100%
June	100%	100%	77%	100%	77%	100%	77%	100%	100%	100%
July	95%	100%	0%	100%	0%	100%	0%	100%	100%	100%
Aug.	100%	100%	0%	100%	0%	100%	0%	100%	100%	100%
Sept.	95%	100%	95%	100%	95%	100%	95%	100%	100%	100%
Oct.	100%	100%	95%	100%	95%	100%	95%	100%	100%	100%
Nov.	95%	100%	81%	100%	81%	100%	81%	100%	100%	100%
Dec.	95%	100%	64%	100%	64%	100%	64%	100%	100%	100%
	Hospitality		Multi-Unit Residential		Research Laboratories		Retail		Warehouse	
Month	Week-day	Week-end	Week-day	Week-end	Week-day	Week-end	Week-day	Week-end	Week-day	Week-end
Jan.	100%	100%	100%	100%	91%	100%	95%	100%	91%	100%
Feb.	100%	100%	100%	100%	95%	100%	100%	100%	95%	100%
March	100%	100%	100%	100%	100%	100%	100%	100%	100%	100%
April	100%	100%	100%	100%	100%	100%	100%	100%	100%	100%
May	100%	100%	100%	100%	95%	100%	100%	100%	95%	100%
June	100%	100%	100%	100%	100%	100%	100%	100%	100%	100%
July	100%	100%	100%	100%	95%	100%	95%	100%	95%	100%
Aug.	100%	100%	100%	100%	100%	100%	100%	100%	100%	100%
Sept.	100%	100%	100%	100%	95%	100%	100%	100%	95%	100%
Oct.	100%	100%	100%	100%	100%	100%	100%	100%	100%	100%
Nov.	100%	100%	100%	100%	95%	100%	95%	100%	95%	100%
Dec.	100%	100%	100%	100%	95%	100%	95%	100%	95%	100%

Appendix F

Normative Quantities

Normative Quantities

Table F-1 through F-8 presents the normative quantity information for the occupancies that are supported by the methodology:

- Commercial office
- Education (K-12)
- Healthcare – general hospital
- Hospitality
- Multi-unit Residential
- Research Laboratories
- Retail (shopping malls)
- Warehouse

The normative quantity information is provided for 10^{th}-, 50^{th}- and 90^{th}-percentile quantities. The units of measurement are consistent with those used in the fragility specifications to determine repair cost and repair time consequences.

Table F-1 Normative Quantities for Commercial Office Occupancy

Normative Quantity Type	Unit of Measurement	10-Percentile Quantity	50-Percentile Quantity	90-Percentile Quantity
Gross Area	Square Feet (SF)	10,000	85,000	1,103,000
Volume	Cubic Feet (CF) per 1 Gross Square Foot (gsf)	10.300	13.600	18.000
Cladding				
Gross Wall Area	SF per 1 gsf	0.380	0.645	1.200
Windows or Glazing Area	100 SF per 1 gsf	8.0E-04	3.0E-03	6.0E-03
Roof Area - Total	SF per 1 gsf	0.025	0.270	1.300
Interior Partition Length	100 Linear Feet (LF) per 1 gsf	7.0E-04	1.0E-03	1.2E-03
Ceramic tile floors	SF per 1 gsf	0.020	0.042	0.104
Ceramic tile walls	100 LF per 1 gsf	3.6E-05	7.6E-05	1.9E-04
Ceilings				
Ceiling - Lay in tile percentage	%		90%	

Table F-1 Normative Quantities for Commercial Office Occupancy (continued)

Normative Quantity Type	Unit of Measurement	10-Percentile Quantity	50-Percentile Quantity	90-Percentile Quantity
Ceiling - Gypsum board percentage	%		5%	
Ceiling - Exposed percentage	%		3%	
Ceiling - Other (high end) percentage	%		2%	
Stairs	Flights (FL) per 1 gsf	8.0E-05	1.0E-04	1.2E-04
Elevators	Each (EA) per 1 gsf	1.5E-05	2.8E-05	7.9E-05
Plumbing				
Plumbing Fixtures	EA per 1 gsf	5.0E-04	1.1E-03	2.6E-03
Piping				
Cold Domestic Water Piping - 2 ½ inch diameter or smaller	1,000 LF per 1 gsf	2.0E-05	4.2E-05	1.0E-04
Cold Domestic Water Piping – greater than 2 ½ diameter	1,000 LF per 1 gsf	1.0E-05	1.5E-05	2.0E-05
Hot Domestic Water Piping - 2 ½ inch diameter or smaller	1,000 LF per 1 gsf	4.0E-05	8.4E-05	2.1E-04
Hot Domestic Waster Piping – greater than 2 ½ diameter	1,000 LF per 1 gsf	2.0E-05	3.0E-05	4.0E-05
Gas supply piping	1,000 LF per 1 gsf	1.0E-05	1.5E-05	2.0E-05
Sanitary Waste Piping	1,000 LF per 1 gsf	3.0E-05	5.7E-05	1.2E-04
HVAC				
Chiller capacity	TN per 1 gsf	2.5E-03	2.9E-03	3.3E-03
Cooling Tower capacity	TN per 1 gsf	2.5E-03	2.9E-03	3.3E-03
Boiler capacity	BTU per 1 gsf	30.000	45.000	60.000
Air Handling Units	Cubic Feet per Minute (CFM) per 1 gsf	0.500	0.700	0.900
Fans	CFM per 1 gsf	0.000	0.000	0.000
HVAC Ducts – 6 sq. feet for larger	1,000 LF per 1 gsf	1.5E-05	2.0E-05	2.5E-05
HVAC Ducts – less than 6 sq. feet	1,000 LF per 1 gsf	5.0E-05	7.5E-05	9.0E-05
HVAC in-line Drops & Diffusers	EA per 1 gsf	6.0E-03	9.0E-03	2.0E-02
HVAC in-line Coils	EA per 1 gsf	3.0E-03	5.0E-03	6.0E-03
VAV Boxes	EA per 1 gsf	1.0E-03	2.0E-03	4.0E-03
Piping				
Steam & Chilled Water Piping - 2 ½ inch diameter or smaller	1,000 LF per 1 gsf	0.0E+00	0.0E+00	5.0E-06
Steam & Chilled Water Piping – greater than 2 ½ diameter	1,000 LF per 1 gsf	0.0E+00	0.0E+00	5.0E-06

Table F-1 Normative Quantities for Commercial Office Occupancy (continued)

Normative Quantity Type	Unit of Measurement	10-Percentile Quantity	50-Percentile Quantity	90-Percentile Quantity
Heating Water Piping - 2 ½ inch diameter or smaller	1,000 LF per 1 gsf	0.0E+00	5.0E-06	1.0E-05
Heating Water Piping – greater than 2 ½ diameter	1,000 LF per 1 gsf	0.0E+00	5.0E-06	1.0E-05
Electrical				
Electrical Load	W per 1 gsf	6.000	16.200	27.000
Electrical Distribution conduits	LF per 1 gsf	7.0E-02	2.0E-01	4.0E-01
Electrical Distribution – cable trays	LF per 1 gsf	0.0E+00	2.0E-02	5.0E-02
Wall mounted switchgear	EA per 1 gsf	1.0E-04	1.5E-04	2.0E-04
Lighting Fixtures – Lay in fluorescent	EA per 1 gsf	1.0E-02	1.5E-02	2.0E-02
Lighting Fixtures – Stem hung fluorescent	EA per 1 gsf	1.0E-02	1.5E-02	2.0E-02
Standby generators	KVA per 1 gsf	0.0E+00	0.0E+00	0.0E+00
Fire Protection				
Sprinkler Piping	20 LF per 1 gsf	8.5E-03	1.0E-02	1.1E-02
Sprinkler Drops	EA per 1 gsf	7.0E-03	9.0E-03	1.2E-02

Table F-2 Normative Quantities for Education (K-12) Occupancy

Normative Quantity Type	Unit of Measurement	10-Percentile Quantity	50-Percentile Quantity	90-Percentile Quantity
Gross Area	SF	3,100	36,400	218,900
Volume	CF per 1 gsf	10.400	13.370	19.200
Cladding				
Gross Wall Area	SF per 1 gsf	0.380	0.750	1.700
Windows or Glazing Area	100 SF per 1 gsf	3.0E-04	1.1E-03	2.9E-03
Roof Area - Total	SF per 1 gsf	0.150	0.680	1.280
Interior Partition Length	100 LF per 1 gsf	3.0E-04	5.6E-04	9.8E-04
Ceramic tile floors	SF per 1 gsf	0.024	0.079	0.166
Ceramic tile walls	100 LF per 1 gsf	4.4E-05	1.4E-04	3.0E-04
Ceilings				
Ceiling - Lay in tile percentage	%		95%	
Ceiling - Gypsum board percentage	%		3%	
Ceiling - Exposed percentage	%		2%	
Ceiling - Other (high end) percentage	%		0%	
Stairs	FL per 1 gsf	6.0E-05	7.0E-05	9.0E-05
Elevators	EA per 1 gsf	9.0E-06	2.0E-05	1.3E-04
Plumbing				
Plumbing Fixtures	EA per 1 gsf	6.1E-04	2.0E-03	4.2E-03
Piping				
Cold Domestic Water Piping - 2 ½ inch diameter or smaller	1,000 LF per 1 gsf	2.0E-05	3.0E-05	4.0E-05
Cold Domestic Water Piping – greater than 2 ½ diameter	1,000 LF per 1 gsf	1.0E-05	1.5E-05	2.0E-05
Hot Domestic Water Piping - 2 ½ inch diameter or smaller	1,000 LF per 1 gsf	4.0E-05	6.0E-05	8.0E-05
Hot Domestic Waster Piping – greater than 2 ½ diameter	1,000 LF per 1 gsf	2.0E-05	3.0E-05	4.0E-05
Gas supply piping	1,000 LF per 1 gsf	2.0E-05	4.0E-05	4.5E-05
Sanitary Waste Piping	1,000 LF per 1 gsf	3.0E-05	4.5E-05	6.0E-05
HVAC				
Chiller capacity	TN per 1 gsf	0.0E+00	0.0E+00	2.5E-03
Cooling Tower capacity	TN per 1 gsf	0.0E+00	0.0E+00	2.5E-03
Boiler capacity	BTU per 1 gsf	30.000	45.000	60.000
Air Handling Units	CFM per 1 gsf	0.000	0.000	0.600
HVAC Ducts – 6 sq. feet for larger	1,000 LF per 1 gsf	0.0E+00	0.0E+00	1.5E-05
HVAC Ducts – less than 6 sq. feet	1,000 LF per 1 gsf	0.0E+00	5.0E-05	8.0E-05
HVAC in-line Drops & Diffusers	EA per 1 gsf	0.0E+00	5.0E-03	8.0E-03

Table F-2 Normative Quantities for Education (K-12) Occupancy (continued)

Normative Quantity Type	Unit of Measurement	10-Percentile Quantity	50-Percentile Quantity	90-Percentile Quantity
HVAC in-line Coils	EA per 1 gsf	0.0E+00	0.0E+00	1.5E-03
VAV Boxes	EA per 1 gsf	0.0E+00	0.0E+00	1.5E-03
Fan Coil Units	EA per 1 gsf	2.0E-03	4.0E-03	0.0E+00
Piping				
Steam & Chilled Water Piping - 2 ½ inch diameter or smaller	1,000 LF per 1 gsf	0.0E+00	0.0E+00	5.0E-06
Steam & Chilled Water Piping – greater than 2 ½ diameter	1,000 LF per 1 gsf	0.0E+00	5.0E-06	1.0E-05
Heating Water Piping - 2 ½ inch diameter or smaller	1,000 LF per 1 gsf	0.0E+00	2.5E-05	4.0E-05
Heating Water Piping – greater than 2 ½ diameter	1,000 LF per 1 gsf	0.0E+00	5.0E-06	1.0E-05
Electrical				
Electrical Load	W per 1 gsf	7.000	18.800	23.000
Electrical Distribution conduits	LF per 1 gsf	1.0E-01	2.0E-01	3.0E-01
Electrical Distribution – cable trays	LF per 1 gsf	0.0E+00	0.0E+00	0.0E+00
Wall mounted switchgear	EA per 1 gsf	1.0E-04	1.5E-04	2.0E-04
Lighting Fixtures – Lay in fluorescent	EA per 1 gsf	1.0E-02	1.5E-02	1.7E-02
Lighting Fixtures – Stem hung fluorescent	EA per 1 gsf	1.0E-02	1.5E-02	1.7E-02
Standby generators	KVA per 1 gsf	0.0E+00	0.0E+00	0.0E+00
Fire Protection				
Sprinkler Piping	20 LF per 1 gsf	7.5E-03	9.0E-03	1.0E-02
Sprinkler Drops	EA per 1 gsf	6.0E-03	8.0E-03	1.0E-02

Table F-3 Normative Quantities for Healthcare Occupancy

Normative Quantity Type	Unit of Measurement	10-Percentile Quantity	50-Percentile Quantity	90-Percentile Quantity
Gross Area	SF	20,000	127,700	1,515,000
Volume	CF per 1 gsf	13.000	15.750	18.000
Cladding				
Gross Wall Area	SF per 1 gsf	0.260	0.500	1.000
Windows or Glazing Area	100 SF per 1 gsf	4.0E-04	1.4E-03	3.1E-03
Roof Area - Total	SF per 1 gsf	0.090	0.290	1.050
Interior Partition Length	100 LF per 1 gsf	7.5E-04	1.1E-03	1.4E-03
Ceramic tile floors	SF per 1 gsf	0.035	0.071	0.159
Ceramic tile walls	100 LF per 1 gsf	6.2E-05	1.3E-04	2.9E-04
Ceilings				
Ceiling - Lay in tile percentage	%		80%	
Ceiling - Gypsum board percentage	%		8%	
Ceiling - Exposed percentage	%		8%	
Ceiling - Other (high end) percentage	%		4%	
Stairs	FL per 1 gsf	7.0E-05	8.0E-05	1.0E-04
Elevators	EA per 1 gsf	1.2E-05	2.8E-05	9.8E-05
Plumbing				
Plumbing Fixtures	EA per 1 gsf	1.2E-03	2.4E-03	5.3E-03
Piping				
Cold Domestic Water Piping - 2 ½ inch diameter or smaller	1,000 LF per 1 gsf	8.0E-05	1.1E-04	1.3E-04
Cold Domestic Water Piping – greater than 2 ½ diameter	1,000 LF per 1 gsf	3.0E-05	4.0E-05	5.0E-05
Hot Domestic Water Piping - 2 ½ inch diameter or smaller	1,000 LF per 1 gsf	1.6E-04	2.2E-04	2.6E-04
Hot Domestic Waster Piping – greater than 2 ½ diameter	1,000 LF per 1 gsf	6.0E-05	8.0E-05	1.0E-04
Gas supply piping	1,000 LF per 1 gsf	5.0E-06	1.0E-05	1.5E-05
Sanitary Waste Piping	1,000 LF per 1 gsf	1.1E-04	1.5E-04	1.8E-04
Process Piping - 2 ½ inch diameter or smaller	1,000 LF per 1 gsf	1.2E-04	1.6E-04	2.0E-04
Process Piping – greater than 2 ½ diameter	1,000 LF per 1 gsf	4.0E-05	6.0E-05	7.0E-05
Acid Waste Piping	1,000 LF per 1 gsf	4.0E-05	6.0E-05	7.0E-05
HVAC				
Chiller capacity	TN per 1 gsf	2.9E-03	3.3E-03	3.7E-03
Cooling Tower capacity	TN per 1 gsf	2.9E-03	3.3E-03	3.7E-03
Boiler capacity	BTU per 1 gsf	40.000	50.000	65.000
Air Handling Units	CFM per 1 gsf	0.800	1.000	1.250

Table F-3 Normative Quantities for Healthcare Occupancy (continued)

Normative Quantity Type	Unit of Measurement	10-Percentile Quantity	50-Percentile Quantity	90-Percentile Quantity
Fans	CFM per 1 gsf	0.800	1.000	1.250
HVAC Ducts – 6 sq. feet for larger	1,000 LF per 1 gsf	2.5E-05	3.5E-05	4.0E-05
HVAC Ducts – less than 6 sq. feet	1,000 LF per 1 gsf	5.0E-05	7.5E-05	9.0E-05
HVAC in-line Drops & Diffusers	EA per 1 gsf	1.6E-02	2.0E-02	2.2E-02
HVAC in-line Coils	EA per 1 gsf	3.0E-03	5.0E-03	6.0E-03
VAV Boxes	EA per 1 gsf	3.0E-03	5.0E-03	6.0E-03
Piping				
Steam & Chilled Water Piping - 2 ½ inch diameter or smaller	1,000 LF per 1 gsf	0.0E+00	2.0E-05	1.5E-05
Steam & Chilled Water Piping – greater than 2 ½ diameter	1,000 LF per 1 gsf	2.0E-05	3.0E-05	2.5E-05
Heating Water Piping - 2 ½ inch diameter or smaller	1,000 LF per 1 gsf	6.0E-05	8.0E-05	1.0E-04
Heating Water Piping – greater than 2 ½ diameter	1,000 LF per 1 gsf	2.0E-05	3.0E-05	3.5E-05
Electrical				
Electrical Load	W per 1 gsf	14.000	23.100	35.600
Electrical Distribution conduits	LF per 1 gsf	3.0E-01	5.0E-01	6.0E-01
Electrical Distribution – cable trays	LF per 1 gsf	0.0E+00	4.0E-02	7.5E-02
Wall mounted switchgear	EA per 1 gsf	2.0E-04	4.0E-04	5.0E-04
Lighting Fixtures – Lay in fluorescent	EA per 1 gsf	1.0E-02	1.5E-02	1.7E-02
Lighting Fixtures – Stem hung fluorescent	EA per 1 gsf	1.0E-02	1.5E-02	1.7E-02
Standby generators	KVA per 1 gsf	3.5E-03	5.0E-03	1.5E-02
Fire Protection				
Sprinkler Piping	20 LF per 1 gsf	1.0E-02	1.1E-02	1.3E-02
Sprinkler Drops	EA per 1 gsf	1.0E-02	1.2E-02	1.4E-02

Table F-4 Normative Quantities for Hospitality Occupancy

Normative Quantity Type	Unit of Measurement	10-Percentile Quantity	50-Percentile Quantity	90-Percentile Quantity
Gross Area	SF			
Volume	CF per 1 gsf	9.000	11.000	14.000
Cladding				
Gross Wall Area	SF per 1 gsf	0.300	0.350	0.500
Windows or Glazing Area	100 SF per 1 gsf	7.0E-04	1.2E-03	1.7E-03
Roof Area - Total	SF per 1 gsf	0.600	0.200	0.060
Interior Partition Length	100 LF per 1 gsf	5.5E-04	6.0E-04	8.0E-04
Ceramic tile floors	SF per 1 gsf	0.120	0.160	0.240
Ceramic tile walls	100 LF per 1 gsf	2.2E-04	2.9E-04	4.3E-04
Ceilings				
Ceiling - Lay in tile percentage	%		15%	
Ceiling - Gypsum board percentage	%		70%	
Ceiling - Exposed percentage	%		8%	
Ceiling - Other (high end) percentage	%		7%	
Stairs	FL per 1 gsf	9.0E-05	1.1E-04	1.2E-04
Elevators	EA per 1 gsf	1.4E-05	1.5E-05	4.0E-05
Plumbing				
Plumbing Fixtures	EA per 1 gsf	3.0E-03	4.0E-03	6.0E-03
Piping				
Cold Domestic Water Piping - 2 ½ inch diameter or smaller	1,000 LF per 1 gsf	6.0E-05	8.0E-05	1.2E-04
Cold Domestic Water Piping – greater than 2 ½ diameter	1,000 LF per 1 gsf	1.0E-05	1.5E-05	2.0E-05
Hot Domestic Water Piping - 2 ½ inch diameter or smaller	1,000 LF per 1 gsf	1.2E-04	1.6E-04	2.4E-04
Hot Domestic Waster Piping – greater than 2 ½ diameter	1,000 LF per 1 gsf	2.0E-05	3.0E-05	4.0E-05
Gas supply piping	1,000 LF per 1 gsf	2.0E-05	4.0E-05	4.5E-05
Sanitary Waste Piping	1,000 LF per 1 gsf	7.0E-05	9.5E-05	1.4E-04
HVAC				
Chiller capacity	TN per 1 gsf	0.0E+00	0.0E+00	2.0E-03
Cooling Tower capacity	TN per 1 gsf	0.0E+00	0.0E+00	2.0E-03
Boiler capacity	BTU per 1 gsf	30.000	45.000	50.000
Air Handling Units	CFM per 1 gsf	0.000	0.000	0.600
HVAC Ducts – 6 sq. feet for larger	1,000 LF per 1 gsf	0.0E+00	0.0E+00	1.5E-05
HVAC Ducts – less than 6 sq. feet	1,000 LF per 1 gsf	0.0E+00	5.0E-05	8.0E-05
HVAC in-line Drops & Diffusers	EA per 1 gsf	4.0E-03	8.0E-03	1.2E-02

Table F-4 Normative Quantities for Hospitality Occupancy (continued)

Normative Quantity Type	Unit of Measurement	10-Percentile Quantity	50-Percentile Quantity	90-Percentile Quantity
HVAC in-line Coils	EA per 1 gsf	0.0E+00	0.0E+00	1.5E-03
VAV Boxes	EA per 1 gsf	0.0E+00	0.0E+00	1.5E-03
Fan Coil Units	EA per 1 gsf	4.0E-03	6.0E-03	0.0E+00
Piping				
Steam & Chilled Water Piping - 2 ½ inch diameter or smaller	1,000 LF per 1 gsf	0.0E+00	0.0E+00	5.0E-06
Steam & Chilled Water Piping – greater than 2 ½ diameter	1,000 LF per 1 gsf	0.0E+00	0.0E+00	5.0E-06
Heating Water Piping - 2 ½ inch diameter or smaller	1,000 LF per 1 gsf	0.0E+00	5.0E-06	1.0E-05
Heating Water Piping – greater than 2 ½ diameter	1,000 LF per 1 gsf	0.0E+00	5.0E-06	1.0E-05
Electrical				
Electrical Load	W per 1 gsf	6.000	11.000	15.000
Electrical Distribution conduits	LF per 1 gsf	0.0E+00	2.0E-01	3.0E-01
Electrical Distribution – cable trays	LF per 1 gsf	0.0E+00	0.0E+00	0.0E+00
Wall mounted switchgear	EA per 1 gsf	1.0E-04	1.5E-04	2.0E-04
Lighting Fixtures – Lay in fluorescent	EA per 1 gsf	0.0E+00	0.0E+00	4.0E-03
Lighting Fixtures – Stem hung fluorescent	EA per 1 gsf	0.0E+00	0.0E+00	4.0E-03
Standby generators	KVA per 1 gsf	0.0E+00	0.0E+00	0.0E+00
Fire Protection				
Sprinkler Piping	20 LF per 1 gsf	1.0E-02	1.1E-02	1.3E-02
Sprinkler Drops	EA per 1 gsf	1.0E-02	1.2E-02	1.4E-02

Table F-5 Normative Quantities for Multi-unit Residential Occupancy

Normative Quantity Type	Unit of Measurement	10-Percentile Quantity	50-Percentile Quantity	90-Percentile Quantity
Gross Area	SF	5,000	34,000	582,200
Volume	CF per 1 gsf	7.440	10.460	14.500
Cladding				
Gross Wall Area	SF per 1 gsf	0.320	0.770	1.300
Windows or Glazing Area	100 SF per 1 gsf	6.0E-04	1.5E-03	3.0E-03
Roof Area - Total	SF per 1 gsf	0.090	0.320	1.000
Interior Partition Length	100 LF per 1 gsf	7.0E-04	1.2E-03	1.6E-03
Ceramic tile floors	SF per 1 gsf	0.108	0.212	0.340
Ceramic tile walls	100 LF per 1 gsf	1.9E-04	3.8E-04	6.1E-04
Ceilings				
Ceiling - Lay in tile percentage	%		0%	
Ceiling - Gypsum board percentage	%		95%	
Ceiling - Exposed percentage	%		5%	
Ceiling - Other (high end) percentage	%		0%	
Stairs	FL per 1 gsf	1.0E-04	1.2E-04	1.4E-04
Elevators	EA per 1 gsf	7.0E-06	3.4E-05	8.0E-05
Plumbing				
Plumbing Fixtures	EA per 1 gsf	2.7E-03	5.3E-03	8.5E-03
Piping				
Cold Domestic Water Piping - 2 ½ inch diameter or smaller	1,000 LF per 1 gsf	5.4E-05	1.1E-04	1.7E-04
Cold Domestic Water Piping – greater than 2 ½ diameter	1,000 LF per 1 gsf	1.0E-05	1.5E-05	2.0E-05
Hot Domestic Water Piping - 2 ½ inch diameter or smaller	1,000 LF per 1 gsf	1.1E-04	2.1E-04	3.4E-04
Hot Domestic Waster Piping – greater than 2 ½ diameter	1,000 LF per 1 gsf	2.0E-05	3.0E-05	4.0E-05
Gas supply piping	1,000 LF per 1 gsf	2.0E-05	4.0E-05	4.5E-05
Sanitary Waste Piping	1,000 LF per 1 gsf	6.4E-05	1.2E-04	1.9E-04
HVAC				
Chiller capacity	TN per 1 gsf	0.0E+00	0.0E+00	2.0E-03
Cooling Tower capacity	TN per 1 gsf	0.0E+00	0.0E+00	2.0E-03
Boiler capacity	BTU per 1 gsf	30.000	45.000	60.000
Air Handling Units	CFM per 1 gsf	0.000	0.000	0.600
HVAC Ducts – 6 sq. feet for larger	1,000 LF per 1 gsf	0.0E+00	0.0E+00	1.5E-05
HVAC Ducts – less than 6 sq. feet	1,000 LF per 1 gsf	0.0E+00	5.0E-05	8.0E-05
HVAC in-line Drops & Diffusers	EA per 1 gsf	4.0E-03	8.0E-03	1.2E-02

Table F-5 Normative Quantities for Multi-unit Residential Occupancy (continued)

Normative Quantity Type	Unit of Measurement	10-Percentile Quantity	50-Percentile Quantity	90-Percentile Quantity
HVAC in-line Coils	EA per 1 gsf	0.0E+00	0.0E+00	1.5E-03
VAV Boxes	EA per 1 gsf	0.0E+00	0.0E+00	1.5E-03
Fan Coil Units	EA per 1 gsf	2.0E-03	4.0E-03	0.0E+00
Piping				
Steam & Chilled Water Piping - 2 ½ inch diameter or smaller	1,000 LF per 1 gsf	0.0E+00	0.0E+00	5.0E-06
Steam & Chilled Water Piping – greater than 2 ½ diameter	1,000 LF per 1 gsf	0.0E+00	0.0E+00	5.0E-06
Heating Water Piping - 2 ½ inch diameter or smaller	1,000 LF per 1 gsf	0.0E+00	5.0E-06	1.0E-05
Heating Water Piping – greater than 2 ½ diameter	1,000 LF per 1 gsf	0.0E+00	5.0E-06	1.0E-05
Electrical				
Electrical Load	W per 1 gsf	8.300	11.400	19.500
Electrical Distribution conduits	LF per 1 gsf	0.0E+00	2.0E-01	3.0E-01
Electrical Distribution – cable trays	LF per 1 gsf	0.0E+00	0.0E+00	0.0E+00
Wall mounted switchgear	EA per 1 gsf	1.0E-04	1.5E-04	2.0E-04
Lighting Fixtures – Lay in fluorescent	EA per 1 gsf	0.0E+00	0.0E+00	4.0E-03
Lighting Fixtures – Stem hung fluorescent	EA per 1 gsf	0.0E+00	0.0E+00	4.0E-03
Standby generators	KVA per 1 gsf	0.0E+00	0.0E+00	0.0E+00
Fire Protection				
Sprinkler Piping	20 LF per 1 gsf	1.0E-02	1.1E-02	1.3E-02
Sprinkler Drops	EA per 1 gsf	1.0E-02	1.2E-02	1.4E-02

Table F-6 Normative Quantities for Research Laboratories Occupancy

Normative Quantity Type	Unit of Measurement	10-Percentile Quantity	50-Percentile Quantity	90-Percentile Quantity
Gross Area	SF	35,000	96,000	330,000
Volume	CF per 1 gsf	13.000	16.000	20.000
Cladding				
Gross Wall Area	SF per 1 gsf	0.400	0.520	1.100
Windows or Glazing Area	100 SF per 1 gsf	7.0E-04	1.5E-03	4.3E-03
Roof Area - Total	SF per 1 gsf	1.050	0.245	0.110
Interior Partition Length	100 LF per 1 gsf	6.0E-04	8.5E-04	1.1E-03
Ceramic tile floors	SF per 1 gsf	0.010	0.028	0.080
Ceramic tile walls	100 LF per 1 gsf	1.8E-05	5.0E-05	1.4E-04
Ceilings				
Ceiling - Lay in tile percentage	%		85%	
Ceiling - Gypsum board percentage	%		5%	
Ceiling - Exposed percentage	%		8%	
Ceiling - Other (high end) percentage	%		2%	
Laboratory Casework	LF per 1 gsf	0.0E+00	2.2E-02	4.0E-02
Fume Hoods	EA per 1 gsf	0.0E+00	9.0E-04	1.9E-03
Stairs	FL per 1 gsf	8.0E-05	1.0E-04	1.2E-04
Elevators	EA per 1 gsf	1.3E-05	1.7E-05	1.0E-04
Plumbing				
Plumbing Fixtures				
Domestic	EA per 1 gsf	2.5E-04	7.0E-04	2.0E-03
Lab	EA per 1 gsf	7.0E-05	2.7E-04	3.0E-03
Piping				
Cold Domestic Water Piping - 2 ½ inch diameter or smaller	1,000 LF per 1 gsf	4.0E-05	6.0E-05	8.0E-05
Cold Domestic Water Piping – greater than 2 ½ diameter	1,000 LF per 1 gsf	1.0E-05	2.0E-05	3.0E-05
Hot Domestic Water Piping - 2 ½ inch diameter or smaller	1,000 LF per 1 gsf	8.0E-05	1.2E-04	1.6E-04
Hot Domestic Waster Piping – greater than 2 ½ diameter	1,000 LF per 1 gsf	2.0E-05	4.0E-05	6.0E-05
Gas supply piping	1,000 LF per 1 gsf	5.0E-06	1.0E-05	1.5E-05
Sanitary Waste Piping	1,000 LF per 1 gsf	5.0E-05	8.0E-05	1.1E-04
Process Piping - 2 ½ inch diameter or smaller	1,000 LF per 1 gsf	3.0E-04	4.0E-04	5.0E-04
Process Piping – greater than 2 ½ diameter	1,000 LF per 1 gsf	1.0E-04	1.5E-04	1.8E-04
Acid Waste Piping	1,000 LF per 1 gsf	1.0E-04	1.5E-04	1.8E-04
HVAC				

Table F-6 Normative Quantities for Research Laboratories Occupancy (continued)

Normative Quantity Type	Unit of Measurement	10-Percentile Quantity	50-Percentile Quantity	90-Percentile Quantity
Chiller capacity	TN per 1 gsf	2.9E-03	3.3E-03	3.7E-03
Cooling Tower capacity	TN per 1 gsf	2.9E-03	3.3E-03	3.7E-03
Boiler capacity	BTU per 1 gsf	55.000	65.000	75.000
Air Handling Units	CFM per 1 gsf	1.000	1.250	1.500
Fans	CFM per 1 gsf	1.000	1.250	1.500
HVAC Ducts – 6 sq. feet for larger	1,000 LF per 1 gsf	3.5E-05	5.0E-05	7.0E-05
HVAC Ducts – less than 6 sq. feet	1,000 LF per 1 gsf	8.0E-05	1.0E-04	1.2E-04
HVAC in-line Drops & Diffusers	EA per 1 gsf	1.3E-02	1.6E-02	2.0E-02
HVAC in-line Coils	EA per 1 gsf	1.3E-03	2.0E-03	2.5E-03
VAV Boxes	EA per 1 gsf	0.0E+00	3.0E-04	5.0E-04
Pressure Dependent Air Valves (Phoenix type boxes)	EA per 1 gsf	6.0E-03	1.0E-02	1.2E-02
Piping				
Steam & Chilled Water Piping - 2 ½ inch diameter or smaller	1,000 LF per 1 gsf	0.0E+00	1.0E-05	1.5E-05
Steam & Chilled Water Piping – greater than 2 ½ diameter	1,000 LF per 1 gsf	1.5E-05	2.0E-05	2.5E-05
Heating Water Piping - 2 ½ inch diameter or smaller	1,000 LF per 1 gsf	6.0E-05	8.0E-05	1.0E-04
Heating Water Piping – greater than 2 ½ diameter	1,000 LF per 1 gsf	2.0E-05	3.0E-05	3.5E-05
Electrical				
Electrical Load	W per 1 gsf	14.500	22.800	48.800
Electrical Distribution conduits	LF per 1 gsf	3.0E-01	5.0E-01	6.0E-01
Electrical Distribution – cable trays	LF per 1 gsf	0.0E+00	4.0E-02	7.5E-02
Wall mounted switchgear	EA per 1 gsf	1.0E-03	3.0E-03	4.0E-03
Lighting Fixtures – Lay in fluorescent	EA per 1 gsf	1.0E-02	1.5E-02	1.7E-02
Lighting Fixtures – Stem hung fluorescent	EA per 1 gsf	1.0E-02	1.5E-02	1.7E-02
Standby generators	KVA per 1 gsf	3.5E-03	5.0E-03	1.5E-02
Fire Protection				
Sprinkler Piping	20 LF per 1 gsf	9.0E-03	1.0E-02	1.1E-02
Sprinkler Drops	EA per 1 gsf	8.0E-03	1.0E-02	1.3E-02

Table F-7 Normative Quantities for Retail Occupancy

Normative Quantity Type	Unit of Measurement	10-Percentile Quantity	50-Percentile Quantity	90-Percentile Quantity
Gross Area	SF	25,000	40,000	90,000
Volume	CF per 1 gsf	18.000	20.000	23.000
Cladding				
Gross Wall Area	SF per 1 gsf	0.250	0.300	0.400
Windows or Glazing Area	100 SF per 1 gsf	4.0E-04	6.0E-04	8.0E-04
Roof Area - Total	SF per 1 gsf	0.700	0.500	0.300
Interior Partition Length	100 LF per 1 gsf	6.0E-05	1.0E-04	1.2E-04
Ceramic tile floors	SF per 1 gsf	0.040	0.060	0.072
Ceramic tile walls	100 LF per 1 gsf	7.2E-05	1.1E-04	1.3E-04
Ceilings				
Ceiling - Lay in tile percentage	%		90%	
Ceiling - Gypsum board percentage	%		3%	
Ceiling - Exposed percentage	%		2%	
Ceiling - Other (high end) percentage	%		5%	
Stairs	FL per 1 gsf	5.0E-05	1.0E-04	1.2E-04
Elevators	EA per 1 gsf	5.0E-05	1.0E-04	1.2E-04
Plumbing				
Plumbing Fixtures	EA per 1 gsf	1.0E-03	1.5E-03	1.8E-03
Piping				
Cold Domestic Water Piping - 2 ½ inch diameter or smaller	1,000 LF per 1 gsf	2.0E-05	3.0E-05	4.0E-05
Cold Domestic Water Piping – greater than 2 ½ diameter	1,000 LF per 1 gsf	1.0E-05	1.5E-05	2.0E-05
Hot Domestic Water Piping - 2 ½ inch diameter or smaller	1,000 LF per 1 gsf	4.0E-05	6.0E-05	8.0E-05
Hot Domestic Waster Piping – greater than 2 ½ diameter	1,000 LF per 1 gsf	2.0E-05	3.0E-05	4.0E-05
Gas supply piping	1,000 LF per 1 gsf	2.0E-05	4.0E-05	4.5E-05
Sanitary Waste Piping	1,000 LF per 1 gsf	3.0E-05	4.5E-05	6.0E-05
HVAC				
Chiller capacity	TN per 1 gsf	0.0E+00	0.0E+00	2.5E-03
Cooling Tower capacity	TN per 1 gsf	0.0E+00	0.0E+00	2.5E-03
Boiler capacity	BTU per 1 gsf	30.000	45.000	60.000
Air Handling Units	CFM per 1 gsf	0.000	0.000	0.600
Fans	CFM per 1 gsf	0.000	0.000	15.000
HVAC Ducts – 6 sq. feet for larger	1,000 LF per 1 gsf	0.0E+00	5.0E-05	8.0E-05
HVAC Ducts – less than 6 sq. feet	1,000 LF per 1 gsf	0.0E+00	5.0E-06	8.0E-06

Table F-7 Normative Quantities for Retail Occupancy (continued)

Normative Quantity Type	Unit of Measurement	10-Percentile Quantity	50-Percentile Quantity	90-Percentile Quantity
HVAC in-line Drops & Diffusers	EA per 1 gsf	0.0E+00	0.0E+00	1.5E-03
HVAC in-line Coils	EA per 1 gsf	0.0E+00	0.0E+00	1.5E-03
VAV Boxes	EA per 1 gsf	2.0E-03	4.0E-03	0.0E+00
Piping				
Steam & Chilled Water Piping - 2 ½ inch diameter or smaller	1,000 LF per 1 gsf	0.0E+00	0.0E+00	5.0E-06
Steam & Chilled Water Piping – greater than 2 ½ diameter	1,000 LF per 1 gsf	0.0E+00	5.0E-06	1.0E-05
Heating Water Piping - 2 ½ inch diameter or smaller	1,000 LF per 1 gsf	0.0E+00	2.5E-05	4.0E-05
Heating Water Piping – greater than 2 ½ diameter	1,000 LF per 1 gsf	0.0E+00	5.0E-06	1.0E-05
Electrical				
Electrical Load	W per 1 gsf	7.000	18.800	23.000
Electrical Distribution conduits	LF per 1 gsf	1.0E-01	2.0E-01	3.0E-01
Electrical Distribution – cable trays	LF per 1 gsf	0.0E+00	0.0E+00	0.0E+00
Wall mounted switchgear	EA per 1 gsf	1.0E-04	1.5E-04	2.0E-04
Lighting Fixtures – Lay in fluorescent	EA per 1 gsf	1.0E-02	1.5E-02	1.7E-02
Lighting Fixtures – Stem hung fluorescent	EA per 1 gsf	1.0E-02	1.5E-02	1.7E-02
Standby generators	KVA per 1 gsf	0.0E+00	0.0E+00	0.0E+00
Fire Protection				
Sprinkler Piping	20 LF per 1 gsf	7.5E-03	9.0E-03	1.0E-02
Sprinkler Drops	EA per 1 gsf	6.0E-03	8.0E-03	1.0E-02

Table F-8 Normative Quantities for Warehouse Occupancy

Normative Quantity Type	Unit of Measurement	10-Percentile Quantity	50-Percentile Quantity	90-Percentile Quantity
Gross Area	SF			
Volume	CF per 1 gsf	20.000	28.000	40.000
Cladding				
Gross Wall Area	SF per 1 gsf	0.200	0.220	0.300
Windows or Glazing Area	100 SF per 1 gsf	0.0E+00	1.0E-05	2.0E-05
Roof Area - Total	SF per 1 gsf	1.000	1.000	1.000
Interior Partition Length	100 LF per 1 gsf	3.0E-05	3.0E-05	4.0E-05
Ceramic tile floors	SF per 1 gsf	0.001	0.002	0.004
Ceramic tile walls	100 LF per 1 gsf	2.2E-06	4.3E-06	7.2E-06
Ceilings				
Ceiling - Lay in tile percentage	%		5%	
Ceiling - Gypsum board percentage	%		5%	
Ceiling - Exposed percentage	%		90%	
Ceiling - Other (high end) percentage	%		0%	
Stairs	FL per 1 gsf	0.0E+00	0.0E+00	0.0E+00
Elevators	EA per 1 gsf	0.0E+00	0.0E+00	0.0E+00
Plumbing				
Plumbing Fixtures	EA per 1 gsf	3.0E-05	6.0E-05	1.0E-04
Piping				
Cold Domestic Water Piping - 2 ½ inch diameter or smaller	1,000 LF per 1 gsf	2.4E-06	4.8E-06	8.0E-06
Cold Domestic Water Piping – greater than 2 ½ diameter	1,000 LF per 1 gsf	1.0E-05	1.5E-05	2.0E-05
Hot Domestic Water Piping - 2 ½ inch diameter or smaller	1,000 LF per 1 gsf	4.8E-06	9.6E-06	1.6E-05
Hot Domestic Waster Piping – greater than 2 ½ diameter	1,000 LF per 1 gsf	2.0E-05	3.0E-05	4.0E-05
Gas supply piping	1,000 LF per 1 gsf	1.0E-05	1.5E-05	2.0E-05
Sanitary Waste Piping	1,000 LF per 1 gsf	1.2E-05	2.0E-05	2.8E-05
HVAC				
Chiller capacity	TN per 1 gsf	0.0E+00	0.0E+00	2.0E-03
Cooling Tower capacity	TN per 1 gsf	0.0E+00	0.0E+00	2.0E-03
Boiler capacity	BTU per 1 gsf	10.000	15.000	20.000
Air Handling Units	CFM per 1 gsf	0.000	0.200	0.400
Fans	CFM per 1 gsf	0.000	0.000	0.300
HVAC Ducts – 6 sq. feet for larger	1,000 LF per 1 gsf	0.0E+00	0.0E+00	1.0E-05
HVAC Ducts – less than 6 sq. feet	1,000 LF per 1 gsf	0.0E+00	4.0E-05	6.0E-05

Table F-8 Normative Quantities for Warehouse Occupancy (continued)

Normative Quantity Type	Unit of Measurement	10-Percentile Quantity	50-Percentile Quantity	90-Percentile Quantity
HVAC in-line Drops & Diffusers	EA per 1 gsf	2.0E-03	3.0E-03	5.0E-03
HVAC in-line Coils	EA per 1 gsf	0.0E+00	0.0E+00	1.0E-03
VAV Boxes	EA per 1 gsf	0.0E+00	0.0E+00	1.0E-03
Piping				
Steam & Chilled Water Piping - 2 ½ inch diameter or smaller	1,000 LF per 1 gsf	0.0E+00	0.0E+00	5.0E-06
Steam & Chilled Water Piping – greater than 2 ½ diameter	1,000 LF per 1 gsf	0.0E+00	0.0E+00	5.0E-06
Heating Water Piping - 2 ½ inch diameter or smaller	1,000 LF per 1 gsf	0.0E+00	5.0E-06	1.0E-05
Heating Water Piping – greater than 2 ½ diameter	1,000 LF per 1 gsf	0.0E+00	5.0E-06	1.0E-05
Electrical				
Electrical Load	W per 1 gsf	4.000	6.000	12.000
Electrical Distribution conduits	LF per 1 gsf	2.0E-02	1.0E-01	1.5E-01
Electrical Distribution – cable trays	LF per 1 gsf	0.0E+00	0.0E+00	0.0E+00
Wall mounted switchgear	EA per 1 gsf	5.0E-05	8.0E-05	1.0E-03
Lighting Fixtures – Lay in fluorescent	EA per 1 gsf	0.0E+00	0.0E+00	0.0E+00
Lighting Fixtures – Stem hung fluorescent	EA per 1 gsf	1.0E-02	1.5E-02	2.0E-02
Standby generators	KVA per 1 gsf	0.0E+00	0.0E+00	0.0E+00
Fire Protection				
Sprinkler Piping	20 LF per 1 gsf	4.5E-03	5.5E-03	6.5E-03
Sprinkler Drops	EA per 1 gsf	6.0E-03	8.0E-03	1.0E-02

Appendix G
Generation of Simulated Demands

G.1 Loss Computations

The loss-calculation algorithm embedded in PACT generates a large number of simulations (or vectors) of demand per intensity level to develop a loss curve. This appendix describes the two PACT algorithms that are used to transform the computed demands into a large number of simulations[1]. Section G.2 presents the algorithm for assessment using nonlinear response-history analysis (multiple demand vectors per intensity level). Section G.3 presents the algorithm for assessment using the simplified analysis procedure (one demand vector per intensity level). The simulations are used to determine the values of performance measures in realizations rather than the analytically-determined vectors, which are not by themselves used for this purpose.

G.2 Simulations for Assessment Using Nonlinear Response-History Analysis

G.2.1 Introduction

Section G.2.2 introduces the algorithm implemented in PACT to transform a limited number of vectors of calculated demand parameters determined by response-history analysis to the large number of simulated demand vectors used for loss calculations. Section G.2.3 presents sample calculations to

[1] In these *Guidelines*, either nonlinear response-history analysis or a simplified linear static procedure can be used to generate estimates of median response parameters. In the case of response history analysis, a correlation matrix for these demands is also generated. Then a large number of simulated demand vectors are generated per intensity level and the values of performance measures is determined for each realization. The minimum number of nonlinear analyses required per intensity level depends on many parameters, including the required accuracy of the loss calculation, the dynamic properties of the building, and the properties of the ground motion. This appendix uses a default number of demand vectors per intensity level [11 for nonlinear response-history analysis and 1 for simplified analysis] to illustrate the algorithms included in PACT to generate a large number of simulations.

illustrate the procedure. A Matlab script is presented in G.2.4 to enable the reader to generate correlated vectors outside of PACT, as described below.

G.2.2 Algorithm

The technical basis for the algorithm described herein was developed by Yang (Yang, 2006; Yang et al., 2009). The algorithm was extended by Huang et al. (2008) to address modeling uncertainty, β_m, record-to-record variability, β_a, and ground motion variability, β_{gm}.

For typical assessment, a limited number, *m*, of response analyses are performed at each intensity level. For each analysis, the peak absolute value of each demand parameter (e.g., third story drift, roof acceleration) is assembled into a row vector with *n* entries, where *n* is the number of demand parameters. The *m* row vectors are catenated to form an *m*×*n* matrix (rows × columns; analyses × demand parameters) – each column presents *m* values of one demand parameter.

The minimum number of response analyses, *m*, depends on many parameters, including the dynamic properties of the building, the chosen ground motion intensity measures, the care taken to choose the ground motions, and the required accuracy of the loss calculations. For a regular building located in a region of low-to-moderate seismic hazard, it is likely that a relatively small number of ground motion records, *m*, will provide an acceptable characterization of structural response at each intensity level, with the required number of records reducing as match to spectral shape is improved.

Denote the matrix of demand parameters, $\mathbf{X}$. The entries in $\mathbf{X}$ are assumed to be jointly lognormal. The natural logarithm of each entry in $\mathbf{X}$ is computed to form an *m*×*n* matrix, $\mathbf{Y}$. The entries in $\mathbf{Y}$ are assumed to be jointly normal and can be characterized by a 1×*n* mean vector, $\mathbf{M}_\mathbf{Y}$, an *n*×*n* correlation coefficient matrix, $\mathbf{R}_{\mathbf{YY}}$, and an *n*×*n* diagonal matrix of standard deviations, $\mathbf{D}_\mathbf{Y}$.

A vector of demand parameters, $\mathbf{Z}$, can be generated with the same statistical distribution as $\mathbf{Y}$ using a vector of uncorrelated standard normal random variables, $\mathbf{U}$, with a mean of 0 and a standard deviation of 1 for each random variable. For this case

$$\mathbf{Z} = \mathbf{AU} + \mathbf{B} = \mathbf{D}_\mathbf{Y}\mathbf{L}_\mathbf{Y}\mathbf{U} + \mathbf{M}_\mathbf{Y} \quad \text{(G-1)}$$

where $\mathbf{A}$ is a matrix of constant coefficients that linearly transforms $\mathbf{U}$ to $\mathbf{Z}$ and $\mathbf{B}$ is a vector of constant coefficients that translates $\mathbf{U}$ to $\mathbf{Z}$. Matrix $\mathbf{A}$

and vector $\mathbf{B}$ are derived in Yang (2006). The matrix $\mathbf{L_Y}$ is the transposed Cholesky-like decomposition[2] of $\mathbf{R_{YY}}$; all other terms are defined above.

One simulated demand is generated by 1) computing $\mathbf{M_Y}$, $\mathbf{D_Y}$ and $\mathbf{L_Y}$ by sampling $\mathbf{Y}$; (2) updating $\mathbf{D_Y}$ for modeling uncertainty per Section G.2.4; (3) populating $\mathbf{U}$ by random sampling each demand parameter on a distribution with a mean of 0 and a standard deviation of 1.0; (4) computing $\mathbf{Z}$ per (G-1); and (5) taking the exponential of every entry in $\mathbf{Z}$ to recover the Vector of simulated demand parameters, $\mathbf{W}$. N vectors of $\mathbf{U}$ are required for the N simulations: one vector per simulation. The process is computationally efficient because $\mathbf{M_Y}$, $\mathbf{D_Y}$ and $\mathbf{L_Y}$ are computed just once for each intensity of shaking. The process is illustrated in Figure G-1 (from Yang, 2006) below.

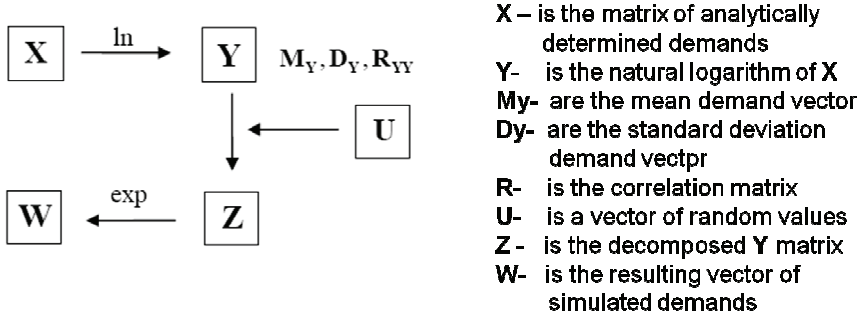

Figure G-1 Generation of simulated vectors of correlated demand parameters (Yang, 2006)

G.2.3 Sample Application of the Algorithm

Description

The sample building is a three story steel moment frame. For this sample application, analysis is performed along one axis and the number of simulations, *N*, is selected as 200. Seven demand parameters (n=7) are used for performance assessment for this building: 1st, 2nd and 3rd story drift (expressed as a percentage of the story height); and 1st, 2nd and 3rd floor and roof acceleration: δ_1, δ_2, δ_3, a_1, a_2, a_3 and a_r, respectively. Eleven analyses (m=11) are performed for each intensity of motion. Residual story drift and floor velocities are not considered in this example, but are included

[2] If matrix $\mathbf{K}$ is symmetric and positive -definite (e.g., a full rank, covariance matrix), it can be decomposed into a lower triangular matrix, $\mathbf{L}$, the Cholesky triangle, and the transpose of the lower triangular matrix, such that $\mathbf{K} = \mathbf{L}\mathbf{L}^T$. If $\mathbf{K}$ is positive semi-definite, $\mathbf{L}$ is computed from an eigenvalue decomposition of $\mathbf{K}$ and is not necessarily triangular or square in this case. To solve $\mathbf{K}\mathbf{u} = \mathbf{R}$, one solves first $\mathbf{L}\mathbf{y} = \mathbf{R}$ for $\mathbf{y}$ and then $\mathbf{L}^T\mathbf{u} = \mathbf{y}$ for $\mathbf{u}$.

in the actual implementation. The matrix $\mathbf{X}$ of demand parameters, 11 rows (one per analysis) × 7 columns (one per demand parameter), is presented in Table G-1. Modeling uncertainty, record-to-record variability and ground motion variability are set aside here to simplify the presentation.

Probability Distributions

Consider the matrix $\mathbf{X} = [\mathbf{X}_1, \mathbf{X}_2 ..... \mathbf{X}_7]$ in Table G-1, below, with: 7 column vectors of demand, with 11 entries per vector. For each vector, the mean (expected) value, μ_x and the variance, s_x^2, can be established as follows:

$$\mu_x = \frac{1}{n}\sum_{i=1}^{i=n} x_i \tag{G-2}$$

$$s_x^2 = \frac{1}{n-1}\sum_{i=1}^{i=n} (x_i - \mu_x)^2 \tag{G-3}$$

The mean and variance of $\mathbf{X} = [\mathbf{X}_1, \mathbf{X}_2 ..... \mathbf{X}_7]$ are presented in Table G-2.

Table G-1 Matrix of Analytically Determined Demand Parameters, *X*

	δ_1 (%)	δ_2 (%)	δ_3 (%)	a_1 (g)	a_2 (g)	a_3 (g)	a_r (g)
1	1.26	1.45	1.71	0.54	0.87	0.88	0.65
2	1.41	2.05	2.43	0.55	0.87	0.77	0.78
3	1.37	1.96	2.63	0.75	1.04	0.89	0.81
4	0.97	1.87	2.74	0.55	0.92	1.12	0.75
5	0.94	1.8	2.02	0.40	0.77	0.74	0.64
6	1.73	2.55	2.46	0.45	0.57	0.45	0.59
7	1.05	2.15	2.26	0.38	0.59	0.49	0.52
8	1.40	1.67	2.1	0.73	1.50	1.34	0.83
9	1.59	1.76	2.01	0.59	0.94	0.81	0.72
10	0.83	1.68	2.25	0.53	1.00	0.9	0.74
11	0.96	1.83	2.25	0.49	0.90	0.81	0.64

Table G-2 Mean and Variance of *X*

	δ_1 (%)	δ_2 (%)	δ_3 (%)	a_1 (g)	a_2 (g)	a_3 (g)	a_r (g)
μ_x	1.2282	1.8882	2.2600	0.5418	0.9064	0.8364	0.6973
s_x^2	0.0878	0.0849	0.0885	0.0139	0.0615	0.0627	0.0094

Joint probability distributions can be developed for pairs of vectors, for examples, between (a) $\mathbf{X}_1$ (first story drift) and $\mathbf{X}_3$ (third story drift), and (b) $\mathbf{X}_4$ (ground floor acceleration) and $\mathbf{X}_7$ (roof acceleration). The black solid circles in Figure G-2 below presents the relationships between $\mathbf{X}_1$ and $\mathbf{X}_3$ (part a) and $\mathbf{X}_4$ and $\mathbf{X}_7$ (part b) constructed using the data of Table G-1: $\mathbf{X}_1$ and $\mathbf{X}_3$ are weakly correlated and $\mathbf{X}_4$ and $\mathbf{X}_7$ are strongly correlated.

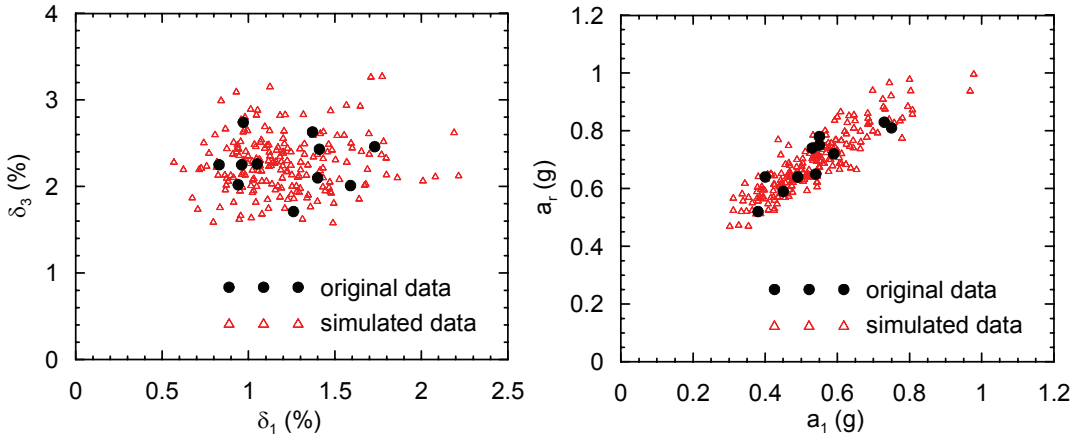

a. $\mathbf{X}_1$ and $\mathbf{X}_3$ b. $\mathbf{X}_4$ and $\mathbf{X}_7$

Figure G-2 Relationships between demand parameters

A joint probability density function of the type shown in Figure G-3 can be constructed for any pair of vectors given two means, two variances, a covariance and type of distribution (normal, log-normal). This figure presents the joint probability density functions for $\mathbf{X}_1$ and $\mathbf{X}_3$ (part a) and $\mathbf{X}_4$ and $\mathbf{X}_7$ (part c) constructed using the data of Table G-2—termed the *original* data hereafter.

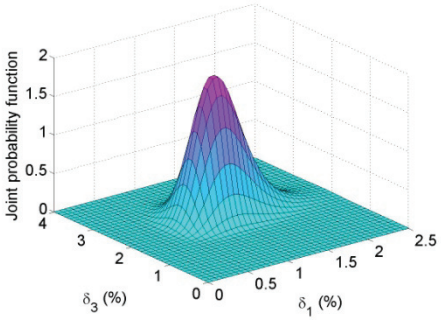

a. joint pdf for $\mathbf{X}_1$, $\mathbf{X}_3$, analytical data

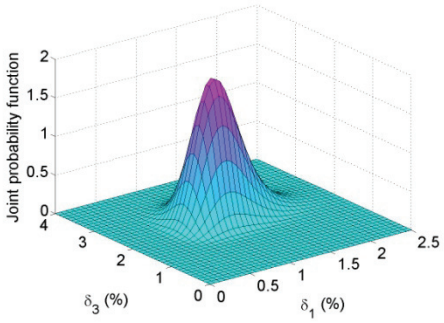

b. joint pdf for $\mathbf{X}_1$, $\mathbf{X}_3$, simulated data

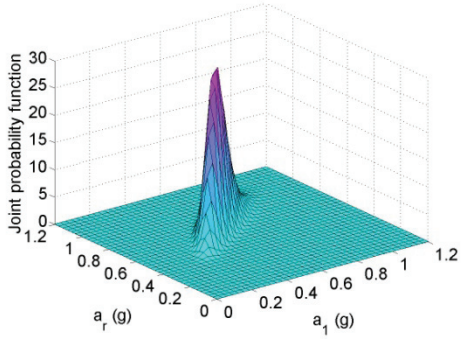

c. joint pdf for $\mathbf{X}_4$, $\mathbf{X}_7$, analytical data

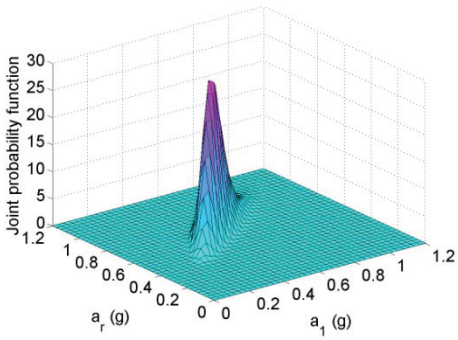

joint pdf for $\mathbf{X}_4$, $\mathbf{X}_7$, simulated data

Figure G-3 Joint probability density functions

Analysis

The entries in matrix $\mathbf{X}$ are assumed to be jointly lognormal. The log of each entry in $\mathbf{X}$ is used to construct the entries in matrix $\mathbf{Y}$, which are now assumed to be jointly normal. Table G-3 below presents the entries in $\mathbf{Y}$; the last two rows in the table present the mean and variance of each column vector in $\mathbf{Y}$. (Note that the natural logarithm of any number less than 1.00 will be negative.)

The row vector μ_y in Table G-2 is the mean vector $\mathbf{M_Y}$ of Equation G-1. The diagonal matrix of standard deviations $\mathbf{D_Y}$ in (Equation G-1) is formed by first taking the square root of each entry in the last row of Table G-3 (standard deviation, s_y, is the square root of the variance, s_y^2) and placing the first entry ($0.2431 = \sqrt{0.059}$) in cell (1,1), the second entry in cell (2,2) and so on. Matrix $\mathbf{D_Y}$ for this example is presented in Table G-4. Sources of uncertainty that are not included in the response-history analysis, including modeling uncertainty herein because a best-estimate model was used for nonlinear analysis, can be included indirectly by adjusting each diagonal entry of Table G-4 by $\sqrt{s_{ii}^2 + \beta^2}$, where s_{ii} is the *i*th diagonal entry and β is the dispersion to be included.

Table G-3 Natural Logarithm of Demand Parameters, *Y*

	δ_1	δ_2	δ_3	a_1	a_2	a_3	a_r
1	0.231	0.372	0.536	-0.616	-0.139	-0.128	-0.431
2	0.344	0.718	0.888	-0.598	-0.139	-0.261	-0.248
3	0.315	0.673	0.967	-0.288	0.039	-0.117	-0.211
4	-0.030	0.626	1.008	-0.598	-0.083	0.113	-0.288
5	-0.062	0.588	0.703	-0.916	-0.261	-0.301	-0.446
6	0.548	0.936	0.900	-0.799	-0.562	-0.799	-0.528
7	0.049	0.765	0.815	-0.968	-0.528	-0.713	-0.654
8	0.336	0.513	0.742	-0.315	0.405	0.293	-0.186
9	0.464	0.565	0.698	-0.528	-0.062	-0.211	-0.329
10	-0.186	0.519	0.811	-0.635	0.000	-0.105	-0.301
11	-0.041	0.604	0.811	-0.713	-0.105	-0.211	-0.446
μ_y	0.179	0.625	0.807	-0.634	-0.131	-0.222	-0.370
s_y^2	0.059	0.022	0.018	0.046	0.070	0.0993	0.021

Table G-4 Matrix $\mathbf{D}_Y$ for the Sample Problem

0.243	0.000	0.000	0.000	0.000	0.000	0.000
0.000	0.149	0.000	0.000	0.000	0.000	0.000
0.000	0.000	0.135	0.000	0.000	0.000	0.000
0.000	0.000	0.000	0.215	0.000	0.000	0.000
0.000	0.000	0.000	0.000	0.265	0.000	0.000
0.000	0.000	0.000	0.000	0.000	0.315	0.000
0.000	0.000	0.000	0.000	0.000	0.000	0.144

The correlation coefficient matrix, $\mathbf{R}_{YY}$, is a symmetric matrix with entries $\rho_{i,j}$, which is the correlation coefficient between random variables Y_i and Y_j. The range for $\rho_{i,j}$ is -1 to +1, where values close to (a) 1.0 indicate a positive linear relationship between the random variables, (b) -1 indicate a negative linear relationship between the random variables, and (c) values close to or equal to 0 indicate no linear relationship between the random variables. Table G-5 presents the correlation coefficient matrix for this sample problem. The values on the leading diagonal are equal to 1.000, which is an expected result because $\rho_{i,i}$ is the correlation of a given random variable (7 in this example) with itself. Correlation coefficients are dimensionless.

Table G-5 Matrix $\mathbf{R}_{YY}$ for the Sample Problem

1.000	0.339	-0.019	0.375	-0.022	-0.193	0.145
0.339	1.000	0.656	-0.353	-0.646	-0.723	-0.376
-0.019	0.656	1.000	0.136	-0.094	-0.066	0.220
0.375	-0.353	0.136	1.000	0.839	0.731	0.881
-0.022	-0.646	-0.094	0.839	1.000	0.934	0.863
-0.193	-0.723	-0.066	0.731	0.934	1.000	0.820
0.145	-0.376	0.220	0.881	0.863	0.820	1.000

From this table one can judge the linear dependence of one random variable on another. Consider $\rho_{1,3}$, the correlation coefficient between first story drift and third story drift, in the log space. In this example, $\rho_{1,3} = -0.019$, which indicates negligible dependence of $\mathbf{Y}_3$ on $\mathbf{Y}_1$ (and vice-versa). Consider now the linear dependence of the second and third floor and roof accelerations on the ground acceleration, $\rho_{4,5}, \rho_{4,6}, \rho_{4,7}$, respectively. All values are close to 1.0, which indicates strong linear dependence.

The correlation coefficient is closely related to the covariance, which is a measure of how much two random variables vary together. (Variance is a measure of how much a single random variable varies—see the last row of Table G-3 that presents the variance in $\mathbf{Y}_i$ for all seven demand parameters).

The unit of covariance is the product of the units of the random variables. The covariance of random variables $\mathbf{Y_i}$ and $\mathbf{Y_j}$, $\text{cov}(\mathbf{Y_i}, \mathbf{Y_j})$, is computed as

$$\text{cov}(\mathbf{Y_i}, \mathbf{Y_j}) = E(\mathbf{Y_i} \cdot \mathbf{Y_j}) - \mu_{\mathbf{Y}_i} \cdot \mu_{\mathbf{Y_j}} \tag{G-4}$$

where E is the expectation value operator and all other terms have been defined previously. For a sample calculation, return to Table G-3 and compute the $\text{cov}(\mathbf{Y_1}, \mathbf{Y_2})$ as

$$\begin{aligned}
\text{cov}(\mathbf{Y_1}, \mathbf{Y_2}) &= E((\mathbf{Y_1} - \mu_{\mathbf{Y}_1})(\mathbf{Y_2} - \mu_{\mathbf{Y}_2})) \\
&= \frac{1}{n-1}\sum_{i=1}^{n}(\mathbf{Y}_{1,i} - \mu_{\mathbf{Y}_1})(\mathbf{Y}_{2,i} - \mu_{\mathbf{Y}_2}) \\
&= \frac{1}{10}((0.231 - 0.179) \times (0.372 - 0.625).. \\
&\quad +(-0.041 - 0.179) \times (0.604 - 0.625)) \\
&= 0.0123
\end{aligned} \tag{G-5}$$

The correlation coefficient, $\rho_{1,2}$, is calculated as

$$\rho_{1,2} = \frac{\text{cov}(\mathbf{Y_1}, \mathbf{Y_2})}{\sqrt{\text{cov}(\mathbf{Y_1}, \mathbf{Y_1}) \times \text{cov}(\mathbf{Y_2}, \mathbf{Y_2})}} = \frac{0.01226}{\sqrt{0.05910 \times 0.02209}} = 0.339 \tag{G-6}$$

The matrix $\mathbf{L_Y}$ is the Cholesky-like decomposition of $\mathbf{R_{YY}}$, namely, $\mathbf{R_{YY}} = \mathbf{L_Y}\mathbf{L_Y^T}$. For this sample application of the algorithm, the number of simulations (=11) is greater than the number of demand parameters (=7), which results in a full rank correlation coefficient matrix, $\mathbf{R_{YY}}$. Therefore, $\mathbf{L_Y}$ is a lower triangular matrix as shown in Table G-6. (Note the Matlab macro *cholcov* returns the upper triangular matrix, the transpose of which is presented in Table G-6.)

Table G-6 Matrix $\mathbf{L_Y}$ for the Sample Problem

1.000	0.000	0.000	0.000	0.000	0.000	0.000
0.339	0.941	0.000	0.000	0.000	0.000	0.000
-0.019	0.704	0.710	0.000	0.000	0.000	0.000
0.375	-0.510	0.708	0.314	0.000	0.000	0.000
-0.022	-0.678	0.540	0.377	0.325	0.000	0.000
-0.193	-0.699	0.594	0.085	0.315	0.120	0.000
0.145	-0.451	0.761	0.185	0.242	-0.101	0.305

All of the matrices required to generate the correlated vectors have been constructed. The third-to-last step in the process is to compute the 7×1 vector $\mathbf{U}$ of uncorrelated standard normal random variables, with a mean of 0 and a standard deviation of 1 for each random variable. The **randn** function in Matlab is used for this purpose. This process is repeated 199 times to construct the 200 simulations for loss assessment. The next step involves

taking the exponential of each value in the 7×200 matrix to recover the demand parameters. Table G-7 presents the first 10 simulations of the 200.

As a last step, the statistics of the simulated demands should be compared with those of the demands calculated by response-history analysis. Figures G-2 and G-3 enable a partial comparison of demands. A rigorous comparison of the analytical and simulated demands is achieved by computing the ratios of the mean vectors and the correlation coefficient matrices. Table G-8 presents ratios of mean simulated response to mean response-history response—all values are close to 1.0. Table G-9 presents ratios of the simulated to response-history correlation coefficients—all values are close to 1.0 for those correlation coefficients in Table G-5 with an absolute value of greater than 0.5. The data of Tables G-8 and G-9 indicate that the *simulated* vectors of demand have the same underlying statistics as those of the *original* demand vectors.

Table G-7 Matrix of Simulated Demand Parameters (first 10 vectors of 200)

	δ_1 (%)	δ_2 (%)	δ_3 (%)	a_1 (g)	a_2 (g)	a_3 (g)	a_r (g)
1	1.361	2.150	2.361	0.469	0.716	0.681	0.620
2	2.009	2.725	2.640	0.467	0.607	0.504	0.633
3	1.303	2.011	2.080	0.474	0.716	0.564	0.623
4	1.265	1.676	2.060	0.695	1.435	1.136	0.826
5	1.635	2.802	2.985	0.577	0.744	0.500	0.684
6	1.192	1.661	2.474	0.901	1.593	1.347	0.955
7	0.865	1.817	2.328	0.460	0.970	0.965	0.661
8	1.045	2.038	2.830	0.612	0.926	0.801	0.852
9	1.437	2.305	2.424	0.461	0.634	0.494	0.609
10	0.958	1.769	1.973	0.408	0.747	0.686	0.648

Table G-8 Ratio of Simulated to Original Logarithmic Means

δ_1	δ_2	δ_3	a_1	a_2	a_3	a_r
0.9462	0.9870	0.9822	1.0231	1.0715	1.0559	1.0220

Table G-9 Ratio Of Entries in Simulated and Original $\mathbf{R}_{YY}$ Matrices

1.000	0.987	2.128	0.761	2.205	1.161	1.265
0.987	1.000	0.908	1.338	1.077	1.084	1.146
2.128	0.908	1.000	0.916	0.783	1.119	0.926
0.761	1.338	0.916	1.000	1.047	1.069	1.045
2.205	1.077	0.783	1.047	1.000	1.007	1.000
1.161	1.084	1.119	1.069	1.007	1.000	0.964
1.265	1.146	0.926	1.045	1.000	0.964	1.000

G.2.4 Matlab Code

The Matlab macro of Figure G-4 can be used to generate correlated vectors of demand parameters. The vectors of demand parameters established by response-history analysis, DP.txt file, should be constructed per Table G-1, namely, one demand parameter per column, one simulation per row. The file beta.txt includes a $2\times n$ matrix where the values in the two rows are for β_m and β_{gm}, respectively, and those in each column are for each demand parameter in the same order the demand parameters are input to PACT. The file n_rows.txt includes the number of the simulated row vectors, which is taken as 200 for the example of Section G.2.3.3.

For intensity- and time-based assessments and for scenario-based assessments using Section B.7 of Appendix B, the user should input for each demand parameter dispersions for analysis and modeling and set the dispersion for ground motion equal to zero. For scenario-based assessment using the procedures of Chapter 5, the user should input for each demand parameter dispersions for analysis, modeling and ground motion.

```
% Develop underlying statistics of the response-history analysis
X=load('DP.txt');
B=load('beta.txt');%matrix for dispersions βm and βgm ,
nr=load('n_rows.txt');%number of the generated row vectors

Y=log(X);
My=(mean(Y))';
Dy_a=(var(Y))';
n=length(My);

Dy=sqrt(diag((sum(B.*B)))+diag(Dy_a));
Ryy=corrcoef(Y);
Ly=(cholcov(Ryy))';

% Generate correlated demand vectors using a Monte-Carlo technique
U=randn(nr,size(Ly,2));

My=diag(My)*ones(n,nr);
Z=Dy*Ly*U'+My;
W=exp(Z');
save correlated_DP.txt W -ascii -double -tabs;
%Check results
Mz=(mean(Z'))';
Rzz=corrcoef(Z');
Mz./(mean(Y))';% for Table G-8
Rzz./Ryy; % for Table G-9
%end
```

Figure G-4 Matlab macro to generate correlated vectors of demand parameters.

G.3 Simulations for Assessment Using Simplified Analysis

For assessment using the simplified method of analysis per Chapter 6, PACT generates internally a set of N statistically consistent demand vectors, given the column vector of demand parameters, $\{\theta\}$, and a value of the dispersion, β, using the following two-step procedure: (1) randomly generate N values of z, where z is normally distributed with a mean of 0 and a standard deviation of 1.0; and (2) compute $\{\theta\}\exp(z\beta)$ for each value of z. Each vector computed using Step 2 is used to generate one value of loss.

Appendix H
Fragility Development

H.1 Introduction

H.1.1 Purpose

This appendix provides guidelines for development of fragility functions for individual building components for use in building performance assessment. It may be used to set fragility functions for either structural or nonstructural components, elements or systems.

H.1.2 Fragility Function Definition

Fragility functions are probability distributions that are used to indicate the probability that a component, element or system will be damaged to a given or more severe damage state as a function of a single predictive demand parameter such as story drift or floor acceleration. Here, fragility functions take the form of lognormal cumulative distribution functions, having a median value θ and logarithmic standard deviation, or dispersion, β. The mathematical form for such a fragility function is:

$$F_i(D) = \Phi\left(\frac{\ln(D/\theta_i)}{\beta_i}\right) \quad \text{(H-1)}$$

where: $F_i(D)$ is the conditional probability that the component will be damaged to damage state "i" or a more severe damage state as a function of demand parameter, D; Φ denotes the standard normal (Gaussian) cumulative distribution function, θ_i denotes the median value of the probability distribution, and β_i denotes the logarithmic standard deviation. Both θ and β are established for each component type and damage state using one of the methods presented in Section H.2.

The conditional probability that a component will be damaged to damage state "i" and not to a more or less severe state, given that it experiences demand, D, is given by:

$$P[i|D] = F_{i+1}(D) - F_i(D) \quad \text{(H-2)}$$

where $F_{i+1}(D)$ is the conditional probability that the component will be damaged to damage state "i+1" or a more severe state and $F_i(D)$ is as

previously defined. Note that, when β_{i+1} is unequal to β_i, Equation H-2 can produce a meaningless negative probability at some levels of *D*. This case is addressed in Section H.3.4.

Figure H-1 (a) shows the form of a typical fragility function when plotted in the form of a cumulative distribution function and (b) the calculation of the probability that a component will be in damage state, "i", at a particular level of demand, *d*.

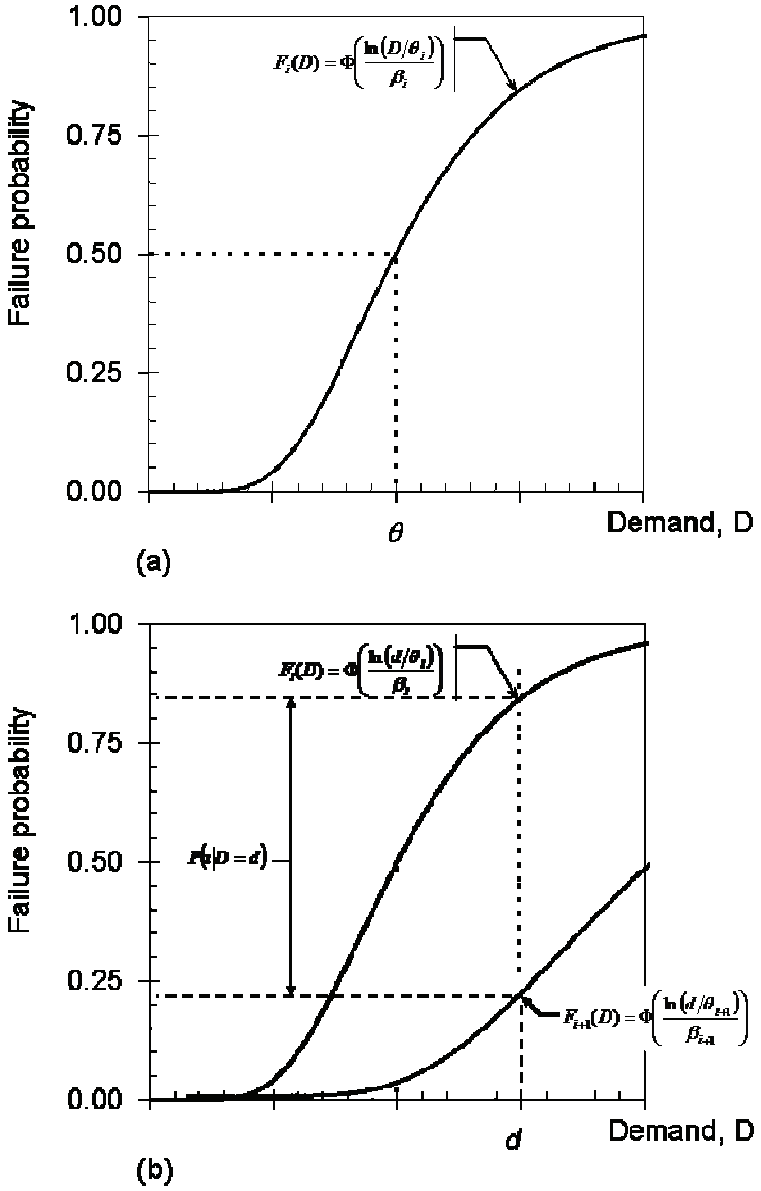

Figure H-1 Illustration of (a) fragility function, and (b) evaluating individual damage-state probabilities

The dispersion, β, represents uncertainty in the actual value of demand, *D*, at which a damage state is likely to initiate in a component . This uncertainty is

a result of variability in the quality of construction and installation of the components in a building, as well as variability in the loading history that the component may experience before it fails. When fragility parameters are determined on the basis of a limited set of test data, two components of the dispersion should be considered. The first of these, termed herein β_r, represents the random variability that is observed in the available test data from which the fragility parameters are determined. The second portion, β_u, represents uncertainty that the tests represent the actual conditions of installation and loading that a real component in a building will experience, or that the available test data is an inadequate sample to accurately represent the true random variability. The dispersion parameter, β, is computed as:

$$\beta = \sqrt{\beta_r^{\,2} + \beta_u^{\,2}} \qquad \text{(H-3)}$$

In these guidelines, the following minimum values of the uncertainty parameter, β_u, are recommended for use: A minimum value of 0.25 should be used if any of the following apply:

- Test data are available for five (5) or fewer specimens
- In an actual building, the component can be installed in a number of different configurations; however, all specimens tested had the same configuration.
- All specimens were subjected to the same loading protocol
- Actual behavior of the component is expected to be dependent on two or more demand parameters, e.g., simultaneous drift in two orthogonal directions; however, specimens were loaded with only one of these parameters.

If none of the above conditions apply, a value of β_u of 0.10 may be used.

H.1.3 Derivation Methods

Fragility functions can best be derived when there is a large quantity of appropriate test data available on the behavior of the component of interest at varying levels of demand. *FEMA 461* provides recommended protocols for performing such tests and recording the data obtained. Since testing is expensive and time consuming, there is not a great body of test data presently available to serve as the basis for determining fragility functions for many building components. Therefore, these guidelines provide procedures for developing the median (θ) and dispersion (β) values for a fragility under five different conditions of data. These are:

a. *Actual Demand Data*: When test data is available from *M* number of specimens and each tested component actually experienced the damage state of interest at a known value of demand, *D*.

b. *Bounding Demand Data*: When test data or earthquake experience data are available from *M* number of specimens; however, the damage state of interest only occurred in some specimens. For the other specimens, testing was terminated before the damage state occurred or the earthquake did not damage the specimens. The value of the maximum demand, D_i, to which each specimen was subjected is known for each specimen. This maximum demand need not necessarily be the demand at which the damage state initiated.

c. *Capable Demand Data*: When test data or earthquake experience data are available from *M* number of specimens; however, the damage state of interest did not occur in any of the specimens. The maximum value of demand, D_i, to which each specimen was subjected is known.

d. *Derivation (analysis)*: When no test data are available; however, it is possible to model the behavior and estimate the level of demand at which the damage state of interest will occur.

e. *Expert Opinion*: When no data are available and analysis of the behavior is not feasible; however, one or more knowledgeable individuals can offer an opinion as to the level of demand at which damage is likely to occur, based either on experience or judgment.

In addition, a procedure is presented for updating existing fragility functions as more data become available. Section H2.6 provides this guidance.

H.1.4 Documentation

This section provides recommendations for documenting the basis for fragility functions. Each fragility function should be accompanied by documentation of the sources of data and procedures used to establish the fragility parameters in sufficient detail that others may evaluate the adequacy of the process and findings. As a minimum, it is recommended that the documentation include the following:

1. *Description of Applicability.* Describe the type of component that the fragility function addresses including any limitations on the type of installation to which the fragility applies.

2. *Description of Specimens*. Describe the specimens used to establish the fragility including identifying the number of specimens examined, their

locations, and the specific details of the specimen fabrication/construction, mounting and installation.

3. *Demands and Load Application*. Detail the loading protocol or characteristics of earthquake motion applied to each specimen. Identify the demand parameters examined that might be most closely related to failure probability and define how demand is calculated or inferred from the loading protocol or excitation. Indicate whether the reported demand quantities are the value at which damage occurred (Method A data) or the maximum to which each specimen was subjected.

4. *Damage State.* Fully describe each damage state for which fragilities are developed including the kinds of physical damage observed and any force-deformation quantities recorded. Define damage states quantitatively in terms of the repairs required or potential downtime or casualty consequences.

5. *Observation Summary, Analysis Method, and Results.* Present a tabular or graphical listing of specimens, demand parameters, and damage states. Identify the method(s) used to derive the fragility parameters per Section H.2 of this Appendix. Present resulting fragility function parameters, θ and β, and results of tests to establish fragility function quality (discussed below). Provide sample calculations.

H.2 Fragility Parameter Derivation

H.2.1 Actual Demand Data

This section defines the procedures for deriving fragility parameters (θ, β) when data are available from a suitable series of tests, and in each specimen, the damage state of interest was initiated at a known value of the demand. In this case, the median value of the demand at which the damage state is likely to initiate, θ, is given by the equation:

$$\theta = e^{\left(\frac{1}{M}\sum_{i=1}^{M}\ln d_i\right)} \quad \text{(H-4)}$$

where:

M = total number of specimens tested to at least the initiation of the damage state

d_i = demand in test "i" at which the damage state was first observed to occur.

The value of the random dispersion, β_r, is given by:

$$\beta_r = \sqrt{\left(\frac{1}{M-1} \sum_{i=1}^{M} \left(\ln\left(d_i / \theta \right) \right)^2 \right)^2} \quad \text{(H-5)}$$

where M, r_i and θ are as defined above.

If one or more of the r_i data appear to lie far from the bulk of the data, either above or below, apply the procedure specified in Section H3.2. Finally, test the resulting fragility parameters using the Lilliefors goodness-of-fit test (Section H3.3). If it passes at the 5% significance level, the fragility function may be deemed acceptable.

Example: Determine the parameters θ and β, from a series of 10 tests, all of which produced the damage state of interest. Demands at which the damage state initiated are respectively story drifts of: 0.9, 0.9, 1.0, 1.1, 1.1, 1.2, 1.3, 1.4, 1.7, and 2 percent.

Test #	Demand di	ln(di)	ln(di/θi)	ln(di/θi)^2
1	0.9	-0.10536	-0.30384	0.092321
2	0.9	-0.10536	-0.30384	0.092321
3	1	0	-0.19848	0.039396
4	1.1	0.09531	-0.10317	0.010645
5	1.1	0.09531	-0.10317	0.010645
6	1.2	0.182322	-0.01616	0.000261
7	1.3	0.262364	0.063881	0.004081
8	1.4	0.336472	0.137989	0.019041
9	1.7	0.530628	0.332145	0.11032
10	2	0.693147	0.494664	0.244692
Σ		1.984833		0.623723

$$\theta = e^{\left(\frac{1}{M} \sum_{i=1}^{M} \ln d_i \right)} = e^{\left(\frac{1}{10}(1.9848) \right)} = 1.22$$

$$\beta_r = \sqrt{\frac{1}{M-1} \sum_{i=1}^{M} \left(\ln\left(d_i / \theta \right) \right)^2} = \sqrt{\frac{1}{(10-1)}(0.6237)} = 0.26$$

H.2.2 Bounding Demand Data

This section defines the procedures for deriving fragility parameters (θ, β) when data are available from a suitable series of tests or earthquake experience records; however, the damage state of interest was initiated in only some of the specimens. For the other specimens, loading applied during the testing or earthquake shaking was insufficient to initiate the damage state of interest. For each specimen "i", it is necessary to know the maximum value of the demand, d_i, to which the specimen was subjected, and whether or not the damage state did occur in the specimen.

Divide the data into a series of N bins. It is suggested, but not essential, that N be taken as the largest integer that is less than or equal to the square root of M, where M is the total number of specimens available, as this will usually result in an appropriate number of approximately equally sized sets.

In order to divide the specimens into the several bins, sort the specimen data in order of ascending maximum demand value, d_i, for each test, then divide the list into N groups of approximately equal size. Each group "j" will have M_j specimens, where:

$$\sum_{i=1}^{N} M_j = M \tag{H-6}$$

Next, determine the average value of the maximum demand for each bin of specimens:

$$\bar{d}_j = \frac{1}{M_j} \sum_{k=1}^{M_j} d_k \tag{H-7}$$

and x_j, the natural logarithm of d_j (i.e., $\ln(d_j)$). Also determine the number of specimens within each bin, m_j, in which the damage state of interest was achieved and the inverse standard normal distribution, y_j, of the failed fraction of specimens in the bin:

$$y_j = \Phi^{-1}\left(\frac{m_j + 1}{M_j + 1}\right) \tag{H-8}$$

That is, determine the number of standard deviations, above the mean that the stated fraction lies, assuming a mean value, $\mu = 0$ and a standard deviation, $\sigma = 1$. This can easily be determined using the "normsinv" function on a Microsoft Excel spreadsheet or by referring to standard tables of the normal distribution. Next, fit a straight line to the data points, x_j, y_j, using a least-squares approach. The straight line will have the form:

$$y = bx + c \tag{H-9}$$

where, b is the slope of the line and c is the y intercept. The slope b is given by:

$$b = \frac{\sum_{i=1}^{M} \left(x_j - \bar{x}\right)\left(y_j - \bar{y}\right)}{\sum_{i=1}^{M} \left(x_j - \bar{x}\right)^2} \tag{H-10}$$

$$\bar{x} = \frac{1}{M}\sum_{j=1}^{M} x_j \tag{H-11}$$

$$\bar{y} = \frac{1}{M}\sum_{j=1}^{M} y_j \tag{H-12}$$

Determine the value of the random dispersion, β_r as:

$$\beta_r = \frac{1}{b} = \frac{\sum_{i=1}^{M}\left(x_j - \bar{x}\right)}{\sum_{i=1}^{M}\left(x_j - \bar{x}\right)\left(y_j - \bar{y}\right)} \tag{H-13}$$

The value of the median, θ, is taken as:

$$\theta = e^{-c\beta_r} = e^{\left(\bar{x} - \bar{y}\beta_r\right)} \tag{H-14}$$

Example: Consider the damage statistics shown in the figure below. The figure depicts the hypothetical performance of motor control centers (MCCs) observed after various earthquakes in 45 facilities. Each box represents one specimen. Several damage states are represented. Crosshatched boxes represent MCCs that experienced a noticeable earthquake effect such as shifting but that remained operable. Black boxes represent those that were found to be inoperable following the earthquake. Each stack of boxes represents one facility. Calculate the fragility function using *PGA* as the demand parameter, binning between halfway points between *PGA* values shown in the figure.

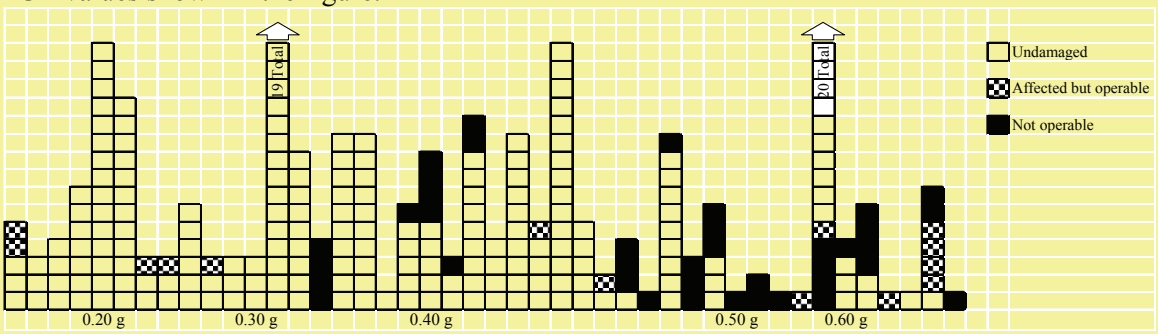

Figure Hypothetical observed earthquake damage data for motor control centers

The number of bins, N, and the lower demand bounds a_i, are dictated by the available data: N is taken as 5 with lower bounds, a_i of 0.15g, 0.25g, 0.35g, 0.45g, and 0.55g respectively. The damage state of interest is loss of post-earthquake functionality (black boxes in figure). The values of M_j and m_j are found by counting all boxes and black boxes, respectively, in the figure in each bin, and are shown in the table below. The value of M is found by summing: $M = \Sigma M_j = 260$. Values x_j and y_j are calculated as $x_j = \ln(\bar{r}_j)$, and $y_j = \Phi^{-1}((m_j+1)/(M_j+1))$. Average values are calculated as shown: $\bar{x} = -0.99$, $\bar{y} = -1.05$, according to Equations H-11 and H-12. For each bin, the values of $x_j - \bar{x}$ and $y_j - \bar{y}$ are calculated as shown.

Table of Example Solution Data

j	a_j (g)	$\bar{r}_j$ (g)	M_j	m_j	x_j	y_j	$x_j - \bar{x}$	$y_j - \bar{y}$	$(x_j - \bar{x})^2$	$(x_j - \bar{x})(y_j - \bar{y})$
1	0.15	0.2	52	0	-1.61	-2.08	-0.623	-1.031	0.388	0.642
2	0.25	0.3	48	4	-1.20	-1.27	-0.217	-0.223	0.047	0.049
3	0.35	0.4	84	8	-0.92	-1.25	0.070	-0.202	0.005	-0.014
4	0.45	0.5	35	15	-0.69	-0.14	0.294	0.907	0.086	0.266
5	0.55	0.6	41	12	-0.51	-0.50	0.476	0.549	0.226	0.261
Σ =			260		-4.93	-5.23			0.753	1.204
		Average =			-0.99	-1.05				

Then, β and θ are calculated as:

$$\beta_r = \frac{\sum_{j=1}^{N}\left(x_j - \bar{x}\right)^2}{\left(x_j - \bar{x}\right)\left(y_j - \bar{y}\right)} = \frac{0.753}{1.204} = 0.63$$

$$\theta = e^{(\bar{x} - \bar{y}\beta_r)} = e^{(-0.99+1.05(0.63))} = e^{(-0.329)} = 0.72g$$

H.2.3 Capable Demand Data

This section defines the procedures for deriving fragility parameters (θ, β) when data are available from a suitable series of specimens; however, the damage state of interest was not initiated in any of the specimens. For each available specimen, "i," the maximum demand at which the specimen was loaded, "d_i", and whether or not the specimen experienced any distress or damage must be known.

From the data for M specimens, determine the maximum demand experienced by each specimen, d_{max}, and the minimum demand for any of the specimens that exhibited any distress or damage, d_{min}. Determine d_a as the smaller of d_{min} or $0.7d_{max}$. Determine M_A as the number of specimens that did not exhibit distress or damage, but that were loaded with demands, $d_i \geq d_a$; M_B as the number of specimens that exhibited distress or damage, but which did not appear to be initiating or on the verge of initiating the damage state of interest; and M_C as the number of specimens appeared to be on the verge of initiating the damage state of interest.

If none of the specimens in any of the tests exhibited any sign of distress or damage, take the value of d_m as d_{max}. If one or more of the specimens exhibited distress or damage of some type, take d_m as:

$$d_m = \frac{d_{\max} + d_a}{2} \tag{H-15}$$

Determine the subjective failure probability S at d_m as:

$$S = \frac{0.5M_C + 0.1M_B}{M_A + M_B + M_C} \tag{H-16}$$

Take the logarithmic standard deviation, β, as having a value of 0.4. Determine the median, θ, as:

$$\theta = d_m e^{-0.4z} \tag{H-17}$$

where, z is determined from Table H-1 based on the value of M_A and S.

Table H-1 Values of z

Conditions	z
$M_A \geq 3$ and $S = 0$	-2.326
$M_A < 3$ and $S \leq 0.075$	-1.645
$0.075 < S \leq 0.15$	-1.282
$0.15 < S \leq 0.3$	-0.842
$S > 0.3$	-0.253

Example: Determine the parameters θ and β, from tests of 10 specimens. Five of the specimens had maximum imposed drift demands of 1% with no observable signs of distress. Three of the specimens had maximum imposed drift demands of 1.5% and exhibited minor distress, but did not appear to be at or near the initiation of the damage state of interest. Two of the specimens had maximum imposed drift demands of 2%, did not enter the damage state of interest during the test, but appeared to be about to sustain such damage. From the given data determine: $d_{max} = 2\%$, $d_{min} = 1.5\%$. d_a is the smaller of $0.7d_{max}$ or d_{min} and therefore, is $0.7(2\%) = 1.4\%$. $M_A = 0$, $M_B=3$, and $M_C=2$.

$$d_m = \frac{d_{\max} + d_a}{2} = \frac{2\% + 1.4\%}{2} = 1.7\%$$

$$S = \frac{0.5M_C + 0.1M_B}{M_A + M_B + M_C} = \frac{0.5(2) + 0.1(3)}{0 + 3 + 2} = 0.26$$

From Table H-1, z is taken as -0.842. Therefore,

$$\theta = d_m e^{-0.4z} = 1.7\% e^{-0.4(-0.842)} = 2.4\%$$

and β is taken as 0.4.

H.2.4 Derivation

There are two methods available for analytical derivation of fragility parameters. The first of these uses a single calculation of the probable capacity and a default value of the logarithmic standard deviation. The second method uses Monte Carlo analysis to explore the effect of variation in material strength, construction quality and other random variables.

Single Calculation

Calculate the capacity of the component, Q in terms of a demand parameter, d, using average material properties and dimensions and estimates of workmanship. Resistance factors should be taken as unity and any conservative bias in code equations, if such equations are used, should be removed. The logarithmic standard deviation, β, is taken as having a value of 0.4. The median capacity θ is taken as:

$$\theta = 0.92Q \qquad \text{(H-18)}$$

Monte Carlo Simulation

Identify all those factors, important to predicting the capacity that are uncertain including material strength, cross section dimensions, member straightness, and workmanship. Estimate a median value and dispersion for each of these random variables. Conduct sufficient analyses, randomly selecting the values of each of these random variables in accordance with their estimated distribution properties, each time calculating the capacity. Determine the median value of the capacity as that capacity exceeded in 50% of the calculations. Determine the random logarithmic standard deviation, β_r, as the standard deviation of the natural logarithm of the calculated capacity values. Use equation H-3 to determine the total logarithmic standard deviation, β, assuming a value of β_u of 0.25.

H.2.5 Expert Opinion

Select one or more experts with professional experience in the design or post-earthquake damage observation of the component of interest. Solicit their advice using the format shown in Figure H-2. Note the suggested inclusion of representative images, which should be recorded with the responses. If an expert refuses to provide estimates or limits them to certain conditions, either narrow the component definition accordingly and iterate, or ignore that expert's response and analyze the remaining ones.

Objective. This form solicits your judgment about the values of a demand parameter (*D*) at which a particular damage state occurs to a particular building component. Judgment is needed because the component may contribute significantly to the future earthquake repair cost, fatality risk, or post-earthquake operability of a building, and because relevant empirical and analytical data are currently impractical to acquire. Your judgment is solicited because you have professional experience in the design or post-earthquake damage observation of the component of interest.

Definitions. Please provide judgment on the damageability of the following component and damage state. Images of a representative sample of the component and damage state may be attached. It is recognized that other demand parameters may correlate better with damage, but please consider only the one specified here.

Component name: _____
Component definition: _____
Damage state name: _____
Damage state definition: _____
_____
Relevant Demand Parameter _____
Definition of *Demand Parameter* _____
_____

Uncertainty; no personal stake. Please provide judgment about this general class of components, not any particular instance, and not one that you personally designed, constructed, checked, or otherwise have any stake in. There is probably no precise threshold level of demand that causes damage, because of variability in design, construction, installation, inspection, age, maintenance, interaction with nearby components, etc. Even if there were such a precise level, nobody might know it with certainty. To account for these uncertainties, **please provide two values of demand at which damage occurs: median and lower bound.**

Estimated median capacity _____ *Definition*. Damage would occur at this level of demand in 5 cases out of 10, or in a single instance, you judge there to be an equal chance that your median estimate is too low or too high.

Estimated lower-bound capacity _____ *Definition*. Damage would occur at this level of demand in 1 case in 10. In a single case, you judge there to be a 10% chance that your estimate is too high. *Judge the lower bound carefully*. Make an initial guess, then imagine all the conditions that might make the actual threshold demand lower, such as errors in design, construction or installation, substantial deterioration, poor maintenance, more interaction with nearby components, etc. Revise accordingly and record your revised estimate. Research shows that without careful thought, expert judgment of the lower bound tends to be too close to the median estimate, so think twice and do not be afraid of showing uncertainty.

On a 1-to-5 scale, please judge your expertise with this component and damage state, where 1 means "no experience or expertise" and 5 means "very familiar or highly experienced."

Your level of expertise: _____

Your name: _____ Date: _____

Figure H-2 Form for soliciting expert judgment on component fragility

Calculate the median value, θ, as:

$$\theta = \frac{\sum_{i=1}^{N} w_i^{1.5} \theta_i}{\sum_{i=1}^{N} w_i^{1.5}} \tag{H-19}$$

where, N is the number of experts providing an opinion; θ_i is expert "i's" opinion as to the median value, and w_i is expert "i's" level of expertise, on a 1-5 scale.

Calculate the lower bound value for the capacity as:

$$d_l = \frac{\sum_{i=1}^{N} w_i^{1.5} d_{li}}{\sum_{i=1}^{N} w_i^{1.5}} \quad \text{(H-20)}$$

where, d_{li} is expert "i's" opinion as to the lower bound value and other terms are as previously defined. The value of the logarithmic standard deviation, β, is taken as:

$$\beta = \frac{\ln(\theta / d_l)}{1.28} \quad \text{(H-21)}$$

If this calculation produces an estimate of β that is less than 0.4, either justify the β, or take β as having a value of 0.4 and recalculate θ as:

$$\theta = 1.67 d_l \quad \text{(H-22)}$$

H.2.6 Updating

This section addresses procedures for re-evaluating fragility parameters for a building component as additional data become available. The pre-existing and updated fragility parameters are respectively termed θ, β, θ', and β'. The additional data are assumed to be a set of M specimens with known maximum demand and damage states. It is not necessary that any of the specimens experienced damage.

Calculate the revised median, θ' and logarithmic standard deviation β' as follows:

$$\theta' = e^{\sum_{j=1}^{5} w'_j \ln(d_j)} \quad \text{(H-23)}$$

$$\beta' = \sum_{j=1}^{5} w'_j \beta_j \quad \text{(H-24)}$$

where:

$$w'_j = \frac{w_j \prod_{i=1}^{M} L(i,j)}{\sum_{j=1}^{5} w_j \prod_{i=1}^{M} L(i,j)} \quad \text{(H-25)}$$

where Π denotes the product of the terms that come after it, and

$L(i,j) = 1 - \Phi\left(\frac{\ln(d_i / x_j)}{0.707 s \beta_j}\right)$ if specimen "i" did not experience the damage state of interest, and

$L(i,j) = \Phi\left(\frac{\ln(d_i / x_j)}{0.707 s \beta_j}\right)$ if specimen "i" did experience the damage state of interest, or a more severe state. and

$x_1 = x_4 = x_5 = \theta$

$x_2 = \theta e^{-1.22\beta}$

$x_3 = \theta e^{1.22\beta}$

$\beta_1 = \beta_2 = \beta_3 = \beta$

$\beta_4 = 0.64\beta$

$\beta_5 = 1.36\beta$

$w_1 = 1/3$

$w_2 = w_3 = w_4 = w_5 = 1/6$

H.3 Assessing Fragility Function Quality

This section provides procedures that can be used to assess the quality of fragility parameters.

H.3.1 Competing Demand Parameters

The behavior of some components may be dependent on several types of demands, for example in-plane and out-of-plane drift, or both drift and acceleration. It may not be clear which demand is the best single predictor of component damage. Assuming that data are available to create fragility functions for each possibly relevant demand, do so. Choose the fragility function that has the lowest β.

H.3.2 Dealing with Outliers using Pierce's Criterion

When fragilities are determined on the basis of actual demand data (Section H2.1), it is possible that one or more tests reported spurious values of demand, d_i, and reflect experimental errors rather than the true demands at which the specimens failed. In cases where one or more d_i values in the data set are obvious outliers from the bulk of the data, investigate whether the data reflects real issues in the damage process that may recur, especially where $d_i << \theta$ for these outliers. If there is no indication that these data reflect a real recurring issue in the damage process, apply the following procedure (Peirce's criterion) to test and eliminate doubtful observations of d_i.

1. Calculate $\ln(\theta)$ and β of the complete data set.
2. Let D denote the number of doubtful observations, and let R denote the maximum allowable deviation of an observation from the data mean to the standard deviation, defined in this case as:

$$R = \frac{\left|\ln(d) - \ln\theta\right|}{\beta} \tag{H-26}$$

   where θ, β, and M are as previously defined, d is a measured demand value, and R is obtained from Table H-2. Assume $D = 1$ first, even if there appears to be more than one doubtful observation.
3. Calculate the maximum allowable deviation, $|\ln(d) - \ln(\theta)|_{max}$, as the product of $\beta \times R$. Note that this can include $d >> \theta$ and $d << \theta$.
4. For any suspicious measurement, d_i, obtain $|\ln(d_i) - \ln(\theta)|$.
5. Eliminate the suspicious measurements if: $\left|\ln(d_i) - \ln(\theta)\right| > \left|\ln(d) - \ln(\theta)\right|_{max}$
6. If this results in the rejection of one measurement, assume D=2, keeping the original values of θ and β, and go to Step 8.
7. If more than one measurement is rejected in the above test, assume the next highest value of doubtful observations. For example, if two measurements are rejected in Step 5, assume the case of $D = 3$, keeping the original values of θ, and β, as the process is continued.
8. Repeat Steps 2 – 5, sequentially increasing D until no more data measurements are eliminated.
9. Obtain θ and β of the reduced data set as for the original data.

H.3.3 Goodness of Fit Testing

Fragility parameters that are developed based on actual demand data (Section H.2.1) should be tested for goodness of fit in accordance with this section. Calculate

$$D = \max_x \left|F_i(d) - S_M(d)\right| \tag{H-27}$$

where $S_M(d)$ denotes the sample cumulative distribution function

$$S_M(d) = \frac{1}{M}\sum_{i=1}^{M} H\left(d_i - d\right) \tag{H-28}$$

Table H-2 Peirce's Criterion Table. Ratio of Maximum Allowable Deviation of a Measured Value from the Data Mean to the Standard Deviation (Ross, 2003)

M	*D*=1	*D*=2	*D*=3	*D*=4	*D*=5	*D*=6	*D*=7	*D*=8	*D*=9
3	1.1960								
4	1.3830	1.0780							
5	1.5090	1.2000							
6	1.6100	1.2990	1.0990						
7	1.6930	1.3820	1.1870	1.0220					
8	1.7630	1.4530	1.2610	1.1090					
9	1.8240	1.5150	1.3240	1.1780	1.0450				
10	1.8780	1.5700	1.3800	1.2370	1.1140				
11	1.9250	1.6190	1.4300	1.2890	1.1720	1.0590			
12	1.9690	1.6630	1.4750	1.3360	1.2210	1.1180	1.0090		
13	2.0070	1.7040	1.5160	1.3790	1.2660	1.1670	1.0700		
14	2.0430	1.7410	1.5540	1.4170	1.3070	1.2100	1.1200	1.0260	
15	2.0760	1.7750	1.5890	1.4530	1.3440	1.2490	1.1640	1.0780	
16	2.1060	1.8070	1.6220	1.4860	1.3780	1.2850	1.2020	1.1220	1.0390
17	2.1340	1.8360	1.6520	1.5170	1.4090	1.3180	1.2370	1.1610	1.0840
18	2.1610	1.8640	1.6800	1.5460	1.4380	1.3480	1.2680	1.1950	1.1230
19	2.1850	1.8900	1.7070	1.5730	1.4660	1.3770	1.2980	1.2260	1.1580
20	2.2090	1.9140	1.7320	1.5990	1.4920	1.4040	1.3260	1.2550	1.1900
>20	$a\ln M + b$								
a	0.4094	0.4393	0.4565	0.4680	0.4770	0.4842	0.4905	0.4973	0.5046
b	0.9910	0.6069	0.3725	0.2036	0.0701	-0.0401	-0.1358	-0.2242	-0.3079

M = Total number of observations (number of specimens)
D = Number of doubtful observations (specimens)

and H is taken as:

- 1.0 if $d_i - d$ is positive
- ½ if $d_i - d$ is zero
- 0 if $d_i - d$ is negative.

If $D > D_{crit}$ from Table H-3, the fragility function fails the goodness of fit test. This result is used in assigning a quality level to the fragility function. Use $\alpha = 0.05$.

Table H-3 Critical Values for the Lilliefors Test

Significance Level	D_{crit}
$\alpha = 0.15$	$0.775 / (M^{0.5} - 0.01 + 0.85M^{-0.5})$
$\alpha = 0.10$	$0.819 / (M^{0.5} - 0.01 + 0.85M^{-0.5})$
$\alpha = 0.05$	$0.895 / (M^{0.5} - 0.01 + 0.85M^{-0.5})$
$\alpha = 0.025$	$0.995 / (M^{0.5} - 0.01 + 0.85M^{-0.5})$

H.3.4 Fragility Functions that Cross

Some components will have two or more possible damage states, with a defined fragility function for each. For any two (cumulative lognormal) fragility functions i and j with medians $\theta_j > \theta_i$ and logarithmic standard deviations $\beta_i \neq \beta_j$, the fragility functions will cross at extreme values. In such a case, adjust the fragility functions by one of the following two methods;

Method 1: adjust the fragility functions such that.

$$F_i(D) = \max_j \left\{ \Phi\left(\frac{\ln(D/\theta_i)}{\beta_i} \right) \right\} \quad \text{for all } j \geq i \tag{H-29}$$

This has the effect that for the damage state with the higher median value, the probability of failure, $F_i(D)$ is never taken as less than the probability of failure for a damage state with a lower median value.

Method 2: First establish θ and β values for the various damage states independently. Next calculate the average of the dispersion values for each of the damage states with crossing fragility curves as:

$$\beta_i' = \frac{1}{N} \sum_{i=1}^{N} \beta_i \tag{H-30}$$

This average logarithmic standard deviation is used as a replacement for the independently calculated values. An adjusted median value must be calculated for each of the crossing fragilities as:

$$\theta_i' = e^{\left(1.28\left(\beta' - \beta_i\right) + \ln \theta_i\right)} \tag{H-31}$$

H.3.5 Assigning a Single Quality Level to a Fragility Function

Assign each fragility function a quality level of high, medium, or low, as shown in Table H-4.

Table H-4 Fragility Function Quality Level

Quality	Method	Peer Reviewed*	Number of Specimens	Other
High	A	Yes	≥ 5	Passes Lilliefors test at 5% significance level. Examine and justify (a) differences of greater than 20% in θ or β, compared with past estimates, and (b) any case of $\beta < 0.2$ or $\beta > 0.6$.
	B	Yes	≥ 20	Examine and justify (a) differences of greater than 20% in θ or β, compared with past estimates, and (b) any case of $\beta < 0.2$ or $\beta > 0.6$.
	U	Yes	≥ 6	Prior was at least moderate quality
Moderate	A		≥ 3	Examine and justify any case of $\beta < 0.2$ or $\beta > 0.6$.
	B		≥ 16	Examine and justify any case of $\beta < 0.2$ or $\beta > 0.6$.
	C	Yes	≥ 6	
	D	Yes		
	E	Yes		At least 3 experts with $w \geq 3$
	U		≥ 6	or prior was moderate quality
Low				All other cases

* Data and derivation published in a peer-reviewed archival journal.

References

ATC (2008), *Interim Guidelines on Modeling and Acceptance Criteria for Seismic Design and Analysis of Tall Buildings,* ATC-72-1 Project Report – 90% Draft, Published by the Applied Technology Council for the Pacific Earthquake Engineering Research Center Tall Buildings Initiative – Task 7 Project Core Group, www.atcouncil.org.

Christopoulos, C., Pampanin, S., Priestley, M.J.N. (2003), "Performance-Based Seismic Response of Frame Structures Including Residual Deformations. Part I: Single-Degree of Freedom Systems", Journal of Earthquake Engineering, 7(1), pg. 97-118.

Christopoulos, C. and Pampanin, S., 2004. "Towards Performance-Based Design of MDOF Structures with Explicit Consideration of Residual Deformations", Invited Paper, *Indian Society for Earthquake Technologies (ISET) Journal of Earthquake Technology*, Special Issue on Performance-Based Design, Vol. 41, No. pp. 172-193.

FEMA 445 (2006), *Next-Generation Performance-Based Seismic Design Guidelines, Program Plan for New and Existing Buildings,* published by the Applied Technology Council for the Federal Emergency Management Agency, Washington, D.C.

FEMA 461 (2007), *Interim Testing Protocols for Determining the Seismic Performance Characteristics of Structural and Nonstructural Components,* published by the Applied Technology Council for the Federal Emergency Management Agency, Washington, D.C.

FEMA P695 (2008), *Quantification of Building Seismic Performance Factors,* ATC-63 Project Report – 90% Draft, published by the Applied Technology Council for the Federal Emergency Management Agency, www.atcouncil.org.

Haselton, C.B., Deierlein, G.G. (2007), *Assessing Seismic Collapse Safety of Modern Reinforced Concrete Moment-Frame Buildings*, PEER 2007/08, www.peer.berkeley.edu.

Ibarra, L.F., Medina, R.A., and Krawinkler, H. (2005). "Hysteretic models that incorporate strength and stiffness deterioration," *International*

Journal for Earthquake Engineering and Structural Dynamics, Vol. 34, No.12, pp. 1489-1511.

Ibarra, L.F., and Krawinkler, H. (2005). *Global Collapse of Frame Structures Under Seismic Excitations*, PEER TR 2005/06, www.peer.berkeley.edu.

Liel, A.B., Haselton, C.B., Deierlein, G.G., Baker, J.W. (2009), "Incorporating modeling uncertainties in the assessment of seismic collapse risk of buildings," Structural Safety, 31(2), pp. 197-211.

Lignos, D.G. (2008), *Sidesway Collapse of Deteriorating Structural Systems, Ph.D Dissertation*, Department of Civil and Environmental Engineering, Stanford University, Stanford California.

MacRae, G.A., Kawashima, K. (1997), "Post-Earthquake Residual Displacements of Bilinear Oscillators," EESD, 26, pp. 701-719.

MacRae G. A., (1994) "*P*-D Effects on Single-Degree-of-Freedom Structures in Earthquakes", *Earthquake Spectra,* Vol. 10, No. 3, August 1994, pp. 539-568

Mahin, S.A., Bertero, V.V. (1981), "Evaluation of Inelastic Seismic Design Spectra," J. Struct. Div., ASCE, 107(9), pp 1777-1795.

Moehle, J., and Deierlein, G., 2004, A Framework Methodology for Performance-Based Earthquake Engineering, *Proceedings*, 13th World Conference on Earthquake Engineering, Vancouver, British Columbia, paper no. 679.

NIST (1999), *UNIFORMAT II Elemental Classification for Building Specifications, Cost Estimating, and Cost Analysis*, NISTIR 6389, National Institute of Standards and Technology, Gaithersberg, Maryland.

Pampanin, S., Christopoulos, C., Priestley, M.J.N. (2003), "Performance-Based Seismic Response of Frame Structures Including Residual Deformations. Part II: Multi-Degree of Freedom Systems", Journal of Earthquake Engineering, 7(1), pg. 119-147.

Riddell, R., Newmark, N. M. (1979), *Statistic Analysis of the Response of Nonlinear Systems Subjected to Earthquakes*, Structural Report Series 468, Civil Engineering, University of Illinois.

Ruiz-Garcia, J., Miranda, E. (2005), "Performance-Based Assessment of Existing Structures Accounting for Residual Displacements", *Technical Report No. 153*, John A. Blume Earthquake Engineering Center, http://blume.stanford.edu, Stanford University, 444 pgs.

Ruiz-Garcia, J., Miranda, E. (2006a), "Direct Estimation of Residual Displacement From Displacement Spectral Ordinates", *Paper No. 1101, Proceedings of 8NCEE, 10 pgs.*

Ruiz-Garcia J, Miranda E., (2006b), "Residual displacement ratios for assessment of existing structures," *EESD,* 35(3):315336.

Ruiz-Garcia J, Miranda E., (2006c), "Evaluation of residual drift demands in regular multi-story frames for performance-based seismic assessment". *EESD*, 35(13)1609-1629.

Yang, T.Y., Moehle, J., Stojadinovic, B., Der Kiureghian, A., 2006, An Application of PEER Performance-Based Earthquake Engineering Methodology, *Proceedings*, 8th US National Conference on Earthquake Engineering, San Francisco, California.

Zareian, F., Krawinkler, H. (2007) "Assessment of probability of collapse and design for collapse safety", *Earthquake Engineering and Structural Dynamics*, **36**(13), 1901-1914.

Project Participants

Project Management

Christopher Rojahn
Project Executive Director
Applied Technology Council
201 Redwood Shores Parkway, Suite 240
Redwood City, CA 94065

Ronald O. Hamburger
Project Technical Director
Simpson Gumpertz & Heger
The Landmark @ One Market, Suite 600
San Francisco, CA 94105

FEMA Oversight

Mike Mahoney
Project Officer
Federal Emergency Management Agency
500 C Street, SW, Room 416
Washington, DC 20472

Robert D. Hanson
Technical Monitor
Federal Emergency Management Agency
2926 Saklan Indian Drive
Walnut Creek, CA 94595-3911

Project Management Committee

Christopher Rojahn, Chair
Ronald Hamburger, Co-Chair

Jon A. Heintz (ex-officio)
Applied Technology Council
201 Redwood Shores Parkway, Suite 240
Redwood City, CA 94065

William T. Holmes (ex-officio)
Rutherford & Chekene
55 Second Street, Suite 600
San Francisco, CA 94105

John Gillengerten
Office of Statewide Health
Planning and Development
1600 9th St., Room 420
Sacramento, CA 95814

Peter J. May
University of Washington
3630 Evergreen Point Road
Medina, WA 98039

Jack P. Moehle
University of California at Berkeley
3444 Echo Springs Road
Lafayette, CA 94549

Maryann T. Phipps (ATC Board Contact)
Estructure
8331 Kent Court, Suite 100
El Cerrito, CA 94530

Steering Committee

William T. Holmes, Chair
Rutherford & Chekene
55 Second Street, Suite 600
San Francisco, CA 94105

Roger D. Borcherdt
U.S. Geological Survey
345 Middlefield Road, MS977
Menlo Park, CA 94025

Anne Bostrom
University of Washington
Parrington Hall, Room 327
Seattle, WA 98195-3055

Bruce Burr
Burr & Cole Consulting Engineers
3485 Poplar Avenue, Suite 200
Memphis, TN 38111

Kelly Cobeen
Wiss, Janney, Elstner Associates, Inc.
2200 Powell Street, Suite 925
Emeryville, CA 94608

Anthony B. Court
A. B. Court & Associates
4340 Hawk Street
San Diego, CA 92103

Terry Dooley
Morley Builders
2901 28th Street, Suite 100
Santa Monica, CA 90405

Dan Gramer
Turner Construction Company
830 4th Avenue South, Suite 400
Seattle, WA 98134

Michael Griffin
CCS Group, Inc.
1415 Elbridge Payne Road, Suite 265
Chesterfield, MO 63017

R. Jay Love
Degenkolb Engineers
300 Frank H Ogawa Plaza, Suite 450
Oakland, CA 94612

David Mar
Tipping-Mar & Associates
1906 Shattuck Avenue
Berkeley, CA 94704

Steven McCabe
NEES Consortium, Inc.
400 F Street
Davis, CA 95616

Brian J. Meacham
Department of Fire Protection Engineering
Worcester Polytechnic Institute
100 Institute Road
Worcester, MA 01609-2280

William J. Petak
University of Southern California
School of Policy Planning and Development
MC 0626 Los Angeles, CA 90089-062

Nonstructural Performance Products Team

Robert E. Bachman, Team Leader
Consulting Structural Engineer
25152 La Estrada Drive
Laguna Niguel, CA 92677

Philip J. Caldwell
Square D/Schneider Electric
7 Sleepy Hollow Lane
Six Mile, SC 29682

Andre Filiatrault
MCEER, University at Buffalo
105 Red Jacket Quadrangle
Buffalo, NY 14261-0025

Robert P. Kennedy
RPK Structural Mechanics Consulting, Inc.
28625 Mountain Meadow Road
Escondido, CA 92026

Helmut Krawinkler
Stanford University
Dept. of Civil & Environmental Eng.
Stanford, CA 94305-4020

Manos Maragakis
University of Nevada, Reno
Department of Civil Engineering
Mail Stop 258
Reno, NV 89557-0152

Eduardo Miranda
Stanford University
Civil & Environmental Engineering
Terman Room 293
Stanford, CA 94305-3707

Keith Porter
University of Colorado
Dept of Civil, Environmental & Architectural Engineering
Engineering Center Office Tower 428
1111 Engineering Drive
Boulder, CO 80309-04

Nonstructural Fragility Development Consultants

Richard Behr
Pennsylvania State University
104 Engineering Unit A
University Park, PA 16802-1416

John Eidinger
G&E Engineering Systems
PO Box 3592
Olympic Valley, CA 96146

Paul Kremer
430 Canterbury Drive
State College, PA 16802

Ali M. Memari
Pennsylvania State University
104 Engineering Unit A
University Park, PA 16802-1416

William O'Brien
The Pointe
501 Vairo Boulevard
State College, PA 16803

John Osteraas
Exponent
149 Commonwealth Drive
Menlo Park, CA 94025

Xin Xu
7 Xibei Xincun, Room 403
Wuxi, Jiangsu 214062, P.R.China

Risk Management Products Team

Craig D. Comartin, Team Leader
Comartin Engineers
7683 Andrea Avenue
Stockton, CA 95207-1705

Mary Comerio
University of California at Berkeley
Department of Architecture
232 Wurster Hall
Berkeley, CA 94720-1800

Gregory Fenves
University of Texas at Austin
Cockrell School of Engineering
Austin, TX 78758

Mahmoud Hachem
Skidmore Owings & Merrill LLP
One Front Street
San Francisco, CA 94111

Gee Heckscher
Architectural Resources Group
1301 53rd St
Port Townsend, WA 98368

Judith Mitrani-Reiser
Johns Hopkins University
Department of Civil Engineering
3400 N. Charles St., Latrobe 109
Baltimore, MD 21218

Farzad Naeim
John A. Martin and Associates, Inc.
950 S. Grand Ave. 4th Fl.
Los Angeles, CA 90015

Keith Porter
University of Colorado
Dept of Civil, Environmental & Architectural Engineering
Engineering Center Office Tower 428
1111 Engineering Drive
Boulder, CO 80309-0428

Hope Seligson
MMI Engineering
2100 Main Street, Suite 150
Huntington Beach, CA 92648

Risk Management Products Team Consultants

Peter Morris
Davis Langdon
1331 Garden Highway
Suite 310
Sacramento, CA 95833

Scott Shell
Esherick Homsey Dodge & Davis Architects
500 Treat Avenue, Suite 201
San Francisco, CA 94110

Structural Performance Products Team

Andrew S. Whittaker, Team Leader
University at Buffalo
Department of Civil Engineering
230 Ketter Hall
Buffalo, NY 14260

Gregory Deierlein
Stanford University
Dept. of Civil & Environmental Eng.
240 Terman Engineering Center
Stanford, CA 94305-4020

John D. Hooper
Magnusson Klemencic Associates
1301 Fifth Avenue, Suite 3200
Seattle, WA 98101

Yin-Nan Huang
127 Paramount Pkwy
Buffalo, NY 14223

Nicolas Luco
U. S. Geological Survey
Box 25046 – DFC – MS 966
Denver, CO 80225

Andrew T. Merovich
A. T. Merovich & Associates, Inc.
1950 Addison Street, Suite 205
Berkeley, CA 94704

Structural Fragility Development Consultants

Charles Ekiert
12 Hillcrest Drive
Hamlin, NY 14464

Andre Filiatrault
MCEER, University at Buffalo
105 Red Jacket Quadrangle
Buffalo, NY 14261-0025

Aysegul Gogus
Department of Civil Engineering
University of California, Los Angeles
Los Angeles, CA 90095-1593

Kerem Gulec
University at Buffalo
Department of Civil Engineering
Buffalo, NY 14260

Dawn Lehman
Department of Civil and Environmental Engineering
214B More Hall
University of Washington
Seattle, WA 98195-2700

Jingjuan Li
4747 30th Ave NE B118
Seattle, WA, 98105

Laura Lowes
Department of Civil & Environmental Engineering
University of Washington
Box 352700
Seattle, WA 98195-2700

Eric Lumpkin
6353 NE Radford Drive Apt. #3917
Seattle, WA 98115

Hussein Okail
University of California San Diego
Department of Structural Engineering
409 University Center
9500 Gilman Dr. – MC0085
La Jolla, CA 92093

Charles Roeder
Department of Civil and Environmental Engineering
233B More Hall
University of Washington
Seattle, WA 98195-2700

P. Benson Shing
University of California San Diego
Department of Structural Engineering
409 University Center
9500 Gilman Dr. – MC0085
La Jolla, CA 92093

Christopher Smith
Department of Civil Engineering
MC:4020, Building 540
Stanford, CA 94305-4020

Victor Victorsson
1742 Sand Hill Road, Apt. 308
Palo Alto, CA 94304

John Wallace
Department of Civil Engineering
University of California, Los Angeles
5731 Boelter Hall
Los Angeles, CA 90095-1593

Fragility Review Panel

Bruce R. Ellingwood
School of Civil and Environmental Eng.
Georgia Institute of Technology
790 Atlantic Drive
Atlanta, GA 30332-0355

Robert P. Kennedy
RPK Structural Mechanics Consulting, Inc.
28625 Mountain Meadow Road
Escondido, CA 92026

Stephen Mahin
Department of Civil Engineering
777 Davis Hall, MC 1710
University of California
Berkeley, CA 94720

Validation/Verification Team

Jack Baker
Stanford University
Terman Engineering Center, Room 240
Stanford, CA 94305-4020

David Bonneville
Degenkolb Engineers
235 Montgomery Street, Suite 500
San Francisco, CA 94104-2908

Charles Scawthorn
C. Scawthorn & Associates
744 Creston Road
Berkeley, CA 94708

Hope Seligson
MMI Engineering
2100 Main Street, Suite 150
Huntington Beach, CA 92648